(4)

AFGL-TR-87-0230

1) Automatic Detection and Recognition of the First Arrival Phase of Seismic Event Signals Contaminated by Noise

2) The Curious Case of the Missing Explosion

1) Kathleen Ann Alden

2) Eugene Herrin

Southern Methodist University
Geophysical Laboratory
Inst for the Study of Earth & Man
Dallas, TX 75275

29 June 1987

FINAL REPORT
1 February 1985-31 January 1987

APPROVED FOR PUBLIC RELEASE; DISTRIBUTION UNLIMITED

AIR FORCE GEOPHYSICS LABORATORY
AIR FORCE SYSTEMS COMMAND
UNITED STATES AIR FORCE
HANSCOM AIR FORCE BASE, MASSACHUSETTS 01731

Unclassified
SECURITY CLASSIFICATION OF THIS PAGE

REPORT DOCUMENTATION PAGE

Form Approved OMB No. 0704-0188

1a. REPORT SECURITY CLASSIFICATION: Unclassified	1b. RESTRICTIVE MARKINGS
2a. SECURITY CLASSIFICATION AUTHORITY	3. DISTRIBUTION / AVAILABILITY OF REPORT: Approved for public release; Distribution unlimited
2b. DECLASSIFICATION / DOWNGRADING SCHEDULE	
4. PERFORMING ORGANIZATION REPORT NUMBER(S)	5. MONITORING ORGANIZATION REPORT NUMBER(S): AFGL-TR-87-0230
6a. NAME OF PERFORMING ORGANIZATION: Southern Methodist University; 6b. OFFICE SYMBOL (If applicable)	7a. NAME OF MONITORING ORGANIZATION: Air Force Geophysics Laboratory
6c. ADDRESS (City, State, and ZIP Code): Geophysical Laboratory, Inst for the Study of Earth & Man, Dallas, TX 75275	7b. ADDRESS (City, State, and ZIP Code): Hanscom AFB, Massachusetts 01731
8a. NAME OF FUNDING / SPONSORING ORGANIZATION; 8b. OFFICE SYMBOL (If applicable)	9. PROCUREMENT INSTRUMENT IDENTIFICATION NUMBER: F19628-85-K-0032
8c. ADDRESS (City, State, and ZIP Code)	10. SOURCE OF FUNDING NUMBERS

PROGRAM ELEMENT NO.	PROJECT NO	TASK NO	WORK UNIT ACCESSION NO
61101E	5A10	DA	AF

11. TITLE (Include Security Classification) (1) Automatic Detection and Recognition of the First Arrival Phase of Seismic Event Signals Contaminated by Noise
(2) The Curious Case of the Missing Explosion

12. PERSONAL AUTHOR(S)
(1) Kathleen Ann Alden (2) Eugene Herrin

13a. TYPE OF REPORT	13b. TIME COVERED	14. DATE OF REPORT (Year, Month, Day)	15. PAGE COUNT
FINAL REPORT	FROM 2/1/85 TO 1/31/87	1987 June 29	272

16. SUPPLEMENTARY NOTATION
There are two papers included in this report with titles and authors as shown above.

17. COSATI CODES			18. SUBJECT TERMS (Continue on reverse if necessary and identify by block number)
FIELD	GROUP	SUB-GROUP	Seismic Lajitas GSE Detector Auto Regressive Decoupling GNOME Amarilla MINOR SCALE

19. ABSTRACT (Continue on reverse if necessary and identify by block number) This report consists of two papers, both of which are based upon data collected at the Lajitas Seismic Station. The abstract for the first paper is as follows:

A historical prospective on the methods that have been used to automatically detect event signals and pick first arrival times is developed. Then the data set used to characterize and test the detection techniques is described. Next the features which discriminate seismic signals effectively from the background noise are characterized.

Two automatic detection methods are investigated: (1) The AR(8)-Spectral estimates of the signal and noise are used to develop the AR(p)-Spectral estimate for a synthetic waveform. (2) Several non-parametric tests are employed in a time domain detector to discriminate event signals from background.

The non-parametric detector chosen, RANK 2700, employs a modified rank sum test to locate the seismic event and pick its first arrival time. Errors in the automatic first arrival picks for 152 of the event traces in the data set are used to analyse the performance (OVER)

20. DISTRIBUTION / AVAILABILITY OF ABSTRACT	21. ABSTRACT SECURITY CLASSIFICATION
☐ UNCLASSIFIED/UNLIMITED ☐ SAME AS RPT ☐ DTIC USERS	Unclassified

22a. NAME OF RESPONSIBLE INDIVIDUAL	22b. TELEPHONE (Include Area Code)	22c. OFFICE SYMBOL
James Lewkowicz	(617) 377-3028	AFGL/LWH

DD Form 1473, JUN 86 — Previous editions are obsolete. — SECURITY CLASSIFICATION OF THIS PAGE: Unclassified

CONT OF BLOCK 19:

of the RANK 2700 detector.

The second paper presents a scenario for a clandestine, decoupled nuclear explosion in southeastern New Mexico based upon data recorded at Lajitas and other stations at regional distances from the hypothetical clandestine test.

Accession For	
NTIS GRA&I	☑
DTIC TAB	☐
Unannounced	☐
Justification	
By	
Distribution/	
Availability Codes	
Dist	Avail and/or Special
A-1	

TABLE OF CONTENTS

LIST OF ILLUSTRATIONS vi

LIST OF TABLES ix

ACKNOWLEDGEMENTS x

INTRODUCTION 1

Historical Prospective on Methods Used to Automatically Detect Events and Pick First Arrival Times 2

Methods Attempted in this Study 11

DESCRIPTION OF THE DATA SET 17

Instruments Used to Record the Data 17

Methods Used to Detect and Record Events in the Event Files 22

EVENT SIGNAL CLASSIFICATION 23

Variation in the Signals to be Distinguished from the Background Noise 23

Appropriateness of the Data Set for Testing the Effectiveness of Any Automatic Techniques Devised 25

Identify the Characteristics of the Seismic Signals Which Define a Class Distinctive from the Background Noise 25

A Threshold Detector to Identify Features 26

Segmentation Using Affinity Techniques to Identify Features 28

Using Rank Quartiles to Identify Features 36

Conclusions 43

DETECTORS 46

AR-Spectral Estimation Used to Develop a Synthetic Waveform 46

Assumptions 46

Description of Method 47

Effectiveness of Method and Conclusions . 51

Non-parametric Detectors 67

Description of the Detector Used to Implement the Non-parametric Tests 67

Two sample sign test 69

Assumptions 69

Procedure 70

Effectiveness 71

Run test 75

Assumptions 75

Procedure 76

Effectiveness 77

Rank sum test 81

Assumptions 81

Procedure 82

Effectiveness 84

Conclusions 84

DETECTION TECHNIQUE AND FIRST ARRIVAL PICKER EMPLOYED TO FIND THE FIRST ARRIVAL PHASE OF EARTHQUAKES AND EXPLOSIONS IN SEISMIC SIGNALS CONTAMINATED BY NOISE 89

Description of Non-parametric Detector and Picker 89

Results 91

CONCLUSIONS AND SUGGESTIONS FOR FUTURE WORK 98

APPENDICES 104

A. Fast Walsh Transform Detector 105

B. Subroutines 109

C. Values of w(alpha,M,N) 132

D. Illustration of the Results of the Automatic Detector and Picker When Run on the Event Traces Recorded by the Four Seismic Stations, Lajitas, Marathon, Shafter and Tres Cuevas for 38 Seismic Events 143

BIBLIOGRAPHY 221

LIST OF ILLUSTRATIONS

Figure

1. A 6.4 Second Detection Window and its Corresponding Normalized Walsh Spectrum Plotted on Top of the Normalized Walsh Spectrum for the Background Noise 12

2. Discrete Density Functions for the Signal and Noise of a Local Event 14

3. Discrete Density Functions for the Signal and Noise of a Regional Event 15

4. Discrete Density Functions for the Signal and Noise of a Teleseismic Event 16

5. Instrument Response for Lajitas, Marathon and Shafter Recording Instruments 19

6. Instrument Response for the Tres Cuevas Recording Instrument 20

7. Examples of the Various Types of Seismic Signals Typically Encountered 24

8. Background Noise Recorded on 11 Different Instruments During a Noise Survey at the Lajitas Test Site, February 8, 1985 27

9. Pattern of Amplitudes and Slopes Exceeding a Threshold Calculated at Plus or Minus Two Standard Deviations of the Mean Background Noise Values for a Local Event 30

10. Pattern of Amplitudes and Slopes Exceeding a Threshold Calculated at Plus or Minus Two Standard Deviations of the Mean Background Noise Values for a Regional Event 31

11. Pattern of Amplitudes and Slopes Exceeding a Threshold Calculated at Plus or Minus Two Standard Deviations of the Mean Background Noise Values for a Teleseismic Event 32

12. Observations for a Local Event Combined into a Finite Number of Segments Using the Nearest Neighbor Decision Rule and Affinity Techniques 33

13. Observations for a Regional Event Combined into a Finite Number of Segments Using the Nearest Neighbor Decision Rule and Affinity Techniques 34

14. Observations for a Teleseismic Event Combined into a Finite Number of Segments Using the Nearest Neighbor Decision Rule and Affinity Techniques 35

15. The Ranks of Amplitudes and Periods are Divided into Rank Quartiles. The Color Changes Graphically Depict any Patterns that Exist in the Features 38

16. The Ranks of Amplitudes and Periods are Divided into Rank Quartiles. The Color Changes Graphically Depict any Patterns that Exist in the Features 39

17. The Ranks of Amplitudes and Periods are Divided into Rank Quartiles. The Color Changes Graphically Depict any Patterns that Exist in the Features 40

18. The Ranks of Amplitudes and Periods are Divided into Rank Quartiles. The Color Changes Graphically Depict any Patterns that Exist in the Features 41

19. The Ranks of Amplitudes and Periods are Divided into Rank Quartiles. The Color Changes Graphically Depict any Patterns that Exist in the Features 42

20. Example of the Slope and "Modified" Slope Calculations 45

21. Proposed AR-Spectral Method for Creating the Spectrum for a Synthetic Waveform 49

22. AR(8)-Spectral Estimates for the Signal and Noise for Event 1 52

23. AR(8)-Spectral Estimates for the Signal and Noise for Event 5 55

24. AR(8)-Spectral Estimates for the Signal and Noise for Event 6 58

25. AR(8)-Spectral Estimates for the Signal and Noise for Event 8 61

26. AR(8)-Spectral Estimates for the Signal and Noise for Event 11 64

27. Example of the Two Sample Sign Test 72

28. The Performance of the Two Sample Sign Test When Used to Detect Seismic Events 73

29. The Performance of the Two Sample Sign Test When Used to Detect Seismic Events 74

30. Example of the Run Test 78

31. The Performance of the Run Test When Used to Detect Seismic Events 79

32. The Performance of the Run Test When Used to Detect Seismic Events 80

33. Example of the Rank Sum Test 85

34. The Performance of the Rank Sum Test When Used to Detect Seismic Events 86

35. The Performance of the Rank Sum Test When Used to Detect Seismic Events 87

LIST OF TABLES

Table

1. Locations and Descriptions of Instruments Used to Record the Event Data 18

2. State Table for Color Changes Used to Graphically Depict the Results of the Threshold Detector 29

3. State Table for Color Changes Used to Graphically Depict the Rank Quartiles 37

4. List of the Errors and Ranges of the Rank Sums for the 152 Events Used to Test the Automatic Event Detector and First Arrival Picker 93

5. List of the Errors and Ranges of the Rank Sums for All of the Events Except Those Which Have Violated the Assumption that the First 100 Observations Represent Background 100

A.1 Sequency Subscript to Bit-Reversed Paley Subscript Conversion 107

C.1 Table for the values of w(alpha,M,N) Used in the Rank Sum Test for Small Values of M and N . 133

D.1 Event File Names, Errors (Automatic Minus Analyst Picks in Seconds), and the Range of Rank Sums for the 38 Events Used to Test the RANK2700 Detector 144

ACKNOWLEGMENTS

The idea for this project resulted from work I started on a seismic event association location bulletin (ALB) for Dr. Eugene Herrin in 1983. I wish to express my appreciation to my major advisor, Dr. Eugene Herrin, for his supervision and assistance, especially with the geophysical aspects, throughout this project. I wish to thank all my advisors, Dr. Eugene Herrin, Dr. Henry L. Gray, Dr. Brian Stump and Dr. John Ferguson, for their constructive criticism, suggestions and advice in addition to all the time and energy they expended in helping me make this thesis a more readable and accurate manuscript. Also, I wish to acknowledge my colleagues, Paul Golden and Chris Hayward, for their support, insightful and thought provoking questions, as well as their willingness to help me locate information pertinent to this research.

Funds for this research were provided by the Defense Advanced Research Projects Agency under Contract AFOSR F49620-81-C-0010 monitored by the U.S. Air Force Office of Scientific Research and Contract AFSC F 19628-85-K-0032 monitored by the Air Force Geophysics Laboratory.

Automatic Detection and Recognition
of the First Arrival Phase of Seismic
Event Signals Contaminated by Noise.

Kathleen Ann Alden

ABSTRACT

A historical prospective on the methods that have been used to automatically detect event signals and pick first arrival times is developed. Then the data set used to characterize and test the detection techniques is described. Next the features which discriminate seismic signals effectively from the background noise are characterized.

Two automatic detection methods are investigated. (1) The AR (8)-spectral estimates of the signal and noise are used to develop the AR (p)-spectral estimate for a synthetic waveform. (2) Several non-parametric tests are employed in a time domain detector to discriminate event signals from background.

The non-parametric detector chosen, RANK 2700, employs a modified rank sum test to locate the seismic event and pick its first arrival time. Errors in the automatic first arrival picks for 152 of the event traces in the data set are used to analyze the performance of the RANK 2700 detector.

INTRODUCTION

Since the advent of the computer, work has been done in many fields to develop techniques to harness the computer to do large tedious jobs more swiftly and with fewer fluctuations in performance than its human counterpart. One of these fields is the identification and classification of seismic signals from digital seismic event records.

There are thousands of seismic events occurring every day and hundreds of seismic stations. It is not practical to evaluate all these seismic records at the speed necessary to keep up with the influx of data. Thus, many studies have been conducted to implement various techniques to (1) determine first arrival times, (2) classify the seismic events correctly and (3) locate the origins of the seismic events.

It is becoming increasingly uneconomical to pick first arrivals by hand and a computer can be used to identify first arrivals more consistently than would be picked by hand on an oscillogram. At the same time, digital recorders are becoming more common on even low-cost seismic systems, and it can be expected that in the future computer techniques will become more attractive.

Historical Prospective on Methods Used To Automatically Detect Events and Pick First Arrival Times

Many scientists, including R.V. Allen (1978), K.R. Anderson (1978), R. Blandford (1983), K.S.Fu (1982), J.E. Gaby (1983), and H.H. Liu (1981) have tried to devise an effective automatic pattern recognition system for seismic signals during the last twenty years. Computer techniques for picking first events have yet to gain widespread acceptance (P.J. Hatherly, 1982). Effective results have been elusive due to the nature of the seismic signals and the methods used to model and predict the observed values.

Both statistical methods; i.e.,maximum likelihood estimator, maximum entropy spectra, etc. (C.H. Chen, 1981), and structural methods; i.e., pattern recognition schemes that use shape features such as slope, radius of curvative, period and amplitude, (J.E. Gaby and K. Anderson, 1983), have been employed to characterize and identify seismic events.

Statistical classification algorithms can be grouped into one of two types, parametric or non-parametric. Parametric algorithms assume a particular class statistical distribution, commonly the normal distribution, and then estimate the parameters of that distribution, such as the mean and variance, to use in algorithm classification. Non-parametric algorithms make

no assumptions about the class distributions. Non-parametric techniques are sometimes termed robust because they work well for a wide variety of class distributions, if the class signatures (mean, variance, etc.) are reasonably distinct. Parametric techniques usually yield good results under the same conditions as the non-parametric techniques if the signatures of the classes are reasonably distinct, even if the assumed class distribution is invalid.

The most effective example of the statistical methods is 94% correct recognition of regional and teleseismic events using maximum entropy spectra and spectral ratio (energy>0.5Hz/energy<0.5Hz), (C.H. Chen, 1982). But even 94% is not a good enough performance record for an automatic pattern recognition system. A system cannot be considered automatic if it requires human watchdogs to monitor its progress and correct mistakes.

Part of the problem of correctly characterizing and classifying seismic signals is in obtaining an accurate first arrival time. There is always ambiguity associated with measuring the first arrival time from seismograms, whether it is done by seismologist or machine, since these signals of finite bandwidth are of unknown shape and contaminated by noise. Such ambiguity can be reduced by combining the processes of picking arrivals in an iterative fashion (C.H. Chen, 1982). Inaccurate first

arrivals distort the structural and statistical characterizations of a seismic event that are used for classification.

Effective results have been elusive due to the nature of the seismic signal which contains events contaminated by noise. In many fields of signal processing: for example, the development of speech recognition systems, the automatic analysis of signals requires the recognition of specific features in the signal. (Gaby and Anderson, 1983) Since more a priori knowledge exists about the characteristic shapes of words, it is easier to automatically identify a word and classify it correctly. The paucity of a priori information available on the morphologies (shapes) of seismic signals inhibits automatic pattern recognition (Gaby and Anderson, 1983).

The lack of a priori knowledge characterizing seismic signals has prompted the recent application of pattern recognition techniques to find and develop methods to discriminate and classify seismic signals. The methods used to find the broad characteristics of a seismic event include storing the trace in a binary tree structure and using affinity techniques, first developed for image processing, to combine small segments of the signal and store the signal within the tree structure at different levels of complexity (Gaby and Anderson, 1983). In other words, this method would use features such as period,

slope and amplitude to divide the event trace into segments and then try to associate those segments with the sequence of arrival phases that make up a seismic event.

Augmented transition networks (ATN), originally created to provide a formal environment to develop grammatical rules describing finite state grammers, have also been used to develop seismic signal structural characteristics interactively (Anderson, 1981).

All the techniqes for seismic pattern recognition schemes require that the first arrival time of the waveform be known. The seismologist uses the morphology (shape) of the seismic signal to identify the first arrival time correctly along with changes in period and amplitude. Determining the correct first arrival time is important in classifying the signal and locating the origin of the seismic event. For an automatic pattern recognition system to replace the seismologist it must identify first arrival times correctly and classify the event with better than the 94% current success rate of techniques previously attempted.

Automatic processes that have been employed to determine first arrival times rely on statistics to distinguish between two populations (signal and noise) occurring on a seismic trace. Since the density distribution functions for both the signal and noise are not known a priori they have traditionally been estimated

by Gaussian density distribution functions. The reason for this is that the statistics (i.e., the divergence and linear discriminant functions) for characterizing Gaussian (normal) distributions are well known and easily available for computation.

The standard statistics for a normal distribution have traditionally been used to characterize the signal and noise making it possible to determine first arrival times by comparing parameters from the two populations. Using the standard statistics for a normal distribution to characterize the noise a predictive model is constructed to predict future seismic noise values.

There should be a failure of the observed data to match the predicted value at the first arrival because the arrival of the seismic signal is not predictable from the background noise. Robinson(1967) wrote subroutines to pass the proposed first arrival if there was a significant prediction error at the first arrival and for two terms after it. Significance was established by making comparisions with the prediction errors within the noise. A test, which predicts the values at the first arrival from the previous values using the technique of linear least-square prediction, was first used by Wadsworth et al(1953) to identify seismic events on the basis of a prediction failure. (P.J. Hatherly, 1982)

Most techniques to distinguish noise from the first

arrival signal use parametric statistics which assume the signal has a known distribution. This is an incorrect assumption for the background noise preceding a seismic event. In general, background noise is a non-stationary process due to seasonal changes and atmospheric variations, with an unknown distribution. Over a short time interval, less than 100 seconds, background noise can usually be considered stationary except in the case where it precedes a seismic event. When a seismic event occurs the mean of the signal often flucuates while the transient signal is being recorded by the seismic instrument.

Non-stationary processes have time changing means and/or variances. Stationary process implies that the mean, the variance and the autocovariances of the process are invariant under time translations. Thus the mean and variance are constant, and the autocovariances depend only on the lag time.

Non-stationary time series have been modeled by several processes: (1) Harrison(1964) used an exponentially weighted moving average, EWMA, to forecast seasonal short term sales. (2) A modified autogressive moving average, ARMA, model with time varying coefficients of the form:

$$\sum_{k=0}^{p} b_{kt} * e_{t-k} = \sum_{j=0}^{r} c_{jt} * x_{t-j} + d_t \ , \ r = \max(p-1, q-m)$$

has been used by P. Whittle (1965), to model non-

stationary time series. Prediction formulas applied in the stationary case are shown by Niemi(1983) to also be valid in the non-stationary case. The effects of the non-stationarity on the estimation of the parameters of the underlying ARMA model are not shown to be significant. (3) The autoregressive integrated moving average, ARIMA, method, based on Gaussian stochastic processes was developed by Box and Jenkins (1970) to model homogeneous non-stationary time series.

Homogeneous non-stationarity implies the changing mean can be described by a low order polynomial in time. However, the coefficients of the polynomial are not constant but vary with time. The observations are described by random stochastic trends (polynomials). Tintner (1940), Yaglom (1955), and Box and Jenkins (1976) argue that homogeneous non-stationary sequences can be transformed into stationary sequences by taking successive differences of the series.

In practice it is usually the first or second integral of a non-stationary process which is stationary. The ARIMA technique integrates the non-stationary time series until it is stationary and then models the resulting time series as an ARMA process. Under fairly general conditions the prediction interval for a future observation in an ARIMA scheme is robust with respect to symmetric non-normality of the error distribution,

Heuts(1981).

Non-parametric methods that make no assumptions about the density distribution of the time series are outlined by Kassam and Thomas(1975). Cobben(1982) outlines a non-parametric detector based on a sign test that discriminates between:

H_0: x(t) = n(t) //data = noise//

H_a: x(t) = s(t) + n(t) //data = signal + noise//

included in Kassam and Thomas (1980). The sign test was extended by Cox (1955) to detect steps and ramps in the presence of additive noise; i.e., signals with sharp onset and gradual onset first arrivals. Cobben's method assumes a stationary signal which may be a valid assumption for a time window of less than 100 seconds, (C.H. Chen, 1978).

Although background noise may possibly be considered stationary, it cannot be assummed to be Gaussian. Various known and unknown processes: microseisms which are "non-Gaussian"; thermal noise due to current across resistors which is "Gaussian"; and seismometer noise which is "distributed as 1/f" contribute to form a non-Gaussian density distribution. Although, Heuts (1981), has shown that an ARIMA prediction model (based on an assumption of Gaussian and stochastic data) is robust with respect to symmetric non-normality of the error distribution. parametric techniques are generally incorrect for

distinguishing noise from the first arrival.

Part of the difficulty in automatically classifying seismic signals and locating their origin is a direct result of incorrect first arrival times picked by methods assuming an underlying Gaussian distribution for the signal. Since the seismic signals have an unknown underlying distribution a method for first arrival detection using non-parametric statistics should be developed in the hopes that it will improve the accuracy of the first arrival time.

Once the first arrival time can be swiftly and accurately located the morphological and statistical methods of classifying seismic signals can be used with greater accuracy since the correct sequence of events (or states) that characterize the seismic signal will be readily available. The first arrival on the seismic trace is identified as the first observation which is statistically different from the observation before. The point chosen is dependent on the signal to noise (S/N) ratio and the amplification of the seismic signal (P.J. Hatherly, 1982).

Some signal detection schemes used to record events in real time use the spectrum found using the Walsh (Goforth and Herrin, 1981) or Fourier (Blandford, 1983) transforms of the signal to distinguish the signal from the background noise. These methods while effective for

real time detection of events can only locate the first arrival time within one window (a block of observed data values transformed to provide a spectrum for comparision). Figure 1 illustrates the fast Walsh transform.

If this window is large enough to detect the first arrival (greater than two times the longest period of the expected signal, 2.5 seconds in our case) it will not be small enough to accurately determine first arrival times for the purpose of classifying and locating the origin of events. This indicates an effective automatic first arrival picker should be implemented in the time domain.

Methods Attempted in this Study

Since the signal is nonstationary with an unknown distribution function it is logical to develop a detector that does not assume stationarity; i.e., constant mean and constant variance, or a "known" distribution function. There is a broad range of amplitudes and bandwidths which characterize local, regional and teleseismic earthquakes and explosions. Thus, we must develop features to distinguish a broad category of signals from the background noise.

Since the seismic signal we record has an unknown distribution, it is important to determine how valid some of the parametric techniques; i.e., techniques that assume a know distribution, are when applied to a seismic signal.

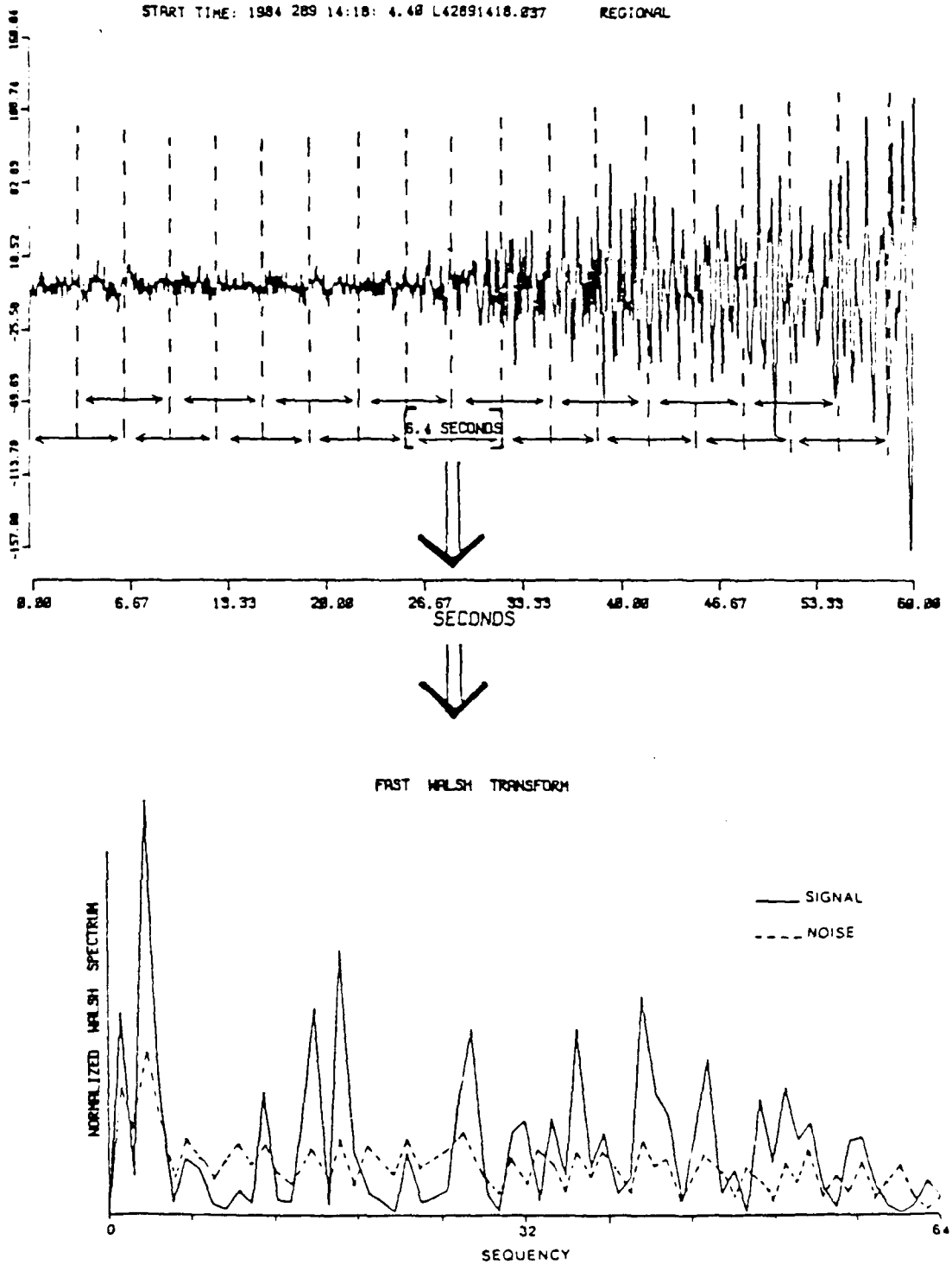

Figure 1. A figurative example of a 6.4 Second Detection Window and its Corresponding Normalized Walsh Spectrum Plotted on Top of the Normalized Walsh Spectrum for the Background Noise.

In particular, Niemi (1983) wrote a paper indicating an ARMA scheme was robust with respect to symmetric non-normality. The discrete density distributions for the signal and noise were plotted for 100 seismic events recorded at each of the four seismic stations in far west Texas (Lajitas, Marathon, Shafter and Tres Cuevas) to find out if the density distributions of the seismic signals and noise from each station could be characterized as symmetric even though the "true" underlying density distributions were unknown. Histograms of the amplitude of the seismic signal were computed to approximate the discrete density functions for the noise and signal plus noise of each event trace. (See figures 2 through 4) In all cases the discrete density functions for both the signal and noise were symmetric. This assumption allows us to model the non-stationary seismic signal with a simplier model than the ARIMA model for which methods of computation have been more fully explored.

Two methods were attempted to develop an automatic first arrival picker. The first technique uses the AR-spectral estimation of the signal and the background noise to develop a synthetic waveform to cross-correlate with the event trace and pick out the first arrival phase. The second technique employs a non-parametric test within a sliding window detector to identify the seismic event signal and pick the first arrival phase.

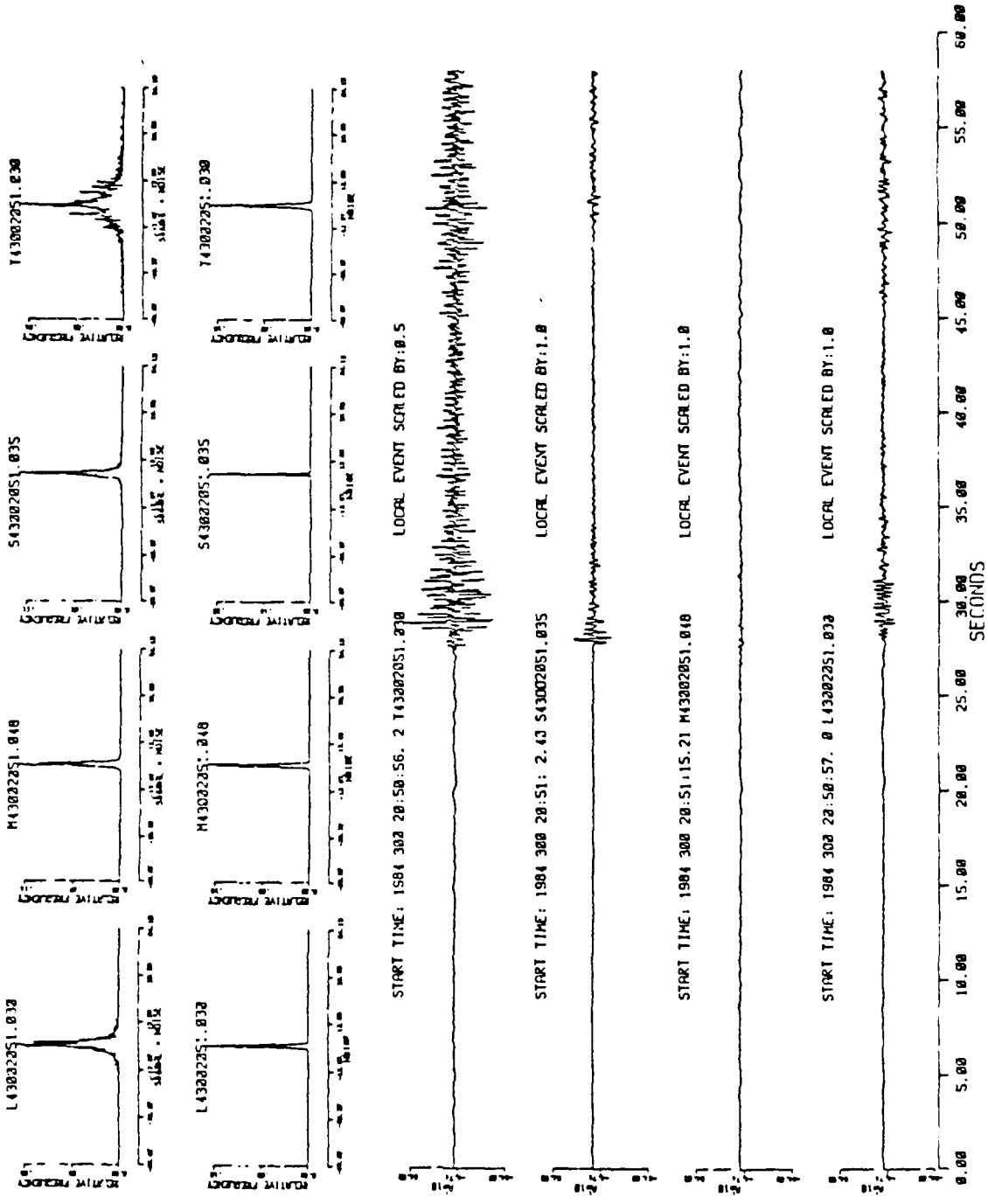

Figure 2. The First 60 Seconds for a Local Event, Recorded at Each of the Four Seismic Stations, Lajitas, Marathon, Shafter and Tres Cuevas, are Plotted from Bottom to Top Respectively. The Corresponding Discrete Density Functions for the First 20 Seconds of Background Noise and the Next 20 Seconds of Signal Plus Noise for Each Trace are Shown from Left to Right.

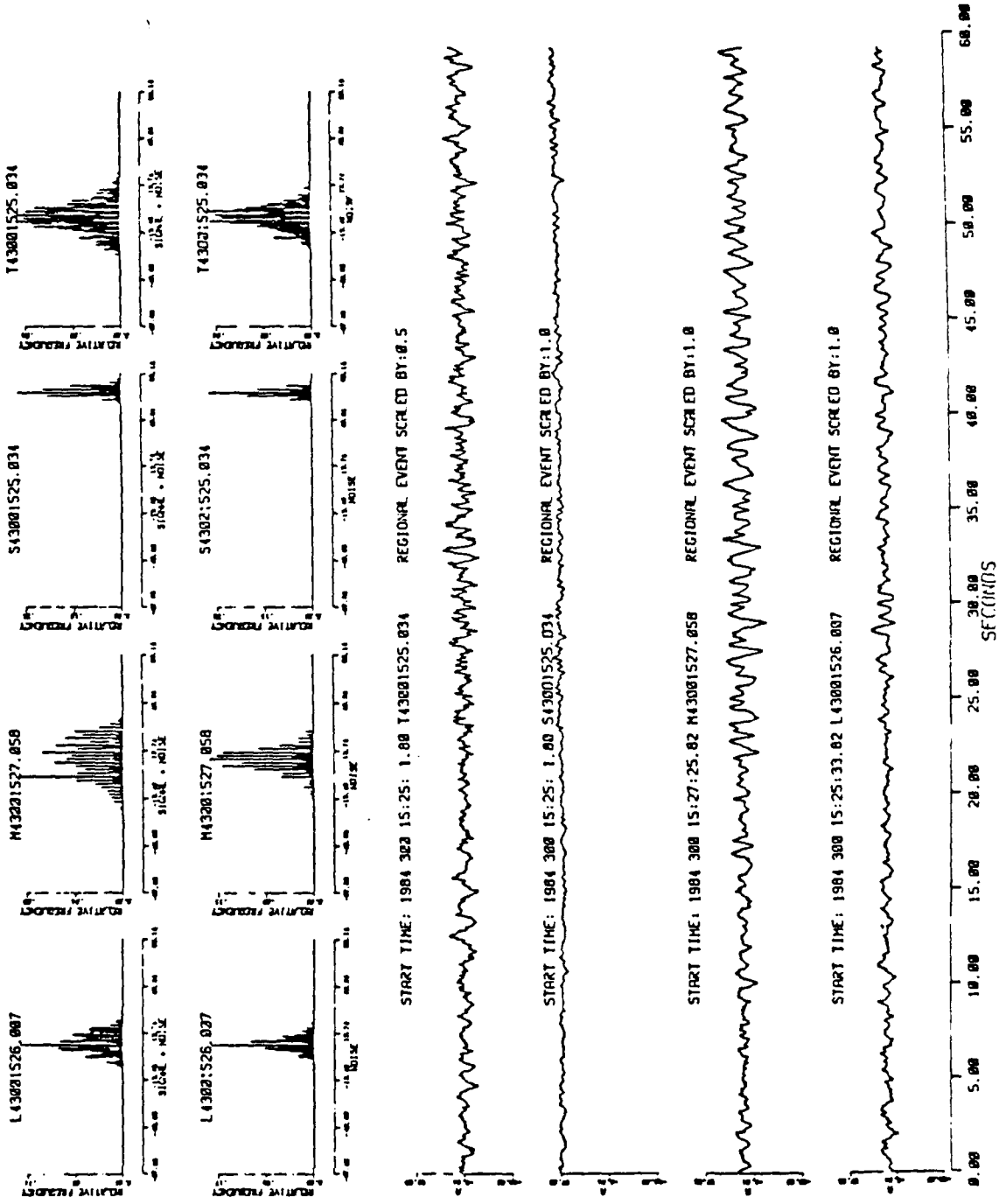

Figure 3. The First 60 Seconds for a Regional Event, Recorded at Each of the Four Seismic Stations, Lajitas, Marathon, Shafter and Tres Cuevas, are Plotted from Bottom to Top Respectively. The Corresponding Discrete Density Functions for the First 20 Seconds of Background Noise and the Next 20 Seconds of Signal Plus Noise for Each Trace are Shown from Left to Right.

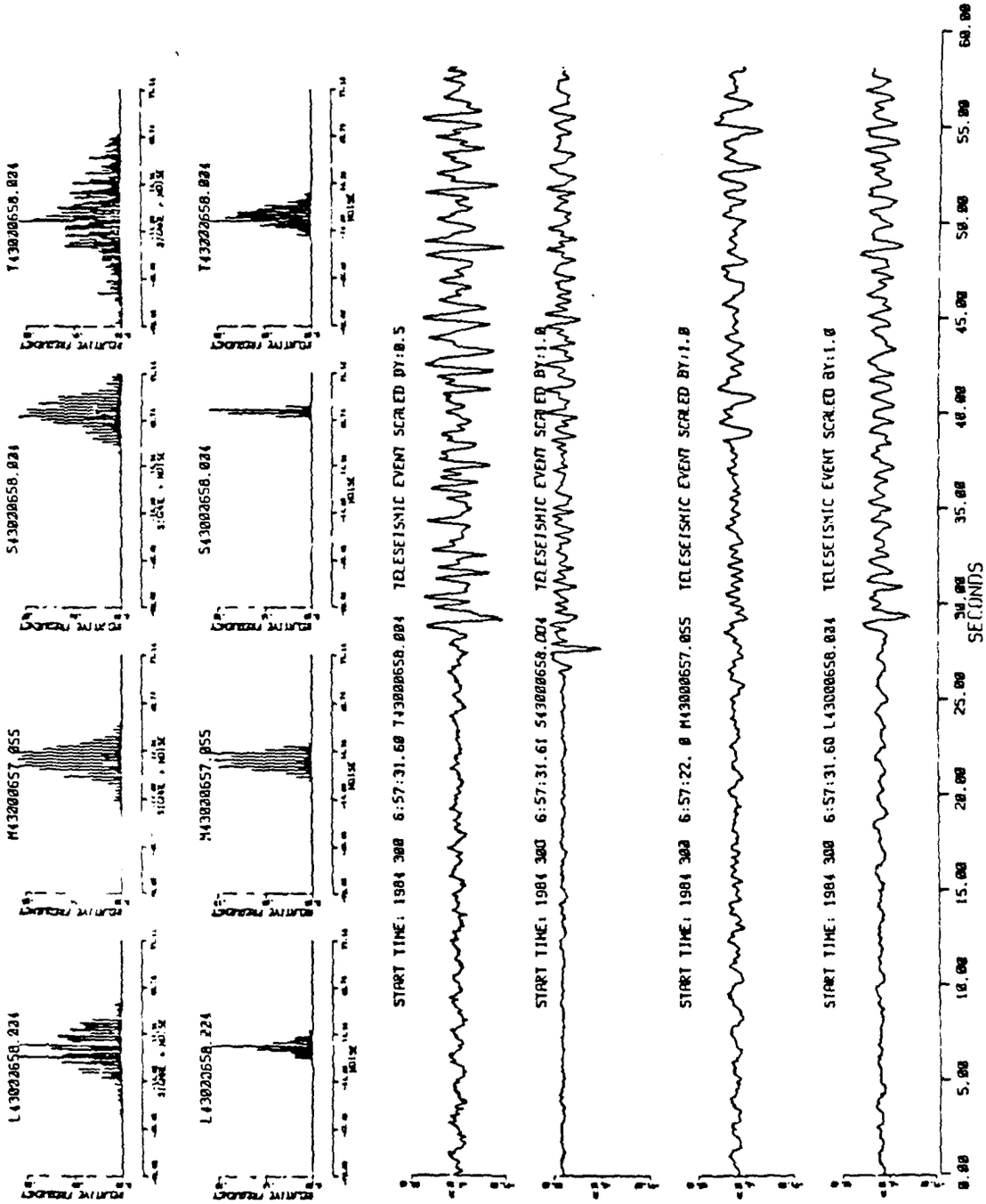

Figure 4. The First 60 Seconds for a Teleseismic Event, Recorded at Each of the Four Seismic Stations, Lajitas, Marathon, Shafter and Tres Cuevas, are Plotted from Bottom to Top Respectively. The Corresponding Discrete Density Functions for the First 20 Seconds of Background Noise and the Next 20 Seconds of Signal Plus Noise for Each Trace are Shown from Left to Right.

DESCRIPTION OF THE DATA SET

Instruments Used to Record the Data

Seismic events recorded at four stations in southwest Texas, Lajitas, Maratnon, Shafter and Tres Cuevas, were collected during the Group of Scientific Experts Technical Test (GSETT) in which Southern Methodist University was a participant. GSETT was conducted from October 15, 1984 to December 14, 1984 to test procedures for exchanging seismic data, which include: the extraction of Level I signal parameters (seismic phase identifiers, arrival times, signal amplitudes and periods); the exchange of these parameters primarily via the Global Telecommunications System of the World Meteorological Organization (WMO/GTS); and the collection and assesment of these data at the Data Center in Washington, D.C.

Table 1 gives the locations and descriptions of the instruments used to record the seismic events during the test. The instrument responses are illustrated in figures 5 and 6.

A real time event detector utilizing the fast Walsh transform (Goforth and Herrin, 1981) implemented on a DEC RT/11 micro-computer received the seismic data from the Lajitas, Marathon, Shafter and Tres Cuevas stations via

TABLE 1. Locations and Descriptions of Instruments Used to Record the Event Data

SEISMOMETER DESCRIPTIONS

NAME	LAJITAS	MARATHON	SHAFTER	TRES CUEVAS
ID	LA	MA	SH	TR
CHANNEL NUMBER	2	3	4	1
INSTRUMENT TYPE	23900	23900	23900	18300
LATITUDE DEG N	29.333	30.306	29.924	29.316
LONGITUDE DEG W	103.667	103.255	104.371	103.717
ELEVATION METERS	1013	1356	1570	1097
VCO HZ	960	1300	1700	2040
LPF CORNER, HZ	5	5	5	15

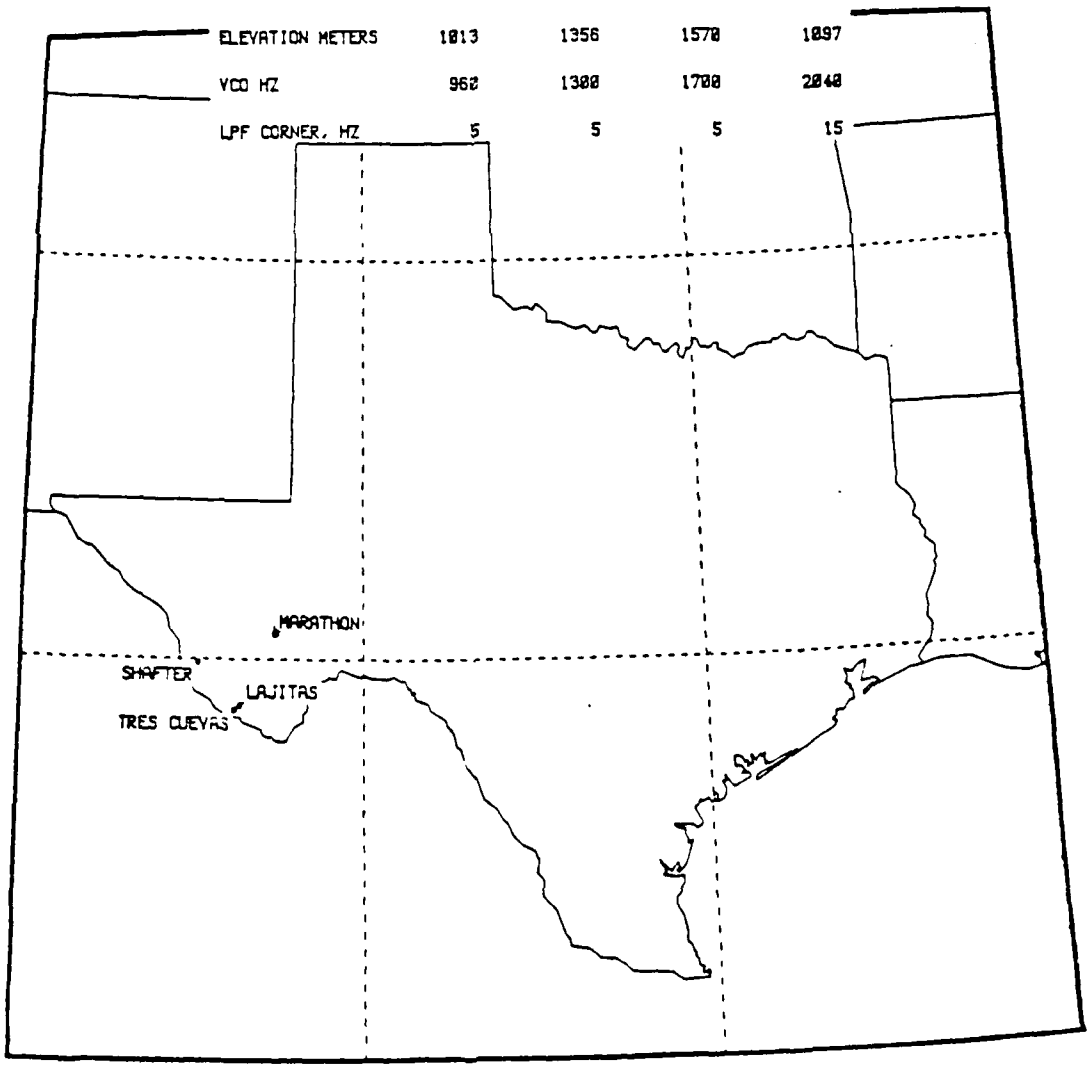

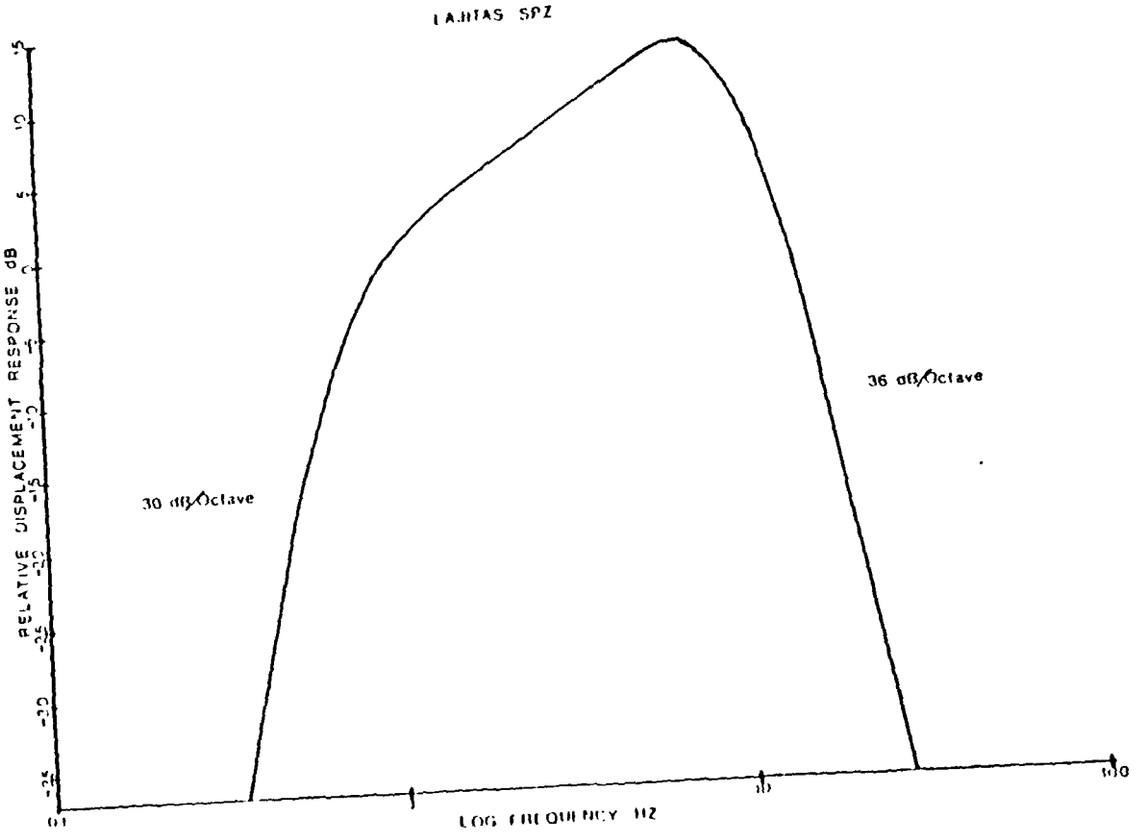

Figure 5. Instrument Response for Lajitas, Marathon and Shafter Recording Instruments

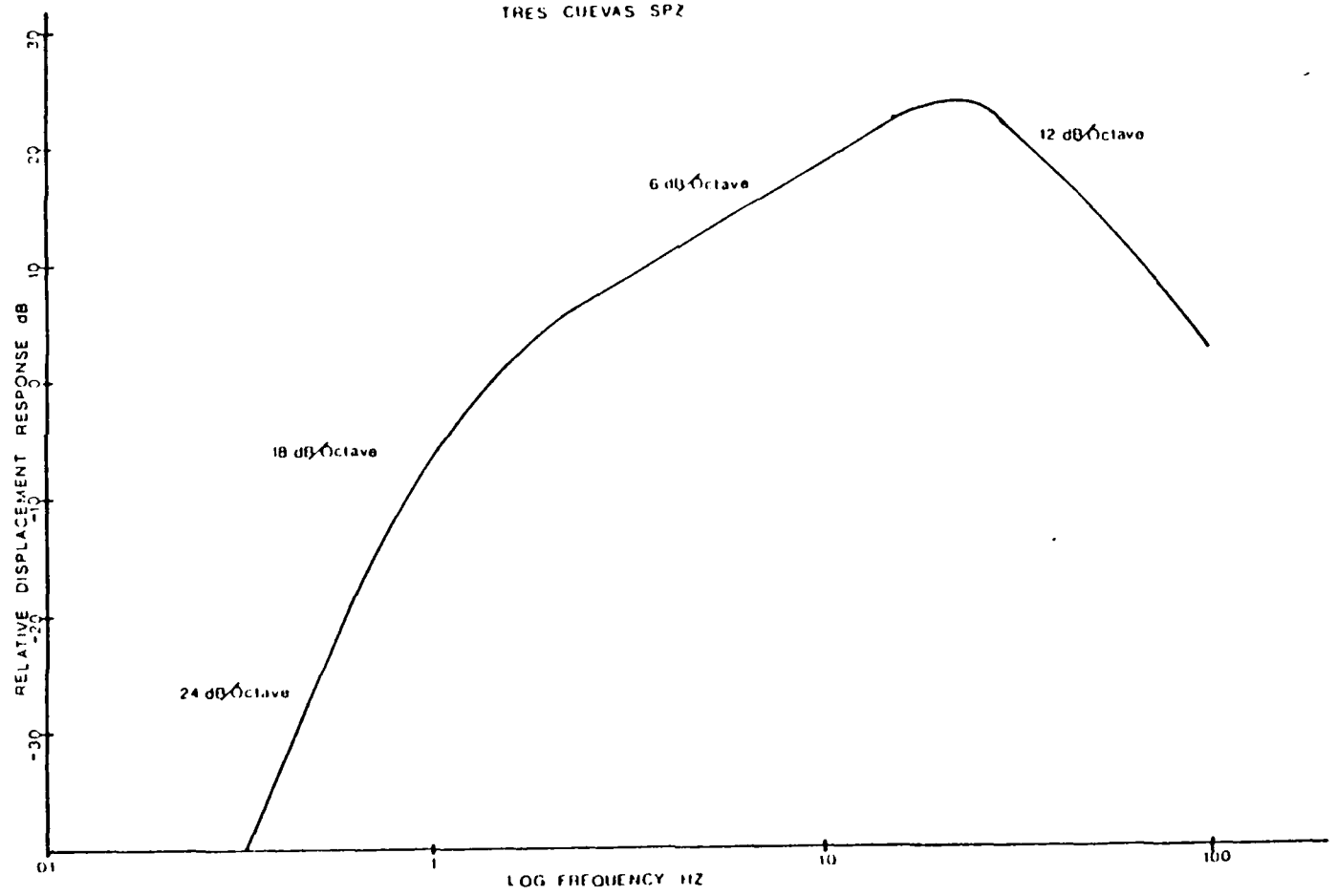

Figure 6. Instrument Response for the Tres Cuevas Recording Instrument.

telephone line. (See appendix A for a description of the fast Walsh transform detector.) The detected events were recorded on magnetic tape for later graphic display and analysis by a seismologist.

The seismic analyst was responsible for identifying phase (Pn,Pg,P or Lg) and picking first arrival times, amplitudes and periods. The bias of the analyst directly effects the choice of local events v.s. "noise". Discrimination of the phase of the first arrival (P or Lg) is dependent on which phase the analyst's experience indicates the waveform matches. Parameters for the events chosen by the analyst as "true" events, not "glitches" or "background noise", were sent to the U.S. National Data center in Washington using the UNIX-net software of the Eunice operating system.

GSETT's Final Event List associated all the event information collected from throughout the world and reported the origin time, location, magnitude and number of stations used to define each event which was detected during the two month time period of the test.

The residual travel time (the difference between the arrival time at the station indicated by the best least squares fit of the stations associated with an event and the first arrival time picked by the analyst) was listed for each station used to define an event. The "true" estimates calculated by least squares, assuming the

correct location of the event was found, allow us to determine if the automatic detection method is doing as well, worse, or better than the human analyst in ambiquous cases.

Methods Used to Detect and Record Events in the Event Files

The fast Walsh transform detection window is 6.4 seconds long with a 50% overlap. (see figure 1) When the spectra of the detection window exceeds the background noise threshold the detection is triggered. Thirty seconds of data preceding the detection window is written at the beginning of the event file so that if the Walsh detector triggered on an Lg arrival the P wave first arrival should be present somewhere in the first 30 seconds of the event file. Thirty seconds was originally thought to be adequate to make sure the P arrival was included in the event trace but experience in working with the data collected during the GSETT experiment has shown that 60 seconds is a better predetection interval for insuring the first arrival (Pn) is included in the event file when the detector triggers on Pg.

EVENT SIGNAL CLASSIFICATION

Variation in the Signals to be Distinguished From the Background Noise

The collection of seismic events we are attempting to distinguish from the background noise, (recorded on short period seismic instruments with a bandwidth of 0-20 Hz), encompasses a broad range of periods and amplitudes. Local events, occurring within 25 to 150 kilometers of the seismic station, are characterized by amplitudes which may be nearly the same as the noise and by periods of 0.3 to 0.4 seconds. Regional events, occuring on the same continent as the seismic station, are characterized by varying amplitudes and periods of 0.5 to 0.7 seconds. Teleseismic events, events that travel distances greater than about 2000 km to reach the seismic recording station, are characterized by periods of 0.8 to 1.2 seconds. The high frequency component of the background noise is similar in spectral content to local seismic event signals while the underlying low frequency component of the background noise is similar in spectral content to teleseismic signals. Pn can often not be discriminated from the background noise by the analyst, thus Lg which follows Pn is often picked as the first arrival phase for

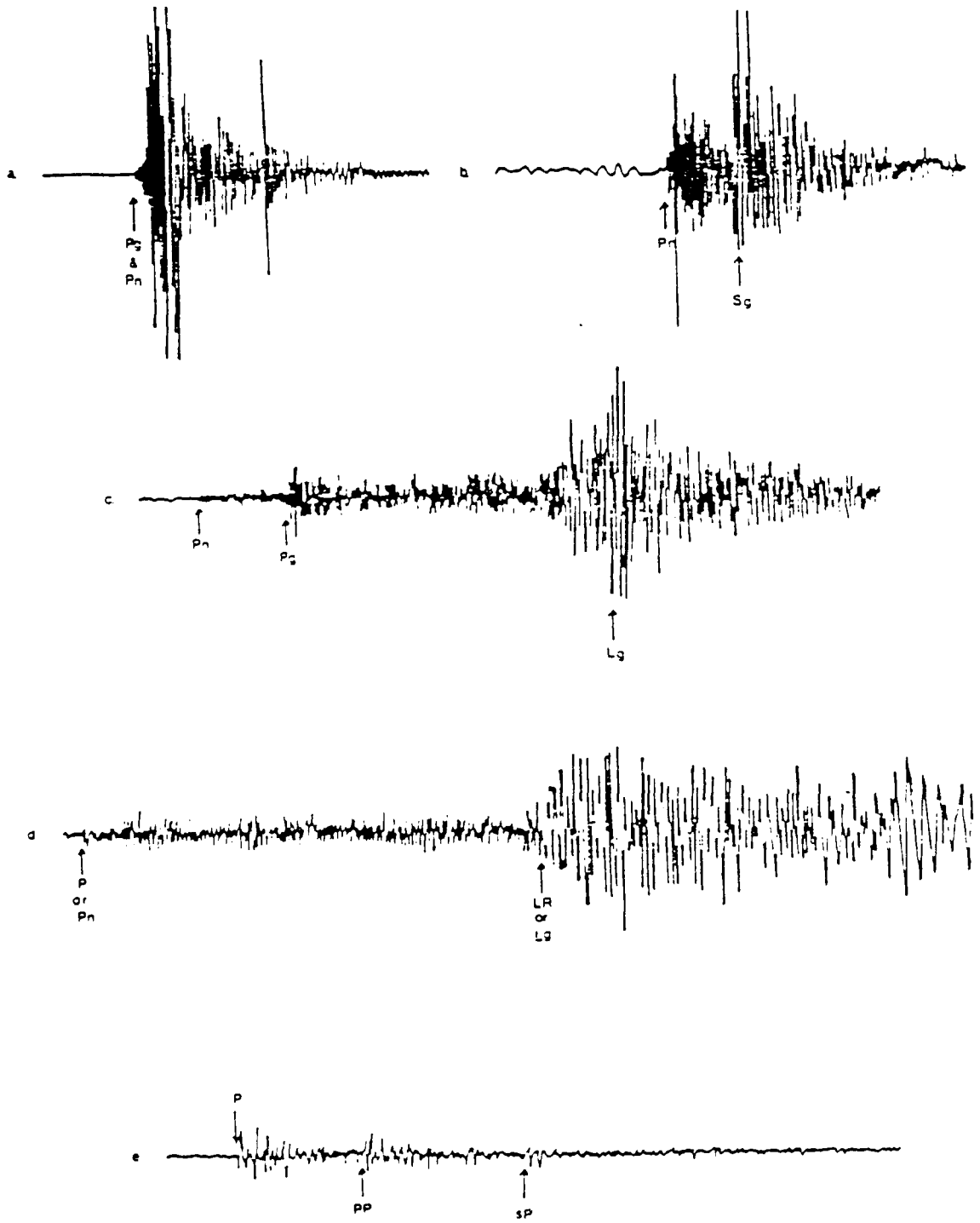

Figure 7. Examples of the Various Types of Seismic Signals Typically Encountered. (a) 33 km - Local Event - SPZ recorded in Berkeley, California. (b) 140 km - Local Event - Closest distance Pn and Pg can be observed separately - SPZ recorded in Colorado. (c) 6^{o} - Regional Earthquake - SPZ recorded in Winner, South Dakota. (d) 13^{o} - Regional to Teleseismic Earthquake - Gulf of California - SPZ recorded in Colorado. (e) 91.5^{o} - Teleseismic Earthquake - Offshore Peru - SPZ recorded in Black Rapids, Alaska.

regional events. Figure 7 illustrates typical examples of the types of seismic signals encountered. (R.B. Simon, 1981)

Appropriateness of the Data Set for Testing the Effectiveness of Any Automatic Techniques Devised

The data set collected during GSETT represents a collection of event records of different types of events with continuous background noise variations from four different seismic stations. This data set has variations in: signal type (local, regional and teleseismic); background noise (due to changes in wind speed, temperature, humidity, barometric pressure and cultural activity); instrument type and local structure at the seismic station. It is concluded that because the data set includes variations in all the parameters normally expected to change when recording seismic events the data set will be a good test of the robustness of any detection method used to pick first arrival times.

Indentify the Characteristics of the Seismic Signals Which Define a Class Distinctive From the Background Noise

Any classification technique actually consists of a one-time calculation of decision boundaries, followed by a comparison of each sample's feature vector and the location of those boundaries. By incorporating these

facts in classification algorithms, their efficiency can be improved by an order of magnitude or more, with little or no reduction in accuracy. (Schowengerdt, R.A., 1983)

Easily calculatable features available in the time domain for discriminating seismic signals and background noise are: period estimates, (intervals between zero-crossings and slope direction changes); amplitude; and slope. Figure 8 is a typical example of the background noise. This noise data was recorded during a background noise study February 8, 1985 at the Lajitas test site. In the next three sections we determine the effectiveness of these features in distinguishing a broad class of seismic signals from the background noise by using: (1) a threshold detector based on an estimate of the mean and variance of the background noise; (2) segmentation of the signal based on the similarity of features to find a pattern; and (3) division of the features based on their ranks into rank quartiles to look for a relative pattern in the feature distribution.

A Threshold Detector to Identify Features

For the threshold detector the mean and variance were calculated for the amplitude and slope (average difference between the ith sample and the samples adjacent to it) of the first 100 observations representating background noise assuming a normal distribution. The threshold for signal

Figure 8. Background Noise Recorded on 11 Different Instruments During a Noise Survey at the Lajitas Test Site, February 8, 1985. Instrument 1 - GS 13 Z (vault), Instrument 2 - GS13N (vault), Instrument 3 - GS13 E (vault), Instrument 4 - 18300 (mine site), Instrument 5 - S750 Z (grouted in), Instrument 6 - S750 Z (vault), Instrument 7 - S750 A (North of mud hut 150m), Instrument 8 - S750A (East of mud hut 150m), Instrument 9 - GS21 (buried 330'), Instrument 10 - GS21 (buried 50'), Instrument 11 - microphones (wind).

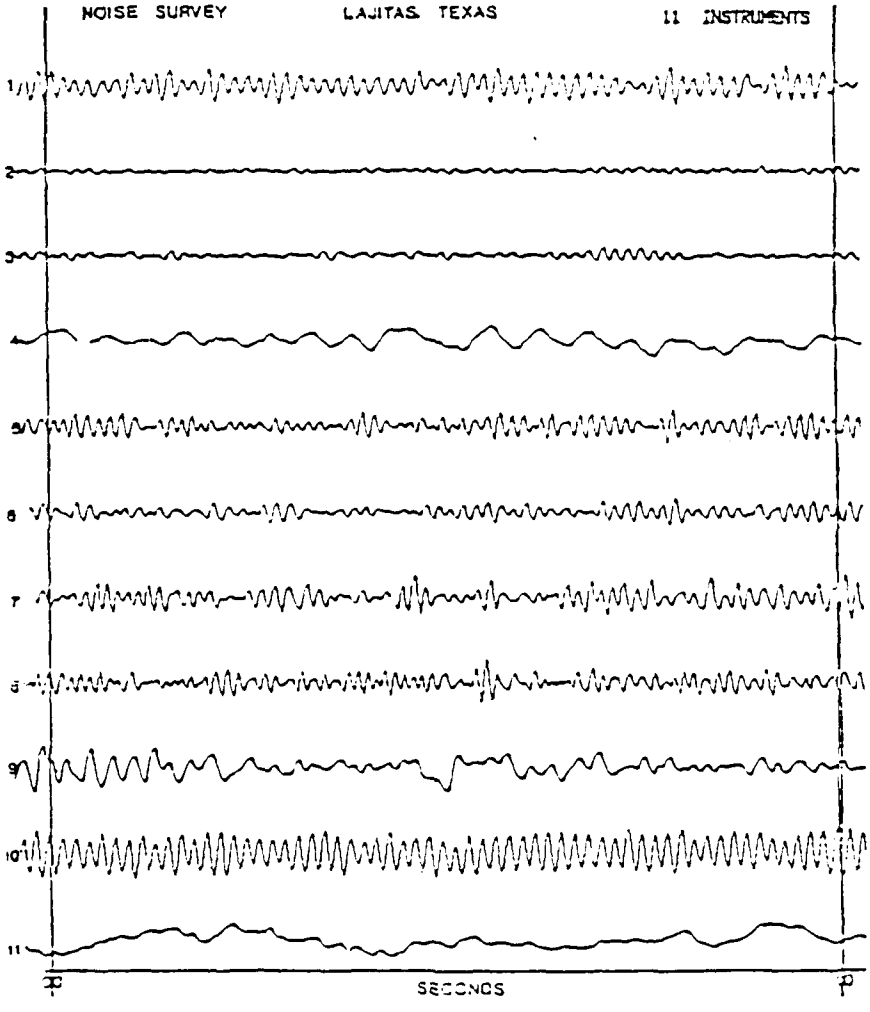

detection was set at two standard deviations from the estimated mean of the background noise. Thus, given that background noise is all that is present in the seismic signal, there is a 95% probability that the amplitude and slope for any observation will be within two standard deviations of its estimated mean. Figures 9 through 11 illustrate the results of this test on three types of seismic events recorded at the four stations Lajitas, Marathon, Shafter and Tres Cuevas. The state table for the color changes occuring along the event traces in figures 9 through 11 is shown in Table 2. The mean and variance estimated for the slope and amplitude were not very effective in clearly distinguishing the background noise from the seismic event signal.

Segmentation Using Affinity Techniques to Identify Features

Segmentation of the trace using the estimated mean and variance of the slope and amplitude of the background noise was done using the nearest neighbor decision rule and an affinity algorithm to combine the samples with the most similar features into a finite number of segments. The nearest neighbor decision rule decides which of a segments neighbors is most similar. Then the affinity algorithm combines those segments which mutually consider each other most similar. Figures 12 through 14 illustrate this technique on the three types of seismic signals,

TABLE 2

State Table for Color Changes Used to Graphically Depict the Results of the Threshold Detector

	AMPLITUDE	SLOPE
BELOW THRESHOLD	0	0
ABOVE THRESHOLD	1	1

COLOR	STATE (AMPLITUDE,SLOPE)
RED	00
BLUE	10
GREEN	01
BLACK	11

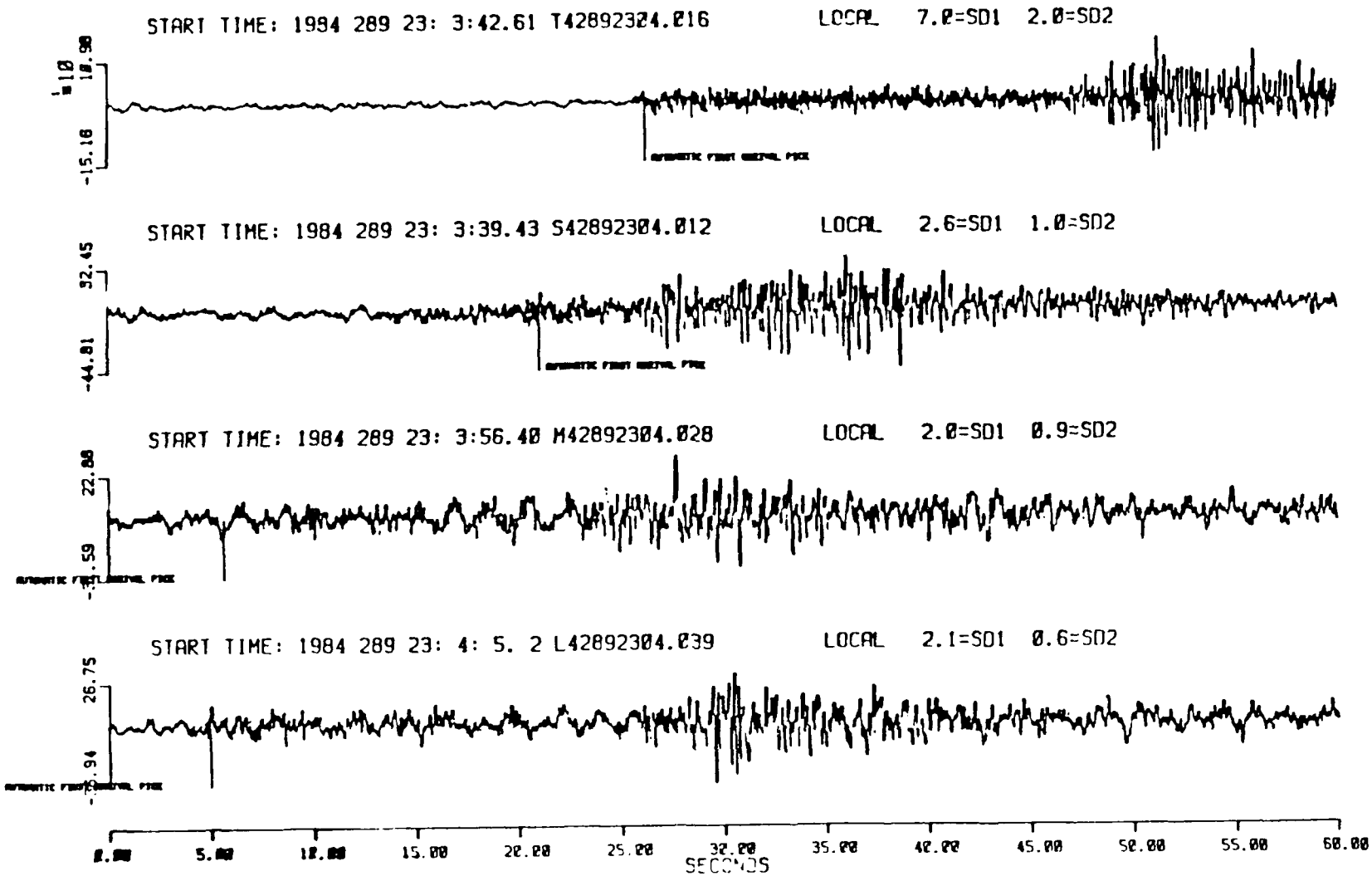

Figure 9. Pattern of Amplitudes and Slopes Exceeding a Threshold Calculated at Plus or Minus Two Standard Deviations of the Mean Background Noise Values for a Local Event. A Vertical Line is Drawn from the Automatic First Arrival Pick and Labeled "AUTOMATIC FIRST ARRIVAL PICK" on Each of the Event Traces for the Lajitas, Marathon, Shafter and Tres Cuevas Stations, Bottom to top

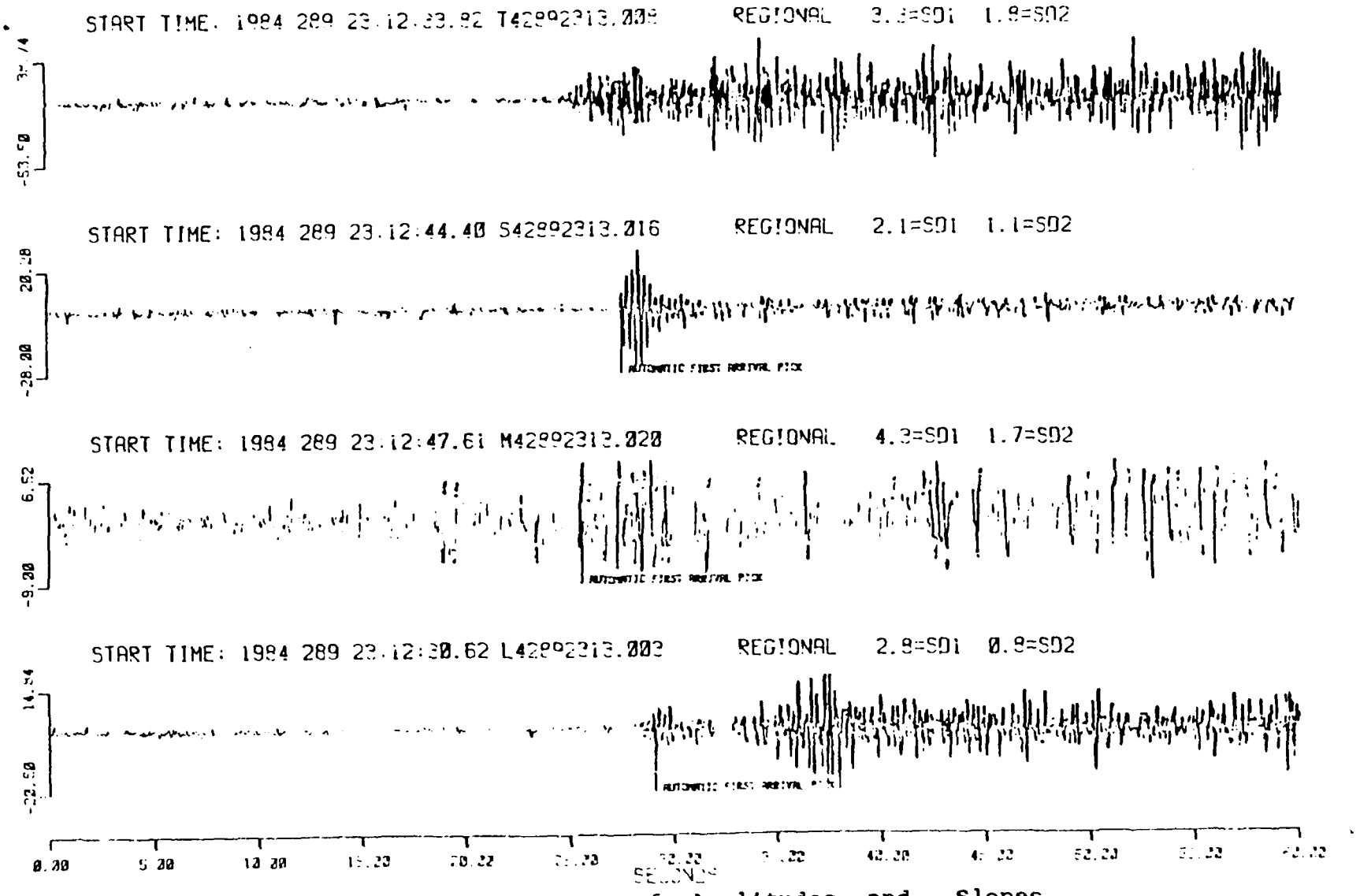

Figure 10. Pattern of Amplitudes and Slopes Exceeding a Threshold Calculated at Plus or Minus Two Standard Deviations of the Mean Background Noise Values for a Regional Event. A Vertical Line is Drawn from the Automatic First Arrival Pick and Labeled "AUTOMATIC FIRST ARRIVAL PICK" on Each of the Event Traces for the Lajitas, Marathon, Shafter and Tres Cuevas Stations, Bottom to Top

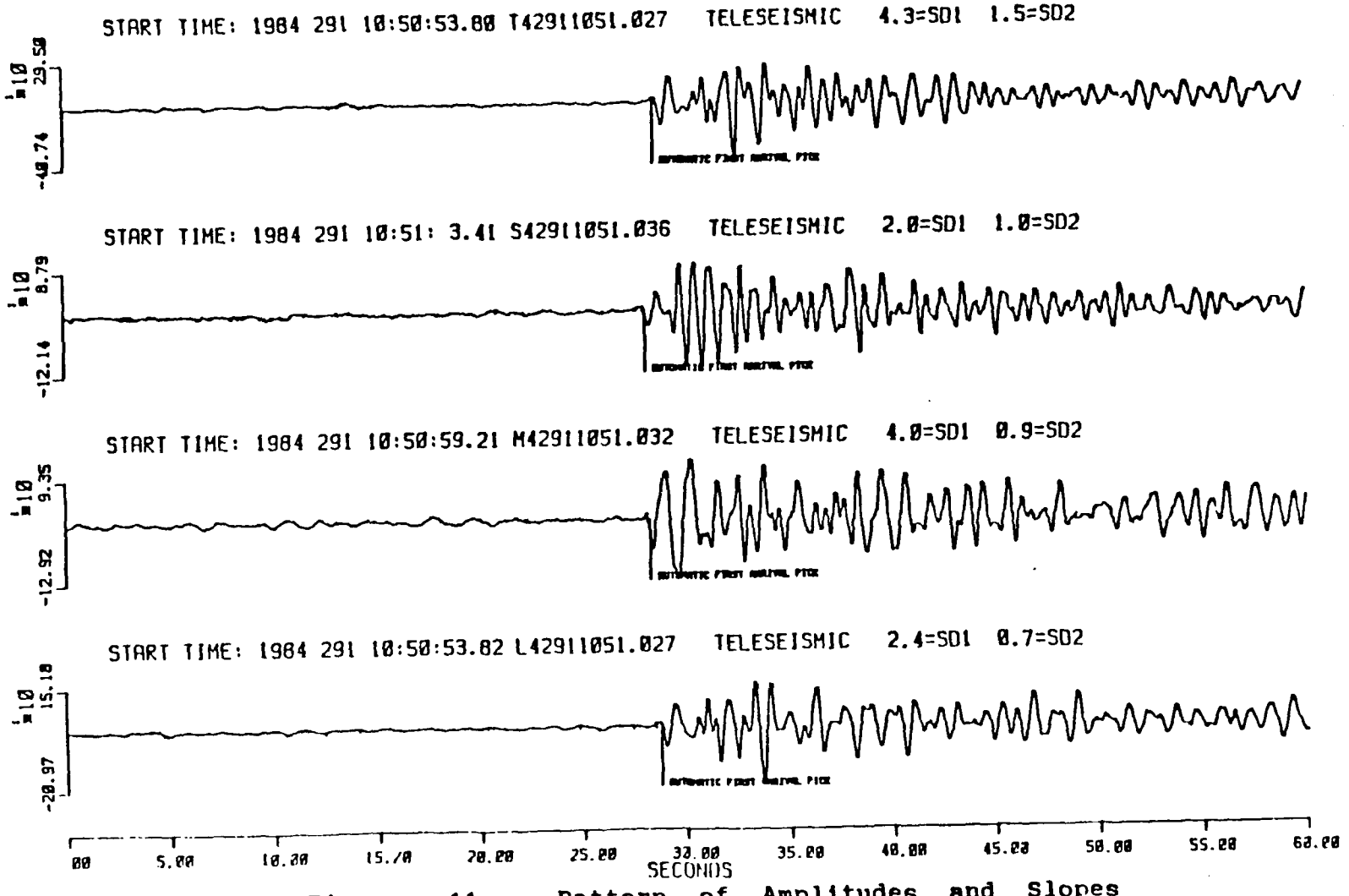

Figure 11. Pattern of Amplitudes and Slopes Exceeding a Threshold Calculated at Plus or Minus Two Standard Deviations of the Mean Background Noise Values for a Teleseismic Event. A Vertical Line is Drawn from the Automatic First Arrival Pick and Labeled "AUTOMATIC FIRST ARRIVAL PICK" on Each of the Event Traces for the Lajitas, Marathon, Shafter and Tres Cuevas Stations, Bottom to Top Respectively. This Event Illustrates a

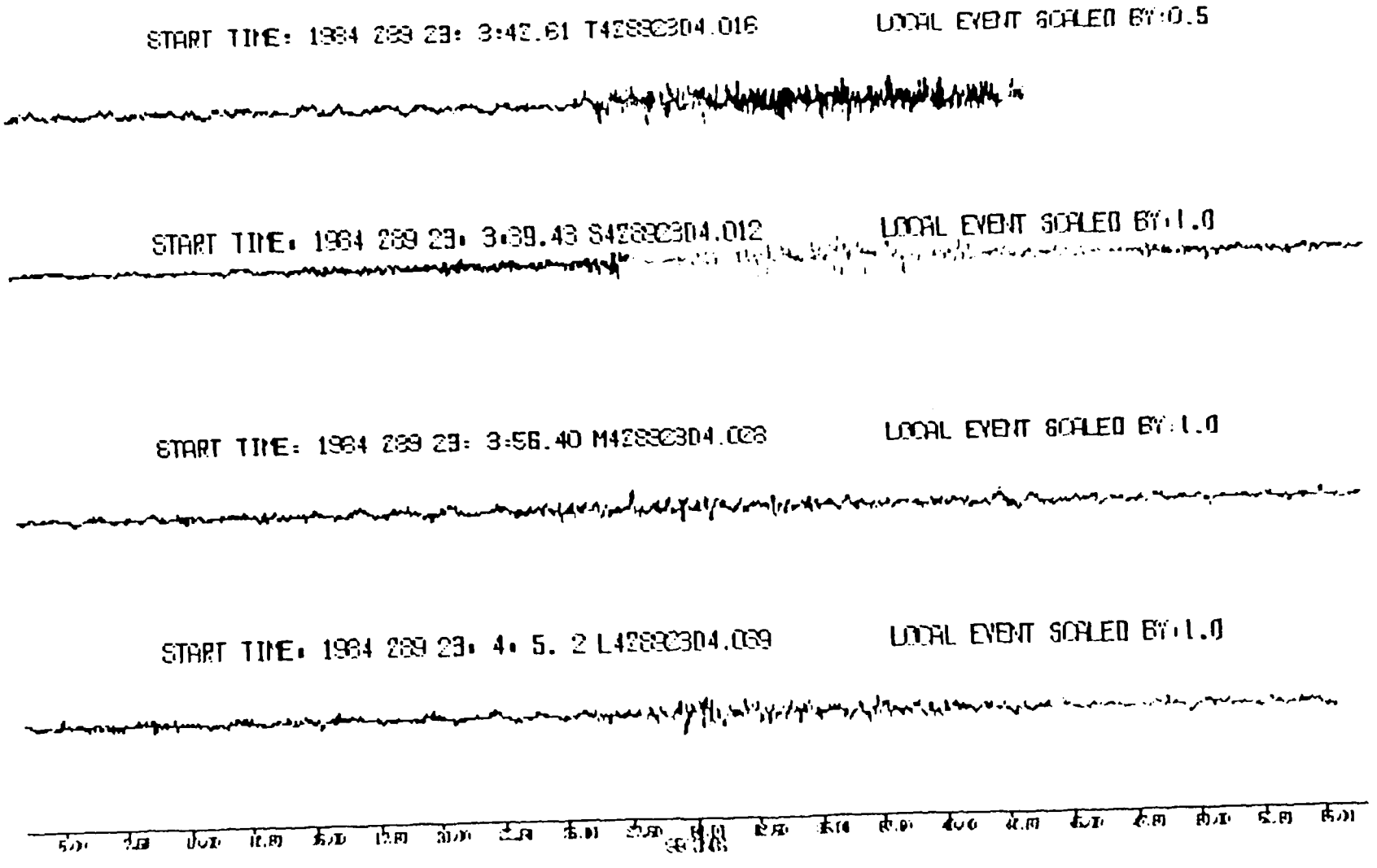

Figure 12. Observations for a Local Event, Recorded at the Four Stations, Lajitas, Marathon, Shafter and Tres Cuevas, are Combined into a Finite Number of Segments Using the Nearest Neighbor Decision Rule and Affinity Techniques.

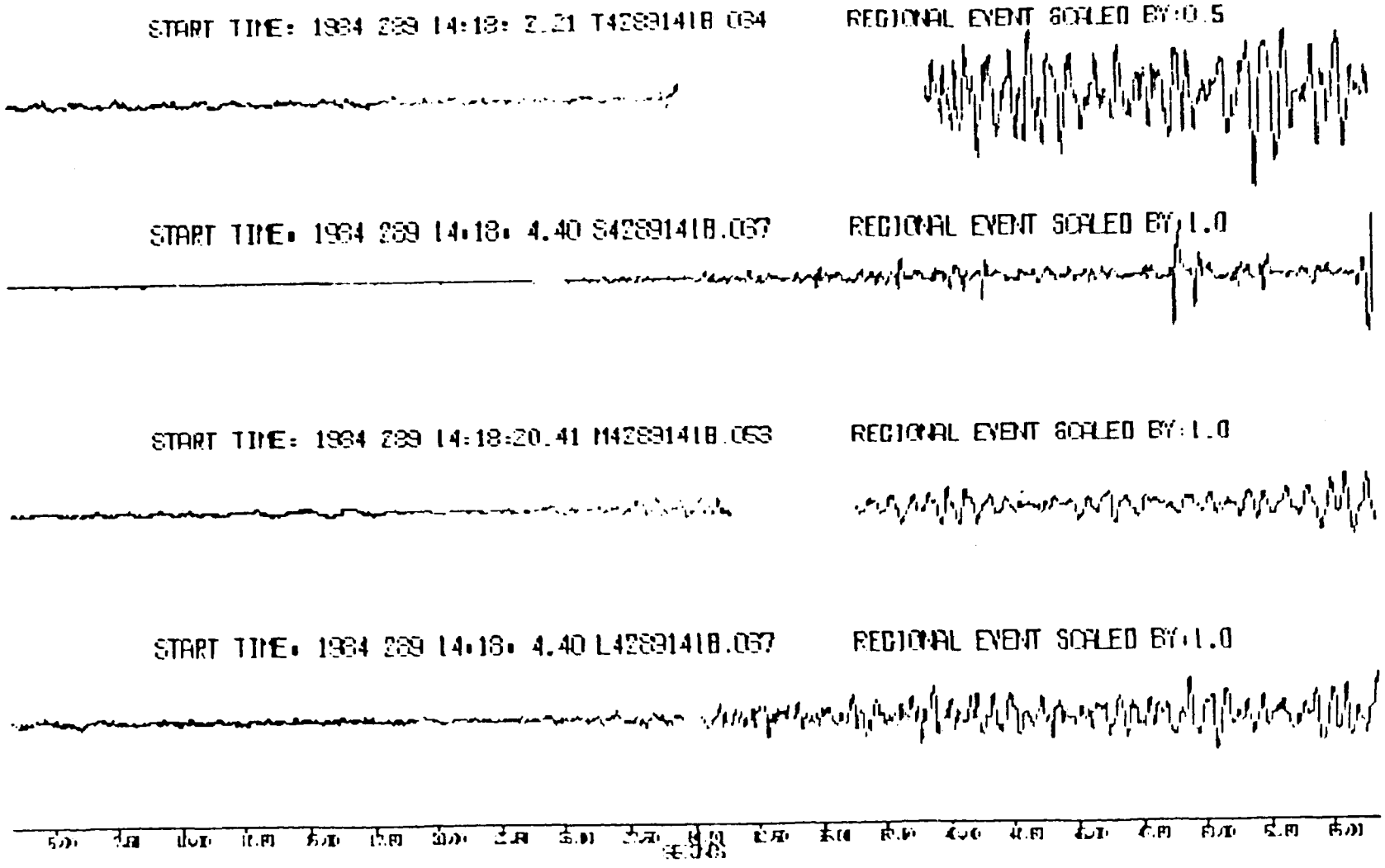

Figure 13. Observations for a Regional Event, Recorded at the Four Stations, Lajitas, Marathon, Shafter and Tres Cuevas, are Combined into a Finite Number of Segments Using the Nearest Neighbor Decision Rule and Affinity Techniques.

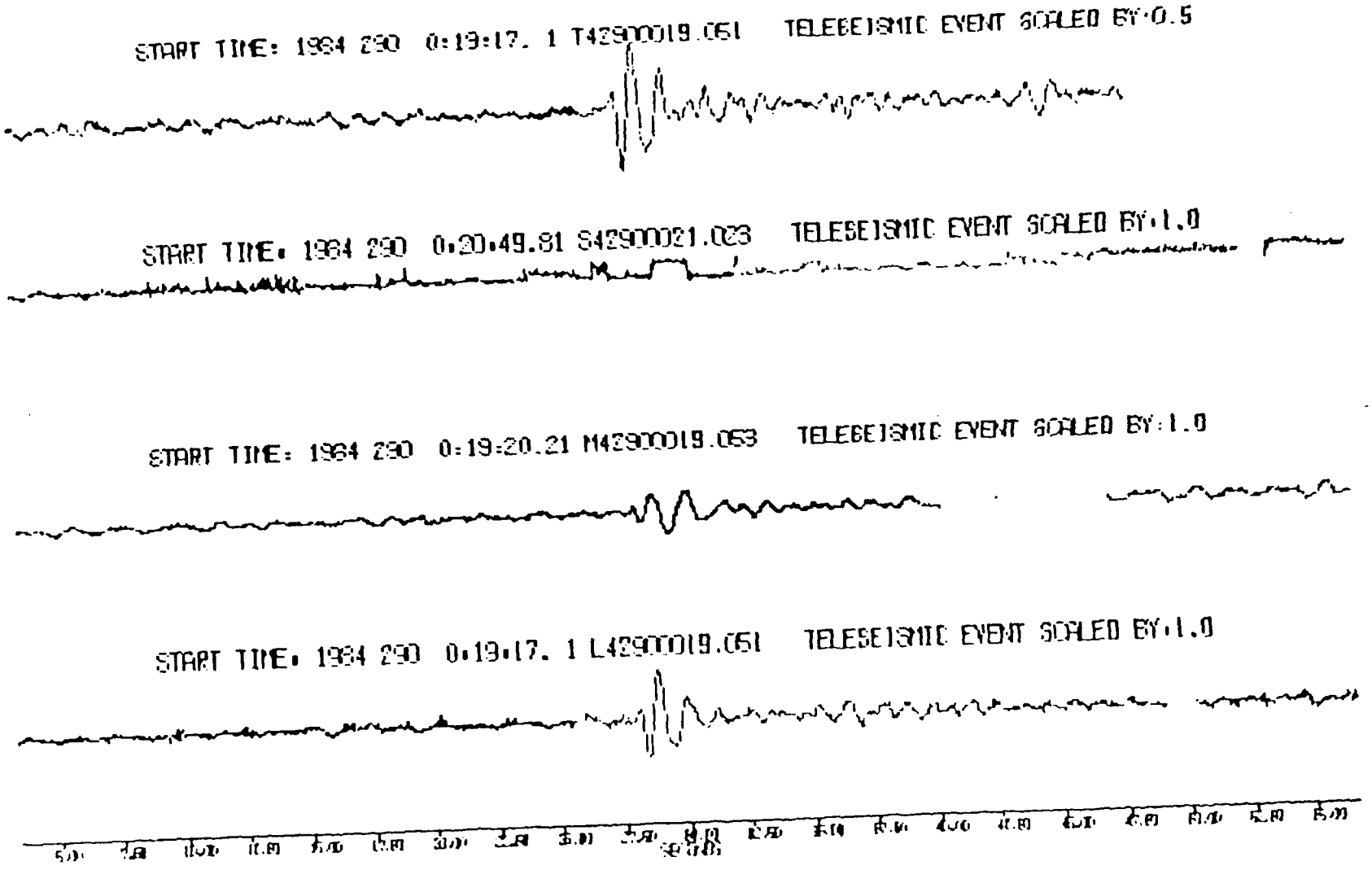

Figure 14. Observations for a Teleseismic Event, Recorded at the Four Stations, Lajitas, Marathon, Shafter and Tres Cuevas, are Combined into a Finite Number of Segments Using the Nearest Neighbor Decision Rule and Affinity Techniques.

local, regional and teleseismic. The colors represent different segments. No clear pattern was identified in the segmentation to make this a useful method for distinguishing signal from noise.

Both the threshold detection and segmentation methods made the assumption that the noise was Gaussian and stationary when the mean and the variance were estimated. Since this is untrue, the noise could not be effectively characterized by the estimated mean and variance and overlap occured between the boundaries defining the signal and noise classes. The subroutine, "NEIGHBOR", listed in appendix B uses the nearest neighbor rule and affinity techniques to combine the segments.

Using Rank Quartiles to Identify Features

The next attempt to characterize the signal and noise categories was to rank the amplitudes and periods, estimated by the distance between zero crossings, of the event trace. Then the ranks were divided into quartiles and color coded on the event trace so any patterns in the features associated with the signal or noise might be identified. Table 3 illustrates the color code used in figures 15 through 19 to identify which rank quartile an observation belongs.

This technique showed a clear pattern for ranked amplitudes of events with large S/N ratios but was

TABLE 3

State Table for Color Changes Used to Graphically Depict the Rank Quartiles

PERIOD RANK QUARTILES	AMPLITUDE RANK QUARTILES: 1st	2nd	3rd	4th
1st	1	2	3	4
2nd	5	6	7	8
3rd	9	10	11	12
4th	13	14	15	8

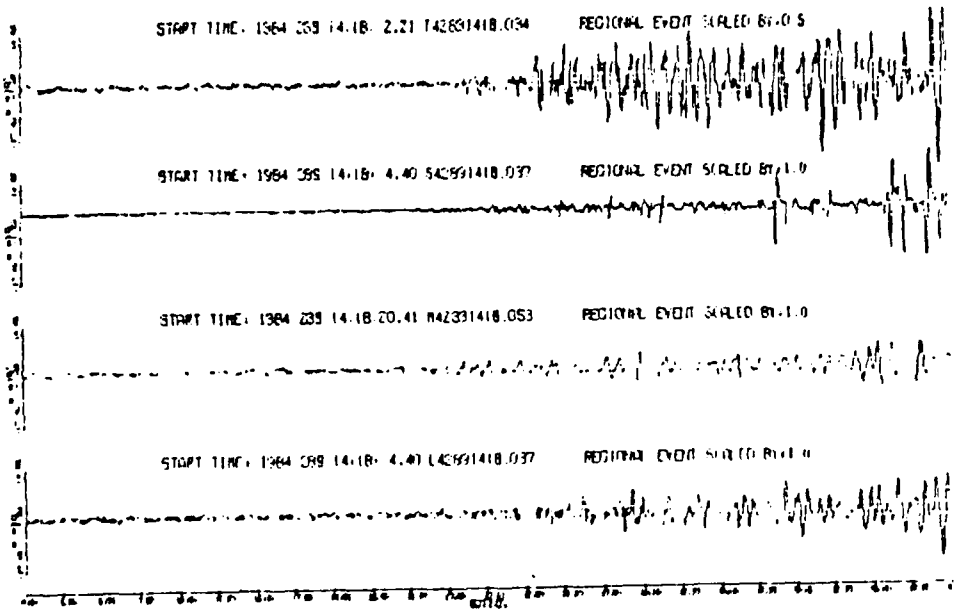

Figure 15.b

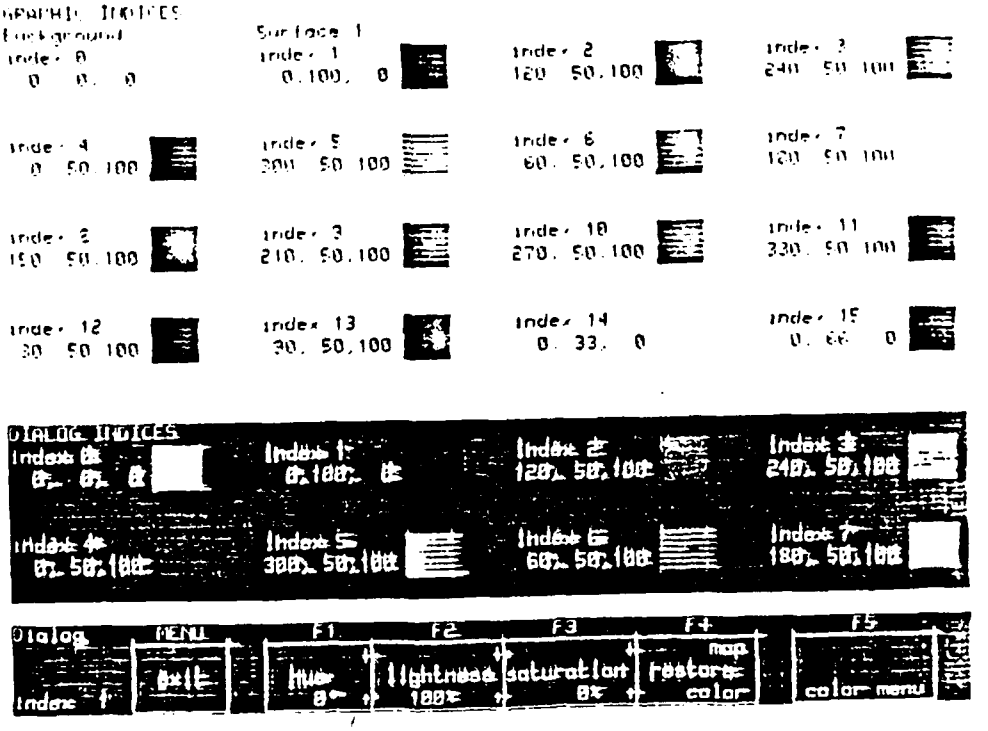

Figure 15.a

Figure 15. The Ranks of Amplitudes and Periods are Divided into Rank Quartiles. The Color Changes in the Event Traces, Recorded at the Stations Lajitas, Marathon, Shafter and Tres Cuevas, Bottom to Top Respectively, Graphically Depict any Patterns that Exist in the Features. (a) The Color Index Corresponding to the 16 Rank Quartiles the Ranks of the Periods and Amplitudes of Each Trace are Divided into as Shown in Table 3. (b) Shows the Rank Quartile Pattern for a Regional Event.

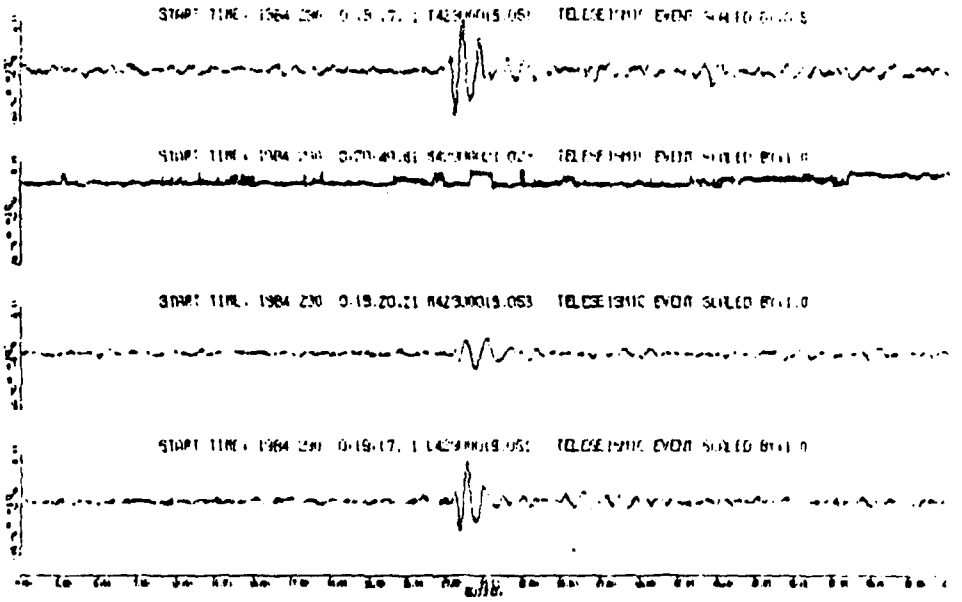

Figure 16.b

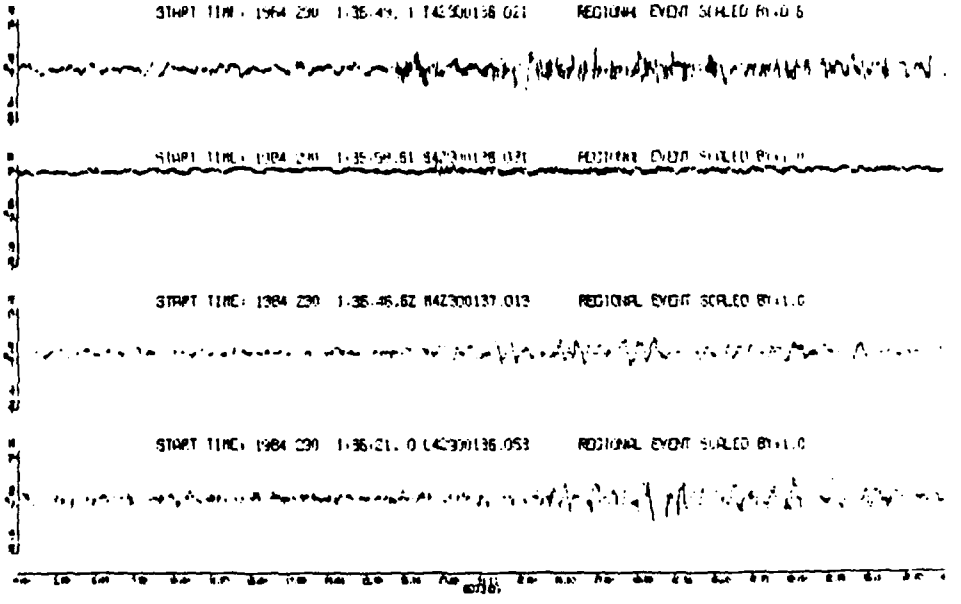

Figure 16.a

Figure 16. The Ranks of Amplitudes and Periods are Divided into Rank Quartiles. The Color Changes in the Event Traces, Recorded at the Stations Lajitas, Marathon, Shafter and Tres Cuevas, Bottom to Top Respectively, Graphically Depict any Patterns that Exist in the Features. (a) Illustrates the Rank Quartile Pattern for a Regional Event. (b) Illustrates the Rank Quartile Pattern for a Regional Event.

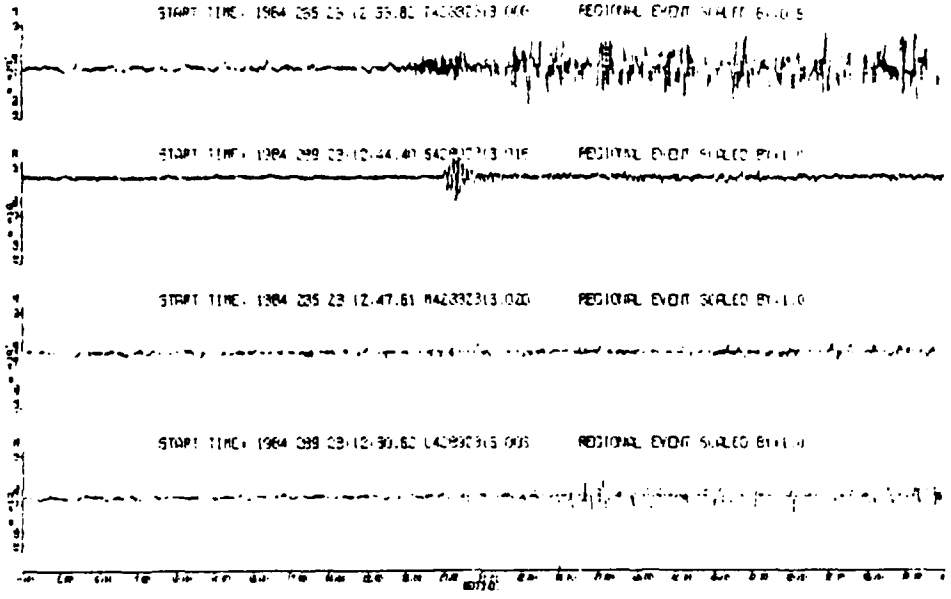

Figure 17.b

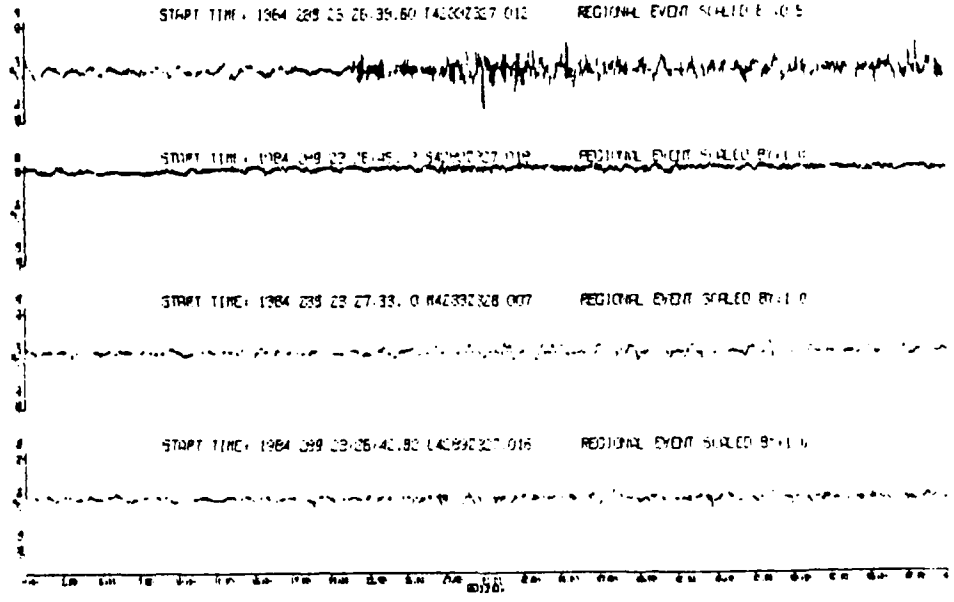

Figure 17.a

Figure 17. The Ranks of Amplitudes and Periods are Divided into Rank Quartiles. The Color Changes in the Event Traces, Recorded at the Stations Lajitas, Marathon, Shafter and Tres Cuevas, Bottom to Top Respectively, Graphically Depict any Patterns that Exist in the Features. (a) Illustrates the Rank Quartile Pattern for a Regional Event. (b) Illustrates the Rank Quartile Pattern for a Regional Event.

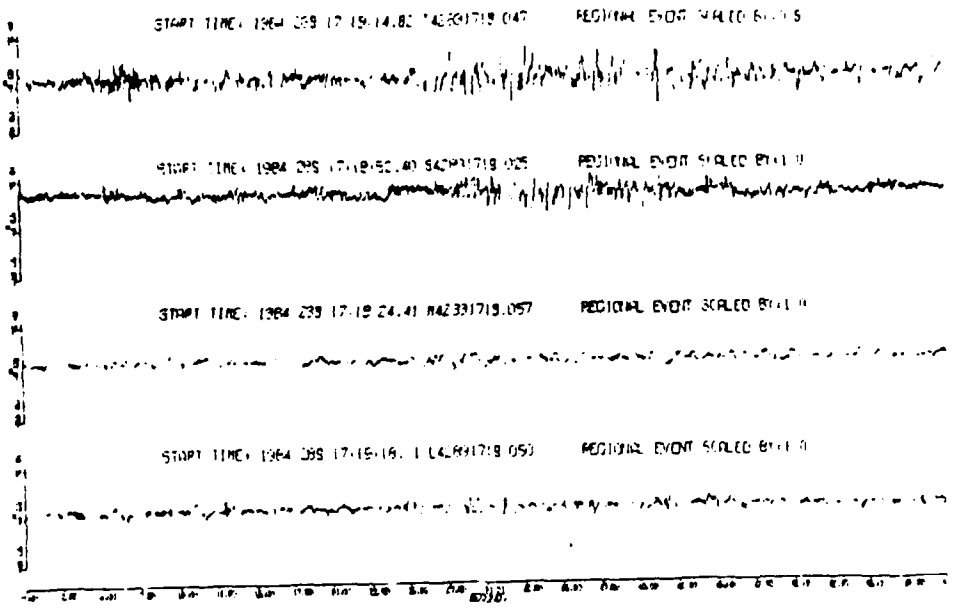

Figure 18.b

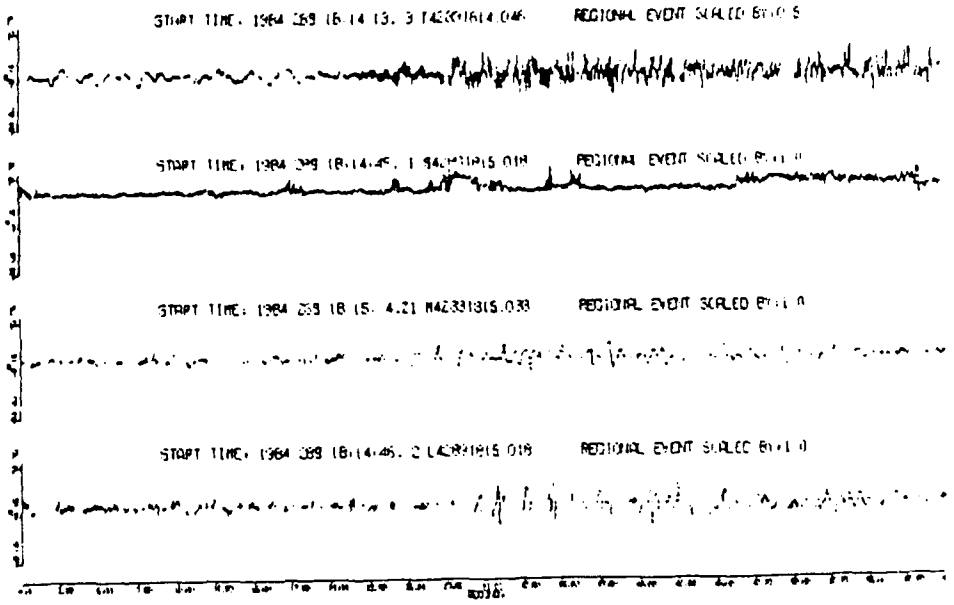

Figure 18.a

Figure 18. The Ranks of Amplitudes and Periods are Divided into Rank Quartiles. The Color Changes in the Event Traces, Recorded at the Stations Lajitas, Marathon, Shafter and Tres Cuevas, Bottom to Top Respectively, Graphically Depict any Patterns that Exist in the Features. (a) Illustrates the Rank Quartile Pattern for a Regional Event. (b) Illustrates the Rank Quartile Pattern for a Regional Event.

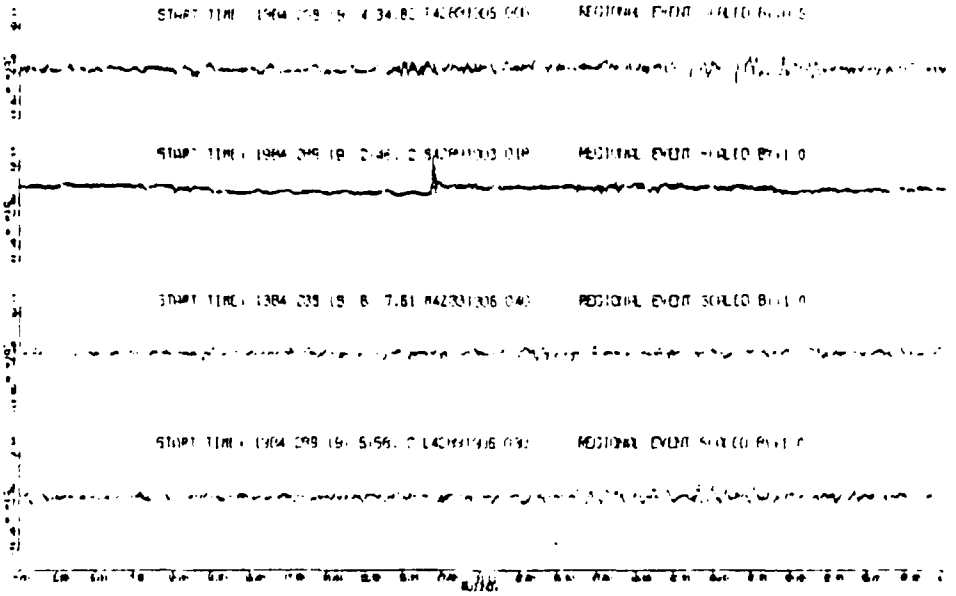

Figure 19.b

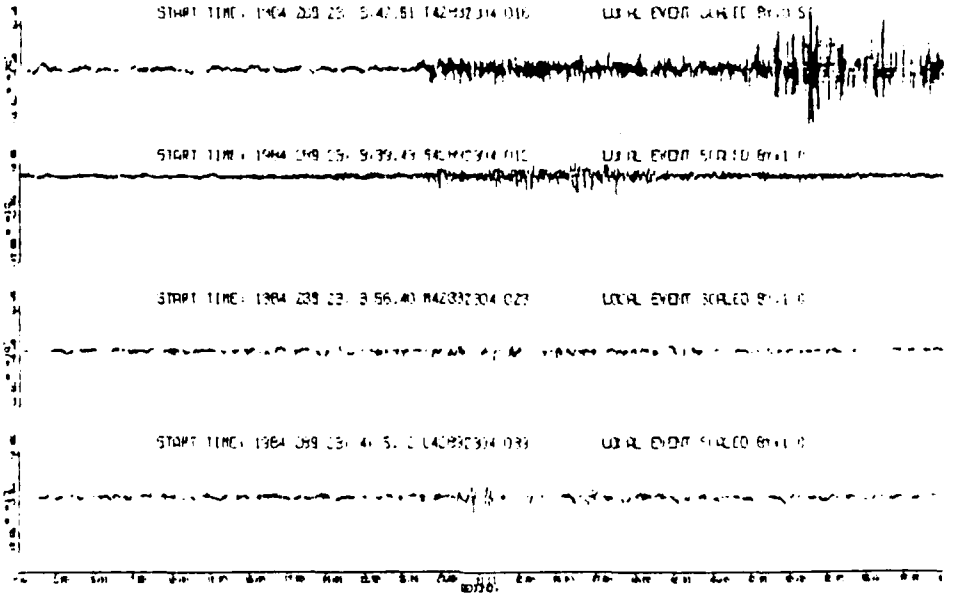

Figure 19.a

Figure 19. The Ranks of Amplitudes and Periods are Divided into Rank Quartiles. The Color Changes in the Event Traces, Recorded at the Stations Lajitas, Marathon, Shafter and Tres Cuevas, Bottom to Top Respectively, Graphically Depict any Patterns that Exist in the Features. (a) Illustrates the Rank Quartile Pattern for a Local Event. (b) Illustrates the Rank Quartile Pattern for a Regional Event.

ambiguous for signals buried in noise. The rank pattern for estimated periods showed no strong pattern for distinguishing signal from noise. However, the ranks for the amplitude and estimated periods, which were added together and divided into quartiles, was the the best indicator of a clear pattern in the features to be used to discriminate signal and noise. This is reasonable since the criteria the human analyst uses to distinguish signal from noise especially in ambiguous cases with low signal to noise ratios is based on changes in both period and amplitude from the preceding background. Slope is sensitive to changes in both amplitude and period which makes it the most favorable feature to use in creating an automatic first arrival detection algorithm.

Conclusions

Since parametric techniques appear to allow too much overlap in the classifications to clearly distinguish signal from noise, a non-parametric technique using the slope of the event trace appears to describe the detection method with the best chance of discriminating background noise from a broad class of seismic event signals.

The feature with the least amount of overlap between background noise and seismic event signals, "modified" slope, was calculated through discrete integration of the event trace slope over segments with the same slope

direction. Figure 20 demonstrates this calculation. Various period estimations of the background noise were too similar to one or more of the local, regional or teleseismic signal classes for effective discrimination between signal and noise. Amplitude was a good discriminator when the S/N ratio was high. However, the detectors failed to trigger on the first arrival for events with low S/N ratios. Both the slope and "modified" slope of the event trace are characterized by a constant mean equal to zero and a variance which changes with time. This makes the "modified" slope of the event trace a more attractive feature for distinguishing between signal and noise than the unmodified event trace whose mean and variance both change with time.

DATA = A(I), SLOPE = S(I), "MODIFIED" SLOPE = $\hat{S}$(I)

SLOPE CALCULATION

$$S(I) = \frac{[A(I) - A(I-1)] + [A(I+1) - A(I)]}{2}$$

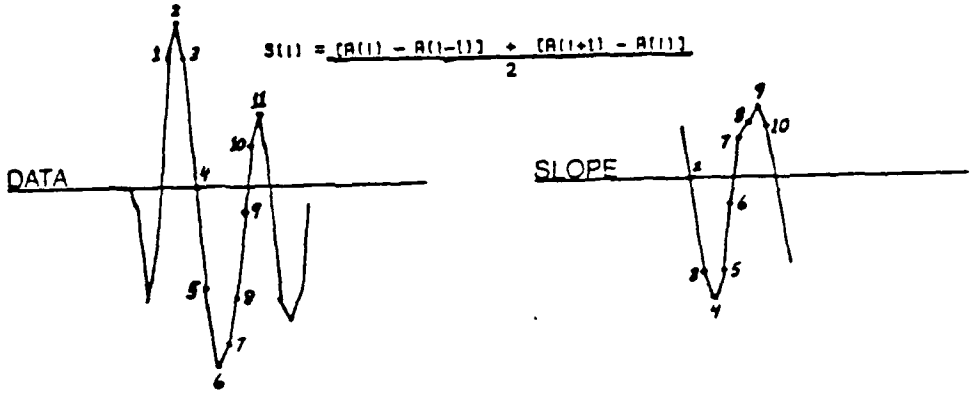

DATA	SLOPE	"MODIFIED" SLOPE
A(1) = 4.	-	-
A(2) = 6.	S(2) = 0.	$\hat{S}$(2) = 0.
A(3) = 4.	S(3) = -3.	$\hat{S}$(3) = -3.
A(4) = 0.	S(4) = -3.75	$\hat{S}$(4) = -6.75
A(5) = -3.5	S(5) = -3.	$\hat{S}$(5) = -8.75
A(6) = -6.	S(6) = -8.75	$\hat{S}$(6) = -18.5
A(7) = -5.	S(7) = 1.25	$\hat{S}$(7) = 1.25
A(8) = -3.5	S(8) = 1.75	$\hat{S}$(8) = 3.
A(9) = -1.5	S(9) = 2.25	$\hat{S}$(9) = 5.25
A(10) = 1.	S(10) = 1.75	$\hat{S}$(10) = 7.
A(11) = 2.	-	-

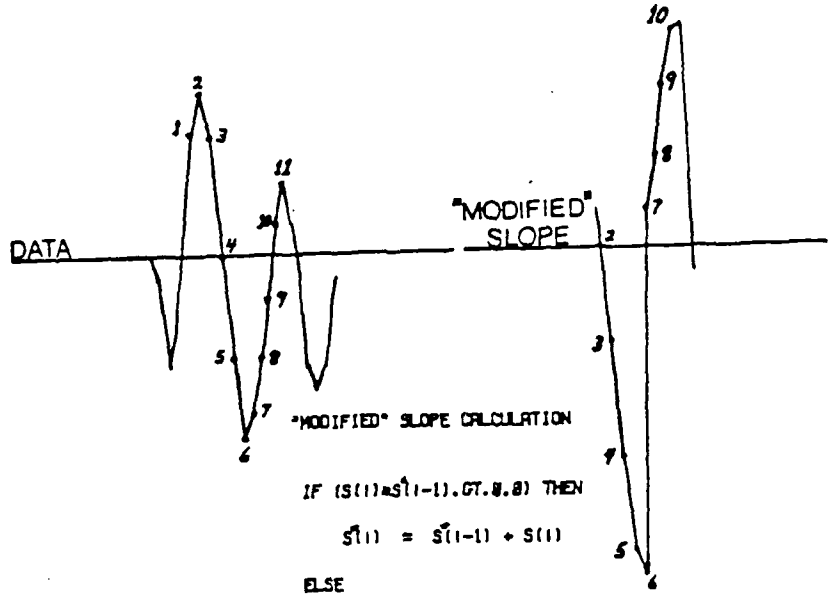

"MODIFIED" SLOPE CALCULATION

```
IF (S(I)≥Ŝ(I-1).GT.0.0) THEN
    Ŝ(I) = Ŝ(I-1) + S(I)
ELSE
    Ŝ(I) = S(I)
END IF
```

Figure 20. Examples to Graphically Illustrate the Slope and "Modified" Slope Calculations for the Slope and "Modified" Slope Features used to Distinguish Event Signals from Background Noise.

DETECTORS

AR-Spectral Estimation Used to Develop a Synthetic Waveform

Assumptions

The autoregressive (AR) model is correct for modeling minimum phase stationary processes. To estimate the spectral density function we must assume that we can obtain an "adequate approximation" by using a finite order AR model (Priestley, 1981). The development of a synthetic waveform to pick out the first arrival phase in an event trace from the autoregressive spectral estimate of that same event trace requires several assumptions. First, in order to use this technique, we must assume the first arrival phase of the seismic signal generated by an earthquake or explosion is minimum phase. Second we assume the corner frequency, or dominate period, of the seismic signal has the same period as the first arrival phase. Third we assume that the background noise does not contain an obvious corner frequency. Forth we assume the seismic signal is stationary or at least can be estimated by a process that assumes the driving function is white noise. Seismic signals contaminated by noise are nonstationary processes with unknown distributions. Hannu

Niemi, (1983), studied the effects of nonstationary noise on ARMA models and concluded that the prediction formulas applied in the stationary case were also valid in the nonstationary case provided the underlying density distribution of the nonstationary process was symmetric. Discrete density distributions for 400 seismic signals and their associated background noise were plotted and in all cases the density distributions were symmetric. This allows us to conclude that an AR model is appropriate for estimating the spectra of the event trace given our initial assumptions.

Description of Method

The first step in developing a synthetic waveform was to compute the coefficients for an eighth order AR model using the Burg algorithm. See appendix B for the subroutines, "Polr_ArBURG" and "AR_SPECTRA", to compute the Burg coefficients and the AR-spectra. Coefficients were computed for the first 800 samples of the event file representing the background noise and the next 800 samples of the event file thought to contain the first arrival phase. Then the AR(8) spectra, $\hat{p}(f)$, was computed for both the signal and the noise and plotted (Priestley, 1981).

$$\hat{p}(f) = \frac{2\hat{\sigma}^2}{\left|1 - \hat{\theta}_1 e^{-i2\pi f} - \ldots - \hat{\theta}_8 e^{-i16\pi f}\right|^2}$$

$(\hat{\theta}_1 \ldots \hat{\theta}_8)$ = AR(8) coefficients

$\hat{\sigma}^2$ = variance of the white noise

f = frequency Hz

To determine the shape of the synthetic waveform's AR power spectral density we employ the doctrine of parsimony. The minimum number of poles needed to describe the spectral shape with the information we have available is three. The poles are located at the low cut-off, high cut-off and corner frequencies of the signal bandwidth. The corner frequency is assumed to be the frequency with the signal spectra's peak amplitude. The low and high frequency cut-offs define the signal spectra interval where the signal spectra is consistently above the noise spectra. The amplitude of the low frequency cut-off is determined by the roll-off below the corner frequency due to the sensivity of the recording instrument, approximately 6dB per octave for the Lajitas station instrument. The amplitude of the high frequency cut-off is determined by the roll-off above the corner frequency due to attenuation. The expected roll-off is -3dB to -4dB per octave. Figure 21 illustrates the proposed method.

The coefficients of the synthetic AR(p) model are derived from the synthetic AR power spectral density,

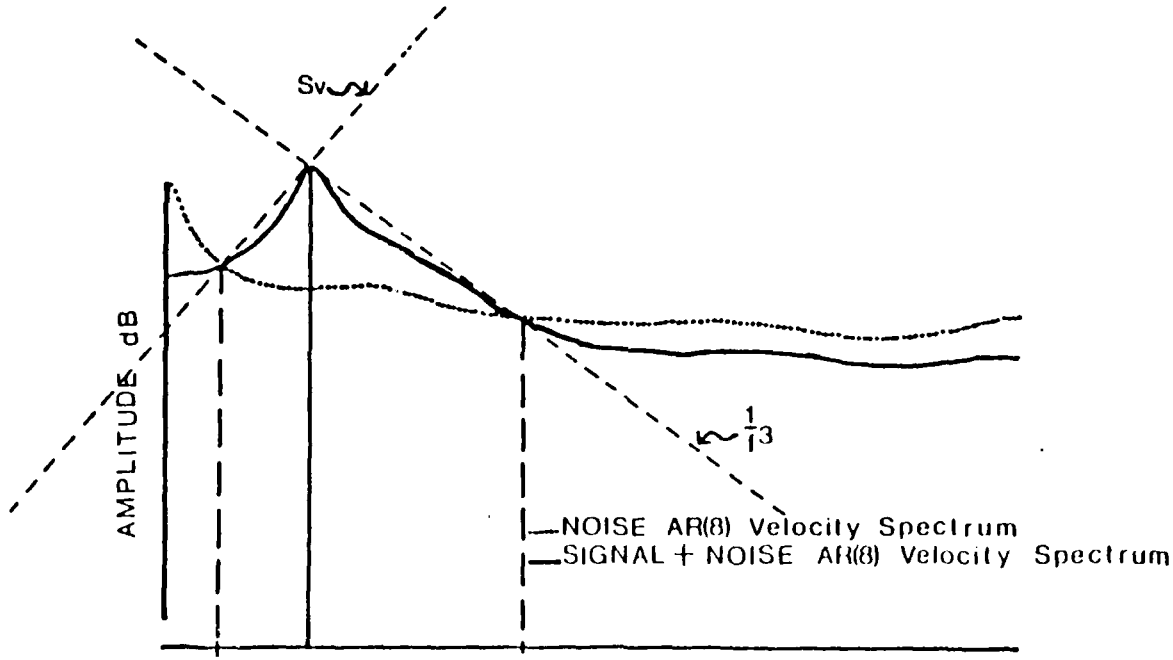

Figure 21. Proposed AR-Spectral Method for Creating the Spectrum for a Synthetic Waveform. *Sv* Denotes the Sensitivity of the Recording Instrument. $1/f^3$ Denotes the Roll-off with Frequency Due to Attenuation.

$\hat{p}(f)$, described in the preceding paragraph. The AR theoretical power spectral density, $p(f)$, is defined by

$$p(f) = \left| S(f) \right|^2$$

where

$$\left| S(f) \right|^2 = S(f)S^*(f)$$

and

$$S(f) = \frac{\sqrt{2\sigma}}{\left[1 - \theta_1 e^{-i2\pi f} - \cdots - \theta_p e^{-i2\pi fp}\right]}$$

Now by making use of the fact that the theoretical power spectral density, $p(f)$, can also be written in terms of the autocovariance, $R(k)$,

$$p(f) = \int_{-\infty}^{\infty} e^{-i2\pi fk} R(k)dk$$

we can obtain the autocovariance, $R(k)$, of the synthetic AR model by taking the inverse fast fourier transform (IFFT) of the synthetic AR power spectral density, $p(f)$.

$$p(f) = \int_{-\infty}^{\infty} e^{-i2\pi fk} R(k)dk \xleftrightarrow{\text{IFFT}} \int_{-\infty}^{\infty} x(k)x(k-t)dt = R(k)$$

Then the autocovariance, $R(k)$, of the synthetic process, $x(t)$, is used by the Yule-Walker algorithm (Kay and Marple, 1981), (see subroutine "AKAIKE" in appendix B), to obtain the AR(p) coefficients for an AR model of order p (determined by Akaike's information criteria ,AIC, Priestley, 1981). This synthetic AR(p) model is then convolved with a spike plus white noise to create the synthetic waveform. The synthetic waveform is then cross-correlated with the event trace to try and pick out the first arrival phase.

Effectiveness of Method and Conclusions

The method hypothesized above started to break down with the assumptions that the first arrival phase has the same period as the corner frequency and the background noise had no obvious corner frequency. The period estimated by the analyst for the first arrival phase of the Lajitas event traces only correlated well with the corner frequencies of the corresponding AR(8) spectral estimates in 25% of the events studied; i.e., teleseismic events with a high signal to noise (S/N) ratio.

Often a corner appeared in the background noise making it difficult to determine the correct spectral bandwidth for the signal automatically. For the above reasons this method for identifying the first arrival phase for a broad category of seismic events was abandoned in favor of a more robust non-parametric technique, the rank sum detector. Representative examples of the AR(8) spectral estimations for several of the events studied are shown in figures 22 through 26 with the analyst's estimations of the dominate periods for the noise and the first arrival phase marked for the Lajitas seismic events.

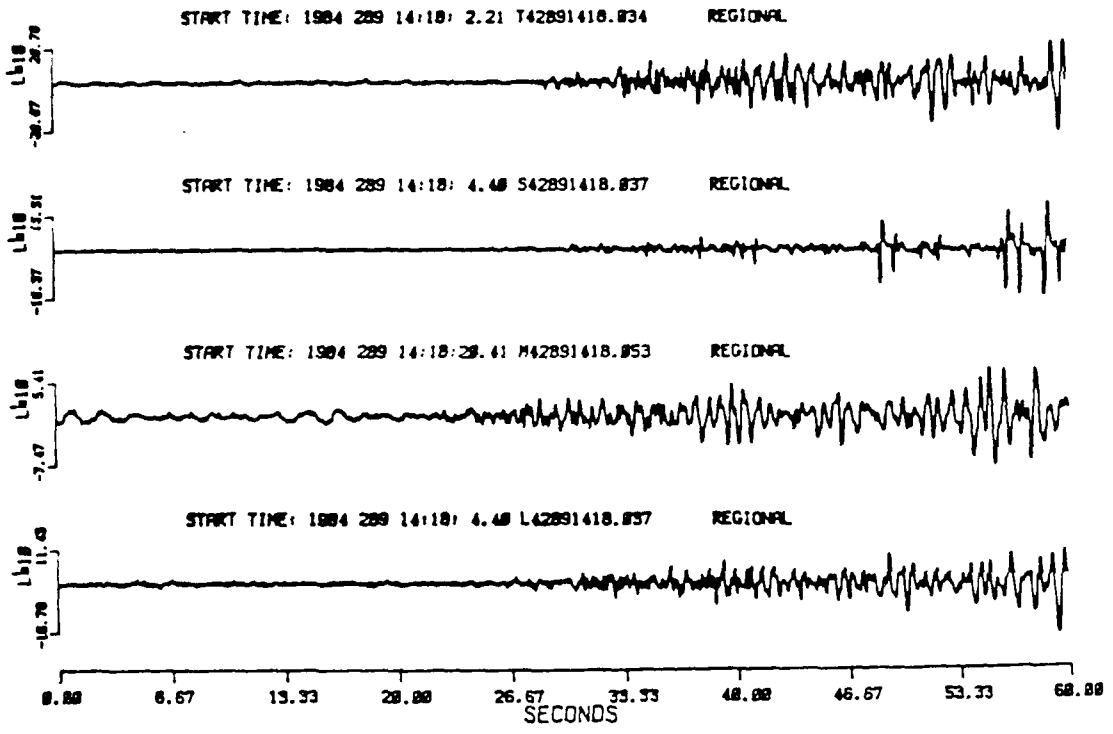

Figure 22.a

Figure 22. AR(8)-Spectral Estimates for the Signal and Noise for Event 1. (a) Event traces recorded at each of the four stations, Lajitas, Marathon, Shafter and Tres Cuevas, for Event 1. (b) Lajitas AR(8)-Spectral Estimates. The Analyst Estimates for the Dominate Period of the Noise and the First Arrival Phase are Indicated with Dashed Lines Drawn to their Respective Spectral Estimates. (c) Marathon AR(8)-Spectral Estimates. (d) Shafter AR(8) Spectral Estimates. (e) Tres Cuevas AR(8) Spectral Estimates.

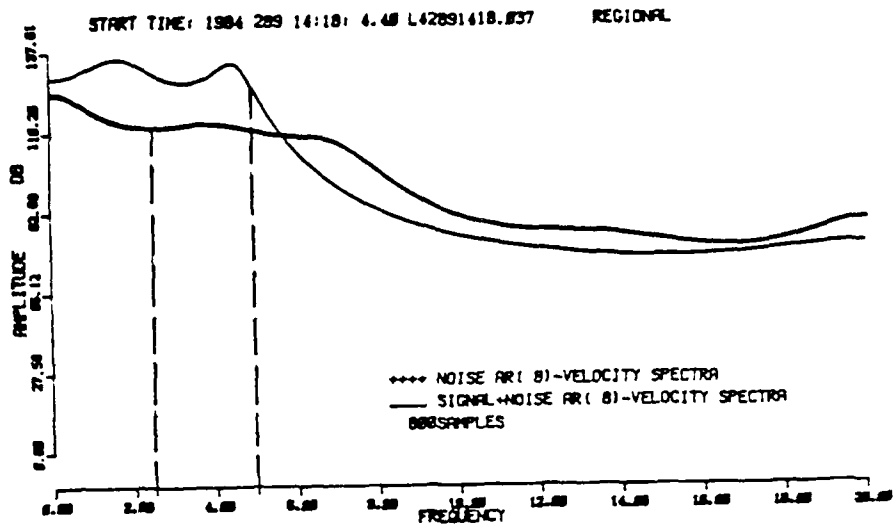

Figure 22.b

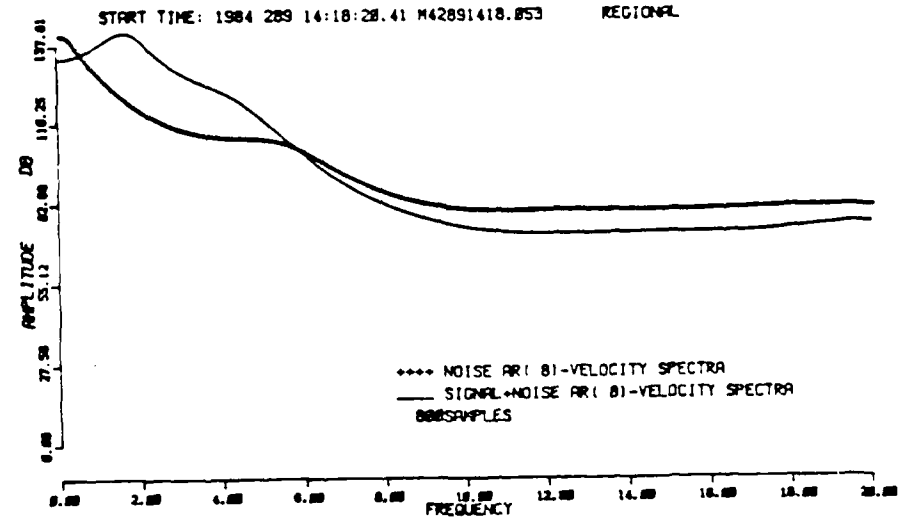

Figure 22.c

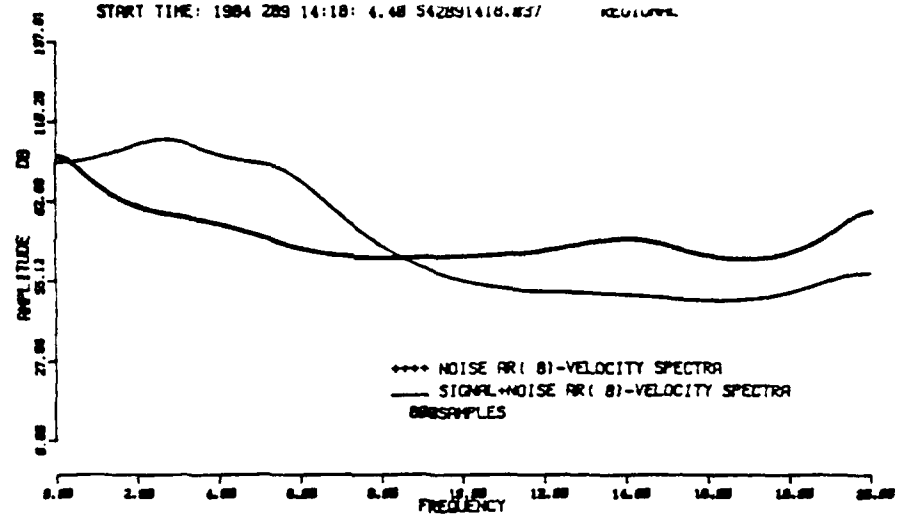

Figure 22.d

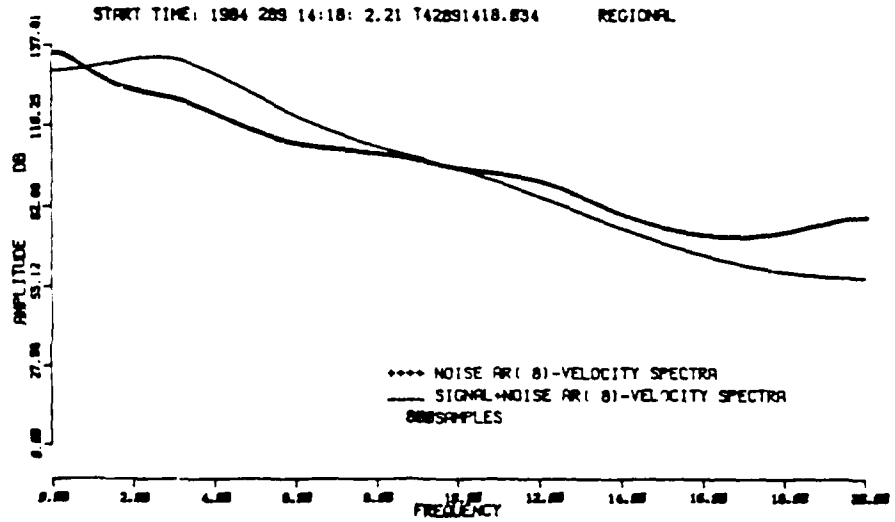

Figure 22.e

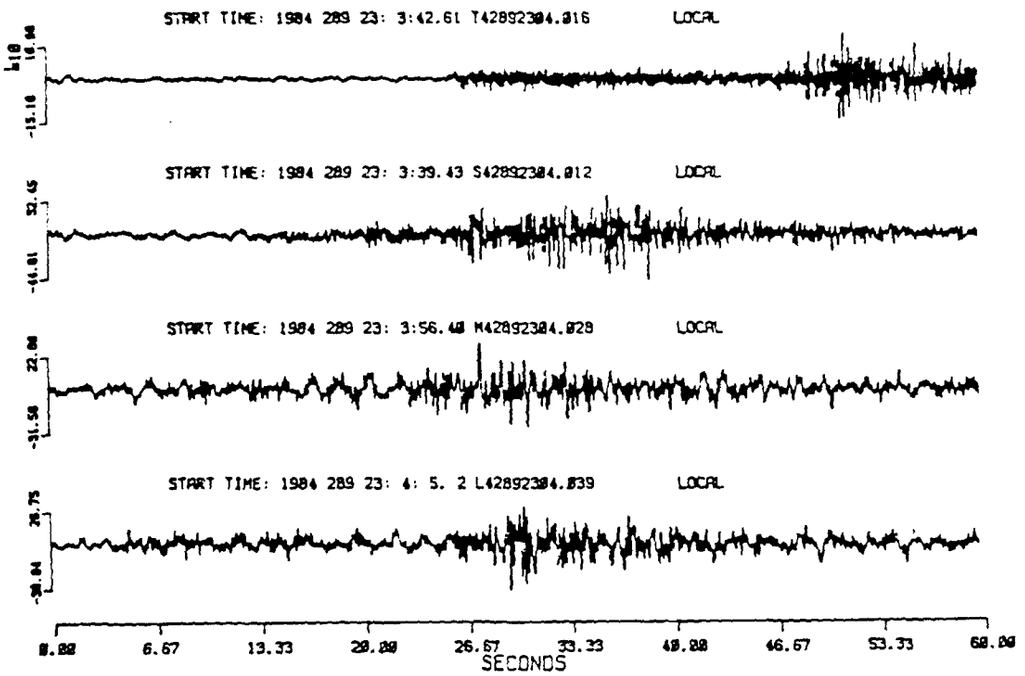

Figure 23.a

Figure 23. AR(8)-Spectral Estimates for the Signal and Noise for Event 5 are Normalized by the Variance of the Noise. (a) Event Traces Recorded at Each of the Four Stations, Lajitas, Marathon, Shafter and Tres Cuevas, for Event 5. (b) Lajitas AR(8)-Spectral Estimates. The Analyst Estimates for the Dominate Period of the Noise and the First Arrival Phase are Indicated with Dashed Lines Drawn to their Respective Spectral Estimates. (c) Marathon AR(8)-Spectral Estimates. (d) Shafter AR(8) Spectral Estimates. (e) Tres Cuevas AR(8) Spectral Estimates.

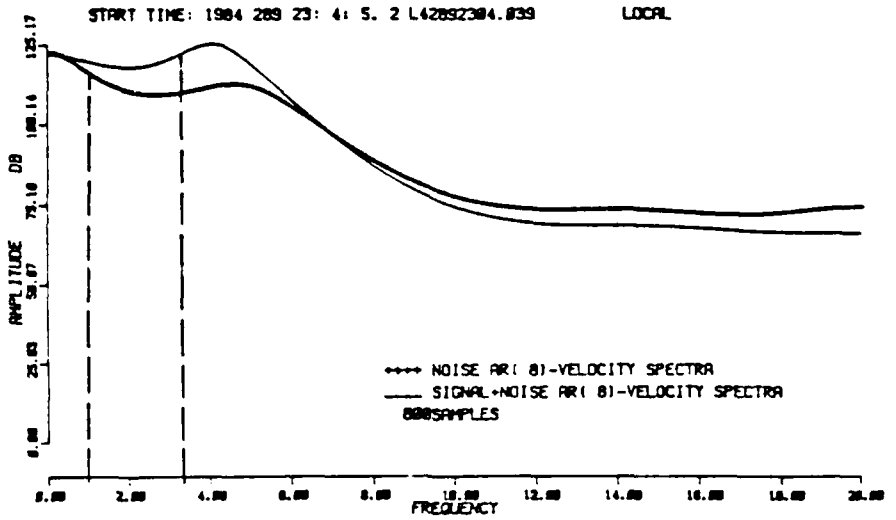

Figure 23.b

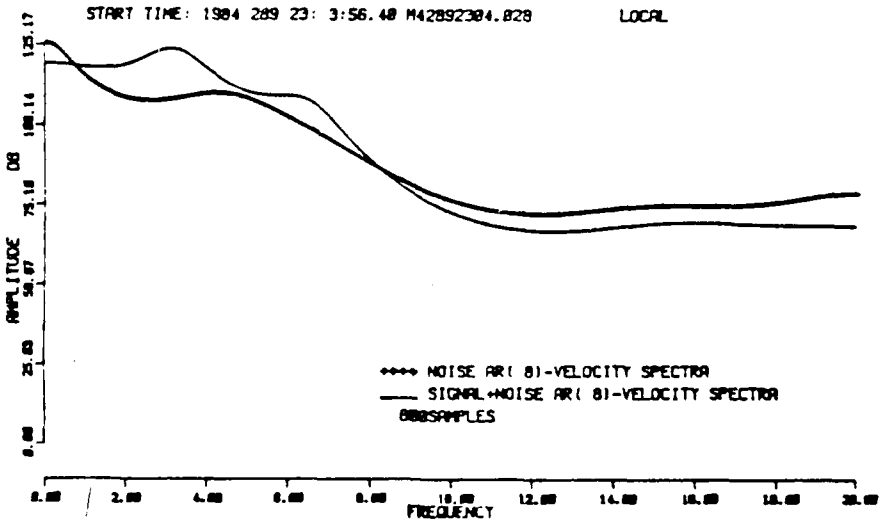

Figure 23.c

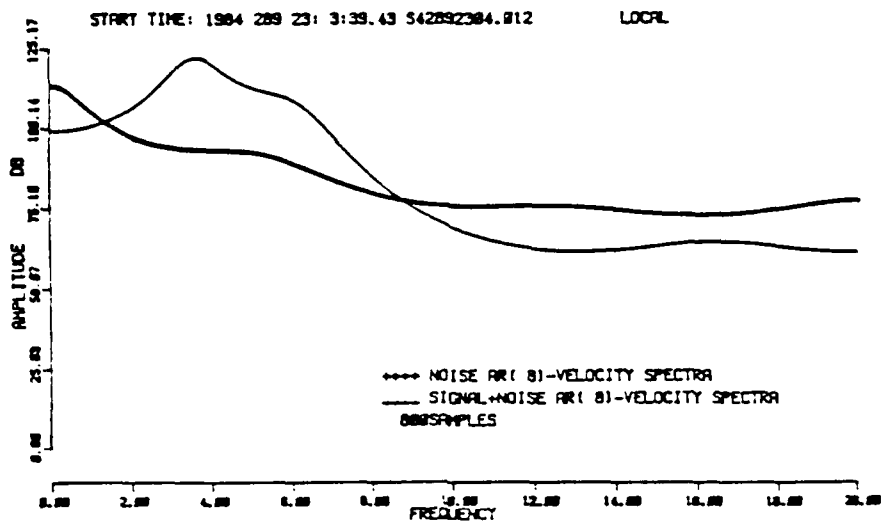

Figure 23.d

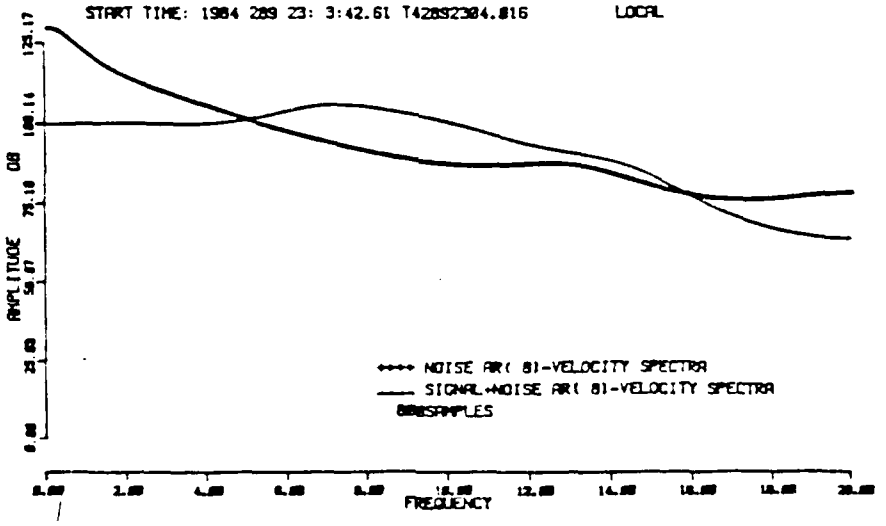

Figure 23.e

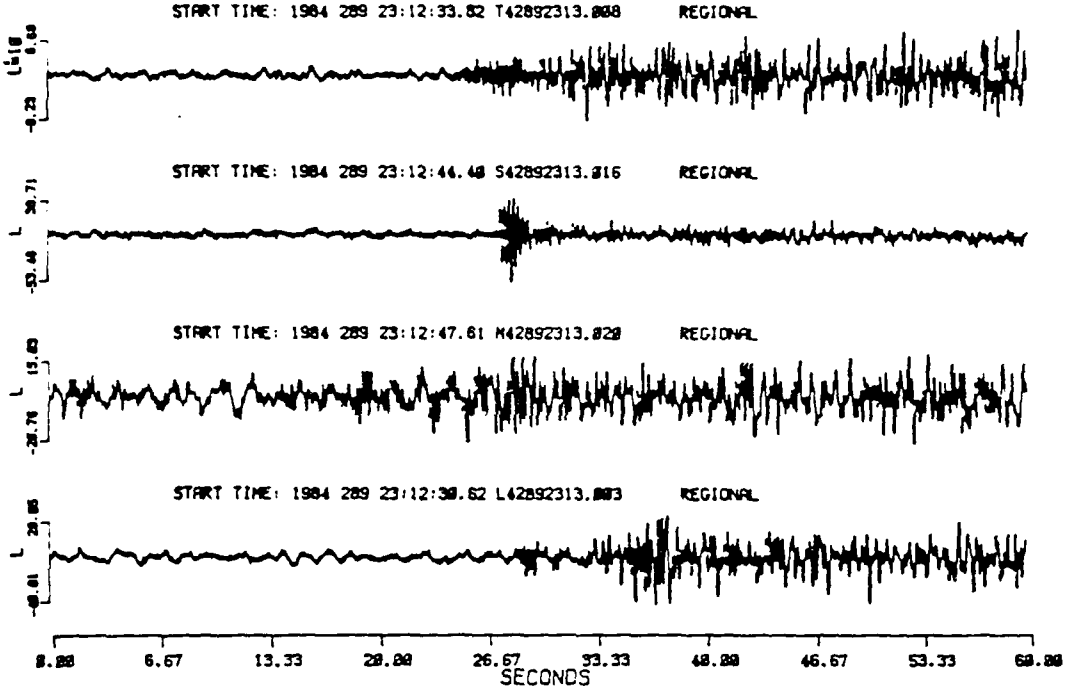

Figure 24.a

Figure 24. AR(8)-Spectral Estimates for the Signa_ and Noise for Event 6 are Normalized by the Variance of the Noise. (a) Event Traces Recorded at Each of the Four Stations, Lajitas, Marathon, Shafter and Tres Cuevas, for Event 6. (b) Lajitas AR(8)-Spectral Estimates. The Analyst Estimates for the Dominate Period of the Noise and the First Arrival Phase are Indicated with Dashed Lines Drawn to their Respective Spectral Estimates. (c) Marathon AR(8)-Spectral Estimates. (d) Shafter AR(8) Spectral Estimates. (e) Tres Cuevas AR(8) Spectral Estimates.

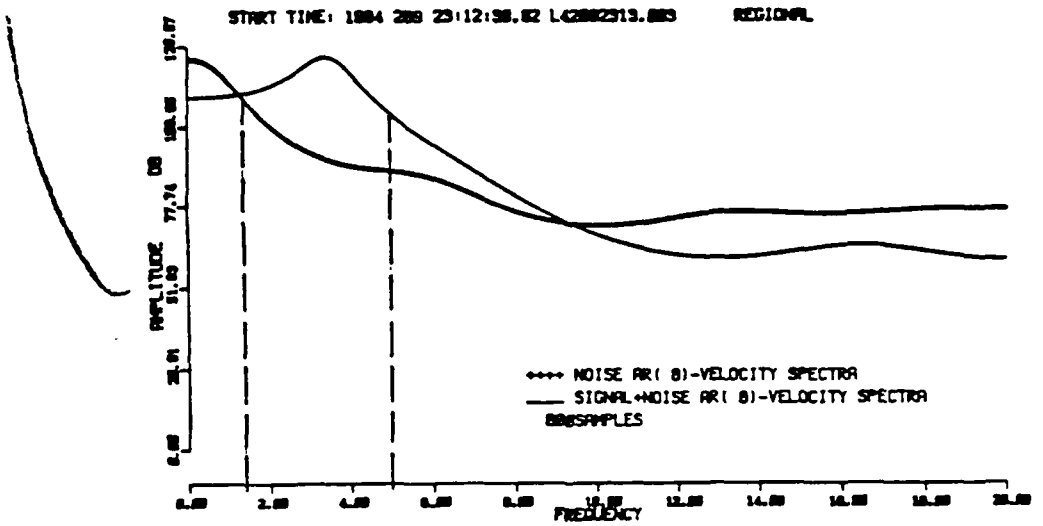

Figure 24.b

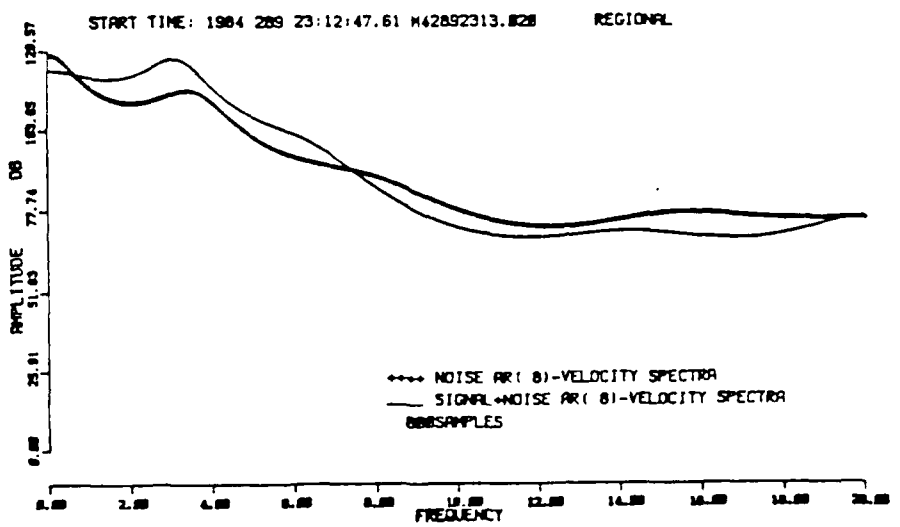

Figure 24.c

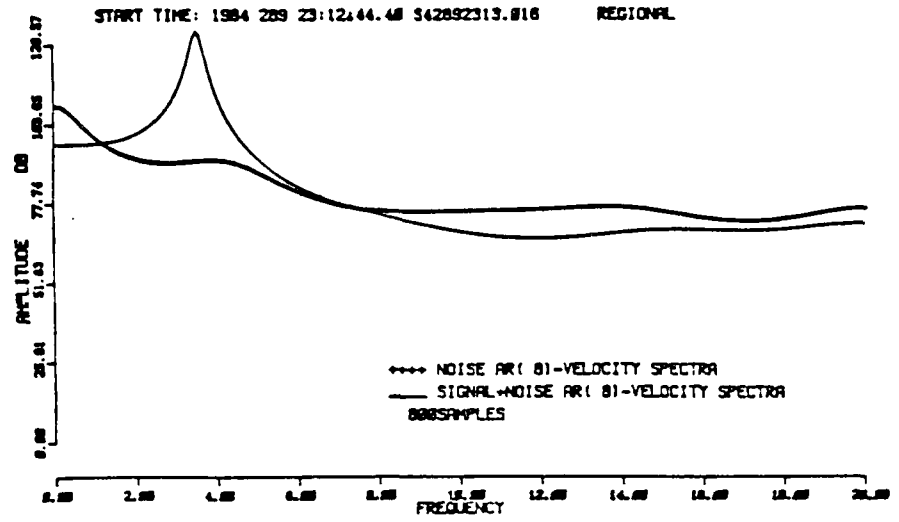

Figure 24.d

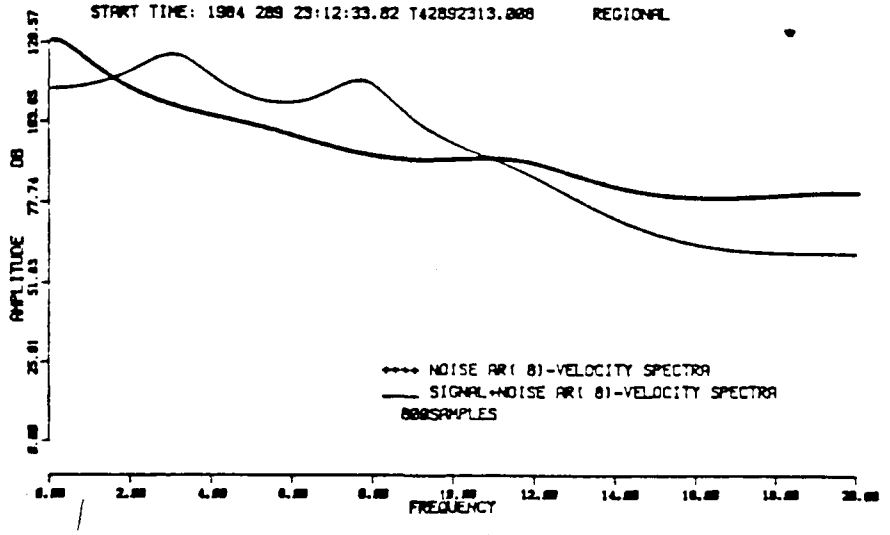

Figure 24.e

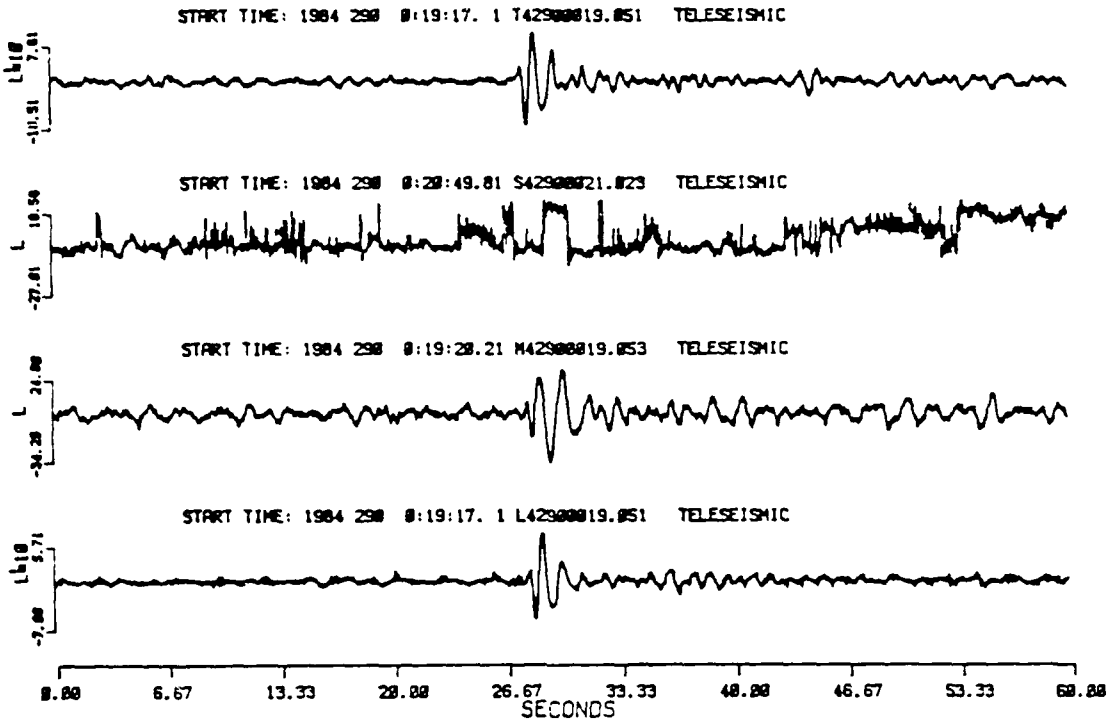

Figure 25.a

Figure 25. AR(8)-Spectral Estimates for the Signal and Noise for Event 8 are Normalized by the Variance of the Noise. (a) Event Traces Recorded at Each of the Four Stations, Lajitas, Marathon, Shafter and Tres Cuevas, for Event 8. (b) Lajitas AR(8)-Spectral Estimates. The Analyst Estimates for the Dominate Period of the Noise and the First Arrival Phase are Indicated with Dashed Lines Drawn to their Respective Spectral Estimates. (c) Marathon AR(8)-Spectral Estimates. (d) Shafter AR(8) Spectral Estimates. (e) Tres Cuevas AR(8) Spectral Estimates.

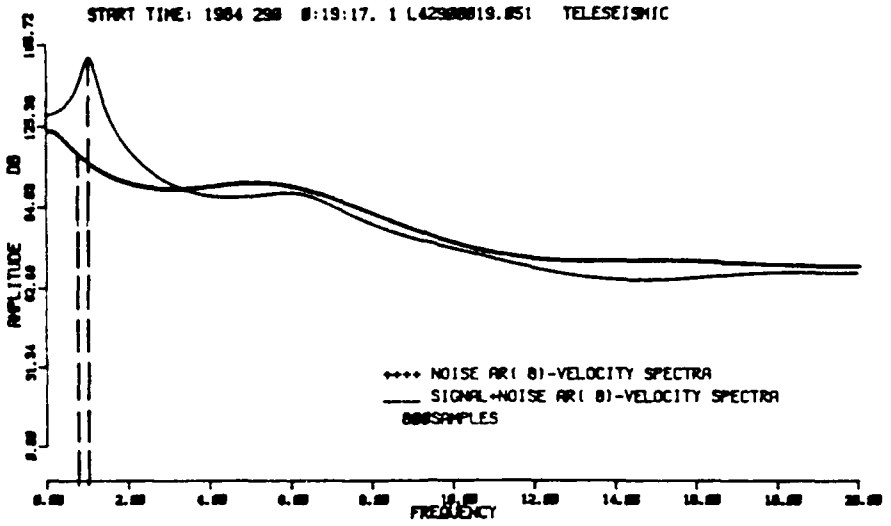

Figure 25.b

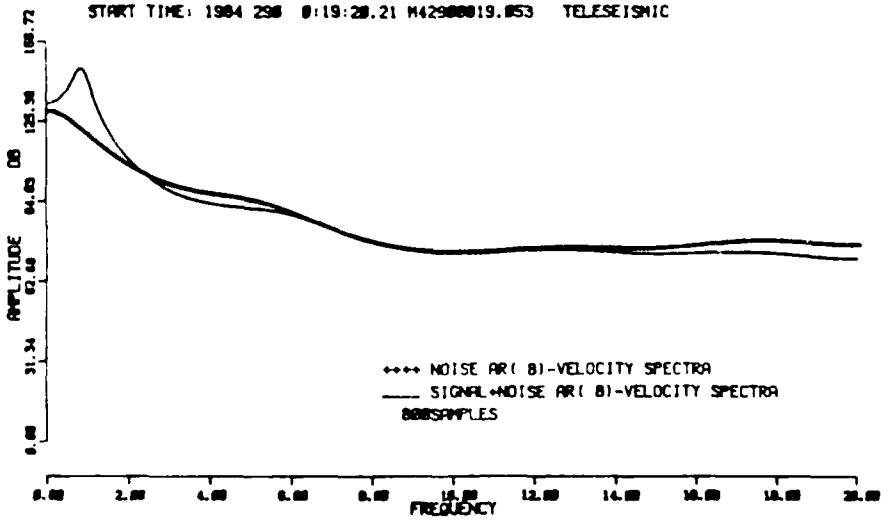

Figure 25.c

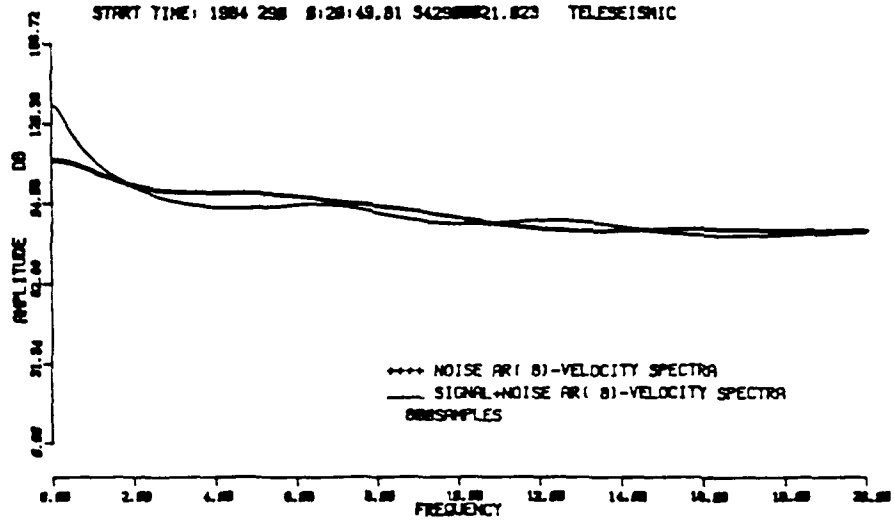

Figure 25.d

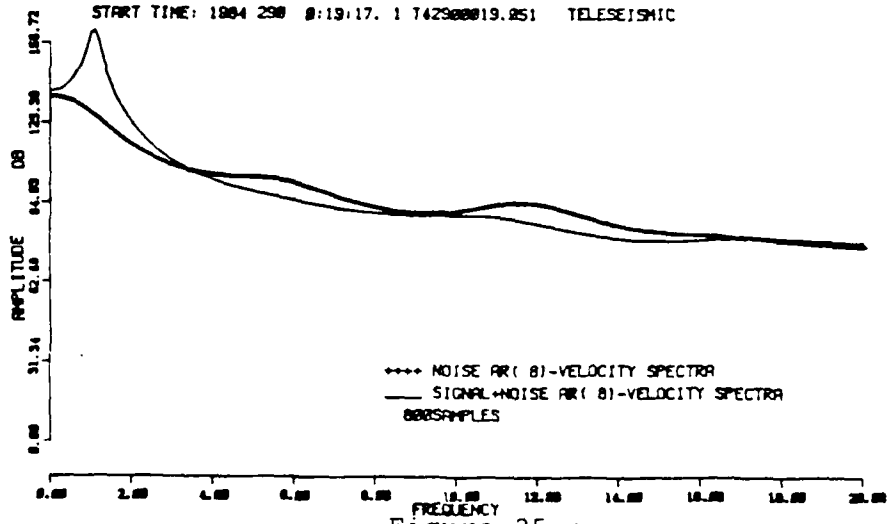

Figure 25.e

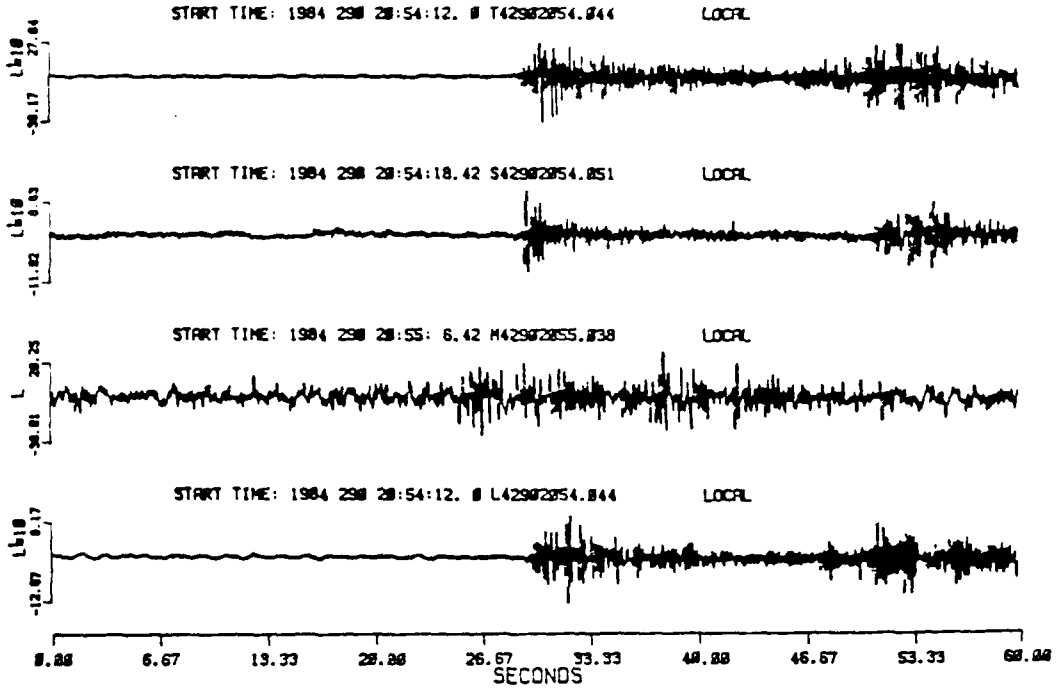

Figure 26.a

Figure 26. AR(8)-Spectral Estimates for the Signal and Noise for Event 11 are Normalized by the Variance of the Noise. (a) Event Traces Recorded at Each of the Four Stations, Lajitas, Marathon, Shafter and Tres Cuevas, for Event 11. (b) Lajitas AR(8)-Spectral Estimates. The Analyst Estimates for the Dominate Period of the Noise and the First Arrival Phase are Indicated with Dashed Lines Drawn to their Respective Spectral Estimates. (c) Marathon AR(8)-Spectral Estimates. (d) Shafter AR(8) Spectral Estimates. (e) Tres Cuevas AR(8) Spectral Estimates.

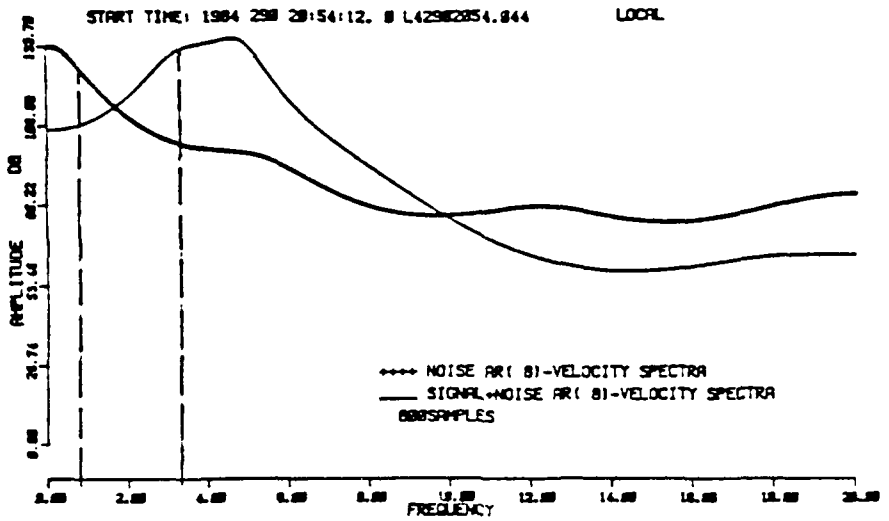

Figure 26.b

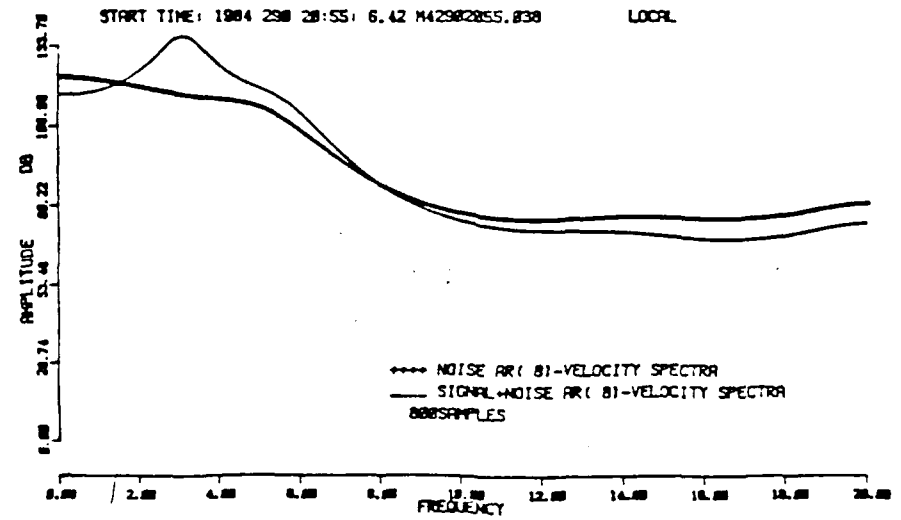

Figure 26.c

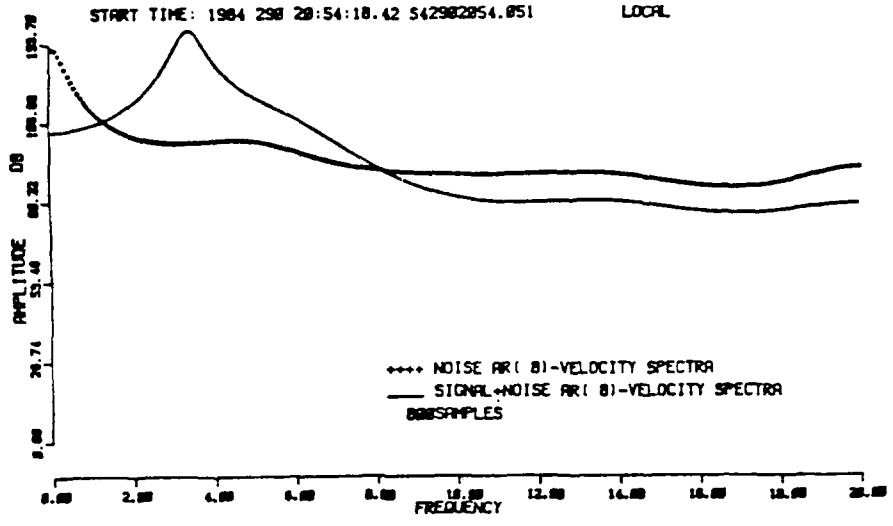

Figure 26.d

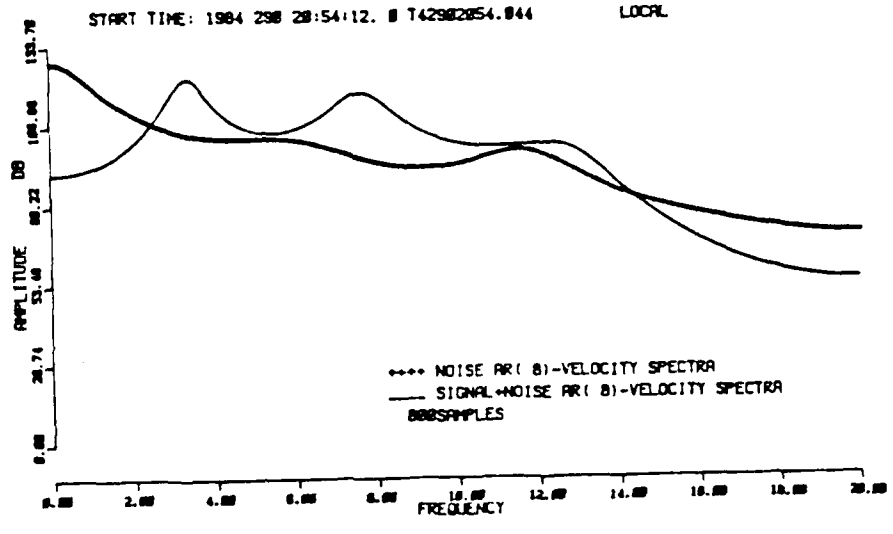

Figure 26.e

Non-parametric Detectors

Description of the Detector Used to Implement the Non-parametric Tests

The non-parametric tests used to distinguish signal from noise in the detector were performed on the "modified" slope of the event trace observation data. This "modified" slope is obtained by discrete integration of the slope of the event trace over segments with the same slope direction. Figure 20 illustrates how the slope and "modified" slope were calculated for each data point in the event traces. The subroutine, "SLOPE", in appendix B calculates the "modified" slope of the event trace.

The number of observations selected for testing the performance of each non-parametric technique as a detector was 100. The sample size was chosen so that the time period of each observation window would be greater than the largest period expected to occur in the event trace. The periods of the various components of the event trace signal and noise range from 0.1 to 1.2 seconds. A window of 100 observations, taken at a sample rate of 40 samples per second, correspondes to two and one-half seconds. The first 100 observations of each event trace is assummed to be a representative example of the background noise for the time period of the event trace. The first 100 observations representing background noise are denoted by

X(i), i=1,100, in the descriptions of the non-parametric tests following this description of the detector. The groups of 100 sequential observations taken at later times in the event trace and compared with the background noise, X(i), are denoted by Y(i), i=1,100. The null hypothesis used for each non-parametric test, H_0, is the assumption that both X(i) and Y(i) are taken from the same population; i.e., that the cummulative distribution functions for X(i) and Y(i), F(x) and F(y), respectively are the same.

Since we know the first 30 seconds into the event trace precedes the 6.4 second window which triggered the fast Walsh detector, we make the assumption that the first arrival phase of the seismic event (P or Lg) is within the first 60 seconds of the event trace. To detect the seismic signal a window of 100 observations is moved in increments of 10 samples, 0.25 seconds, down the event trace. Each window of 100 samples is compared to the first 100 samples of the trace representing background noise using a non-parametric statistical test. Detection occurs when the non-parametric test indicates the two windows of 100 samples are not from the same population; i.e., the underlying distributions, F(x) and F(y), are not the same.

Three non-parametric tests, (1) the two sample sign test, (2) the run test, and (3) the rank sum test, were

tried in the detector to determine the most effective test for discriminating between signal and noise. The following describes each test, the assumptions each test made, the validity of those assumptions with respect to the data set and the effectiveness of each test in discriminating between the background noise and the signal plus noise. The detector subroutine, "DETECTOR", is listed in appendix B.

Two sample sign test

Assumptions

The data for the two sample sign test consists of two random samples, N observations from the control population; i.e., background noise, and N observations from the treatment population; i.e., signal plus noise. In our case we choose N observations, X(1),...,X(N), from the beginning of the event trace representative of the background noise and N observations, Y(1),...,Y(N), from the remaining portion of the event trace. Unfortunately, the observations taken from a seismic signal are not independent random variables. Instead there is a dependency between the observations. Walsh (1949,1951) has shown that the sign test will have similar results if the observations in the two samples are mildly dependent.

The two sample sign test is sensitive to changes in

the location and spread of the distribution. If a signal is present the spread of the X(i) observations should be significantly different from the spread of the background noise, Y(i) observations. The sign test run on the seismic data assumed that no ties, (i.e., X(i) = Y(i)), were present.

Procedure

To test

$$H_0: \quad F(x) = F(y)$$

1. Define indicator variables

$$Z(i) = \begin{cases} 1 & \text{if } [Y(i) - X(i)] > 0 \\ 0 & \text{if } [Y(i) - X(i)] = 0 \\ -1 & \text{if } [Y(i) - X(i)] < 0 . \end{cases}$$

$$\delta(i) = \begin{cases} 1 & \text{if } Z(i) > 0 \\ 0 & \text{if } Z(i) \leq 0 \end{cases}$$

2. Set

$$Sn = \sum_{i=1}^{N} Z(i)\,\delta(i).$$

The statistic Sn is the number of positive Z's.

3. For a one-sided test of HO versus the alternative,

$$H_a: \quad F(x) = F(y),$$

at the alpha level of significance,

Reject H_0 if Sn < [N - b(alpha,N,1/2)]

Accept H_0 if Sn > [N - b(alpha,N,1/2)],

where the constant b(alpha,N,1/2) under the null

hypothesis satifies P[Sn > b(alpha,N,1/2)] = alpha. That is, b(alpha,N,1/2) is the upper alpha percentile point of the binomial distribution with sample size N and p = 1/2.

For large sample approximation under the null hypothesis define:

$$Sn^* = \frac{Sn - E(Sn)}{SQRT[Var(Sn)]} = \frac{Sn - N/2}{SQRT(N/4)} \quad .$$

When H_0 is true, the statistic Sn has an asymptotic (N tending to infinity) standard normal distribution, z(alpha). The normal theory approximation test of H_0 versus the alternative H_a, at the alpha level of significance is

Reject H_0 if $Sn^* \geq z(alpha)$

Accept H_0 if $Sn^* < z(alpha)$.

In regard to ties, X(i) = Y(j), if there are zero values among the Z's, discard them and redefine N to be the number of nonzero Z's. Figure 27 is an example of the two sample sign test with N = 30, k = 10 for a confidence interval (0.137-0.583), and alpha = 0.01.

Effectiveness

A large number of ties occur when the X(i) and Y(i) observations taken from seismic signals are compared. These ties are due to the limited dynamic range for small values of seismic observations near zero; i.e., the same values occur more often near zero since there is a more limited range of values to choose from. Since the ties

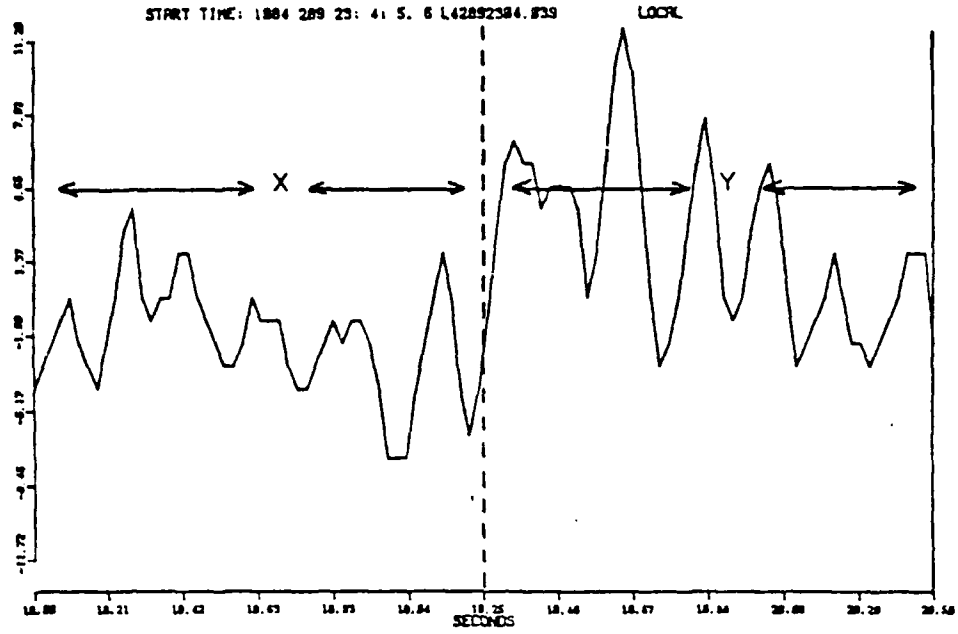

X	Y	SIGN
-2.0	-1.0	-1
4.0	1.0	-1
5.0	2.0	-1
0.0	1.0	1
-8.0	-3.0	-1
-11.0	-7.0	-1
-11.0	-13.0	1
-10.0	-15.0	1
-7.0	-13.0	1
-4.0	-6.0	1
0.0	2.0	1
3.0	7.0	1
7.0	11.0	1
6.0	10.0	1
5.0	7.0	1
3.0	1.0	-1
4.0	-4.0	0
8.0	0.0	-1
9.0	9.0	0
9.0	20.0	1
10.0	29.0	1
12.0	28.0	1
16.0	18.0	1
18.0	6.0	-1
20.0	0.0	-1
17.0	-4.0	-1
11.0	1.0	-1
4.0	12.0	1
-1.0	17.0	1
-4.0	19.0	1

TWO SAMPLE SIGN TEST

H_0: $F(x) = F(y)$
H_a: $F(x) \neq F(y)$
N = 30
E(Sn) = 15.0
$|Sn - E(Sn)| = 2.0$
K = 10
REJECT THE NULL HYPOTHESIS

Figure 27. Example of the Two Sample Sign Test. The Sign, (1,0,-1), Indicates the Absolute Value of the X(i) Observation is, Greater Than, Equal, or Less Than, the Absolute Value of the Y(i) Observation. Sn is the Summation of the Positive Signs.

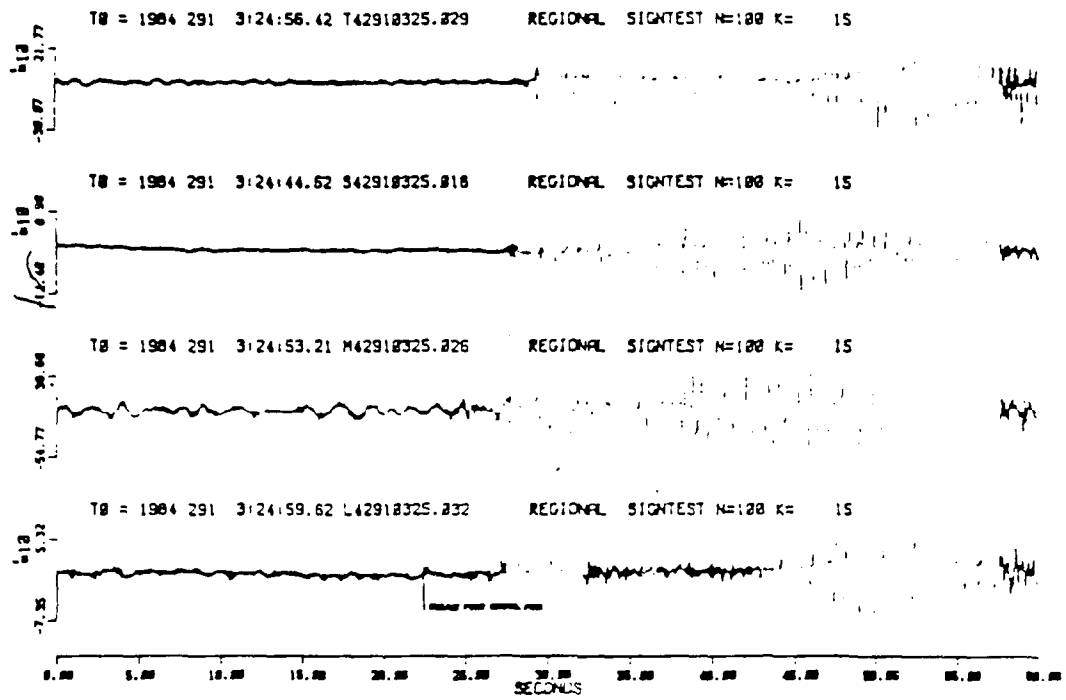

Figure 28.b

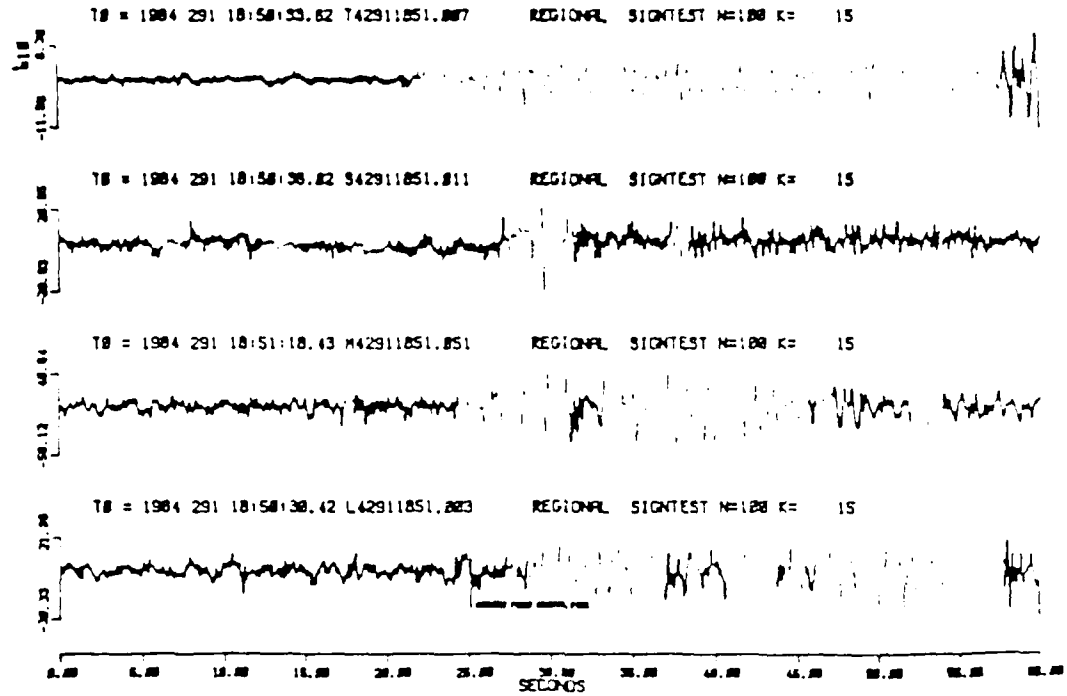

Figure 28.a

Figure 28. The Performance of the Two Sample Sign Test When Used to Detect Seismic Events. The Null Hypothesis for this Test Assumes all the Observations, X(i) and Y(i), Come from the Same Population, the Background Noise. The Blue Color Indicates a Rejection of the Null Hypothesis, i.e. a Signal is Present. (a) Event 19. (b) Event 14.

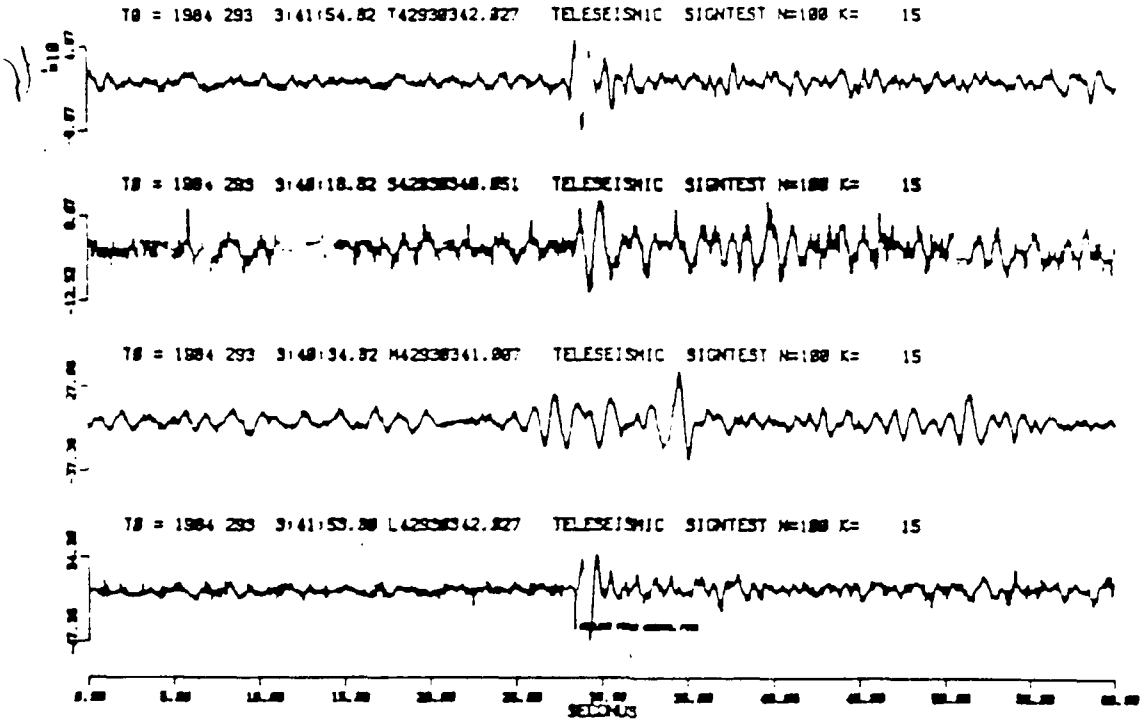

Figure 29.b

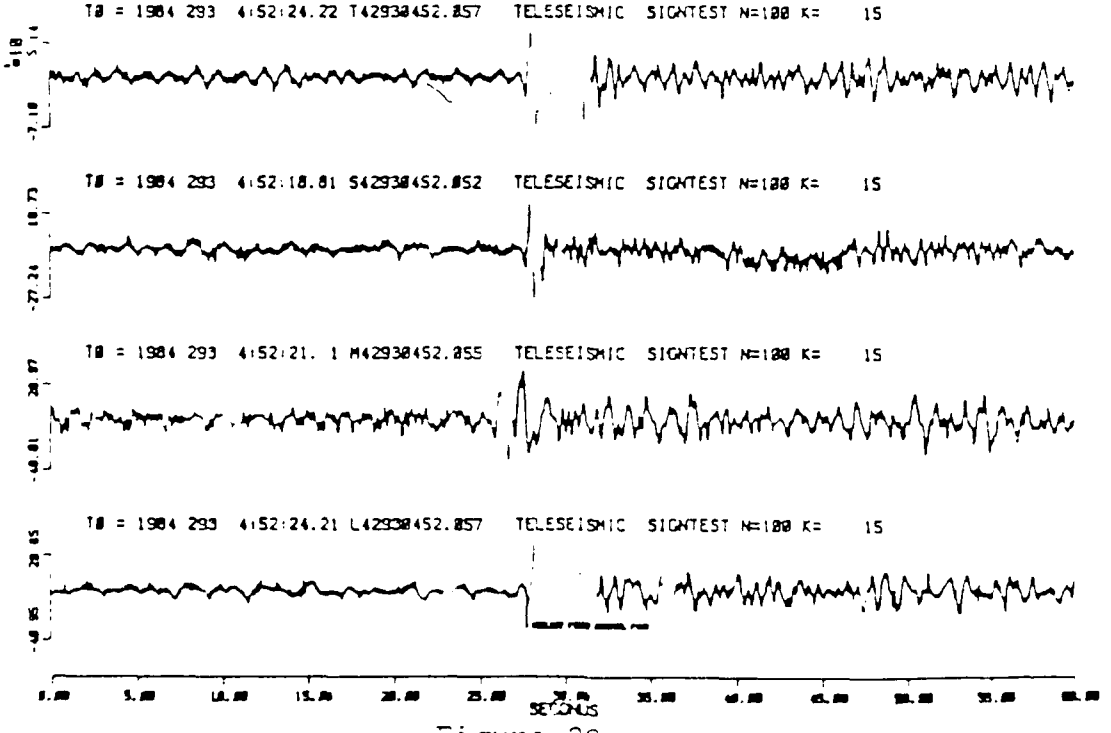

Figure 29.a

Figure 29. The Performance of the Two Sample Sign Test When Used to Detect Seismic Events. The Null Hypothesis for this Test Assumes all the Observations, X(i) and Y(i), Come from the Same Population, the Background Noise. The Blue Color Indicates a Rejection of the Null Hypothesis, i.e. a Signal is Present.

were not taken into consideration in calculating the value of the sign test they dilute its sensitivity to differences in the spread of the distributions. Ties were not accounted for because of the increase in computation time it would require; i.e., recalculation of the test for the reduced number of untied observations. Figures 28 and 29 illustrate the performance of the two sample sign test when used to detect signals. The sign test subroutine, "SIGNEXP", is listed in appendix B.

Run test

Assumptions

The run test selects N observations, X(1),...,X(N), of representative background noise taken from the beginning of the event trace and M observations, Y(1),...,Y(M), at some time later in the event trace. Then the observations are ordered in ascending order and the number of runs (groups of X or Y observations) are counted. The run test in this application assumes the two samples, X and Y, are independent random variables. Since there is a dependence between the observations in each sample the designated level of significance for the run test will not be preserved.

If X(i) and Y(j) are from the same population then X and Y will be well mixed and the number of runs will be large. However, if X(i) and Y(j) are from widely separate

populations then there will only be two runs. The run test is sensitive to differences in both shape and location of the distributions.

Procedure

To test

$$H_0: \quad F(x) = F(y) \ .$$

1. Order the observations, X(i), i=1,N and Y(i), i=1,M, together in ascending order from least to greatest.

2. Set Z equal to the number of distinct groups of Y's. The statistic Z is the number of runs in the ordered array of observations.

3. For a one-sided test of H_0 versus the alternative

$$H_a: \quad F(x) = F(y) \ ,$$

at the alpha level of significance,

$$\text{Reject } H_0 \quad \text{if } Z \geq z0$$

$$\text{Accept } H_0 \quad \text{if } Z < z0 \ ,$$

where the constant z0 is the largest integer which satisfies

$$\sum_{z=2}^{z\phi} P[Z = z] = \text{alpha}.$$

That is, z0 is the lower percentile point of the distribution of Z for sample sizes N and M.

The following specifies P[Z = z] under the null hypothesis so that we can determine the integer z0 for a given test size.

$$P[Z = z] = P[Z = 2k] = \frac{2\binom{M-1}{k-1}\binom{N-1}{k-1}}{\binom{M+N}{M}}$$

$$P[Z = z] = P[Z = 2k+1] = \frac{\binom{M-1}{k}\binom{N-1}{k-1} + \binom{M-1}{k-1}\binom{N-1}{k}}{\binom{M+N}{M}}$$

For large sample approximation define

$$Z^* = \frac{Z - E(Z)}{SQRT[Var(Z)]}$$

$$E(Z) = \frac{2MN}{M+N} + 1$$

$$Var(Z) = \frac{2MN(2MN-M-N)}{((M+N)**2)(M+N-1)}.$$

When H_0 is true, the statistic z0 has an asymptotic (N tending to infinity) standard normal distribution. The normal theory approximation for the one-sided run test is

Reject H_0 if $Z^* \geq z(alpha)$

Accept H_0 if $Z^* < z(alpha)$.

For $M \geq 10$ and $N \geq 10$ the asymptotic normal distribution can be used to determine z0 (Mood, Graybill and Boes, 1974). If there are ties, Z(i) = Z(j), we delete the tied observations and recalculate z0 for the new value of N. Figure 30 illustrates an example of the run test for N = 30, M = 30, z0 = 40, and alpha = 0.01. The run test subroutine, "RUNEXP", is listed in appendix B.

Effectiveness

Due to the way seismic signals are recorded digitally, there are a large number of ties which impede

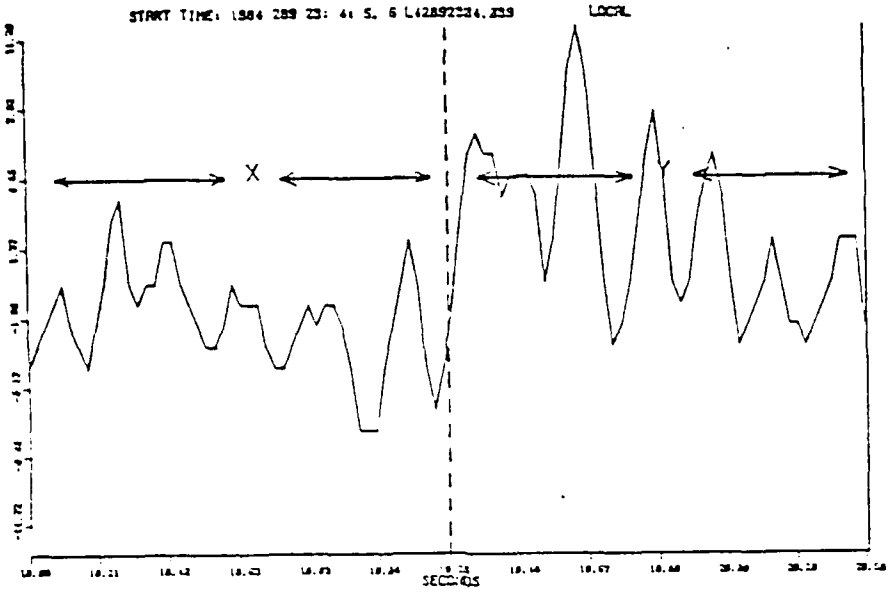

INDEX	DATA	TYPE
1	0.3	X
2	0.3	X
3	0.3	Y
4	0.3	Y
5	1.3	Y
6	1.3	Y
7	1.3	Y
8	1.3	X
9	1.3	Y
10	1.3	Y
11	2.3	X
12	2.3	Y
13	2.3	Y
14	3.3	Y
15	3.3	X
16	3.3	X
17	4.3	X
18	4.3	X
19	4.3	Y
20	4.3	X
21	4.3	X
22	4.3	Y
23	4.3	X
24	5.3	X
25	5.3	X
26	6.3	X
27	6.3	Y
28	6.3	Y
29	7.3	X
30	7.3	Y

INDEX	DATA	TYPE
31	7.3	Y
32	7.3	Y
33	7.3	X
34	8.3	X
35	8.3	X
36	9.3	X
37	9.3	Y
38	9.3	X
39	10.3	X
40	10.3	X
41	10.3	Y
42	11.3	X
43	11.3	Y
44	11.3	X
45	11.3	X
46	12.3	X
47	12.3	Y
48	13.3	Y
49	13.3	Y
50	15.3	Y
51	16.3	X
52	17.3	X
53	17.3	Y
54	18.3	X
55	18.3	Y
56	19.3	Y
57	20.3	X
58	20.3	Y
59	28.3	Y
60	29.3	Y

RUN TEST

H_0: F(x) = F(y)

H_a: F(x) ≠ F(y)

N = 30 M = 30

E(Z) = 31.0

VAR(Z) = 14.7

z = 28

z0 = 40

REJECT THE NULL HYPOTHESIS

Figure 30. Example of the Run Test. The X(i) and Y(i) Observations are Ordered in Ascending Order. Then the Number of Runs of X and Y Values, Z, are Counted. If the Number of Runs is Less than the Threshold, z0, the Null Hypothesis that X and Y Both Come from the Same Population is Rejected.

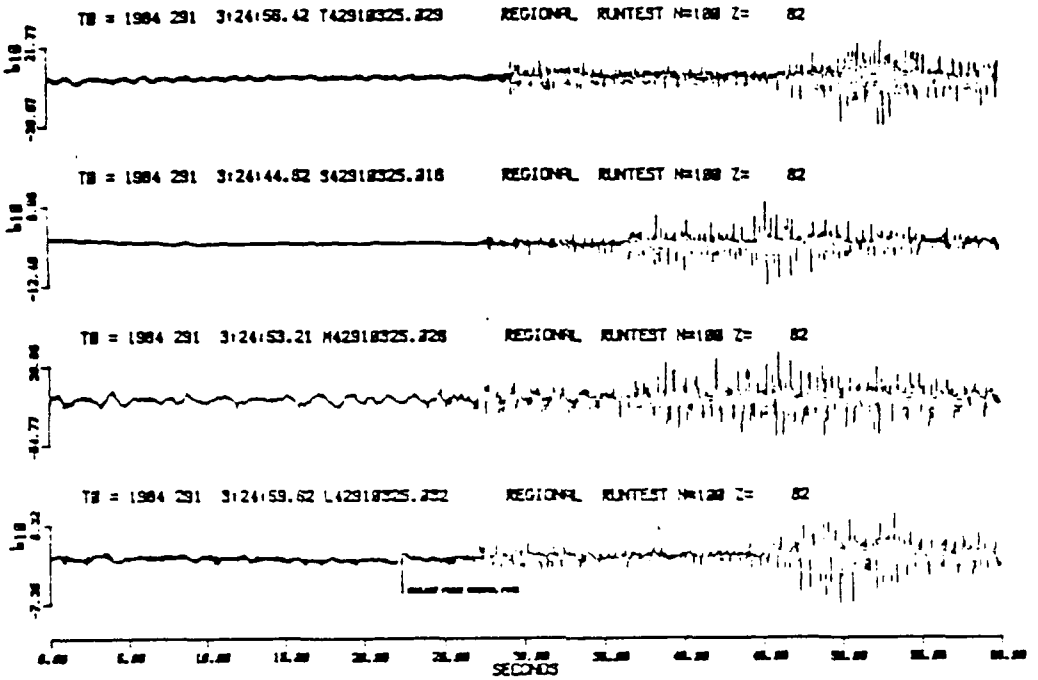

Figure 31.b

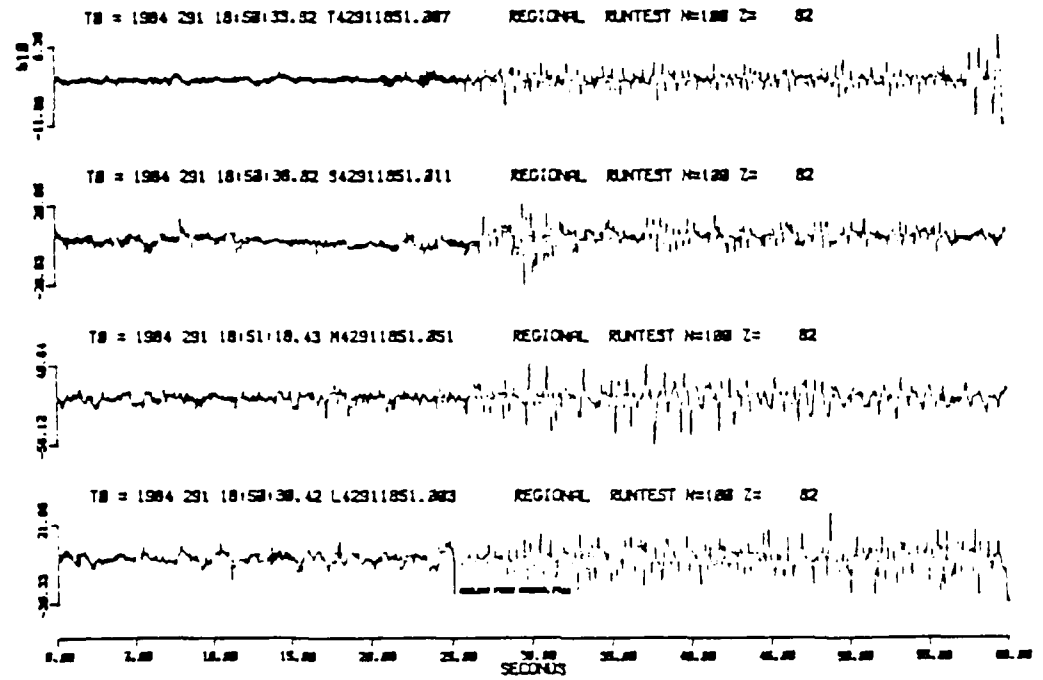

Figure 31.a

Figure 31. The Performance of the Run Test When Used to Detect Seismic Events. The Null Hypothesis for this Test Assumes all the Observations, X(i) and Y(i), Come from the Same Population, the Background Noise. The Blue Color Indicates a Rejection of the Null Hypothesis, i.e. a Signal is Present. (a) Event 19. (b) Event 14.

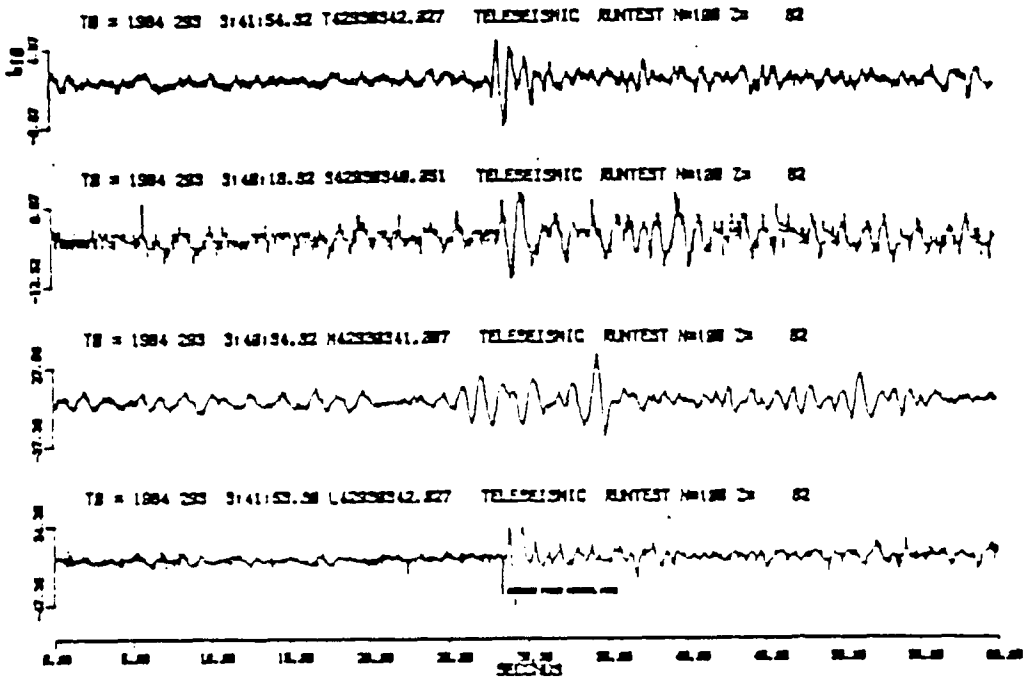

Figure 32.b

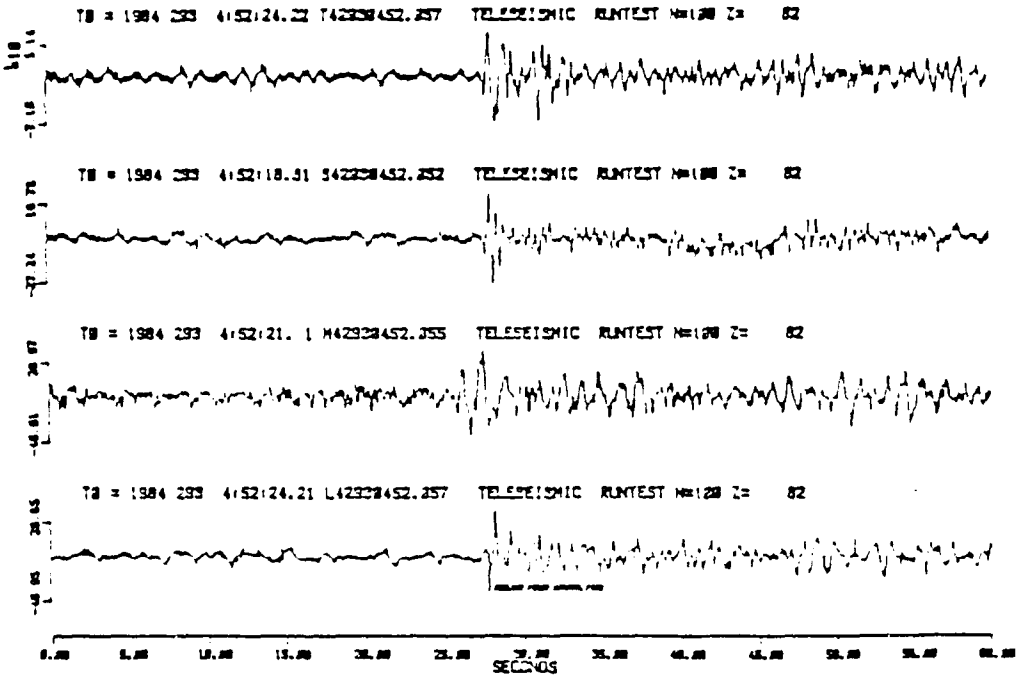

Figure 32.a

Figure 32. The Performance of the Run Test When Used to Detect Seismic Events. The Null Hypothesis for this Test Assumes all the Observations, X(i) and Y(i), Come from the Same Population, the Background Noise. The Blue Color Indicates a Rejection of the Null Hypothesis, i.e. a Signal is Present.

the effectiveness of the run test in distinguishing the differences in shape between two different populations. Since this non-parametric technique does not have a good way of handling the number of ties naturally occurring in seismic signal comparisons, this technique was rejected in favor of the rank sum test. Figures 31 through 32 illustrate the performance of the run test as a signal detector.

Rank sum test

Assumptions

The rank sum test selects N sequential observations, X(1),...,X(N), of the "modified" slope of the representative background noise from the beginning of the event trace. Then M sequential observations of "modified" slope, Y(1),...,Y(M), are chosen from some time later in the event trace. The N plus M observations are ordered in ascending order and assigned a rank based on their position in the ordered sequence. The ranks for the Y(i) observations, Ry(i), are summed and the absolute value of the difference between that rank sum, Ty, and the estimated mean, E(Ty), is compared with a predetermined threshold value, k.

The rank sum test assumes the X(i) and Y(i) observations are independent random variables. Since background noise is not a purely random process and the

seismic signal can be thought of as the background noise "treated" with the addition of a seismic event, neither the X(i) or the Y(i) observations are independent random variables. Serfling (1968) investigating the robustness of Wilcoxon test, upon which the rank sum test is based, let the two samples, X and Y, be independent of each other but let the random variables within a sample be possible dependent. It is found that the robustness of the test statistic for the Wilcoxon two-sample procedure under the null hypothesis with departures from the standard assumption of random samples depends upon the grade of correlation of the variables X(i) and X(i+1). In other words, similar results for the rank sum test should be obtained when only mild dependence occurs between the observations in the samples. Since we do not know the exact degree of dependence between the observations, there is a probability that the significance level, (alpha), assumed for the rank sum test does not reflect the true significance level.

Procedure

To test

$$H_0: \quad F(x) = F(y) \ .$$

1. Order the N and M observations from least to greatest and let Ry(i) denote the rank of Y(i) in this ordering.

2. Set

$$Ty = \sum_{i=1}^{M} Ry(i).$$

The statistic Ty is the sum of the ranks assigned to the Y's.

3. For a one-sided test of H0 versus the alternative

$$H_a: \quad F(x) = F(y),$$

at the alpha level of significance,

$$\text{Reject } H_0 \quad \text{if} \quad Ty \geq w(\text{alpha},M,N)$$

$$\text{Accept } H_0 \quad \text{if} \quad Ty < w(\text{alpha},M,N) \ ,$$

where the constant w(alpha,M,N) under the null hypothesis satifies

$$P[Ty > w(\text{alpha},M,N)] = \text{alpha}.$$

Values of w(alpha,M,N) are given in Table C.1, Appendix C (Hollander and Wolfe, 1973).

For large sample approximation under the null hypothesis define

$$Ty^* = \frac{Ty - E(Ty)}{SQRT[Var(Ty)]} \ .$$

When H_0 is true, the statistic Ty has an asymptotic (minimum of N or M tending to infinity) standard normal distribution. The one-sided normal approximation theory for the test statistic is

$$\text{Reject } H_0 \quad \text{if } Ty^* \geq z(\text{alpha})$$

$$\text{Accept } H_0 \quad \text{if } Ty^* < z(\text{alpha}).$$

For $M \geq 7$ and $N \geq 7$ the asymptotic normal approximation is quite accurate. (Mood, Graybill and Boes, 1974)

If there are ties; i.e., the ith observation in

ascending order is tied with the k observations following the ith observation then the summation of the indices divided by k+1 is the average rank assigned to each of the tied values. For the large sample approximation, compute Ty using average ranks, and replace Var(Ty) by

$$\mathrm{Var}(Ty) = \frac{MN}{12}\left[M+N+1 - \frac{\sum_{i=p}^{L} f(i)(f(i)^{**2} - 1)}{(M+N)(M+N-1)} \right],$$

where L is the number of tied groups of ranks and f(i) is the size of the ith tied group. An untied observation is considered to be a tied group of size 1. Hence if there are no tied observations the right hand side of Var(Ty) reduces to

$$\frac{MN\ (M+N+1)}{12}\ .$$

Figure 33 illustrates an example of the rank sum test for N=30, M=30, and alpha = 0.001. The rank sum test subroutine, "RANKTEST", is listed in appendix B.

Effectiveness

Since the ties are handled by averaging the ranks this test is sensitive to the relative changes in the shape of the seismic signal's density distribution. Figures 34 and 35 illustrate the application of the rank sum test to detect a seismic event.

Conclusions

The rank sum test was the most effective of the non-

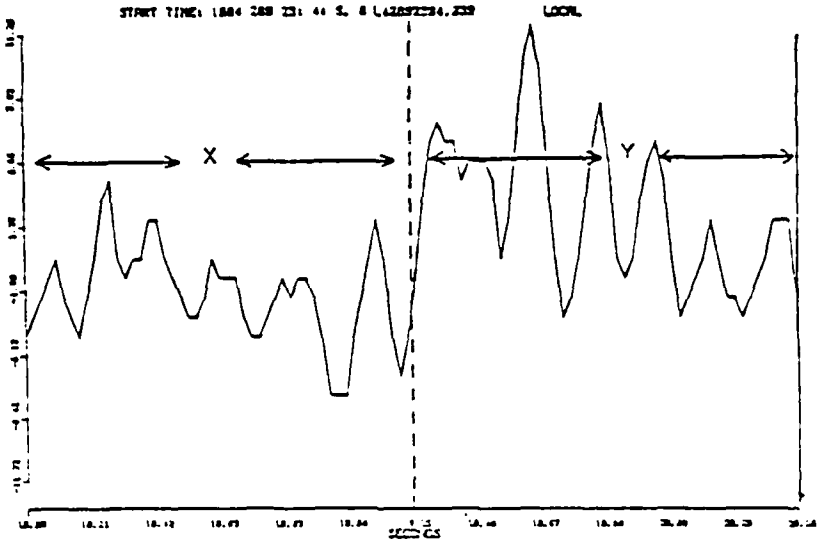

DATA	RANK	FREQ
2.3	12.3	3.3
4.3	20.3	7.3
5.3	24.5	2.3
8.3	2.5	4.3
9.3	34.5	2.3
11.3	43.5	4.3
11.3	43.5	4.3
10.3	40.3	3.3
7.3	31.3	5.3
4.3	20.3	7.3
8.3	2.5	4.3
3.3	15.3	3.3
7.3	31.3	5.3
6.3	27.3	3.3
5.3	24.5	2.3
3.3	15.3	3.3
4.3	20.3	7.3
8.3	34.5	2.3
9.3	37.3	3.3
9.3	37.3	3.3
10.3	40.3	3.3
12.3	46.5	2.3
16.3	51.3	1.3
18.3	54.5	2.3
23.3	57.5	2.3
17.3	52.5	2.3
11.3	43.5	4.3
4.3	20.3	7.3
1.3	7.5	6.3
4.3	20.3	7.3

DATA	RANK	FREQ
1.3	7.5	6.3
1.3	7.5	6.3
2.3	12.3	3.3
1.3	7.5	6.3
3.3	15.3	3.3
7.3	31.3	5.3
13.3	48.5	2.3
15.3	53.3	1.3
13.3	48.5	2.3
6.3	27.3	3.3
2.3	12.3	3.3
7.3	31.3	5.3
11.3	43.5	4.3
10.3	40.3	3.3
7.3	31.3	5.3
1.3	7.5	6.3
4.3	20.3	7.3
8.3	2.5	4.3
9.3	37.3	3.3
23.3	57.5	2.3
29.3	60.3	1.3
28.3	59.3	1.3
18.3	54.5	2.3
6.3	27.3	3.3
3.3	2.5	4.3
4.3	20.3	7.3
1.3	7.5	6.3
12.3	46.5	2.3
17.3	52.5	2.3
19.3	56.3	1.3

RANK TEST

H_0: $F(x) = F(y)$
H_a: $F(x) \neq F(y)$
N = 33 M = 33
E(Ty) = 915.3
VAR(Ty) = 4575.3
$|Ty - E(Ty)|$ = 7.3
K = 222
ACCEPT THE NULL HYPOTHESIS

Figure 33. Example of the Rank Sum Test. The X(i) and Y(i) Observations are Ordered in Ascending Order and Assigned at Rank Indicating their Position in the Sequence. Then the Ranks, Ry(i), for the Y(i) Values are Summed, Ty. If the Absolute Value of the Rank Sum, Ty, minus its Expected Value, E(Ty), is Less than the Threshold, K, we Accept the Null Hypothesis that X(i) and Y(i) Come from the Same Population.

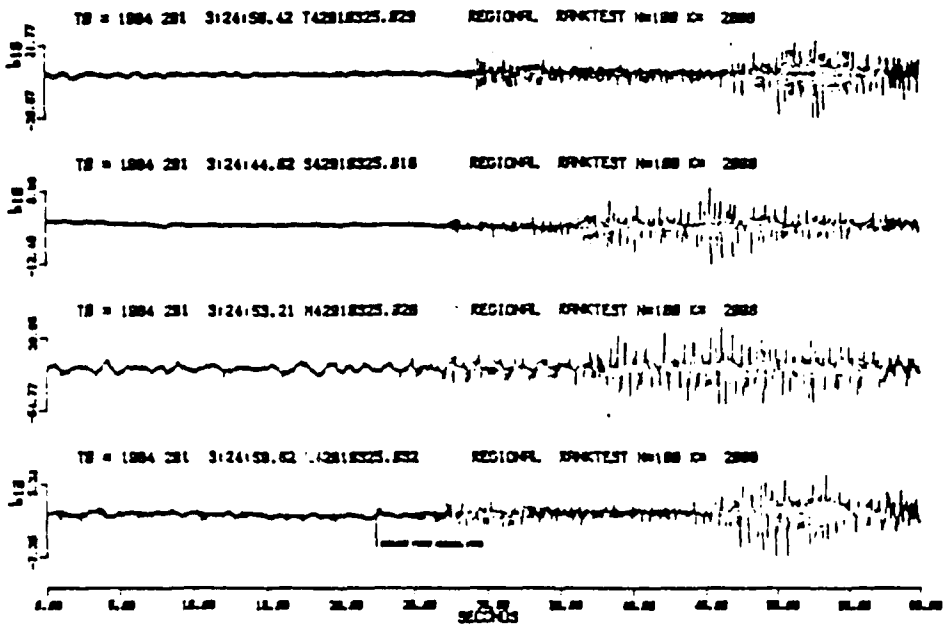

Figure 34.b

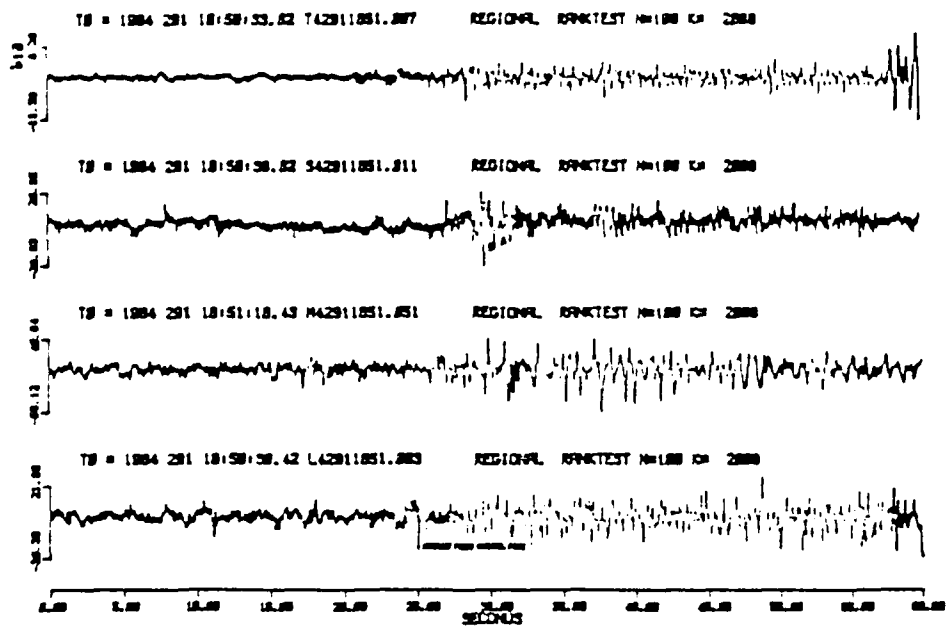

Figure 34.a

Figure 34. The Performance of the Rank Sum Test When Used to Detect Seismic Events. The Null Hypothesis for this Test Assumes all the Observations, X(i) and Y(i), Come from the Same Population, the Background Noise. The Blue Color Indicates a Rejection of the Null Hypothesis, i.e. a Signal is Present. (a) Event 19. (b) Event 14.

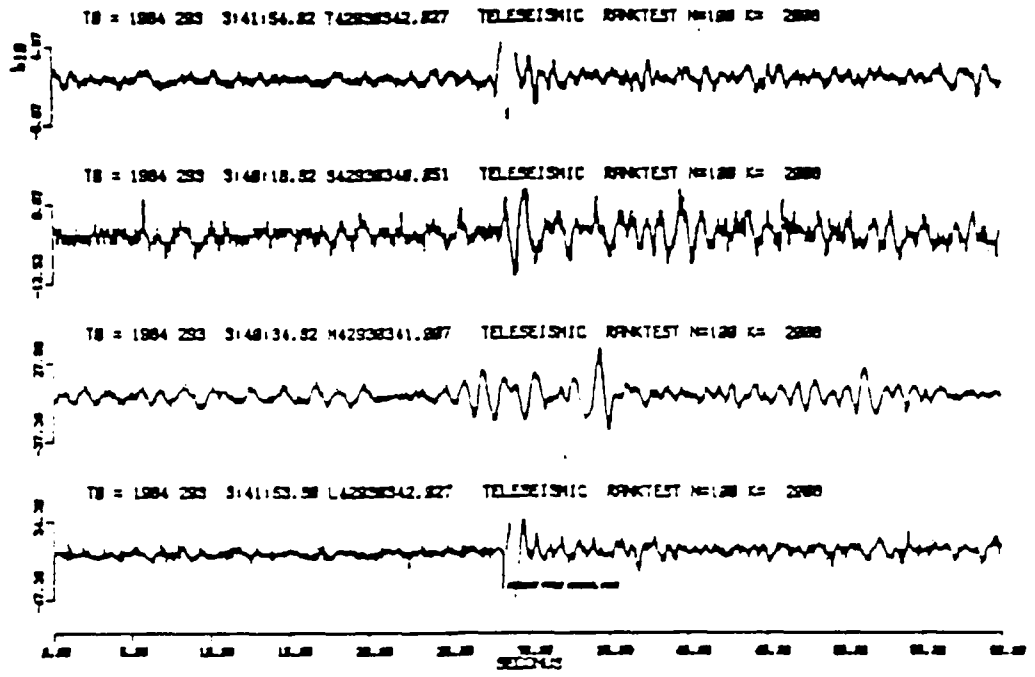

Figure 35.b

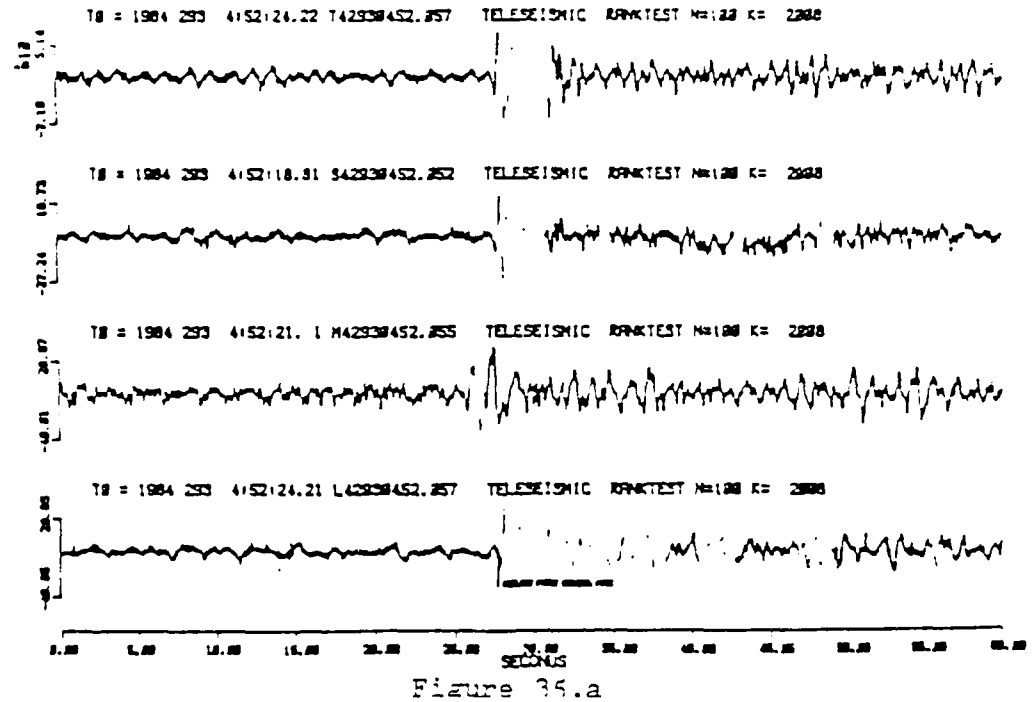

Figure 35.a

Figure 35. The Performance of the Rank Sum Test When Used to Detect Seismic Events. The Null Hypothesis for this Test Assumes all the Observations, X(i) and Y(i), Come from the Same Population, the Background Noise. The Blue Color Indicates a Rejection of the Null Hypothesis, i.e. a Signal is Present.

parametric tests in discriminating between signal and noise. After studying figures 28,29,31,32,34 and 35 one can see that the rank sum test does the best job of discriminating the event signal from background noise in a trace where an event signal is known to be present. The success of the rank sum test is due to its method of handling the large number of ties indigenous to seismic signals.

DETECTION TECHNIQUE AND FIRST ARRIVAL PICKER EMPLOYED TO FIND THE FIRST ARRIVAL PHASE OF EARTHQUAKES AND EXPLOSIONS IN SEISMIC SIGNALS CONTAMINATED BY NOISE

Description of Non-parametric Detector and Picker

The rank sum test applied to the "modified" slope of the event trace observation data most clearly distinguished seismic signals from the background noise of the three non-parametric techniques tested. Several implementations of a detector based on the rank sum test were run on a training set of 48 event traces. The level of significance for the rank sum test was varied to find the threshold for detection which would allow the rank sum test to clearly discriminate between signal and noise. However, the "unmodified" application of the rank sum test to discriminate between signal and noise was not "consistent" in picking the seismic event due to varying S/N ratios. To allow the threshold for detection to change with S/N ratio a "modified" version of the rank sum test was implemented.

The minimum and maximum rank sums for a each trace were determined in this "modified" implementation of the rank sum test. If the range of the rank sums, (i.e., sum of the ranks in each window), for a trace,

maximum rank sum - minimum rank sum,

is greater than 3600, which was observed to constitute the "high" S/N case, then the threshold for signal detection is computed to be the minimum rank sum plus 2700. If the range of the rank sums is less than 3600, which was observed to constitute the "low" S/N case, then the signal detection threshold is computed to be the minimum rank sum plus 75 percent of the range of the rank sums. Based on a detailed analysis of the rank sums test when applied to the event traces in the data set, this allows approximately 99.9 percent of the rank sums due to background noise to fall below the threshold in the "high" S/N cases and 99 percent in the "low" S/N cases.

The automatic first arrival pick is defined as the first zero-crossing preceding the first observation in the first detection window whose modified slope is at least 1.05 times greater than the maximum modified slope value of the representative background noise.

The event detector based on the rank sum test takes the first N=100 observations in the event trace to be a representative sample of the background noise present in that event trace. The rank sum test is computed for observation windows, N equal 100 samples in length, moved in increments of 10 samples, 0.25 seconds, down the event trace. The rank sum of each window is computed and compared with the rank sum of the background noise window.

The subroutine to detect and pick the first arrival phase, "RANK2700", is listed in appendix B.

Results

The detector which used the "modified" version of the rank sum test described in the preceding section to discriminate between signal and noise was run on 152 of the event files recorded during the GSETT experiment. These event files were selected to give the broadest representation of the wide variety of seismic signals we would expect to encounter if the detector were run over all events recorded by the fast Walsh detector on a daily basis.

To analyze the performance of the "modified" rank sum detector we looked at 128 of the event traces. Since 24 of the 152 event traces the detector was run on were also included in the training set used to develop the "modified" version of the rank sum detector they were excluded in this analysis to give us an unbiased look at the detector's performance. One hundred and twenty-four automatic picks were compared to their respective analyst's picks. Sixty-five were within 0.4 seconds of the analyst's pick. After analizing the automatic picks differing from the analyst's picks by more than 0.4 seconds, it was concluded that 5 appeared to be more correct than the analyst's original picks. Twenty-four of

the automatic picks were ambiguous, either the automatic pick or the analyst pick could be correct. Thirty-five of the automatic picks had errors larger than 0.4 seconds relative to the analyst picks: 4 local; 28 regional; and 3 teleseismic events. The representative background noise for 22 of the regional and local automatic picks with errors larger than 0.4 seconds contained P arrivals. This indicates that the violation of the assumption that the first 100 samples is background noise causes a deterioration in the accuracy of the automatic first arrival pick. The apparently erroneous automatic picks that occur for teleseismic events are caused by small emergent precursors to the P-arrival which the analyst picked.

Occasionally, the assumption that the first 100 observations in the event trace represent background noise is violated. Either because the fast Walsh detector did not detect the P arrival but instead triggered on the Lg arrival or because the signatures from two seismic events occurring near the same time overlap each other on the the event trace. This causes either the P arrivals or the coda from a preceding event to contaminate the first 100 observations assummed to contain only background noise.

When the initial assumption that the first 100 samples of the trace represent background noise is violated the detector discriminates between signal and

TABLE 4. Errors (Automatic Minus Analyst Picks in Seconds), and Ranges of the Rank Sums for the 152 Events Used to Test RANK2700

ALL EVENTS

EVENT NAME	RANGE	ERROR
S42891418.037	5057.0	0.0
L42892313.003	4802.5	0.0
M42911851.051	3742.0	0.0
T42932303.019	5323.0	0.0
T42973815.046	5751.5	0.0
L42971753.018	5272.0	0.0
S42971753.018	6174.0	0.0
T42900019.051	5564.5	-0.1
S42900136.031	3581.0	0.1
M42902355.038	4294.0	0.1
T42891418.034	5349.5	-0.1
M42912140.040	5149.0	0.1
T42912213.057	4814.5	0.1
L42920528.008	5145.5	-0.1
S42920528.001	4184.0	0.1
T42920528.008	5536.0	-0.1
L42921533.036	5469.0	0.1
M42921533.023	5871.0	0.1
S42921533.026	5261.5	0.1
L42921859.031	3998.0	0.1
T42921859.028	4275.0	0.1
L42932129.009	5495.5	-0.1
T42932129.006	5797.0	0.1
L42891418.037	4920.5	-0.1
T42951908.057	5539.5	0.1
L42962037.016	3720.5	0.1
S42970815.039	5939.5	0.1
S42892313.016	5454.0	0.1
M42892328.007	3311.5	0.1
M42900019.053	4579.5	0.1
T42902054.044	5934.0	0.2
L42932303.019	5848.0	0.2
M42932303.035	5889.5	0.2
S42921430.030	3994.0	-0.2
M42951908.050	5725.0	0.2
S42911603.000	4508.5	0.2
S42900021.023	4569.5	0.2
M42891418.053	5475.5	0.2
L42900019.051	4862.0	-0.2
L42902054.044	5524.0	-0.2
M42971753.030	5839.5	0.2
T42892304.016	5748.0	0.2
M42901820.047	4772.0	0.3
S42911807.026	4369.0	0.3
M42921430.014	4358.0	0.3
T42911807.032	4579.5	-0.3
L42951908.057	5912.5	0.3
T42921429.018	3944.0	-0.3
T42892327.012	5168.0	0.3
T42911851.007	5859.5	0.3
T42911958.056	4692.5	0.3
L42921829.039	4112.5	0.3
T42891905.008	3880.0	0.3
T42900136.021	4554.5	0.3
T42902209.030	3713.0	0.3

ALL EVENTS

EVENT NAME	RANGE	ERROR
T42921533.036	5751.5	-0.4
M42962038.001	4733.5	0.4
S42901821.025	4187.0	-0.4
L42911807.020	4572.5	0.4
L42912140.015	5738.0	0.4
M42911807.029	4144.5	0.4
L42912213.057	4443.5	-0.4
L42921429.020	2235.0	0.5
M42932129.031	5872.0	-0.5
T42892313.008	5583.5	0.6
L42902247.013	4145.0	-0.6
T42910325.029	5643.0	0.6
S42932129.018	6385.5	-0.6
M42891815.038	3481.5	0.6
L42911851.003	4626.5	-0.6
M42910325.026	5548.0	0.7
M42902210.022	4852.0	0.7
L42911959.017	4392.0	-0.7
S42962038.014	4264.5	0.8
T42911602.003	5197.5	0.8
S42892327.018	4096.0	-0.8
T42902246.038	3742.0	0.9
M42921830.008	3958.5	0.9
M42970815.043	6135.5	-0.9
M42911602.039	3788.0	0.9
M42971951.000	2483.5	-1.0
L42970815.048	6091.0	-1.1
S42951909.000	5251.5	-1.1
T42921829.039	4849.5	-1.2
L42891719.050	4166.5	1.2
T42891814.046	4812.0	1.2
L42971952.007	4583.0	1.2
S42932303.035	5628.5	-1.2
L42910325.030	5958.0	1.4
T42962037.016	3655.0	1.5
M42891719.057	3826.0	1.7
L42892327.016	4615.5	-1.8
T42891719.047	4242.5	1.9
S42921829.023	5681.5	-2.0
M42912214.052	4067.0	2.1
S42921858.056	3923.5	2.3
S42911851.011	5646.0	-2.4
M42891906.040	3349.5	2.7
T42912140.015	5518.5	-2.9
L42902209.027	2860.0	3.0
T42971752.052	5585.0	3.3
M42920528.004	5799.5	-3.4
T42971951.000	3419.5	3.9
M42902246.029	4954.5	4.4
M42892304.028	4193.5	-5.1
S42902211.000	2888.0	5.1
S42902247.016	2987.0	5.4
S42911958.058	6332.0	-6.3
S42892304.012	5496.0	-6.3
L42891815.018	4178.0	6.5

TABLE 4 (Continued)

ALL EVENTS

EVENT NAME	RANGE	ERROR
S42891719.025	4885.5	7.4
L42981821.016	4485.5	7.5
T42981828.037	3292.8	-9.1
S42971958.048	4355.5	10.1
S42912139.038	3748.8	10.4
S42891815.018	3478.5	10.4
M42980137.019	4208.8	12.6
M42911959.008	4199.8	13.4
S42891983.018	3351.2	-15.1
M42892313.022	4762.5	-15.3
L42891986.038	3868.5	-17.5
L42892384.039	5576.5	-19.9
S42918325.016	5376.8	-22.9
M42921859.054	4645.5	-23.6
S42912215.001	5845.8	-23.7
L42980136.053	4227.5	-25.8
S42982854.051	6894.8	-26.8
L42911682.007	4522.8	-33.3

NUMBER OF EVENTS = 128
MEDIAN = 0.5
MEAN = 3.2
VARIANCE = 48.3

LOCAL EVENTS

EVENT NAME	RANGE	ERROR
L42971753.018	5272.8	0.0
S42971753.018	6174.8	0.0
L42962837.016	3722.5	0.1
M42982855.038	4294.8	0.1
M42912148.048	5149.8	0.1
T42892384.016	5748.8	0.2
T42982854.044	5984.8	0.2
M42971753.038	5839.5	0.2
L42982854.044	5524.8	-0.2
M42962838.081	4733.5	0.4
L42912148.015	5738.8	0.4
S42962838.014	4264.5	0.8
M42971951.008	2483.5	-1.0
L42971952.007	4583.8	1.2
T42962837.016	3655.8	1.5
T42912148.015	5518.5	-2.9
T42971752.052	5585.8	3.3
T42971951.008	3419.5	3.9
M42892384.028	4193.5	-5.1
S42892384.012	5496.8	-6.3
S42971958.048	4355.5	10.1
S42912139.038	3748.8	10.4
L42892384.039	5576.5	-19.9
S42982854.051	6894.8	-26.8

NUMBER OF EVENTS = 24
MEDIAN = 0.8
MEAN = 4.8
VARIANCE = 326.3

TABLE 4 (Continued)

REGIONAL EVENTS

EVENT NAME	RANGE	ERROR
S42891418.037	5857.0	0.0
L42892313.003	4882.5	0.0
M42911851.051	3742.0	0.0
T42932303.019	5323.0	0.0
S42892313.016	5454.0	0.1
M42892328.007	3311.5	0.1
S42900136.031	3581.0	0.1
T42891418.034	5349.5	-0.1
T42912213.057	4814.5	0.1
L42921533.036	5469.0	0.1
M42921533.023	5871.0	0.1
S42921533.026	5261.5	0.1
L42921859.031	3998.0	0.1
T42921859.028	4275.0	0.1
L42932129.029	5455.5	-0.1
T42932129.026	5797.0	0.1
L42891418.037	4928.5	-0.1
S42921438.033	3994.0	-0.2
M42891418.053	5475.5	0.2
L42932303.013	5848.0	0.2
M42932303.035	5889.5	0.2
S42911623.002	4528.5	0.2
T42921429.018	3944.0	-0.3
T42902209.030	3713.0	0.3
T42892327.012	5168.0	0.3
S42911807.026	4363.0	0.3
L42921829.039	4112.5	0.3
T42911807.032	4579.5	-0.3
T42891905.008	3888.0	0.3
T42911851.007	5859.5	0.3
T42911958.056	4692.5	0.3
T42900136.021	4554.5	0.3
M42921438.014	4358.0	0.3
M42901828.047	4778.0	0.3
L42911807.029	4572.5	0.4
T42921533.036	5751.5	-0.4
L42912213.057	4443.5	-0.4
M42911807.029	4144.5	0.4
S42901821.025	4187.0	-0.4
L42921429.022	2295.0	0.5
M42932129.021	5872.0	-0.5
T42910325.028	5643.0	0.6
S42932129.018	6385.5	-0.6
T42892313.008	5583.5	0.6
L42911851.003	4626.5	-0.6
M42891815.038	3481.5	0.6
L42902247.013	4145.0	-0.6
M42910325.026	5540.0	0.7
M42902210.022	4852.0	0.7
L42911959.017	4398.0	-0.7
T42911602.003	5197.5	0.8
S42892327.018	4896.0	-0.8
T42902246.038	3742.0	0.9
M42911602.038	3788.0	0.9
M42921838.008	9958.5	0.9

REGIONAL EVENTS

EVENT NAME	RANGE	ERROR
T42891814.046	4812.0	1.2
L42891719.058	4166.5	1.2
S42932303.035	5628.5	-1.2
T42921829.039	4849.5	-1.2
L42910325.032	5353.0	1.4
M42891719.057	3826.0	1.7
L42892327.016	4615.5	-1.8
T42891719.047	4242.5	1.9
S42921829.023	5681.5	-2.0
M42912214.052	4867.0	2.1
S42921858.056	3923.5	2.3
S42911851.011	5646.0	-2.4
M42891906.042	3349.5	2.7
L42902228.027	2860.0	3.0
M42902246.029	4954.5	4.4
S42902211.000	2880.0	5.1
S42902247.016	2987.0	5.4
S42911958.058	6332.0	-6.3
L42891815.018	4178.0	6.5
S42891719.025	4825.5	7.4
L42901821.016	4425.5	7.5
T42901820.037	3292.0	-9.1
S42891815.018	3478.5	10.4
M42900137.019	4288.0	12.6
M42911953.028	4199.0	13.4
S42891903.018	3351.0	-15.1
M42892313.022	4768.5	-15.3
L42891906.038	3868.5	-17.5
S42910325.016	5376.0	-22.9
M42921859.054	4645.5	-22.6
S42912215.001	5845.0	-23.7
L42900136.053	4227.5	-25.0
L42911602.027	4522.0	-33.3

NUMBER OF EVENTS = 88
MEDIAN = 0.6
MEAN = 3.5
VARIANCE = 135.6

TABLE 4 (Continued)

TELESEISMIC EVENTS

EVENT NAME	RANGE	ERROR
T42970815.046	5751.5	0.0
T42980019.051	5564.5	-0.1
L42920528.008	5145.5	-0.1
S42920528.001	4184.0	0.1
T42920528.008	5536.0	-0.1
T42951308.257	5539.5	0.1
S42970815.039	5909.5	0.1
M42980019.053	4573.5	0.1
L42980019.051	4862.0	-0.2
S42980021.023	4569.5	0.2
M42951908.252	5725.0	0.2
L42951908.257	5912.5	0.3
M42970815.043	6135.5	-0.9
L42970815.046	6091.0	-1.1
S42951909.200	5251.5	-1.1
M42920528.004	5799.5	-3.4

NUMBER OF EVENTS = 16
MEDIAN = 0.1
MEAN = 0.5
VARIANCE = 859.8

noise poorly. One way to improve the effectiveness of the detection method is to extend the time preceding the 6.4 second window triggering the fast Walsh detector to 60 seconds. Past experience in picking the first arrival has shown that while the Pn arrival sometimes precedes the Pg arrival triggering the Walsh detector by more than 30 seconds all of the Pn arrivals are included in the first 60 seconds preceding the window triggering the detector. Then only overlapping seismic events will cause the performance of the detector to deteriorate. Of the 400 event traces in the data set only four were overlapping events. Table 4 lists the errors relative to the analyst's picks in the automatic first arrival picks and the range of the rank sums for all the events and for each individual type of event; i.e., local, regional and teleseismic. The illustrations depicting the performance of the automatic detector and first arrival picker on 152 event traces are included in appendix D.

CONCLUSIONS AND SUGGESTIONS FOR FUTURE WORK

The rank sum detector is extremely robust and excellent for distinguishing a broad category of seismic signals from noise. However, the time preceding the window triggering detection in the fast Walsh detector should be increased to 60 seconds. To illustrate this conclusion let us examine an extreme case where we would like the detector to pick either Pn or Lg as the first arrival for later event association and location. Suppose the fast Walsh detector fails to trigger on the Pn arrival from a regional event 13^{o} from the recording station. The maximum time interval between Pn and Pg at 13^{o} is 57 seconds. So if the fast Walsh detector triggered on Pg, the Pn arrival would still be included in the event trace file if the predetection time was increased to 60 seconds. If the fast Walsh detector triggered on Lg instead of Pg, then we conclude the Pn arrival must be too far below the background noise level for even a human analyst to discern otherwise the fast Walsh detector would have triggered on Pg instead of Lg. In this event the human analyst would pick Pg as the first arrival when we would rather have him pick Lg for later association purposes. Since the time interval between Pg and Lg for a regional event 13^{o} from

the recording station is 3 minutes, the automatic detector would select Lg as the first arrival. The real time fast Walsh detector writes seismic events occurring closer together than 60 seconds into a continouous event file. There should be no significant problem with overlapping events in extending the pre-detection time to 60 seconds for each event file. Then 99% of the automatic picks should be correct within a median error of plus or minus 0.2 seconds (see Table 5).

The next step is to develop a criteria to break up the class of signals detected into local, regional and teleseismic events and then into earthquakes and explosions. Decision tree or stratified layer classification is designed to take advantage of such situations (one or two features; i.e. slope, period or amplitude) to improve efficiency and, if possible accuracy. The decision tree classifier progresses through a series of stages or layers; at each layer certain *classes (local, regional and teleseismic)* are separated in the simplest manner possible. It is flexible and permits different features and classifications (boundaries) to be used to separate different classes. (Schowengerdt, R.A., 1983).

TABLE 5. Errors (Automatic Minus Analyst Picks in Seconds), and Ranges of the Rank Sums of Events Which do not Violate the Initial Assumptions

ALL EVENTS EXCEPT THOSE WHICH VIOLATE THE INITIAL ASSUMPTIONS OF THE RANK2700 DETECTOR

EVENT NAME	RANGE	ERROR
S42891418.037	5857.0	0.0
L42892284.039	5576.5	0.0
L42892313.003	4882.5	0.0
M42888137.018	4228.0	0.0
L42881831.016	4425.5	0.0
T42881823.037	3232.0	0.0
L42910325.032	5958.0	0.0
L42911682.007	4522.0	0.0
M42911682.039	3788.0	0.0
T42911682.003	5197.5	0.0
L42911851.003	4626.5	0.0
M42911851.351	3742.0	0.0
M42911959.008	4199.0	0.0
T42912140.015	5518.5	0.0
M42921833.008	3958.5	0.0
S42921858.056	3922.5	0.0
M42922129.031	5070.0	0.0
S42922129.019	6385.5	0.0
S42922283.035	5628.5	0.0
T42922283.013	5322.0	0.0
S42951389.000	5251.5	0.0
S42962039.014	4264.5	0.0
T42962037.016	3655.0	0.0
T42972815.046	5751.5	0.0
L42971753.018	5272.0	0.0
S42971753.018	6174.0	0.0
T42971752.052	5585.0	0.0
M42971951.000	2483.5	0.0
T42971351.000	3413.5	0.0
S42921533.026	5251.5	0.1
M42892229.027	3311.5	0.1
L42921859.021	3958.0	0.1
M42900819.052	4573.5	0.1
T42921859.029	4275.0	0.1
L42932129.009	5495.5	-0.1
T42900819.051	5564.5	-0.1
L42891418.037	4923.5	-0.1
T42932125.006	5737.0	0.1
S42920126.021	3591.0	0.1
T42891418.034	5349.5	-0.1
S42892213.016	5454.0	0.1
T42951989.057	5539.5	0.1
L42962037.016	3722.5	0.1
M42912140.042	5149.0	0.1
M42892255.029	4294.0	0.1
S42972815.039	5589.5	0.1
T42912213.057	4814.5	0.1
L42900519.008	5145.5	-0.1
S42920518.021	4184.0	0.1
T42920518.008	5536.0	-0.1
L42921533.026	5469.0	0.1
M42921533.023	5871.0	0.1
T42982056.044	5984.0	0.2

ALL EVENTS EXCEPT THOSE WHICH VIOLATE THE INITIAL ASSUMPTIONS OF THE RANK2700 DETECTOR

EVENT NAME	RANGE	ERROR
S42921420.038	3994.0	-0.2
T42892284.016	5748.0	0.2
S42900821.022	4569.5	0.2
M42891418.053	5475.5	0.2
L42932283.018	5843.0	0.2
M42932283.035	5889.5	0.2
M42871753.038	5829.5	0.2
S42911683.000	4528.5	0.2
L42982056.044	5584.0	-0.2
M42951988.053	5725.0	0.2
L42900819.051	4862.0	-0.2
S42911887.026	4369.0	0.3
T42911887.032	4573.5	-0.3
T42892327.012	5168.0	0.3
T42900136.021	4554.5	0.3
M42921438.014	4350.0	0.3
T42911851.007	5059.5	0.3
T42921429.018	3944.0	-0.3
T42891985.008	3888.0	0.3
T42911958.056	4692.5	0.3
M42901828.047	4770.0	0.3
L42921829.039	4112.5	0.3
L42951988.057	5912.5	0.3
T42982209.020	3713.0	0.3
M42911887.029	4144.5	0.4
L42912213.057	4443.5	-0.4
T42921533.026	5751.5	-0.4
M42962038.001	4733.5	0.4
S42981821.025	4187.0	-0.4
L42912143.015	5728.0	0.4
L42911887.029	4572.5	0.4
L42982247.013	4145.0	-0.5
T42892313.008	5583.5	0.5
T42910325.029	5643.0	0.6
M42891815.038	3481.5	0.6
M42910325.026	5548.0	0.7
L42911959.017	4398.0	-0.7
M42982218.022	4052.0	0.7
S42892327.018	4096.0	-0.8
T42982246.028	3742.0	0.8
M42972815.043	6135.5	-0.8
L42972815.046	6091.0	-1.1
T42921829.039	4849.5	-1.2
L42971352.037	4583.0	1.2
T42891814.046	4812.0	1.2
L42891719.053	4166.5	1.2
M42891719.057	3826.0	1.7
L42892327.016	4615.5	-1.8
T42891719.047	4242.5	1.8
M42891986.043	3349.5	2.7
L42982229.027	2868.0	3.2
M42928528.004	5799.5	-3.4
M42892234.028	4133.5	-5.1

TABLE 5 (Continued)

ALL EVENTS EXCEPT THOSE WHICH VIOLATE THE INITIAL ASSUMPTIONS OF THE RANK2700 DETECTOR

EVENT NAME	RANGE	ERROR
S42892384.012	5496.0	-6.3
S42891719.025	4805.5	7.4

NUMBER OF EVENTS = 188
MEDIAN = 0.2
MEAN = 0.5
VARIANCE = 1.3

LOCAL EVENTS EXCEPT THOSE WHICH VIOLATE THE INITIAL ASSUMPTIONS OF THE RANK2700 DETECTOR

EVENT NAME	RANGE	ERROR
L42892384.039	5576.5	0.0
T42912140.015	5518.5	0.0
S42962038.014	4264.5	0.0
T42962037.016	3655.0	0.0
L42971753.018	5272.0	0.0
S42971753.018	6174.0	0.0
T42971752.052	5585.0	0.0
M42971551.000	2483.5	0.0
T42971951.000	3419.5	0.0
M42902055.038	4294.0	0.1
L42962037.016	3722.5	0.1
M42912140.040	5149.0	0.1
L42902054.044	5584.0	-0.2
T42892384.016	5742.0	0.2
T42902054.044	5984.0	0.2
M42971753.030	5039.5	0.2
L42912140.015	5732.0	0.4
M42962038.001	4733.5	0.4
L42971952.007	4583.0	1.2
M42892384.028	4193.5	-5.1
S42892384.012	5496.0	-6.3

NUMBER OF EVENTS = 21
MEDIAN = 0.1
MEAN = 0.7
VARIANCE = 11.5

TABLE 5 (Continued)

REGIONAL EVENTS EXCEPT THOSE WHICH VIOLATE THE INITIAL ASSUMPTIONS OF THE RANK2700 DETECTOR

EVENT NAME	RANGE	ERROR
S42891418.037	5057.0	0.0
L42892313.003	4002.5	0.0
M42900137.019	4200.0	0.0
L42901821.016	4405.5	0.0
T42901820.037	3292.0	0.0
L42910325.032	5958.0	0.0
L42911602.007	4522.0	0.0
M42911602.038	3786.0	0.0
T42911602.003	5197.5	0.0
L42911851.003	4626.5	0.0
M42911851.051	3742.0	0.0
M42911959.006	4198.0	0.0
M42921830.008	3958.5	0.0
S42921858.056	3923.5	0.0
M42932129.031	5078.0	0.0
S42932129.010	6385.5	0.0
S42932303.035	5628.5	0.0
T42932303.019	5323.0	0.0
L42921533.036	5469.0	0.1
M42921533.023	5871.0	0.1
S42921533.026	5261.5	0.1
S42900136.031	3581.0	0.1
L42921859.031	3998.0	0.1
L42891418.037	4928.5	-0.1
T42921859.028	4275.0	0.1
L42932129.009	5495.5	-0.1
S42892313.016	5454.0	0.1
M42892328.007	9311.5	0.1
T42932129.006	5797.0	0.1
T42891418.034	5349.5	-0.1
T42912213.057	4814.5	0.1
M42891418.053	5475.5	0.2
L42932303.019	5848.0	0.2
M42932303.035	5889.5	0.2
S42921438.030	3994.0	-0.2
S42911603.000	4508.5	0.2
T42891905.008	9888.0	0.3
T42911851.007	5059.5	0.3
M42901828.047	4778.0	0.3
T42911858.056	4692.5	0.3
T42892327.012	5168.0	0.3
M42921438.014	4358.0	0.3
T42902209.030	3713.0	0.3
T42921429.018	3944.0	-0.3
S42911807.026	4369.0	0.3
T42911807.032	4579.5	-0.3
T42900136.021	4554.5	0.3
L42921829.039	4112.5	0.3
S42901821.025	4187.0	-0.4
T42921533.036	5751.5	-0.4
L42912213.057	4443.5	-0.4
L42911807.029	4572.5	0.4
M42911807.029	4144.5	0.4

REGIONAL EVENTS EXCEPT THOSE WHICH VIOLATE THE INITIAL ASSUMPTIONS OF THE RANK2700 DETECTOR

EVENT NAME	RANGE	ERROR
T42910325.029	5643.0	0.6
T42892313.008	5583.5	0.6
L42902247.013	4145.0	-0.6
M42891815.038	9481.5	0.6
M42902210.022	4852.0	0.7
M42910325.026	5548.0	0.7
L42911959.017	4398.0	-0.7
S42892327.010	4896.0	-0.8
T42902246.038	3742.0	0.9
T42921829.039	4849.5	-1.2
L42891719.050	4166.5	1.2
T42891814.046	4812.0	1.2
M42891719.057	3826.0	1.7
L42892327.016	4615.5	-1.8
T42891719.047	4242.5	1.9
M42891906.040	9349.5	2.7
L42902209.027	2868.0	3.0
S42891719.025	4805.5	7.4

NUMBER OF EVENTS = 71
MEDIAN = 0.2
MEAN = 0.5
VARIANCE = 4.5

TABLE 5 (Continued)

TELESEISMIC EVENTS EXCEPT THOSE WHICH
VIOLATE THE INITIAL ASSUMPTIONS
OF THE RANK2700 DETECTOR

EVENT NAME	RANGE	ERROR
S42951989.000	5251.5	0.0
T42978815.046	5751.5	0.0
L42928528.008	5145.5	-0.1
S42928528.001	4184.0	0.1
T42928528.008	5536.0	-0.1
M42900019.053	4579.5	0.1
T42951988.057	5539.5	0.1
S42978815.039	5909.5	0.1
T42900019.051	5564.5	-0.1
S42900021.023	4569.5	0.2
M42951988.050	5725.0	0.2
L42900019.051	4862.0	-0.2
L42951988.057	5912.5	0.3
M42978815.043	6135.5	-0.9
L42978815.046	6091.0	-1.1
M42928528.004	5799.5	-3.4

NUMBER OF EVENTS = 16
MEDIAN = 0.1
MEAN = 0.4
VARIANCE = 22.9

THE FOLLOWING PAGES CONTAIN

APPENDIXES AND EVENTS

APPENDIX A

FAST WALSH TRANSFORM DETECTOR

The Walsh functions are an ordered set of rectangular waveforms whose amplitudes take the values +1 or -1. They are arranged in order of increasing number of zero-crossings per time interval, so called sequency order.

Sequency is defined as one half the number of zero-crossings per interval. The sequency of Walsh transforms is analogous to the frequency of sines and cosines used in Fourier analysis.

Any time series can be expressed as the weighted sum of a series of Walsh functions. The Walsh transform provides the coefficients for the summation in the same way as done by a Fourier transform. The advantage of the fast Walsh transform is that it can be computed much faster than the Fourier transform because it involves only integer addition and shifting. The macro subroutine for the fast Walsh transform used in the real time event detector is listed in appendix C.

One complication of the fast Walsh transform is that it does not produce a spectrum in sequency order. Instead, it produces a Paley ordered spectrum (sometimes called natural order) in which the subscripts have been bit-reversed. The seismic event detection program uses lookup table A.1 to convert a sequency subscript from the passband into a bit-reversed Paley subscript in the transformed spectrum. (GSETT Report, Paul Golden, 1985)

TABLE A.1 Sequency Subscript to Bit-Reversed Paley Subscript Conversion

SEQUENCY ORDERED SUBSCRIPTS		BIT-REVERSED PALEY ORDERED SUBSCRIPTS	
1	1	1	1
2	64	2	33
3	32	3	49
4	33	4	17
5	16	5	25
6	49	6	57
7	17	7	41
8	48	8	9
9	9	9	13
10	57	10	45
11	25	11	61
12	40	12	29
13	9	13	21
14	56	14	53
15	24	15	37
16	41	16	5
17	4	17	7
18	61	18	39
19	29	19	55
20	36	20	23
21	13	21	31
22	52	22	63
23	20	23	47
24	45	24	15
25	5	25	11
26	60	26	43
27	28	27	59
28	37	28	27
29	12	29	19
30	53	30	51
31	21	31	35
32	44	32	3
33	2	33	4
34	63	34	36
35	31	35	52
36	34	36	20
37	15	37	28
38	50	38	60
39	18	39	44
40	47	40	12
41	7	41	16
42	58	42	40
43	26	43	64
44	39	44	32
45	10	45	24
46	55	46	56
47	23	47	40
48	42	48	8
49	3	49	6
50	62	50	38
51	30	51	54
52	35	52	22
53	14	53	30
54	51	54	62
55	19	55	46
56	46	56	14
57	6	57	10
58	59	58	42
59	27	59	50
60	30	60	26
61	11	61	10
62	54	62	50
63	22	63	34
64	43	64	2

The time series data in the detection window is transformed using the fast Walsh transform. The absolute values of the weighted coefficients are summed across the pass band. The sum is then normalized by shifting to the value it would have had if the weights had all been 1. This normalized sum is the magnitude which is compared to the threshold for the channel. A magnitude below the threshold triggers the detection.

When detection occurs the signal is written to an event file. This event file is later graphically displayed to enable a seismic analyst to discriminate between an "event" signal and "glitches" or "noise" and to pick the event parameters. (Goforth and Herrin, 1981)

APPENDIX B

Subroutines

LIST OF SUBROUTINES

AR_SPECTRA - COMPUTES AR(P) SPECTRAL ESTIMATES

AKAIKE - COMPUTES AR YULE-WALKER COEFFICIENTS

COV - COMPUTES AUTOCORRELATIONS FOR A TIME SERIES

DETECTOR - DETECTOR USED TO TEST NONPARAMETRIC TESTS

IFWM64 - INTEGER FAST WALSH TRANSFORM IN MACRO FOR 64 POINT WINDOW

NEIGHBOR - COMBINES SEGMENTS WITH NEAREST NEIGHBOR DECISION RULE

PDF - COMPUTES DENSITY DISTRIBUTION HISTOGRAMS

Polr_A-BURG - COMPUTES AR BURG COEFFICIENTS

RANKFREQ - COMPUTES RANKS AND FREQUENCIES FOR N OBSERVATIONS

RANKTEST - COMPUTES THE RANK SUM SUM TEST FOR N+M OBSERVATIONS

RANK2700 - DETECTOR BASED ON A MODIFIED RANK SUM TEST

RUNEXP - COMPUTES THE RUN TEST FOR N+M OBSERVATIONS

SIGNEXP - COMPUTES THE SIGN TEST FOR N OBSERVATIONS

SLOPE - COMPUTES MODIFIED SLOPE FOR A TIME SERIES

```
      SUBROUTINE AR_SPECTRA(FMAX,FMIN,COEF,NCOEF,
     +                      PF,PFLOG,NF,VAR,ARMAX)
C
C---     This subroutine computes the AR spectral estimate as
C---  defined by M.B. Priestly in Spectral Analysis and Time Series,
C---  (paperback), p. 881, 1981.
C
      REAL FMAX                                    !FREQUENCY MAXIMUM
      REAL FMIN                                    !FREQUENCY MINIMUM
      REAL COEF(NCOEF)                             !AR COEFFICIENTS
      REAL PF(251)                          !AMPLITUDE OF AR_SPECTRA AT F
      REAL PFLOG(251)                    !AMPLITUDE IN dB OF AR_SPECTRA AT F
      REAL VAR                           !VARIANCE OF WHITE NOISE OF PROCESS
      INTEGER NCOEF                             !NUMBER OF AR COEFFICIENTS
      COMPLEX*8 CMPLXF,CONST,SUM
      COMPLEX*8 TWOPII/(0.0,6.28318530718)/
      REAL TWOPI/6.28318530718/
      INTEGER NF                        !NUMBER OF POINTS IN AR-SPECTRA
C
C---  COMPUTE SPECTRAL ESTIMATE FOR EACH FREQUENCY
C
      F = FMIN
      SRATE = FLOAT(NF-1)/(FMAX-FMIN)     !COMPUTE FREQUENCY INCREMENT
      DO K = 1,NF
        F = (FLOAT(K-1)/SRATE) + FMIN                !(K-1)th FREQUENCY
        SUM = CMPLX(1.0,0.0)
        IF (NCOEF.GE.1) THEN
          DO I=1,NCOEF
            CMPLXF = CMPLX(F*I,0.0)                      !COMPLEX FREQUENCY
            SUM = SUM - CMPLX(COEF(I),0.0)*CEXP(TWOPII*CMPLXF)
          END DO
        END IF
        CONST = SUM*CONJG(SUM)
        PF(K) = 1./REAL(CONST)
        PF(K) = PF(K)*2.*VAR                  !VAR = VARIANCE OF NOISE DATA
        PFLOG(K) = 20.*ALOG10(PF(K))           !AMPLITUDE IN dB OF SPECTRA
        ARMAX = MAX(PFLOG(K),ARMAX)            !MAXIMUM SPECTRAL AMPLITUDE
      END DO !K
      RETURN
      END
```

```
      SUBROUTINE AKAIKE(X,N,M,ACF,ML,COEF)
C
C
C---     Modified from Gray-Woodward ARMA spectral analysis
C---  package for the IBM PC by Kathleen A. Alden 1-30-86.
C---  This subroutine computes the Yule-Walker coefficients
C---  as described by Kay and Marple, (1982).
C
      REAL X(1)  !SERIES
      REAL FPE(30) !WORK ARRAY FOR FINAL PREDICTION ERROR (FPE)
      REAL ACF(1)  !AUTOCORRELATION
      REAL A(30,30) !WORK ARRAY
      REAL COEF(1)  !YULE-WALKER COEFFICIENTS
      INTEGER N     !LENGTH OF X SERIES
      INTEGER M     !MAXIMUM ORDER OF FPE
      INTEGER ML    !ORDER SELECTED BY FPE
C
      MLAG=100
      ICOEF=1
      SUM=0.0
      DO 51 I=1,N
      SUM = SUM + X(I)
   51 CONTINUE
      XBAR=SUM/N
      XSQ=0.0
      DO 52 I=1,N
      X(I) = X(I) - XBAR
      XSQ = XSQ + X(I)*X(I)
   52 CONTINUE
      PV = XSQ/N
C     CALCULATION OF AR COEF'S. USING YULE-WALKER EQUATIONS
      A(1,1) = ACF(2)
      FPE(1) = (1.0-(A(1,1)*A(1,1)))*(N+2)/(N-2)
      M1 = M-1
      DO 2 I=1,M1
      SN = 0.0
      SD = 0.0
      DO 3 J=1,I
      SN = SN + A(I,J)*ACF(I+2-J)
      SD = SD + A(I,J)*ACF(J+1)
    3 CONTINUE
      A(I+1,I+1) = (ACF(I+2) - SN)/(1.0-SD)
      FPE(I+1) = FPE(I)*(N+I+2)*(N-I-1)*(1.0-A(I+1,I+1)*A(I+1,I+1) ) /
     + ( (N-I-2)*(N+I+1) )
      DO 4 J=1,I
      A(I+1,J) = A(I,J) - A(I+1,I+1)*A(I,I-J+1)
    4 CONTINUE
    2 CONTINUE
      IF(ICOEF.EQ. 0) GO TO 15
   16 CONTINUE
   15 CONTINUE
      I=1
      J=2
    7 IF(FPE(I) .LE. FPE(J)) GO TO 5
      I = J
      J = J + 1
      GO TO 8
    5 J = J + 1
    8 IF(J .GT. M) GO TO 6
      GO TO 7
    6 ML=I
      DO 65 I=1,ML
   65 COEF(I)=A(ML,I)
      RETURN
      END
```

```
      SUBROUTINE COV(X,L,XB,GV,D,N)
C
C--       This subroutines calculates N autocorrelations, the
C--    sample mean, and the variance equal to the zero lag auto-
C--    variance for the input time series, x(I), I=1,L.
C--    Taken from the Gray-Woodward ARMA spectral estimation
C--     package, 1985.
C
C--      X=SERIES -INPUT
C--      L=LENGTH OF SERIES - INPUT
C--      XB=MEAN - OUTPUT
C--      GV=VARIANCE  - OUTPUT
C--      D=AUTOCORRELATIONS - OUTPUT
C--      N=NUMBER OF AUTOCORRELATIONS TO CALCULATE -INPUT
C--      NOTE:D(I)=AUTOCORRELATIONS AT LAG I-1
C
      REAL X(1)
      REAL D(1)
C
C--   COMPUTE THE SAMPLE MEAN FOR X(I), I=1,L
C
      XB=0.0
      DO 25 I=1,L
   25 XB=XB+X(I)
      XB=XB/FLOAT(L)
C
C--   COMPUTE THE AUTOCOVARIANCES AT LAGS = 0,(N-1)
C
      DO 30 I=1,N
      D(I)=0.0
      NK=L-I+1
      DO 40 J=1,NK
   40 D(I)=(X(J)-XB)*(X(I+J-1)-XB)+D(I)
   30 CONTINUE
C
C--   SAMPLE VARIANCE EQUALS THE AUTOCOVARIANCE AT LAG = 0.
C
      GV=D(1)
C
C--   NORMALIZE THE AUTOCOVARIANCES TO OBTAIN THE AUTOCORRELATION
C
      DO 50 I=1,N
   50 D(I)=D(I)/GV
      RETURN
      END
```

```
      SUBROUTINE DETECTOR(NSAMPLES,N,MEAN,K,INC,
     +                    TRC,SEGLEN,PATTERN,IST,SN,RANK)
C
C--- SUBROUTINE TO PERFORM TWO SAMPLE SIGN TEST
C--- MOODY,GRAYBILL & BOES
C
      REAL TEST
      REAL PATTERN(1) !1.=H0,2.=HA
      REAL TRC(1) !TRACE CONTAINING SIGNAL
      REAL SEGLEN(1) !SAMPLE LENGTH OF PATTERN
      REAL MEAN
      REAL SN !MAX SIGNAL TO NOISE RATIO FOR TRACE
      INTEGER NSAMPLES
      INTEGER INC !INCREMENT WINDOW MOVES DOWN TRACE
      INTEGER IST !START IN WINDOW
      INTEGER N !NUMBER OF SAMPLES IN NOISE PART OF TEST
      INTEGER K !ACCEPT OR REJECT CRITERIA
      REAL T(300,3) !WORK ARRAY FOR ORDERING SAMPLES
      REAL RANK(1) !SUMATION OF RANKS OF SIGNAL
      LOGICAL ACCEPT/.FALSE./
C
C--- COMPUTE RANK SUM TEST OVER TRACE
C
      N2 = 2*N
      SN = MEAN
      ENMAX = 0.0
      DO I=1,N
        L = I-1
        PATTERN(NSAMPLES-L) = 1.0
        SEGLEN(NSAMPLES-L) = 1.0
        PATTERN(I) = 1.0
        SEGLEN(I) = 1.0
        T(I,1) = ABS(TRC(I*2-1))
        T(I+N,1) = ABS(TRC(I*2))
        ENMAX = MAX(T(I,1),ENMAX)
        ENMAX = MAX(T(I+N,1),ENMAX)
      END DO
      ENMAX = ENMAX*1.05
        IR = 0
        DO I=1,(NSAMPLES-N),INC
          IR = IR + 1
          DO J=1,N
            JJ = J + (I-1)
            T(J+N,1) = ABS(TRC(JJ))
          END DO !J=1,N
          CALL RANKTEST(N,T(1,1),T(N+1,1),K,TY,ACCEPT)
          SN = MAX(TY,SN)
          RANK(IR) = TY
          IF (ACCEPT) THEN
            DO L=I,(I+(INC-1))
              PATTERN(L) = 2.0 !REJECT H0
              SEGLEN(L) = 1.0
            END DO
          ELSE
            DO L=I,(I+(INC-1))
              PATTERN(L) = 1.0 !ACCEPT H0
              SEGLEN(L) = 1.0
            END DO
          END IF
        END DO !I
        SN = SN/RANK(1)  !MAX SIGNAL RANK /NOISE RANK
        RETURN
        END
```

```
        .TITLE      IFWM64

;       LENGTH 64 INTEGER FAST WALSH TRANSFORM.
;       IMPLEMENTS FORTRAN VERSION IN IFWF64.FOR .
;       LABELS AND VARIABLE NAMES IN COMMENTS ARE
;       FROM THE FORTRAN VERSION.
;       BY DWIGHT DEURING ON 22-NOV-82.
;       Modified 12-SEP-84 to handle integer overflow
;
;               INTEGER*2 X(64)
;               CALL IFWM64(X)
;       PRODUCES TRANSFORM IN-PLACE WITH RESULT IN
;       BIT-REVERSED DYADIC (NATURAL) ORDER.
;
;                                               ;# OF ELEMENTS
SIZ=64                                          ;64 = 2**6
PWR=6
L=SIZ/2

;
        .PSECT      IFWM64
        .ENTRY      IFWM64, ^M<R2,R3,R4,R5,R6,R7>
; REGISTER USAGE:
;       R0      I       ITERATION CONTROL
;       R1      L*2       L AS WORD INDEX
;       R2      R
;       R3      POINTS TO X(P)
;       R4      POINTS TO X(PPL)
;       R5      J
;       R6      K*2       K AS WORD INDEX
;       R7      XP
;
        MOVZBL      #PWR,R0                 ;ITERATION COUNT
        MOVL        @#<L*2>,R1              ;L*2
        MOVZBL      #1,R2                   ;R
        MOVZBL      4(AP),R3                ;ADDR(X(P)), P=1
10$:    MOVL        R3,R1,R4                ;ADDR(X(PPL)), PPL=L+1
        ADDL3       #1,R5                   ;J=1
        MOVZBL      #2,R6                   ;2K=2 (WORD INDEX)
20$:    MOVZBL      (R3),R7                 ;XP=X(P)
30$:    MOVW        R7,(R4),(R3)+           ;X(P)=XP+X(PPL), P=P+1
        ADDW3       #^X8001,-2(R3)          ;no overflow, OK
        BVC         40$                     ;sign changed to negative
        BLSS        35$                     ;largest negative+1 (so IABS()
        MOVW        #^X7FFF,-2(R3)          ;use largest positive
        BRB         40$                     ;X(PPL)=XP-X(PPL), PPL=PPL
35$:    MOVW        (R4),R7,(R4)+           ;no overflow, OK
40$:    SUBW3       #^X8001,-2(R4)          ;sign changed to negative
        BVC         50$                     ;largest negative+1 (so IABS()
        BLSS        45$                     ;use largest positive
        MOVW        #^X7FFF,-2(R4)          ;2K=2K+2
        BRB         50$
45$:    MOVW        #2,R6
50$:    ADDL2       R6,R1                   ;IF(K.LE.L)
        CMPL        R1,R3                   ;P=P+L
        BLEQ        30$                     ;PPL=PPL+L
        ADDL2       R1,R4                   ;J=J+1
        ADDL2       R5
        INCL        R5,R2                   ;IF(J.LE.R)
        CMPL        #2$                     ;L=L/2
        BLEQ        #-1,R1,R1               ;R=R*2
        ASHL        #1,R2,R2
        ASHL        R0,10$
        SOBGTR      RET

;
        .END
```

```
      SUBROUTINE NEIGHBOR(MAXLEN,SEG,NSEGMENTS,NMIN)
C
C--       The nearest neighbor decision rule first compares the
C--   feature vector for each segment of an array of observations.
C--   Each segment is tagged with a 0 or 1 to indicate its affinity
C--   to either the previous or next segment respectively.  Then
C--   the segments which have an affinity for each other are combined
C--   and their features are averaged.  This continues until the
C--   number of segments becomes less than or equal to the minimum
C--   number of segments desired.
C
C--   Code written by Kathleen A. Alden, March 14,1984.
C
C     SEG(I,J) - INPUT VECTOR FOR ITH SEGMENT, J=1,8
C                SEG(I,1) = AMPLITUDE
C                SEG(I,2) = ESTIMATED PERIOD
C                SEG(I,3) = NUMBER OF OBSERVATIONS IN ITH SEGMENT
C                SEG(I,4) = ABSOLUTE DIFFERENCE BETWEEN
C                           I-1 AND I SEGMENT AMPLITUDES
C
C                SEG(I,5) = ABSOLUTE DIFFERENCE BETWEEN
C                           I-1 AND I SEGMENT PERIODS
C
C                SEG(I,6) = ABSOLUTE DIFFERENCE BETWEEN
C                           I+1 AND I SEGMENT AMPLITUDES
C
C                SEG(I,7) = ABSOLUTE DIFFERENCE BETWEEN
C                           I+1 AND I SEGMENT PERIODS
C                SEG(I,8) = 0 INDICATES AFFINITY WITH NEXT SEGMENT
C                           1 INDICATES AFFINITY WITH PREVIOUS SEGMENT
C                NSEGMENTSMENTS = NUMBER OFSEGMENTS IN TRACE
C                NMIN = MINIMUM NUMBER OF SEGMENTS IN TRACE
C
      REAL SEG(MAXLEN,8)
      INTEGER NSEGMENTS !TOTAL NUMBER OF SEGMENTS
      INTEGER NMIN !MINIMUM NUMBER OF SEGMENTS
C
C-- DETERMINE AFFINITY OF EACH SEGMENT
C
      DO WHILE(NSEGMENTS.GT.NMIN)
        SEG(1,8) = 0.              !1ST SAMPLE AFFINITY W/NEXT SEGMENT
        SEG(NSEGMENTS,8) = 1.0     !LAST SAMPLE AFFINITY W/PREVIOUS
        DO I=2,NSEGMENTS-1
          SEG(I,4) = ABS(SEG(I-1,1)-SEG(I,1))        !PREV AMPLT DIF
          SEG(I,5) = ABS(SEG(I-1,2)-SEG(I,2))        !PREV PER   DIF
          SEG(I,6) = ABS(SEG(I+1,1)-SEG(I,1))        !NEXT AMPLT DIF
          SEG(I,7) = ABS(SEG(I+1,2)-SEG(I,2))        !NEXT PER   DIF
          IF (SEG(I,4).GT.SEG(I,6)) THEN
            IF (SEG(I,5).GT.SEG(I,7)) THEN
              SEG(I,8) = 0.0  !PERIOD & AMPLITUDE AFFINITY W/NEXT SEG
            ELSE
              SEG(I,8) = 0.0          !AMPLITUDE AFFINITY W/NEXT SEG
            END IF
          ELSE
            IF (SEG(I,5).LE.SEG(I,7)) THEN
              SEG(I,8) = 1.0  !PERIOD & AMPLITUDE AFFINITY W/PREV SEG
            ELSE
              SEG(I,8) = 1.0          !AMPLITUDE AFFINITY W/PREV SEG
            END IF
          END IF
        END DO
C
C--   COMBINE SEGMENTS WITH AN AFFINITY FOR EACH OTHER
C
        K = 0                 !INITIAL NUMBER OF NEW COMBINED SEGMENTS
```

```
- CONTINUED -
      SUBROUTINE NEIGHBOR(MAXLEN,SEG,NSEGMENTS,NMIN)


          IF (SEG(2,8).LT.8.5) THEN
            K = K + 1
          END IF
          DO I = 2,NSEGMENTS
            IF (SEG(I,8).GT.8.5) THEN
              IF (SEG(I-1,8).LT.8.5) THEN !COMBINE FEATURES FOR NEW SEG
                K = K + 1                                          !AMPLITUDE
                SEG(K,1) = (SEG(I-1,1) + SEG(I,1))/2.                !PERIOD
                SEG(K,2) = (SEG(I-1,2) + SEG(I,2))/2.                !LENGTH
                SEG(K,3) = (SEG(I-1,3) + SEG(I,3))
              ELSE
                K = K + 1                                          !AMPLITUDE
                SEG(K,1) = SEG(I,1)                                  !PERIOD
                SEG(K,2) = SEG(I,2)                                  !LENGTH
                SEG(K,3) = SEG(I,3)
              END IF
            ELSE
              IF (SEG(I+1,8).LT.8.5) THEN
                K = K+1                                            !AMPLITUDE
                SEG(K,1) = SEG(I,1)                                  !PERIOD
                SEG(K,2) = SEG(I,2)                                  !LENGTH
                SEG(K,3) = SEG(I,3)
              END IF
            END IF
          END DO
          IF (SEG(I-1,8).LT.8.5) THEN     !COMBINE FEATURES FOR NEW SEG
            K = K + 1                                              !AMPLITUDE
            SEG(K,1) = (SEG(I-1,1) + SEG(I,1))/2.                    !PERIOD
            SEG(K,2) = (SEG(I-1,2) + SEG(I,2))/2.                    !LENGTH
            SEG(K,3) = (SEG(I-1,3) + SEG(I,3))
          END IF
          NSEGMENTS = K
        END DO !WHILE(NSEGMENTS.GT.NMIN)
        RETURN
        END
```

```
      PROGRAM PDF
C
C---     This program calculates the density distribution
C---  histograms for the background noise, first 1000 points,
C---  and the signal + noise, second 1000 points, of the seismic
C---  event traces.
C
      PARAMETER (MAXLEN=3000)
      PARAMETER (MAXNTRC=4)
      PARAMETER (IBUFSIZ=256)
      PARAMETER (NINTERV=1000)
      CHARACTER*80 BLANKS
      CHARACTER*16 FLNAME(MAXNTRC)
      CHARACTER*12 TRCTYPE
      CHARACTER*80 TCHAR
      LOGICAL SAMESCALE/.FALSE./  !ADJUST ALL TRACES TO SAME SCALE IF .TRUE.
      LOGICAL CLASS
      REAL CLASSINT  !CLASS INTERVAL FOR PROB.DENS.CALCULATION
      REAL TRACE(MAXLEN,MAXNTRC) !TRACES FOR SEISMIC EVENTS
      REAL PDNOISE(NINTERV,MAXNTRC)  !PROBABILITY DENSITY DIST. NOISE
      REAL PDSIGNAL(NINTERV,MAXNTRC) !PROBABILITY DENSITY DIST. SIGNAL+NOISE
      REAL SAMPLERATE/40./ !SAMPLES PER SECOND
      REAL SCALETRC(MAXNTRC)/1.0,1.0,1.0,1.0/ !SCALE TRACES FOR PLOTTING
      REAL FSVALUE/0.0/      !FIRST SAMPLE VALUE IN SECONDS
      REAL XINPLOT/24./   !X LENGTH OF PLOT IN INCHES
      REAL YINPLOT/20./   !Y LENGTH OF PLOT IN INCHES
      REAL  AMIN
      REAL  AMAX
      REAL GMIN/100./
      REAL GMAX/-100./
      REAL FMIN/0.0/     !FREQUENCY MINIMUM
      REAL FMAX/0.0/     !FREQUENCY MAXIMUM
      REAL AHT/0.21/      !SIZE OF CHARACTERS IN INCHES
      REAL XIN   !X-AXIS LENGTH
      REAL YIN   !Y-AXIS LENGTH
      REAL EVTXIN/24./  !EVENT X AXIS IN INCHES
      REAL EVTYIN/12./  !EVENT Y AXIS IN INCHES
      REAL PROBXIN/5./  !PROBABILITY DENS X AXIS IN INCHES
      REAL PROBYIN/3./  !PROBABILITY DENS Y AXIS IN INCHES
      REAL EVTMAX/-10.0/ !EVENT MAXIMUM PLOTTED
      REAL EVTMIN/10.0/ !EVENT MINIMUM PLOTTED
      REAL FREQMIN/0.0/ !RELATIVE FREQUENCY MINIMUM PLOTTED
      REAL FREQMAX/1.0/ !RELATIVE FREQUENCY MAXIMUM PLOTTED
      REAL IXOFF/1.0/
      REAL IYOFF/1.0/
      REAL FRC/1.0/  !FACTOR TO SCALE PLOT
      REAL XORIGIN/0.0/ !INITIAL PLOT ORIGIN
      REAL YORIGIN/0.0/ !INITIAL PLOT ORIGIN
      REAL AFACTOR/0.0/   !Y-AXIS TRACES OVERLAPP IF.LE.0.
      INTEGER ITIME(8) !ARRAY TO COMPUTE CORRECT TIME FOR 1ST SAMPLE
      INTEGER NPDFSMPS/1000/ !NUMBER OF SAMPLES IN PROBABILITY DISTR.
      INTEGER NSAMPLES/2400/ !NUMBER OF SAMPLES IN EACH TRACE
      INTEGER NCLASSINT/100/ !NUMBER OF CLASS INTERVALS
      INTEGER NPLOTS/1/  !INITIALIZE THE NUMBER OF PLOTS PLOTTED TO 1
      INTEGER STRTSAMP(MAXNTRC)/1,1,1,1/ !FIRST SAMPLE TO BE PLOTTED
      INTEGER XLABEL(20)  !LABEL FOR X-AXIS
      INTEGER YLABEL(20)  !LABEL FOR Y-AXIS
      INTEGER PLABEL(20)  !LABEL FOR PLOT
      INTEGER NCHARSX/0/
      INTEGER NCHARSY/0/
      INTEGER NCHARSP/0/
      INTEGER NTRACES/4/ !NUMBER OF TRACES
      integer ibuff   !buffer size for standard calcomp
      integer no      !number standard calcomp
      integer lgu     !logical unit number for PLOTSIN namelist
```

```
- CONTINUED -
      PROGRAM PDF


      Integer il/20/  !logical unit number for plotting device input
      Integer io/21/  !logical unit number for plotting device output
      Integer ir/1000/!resolution of plotter inc/inch
      Integer iw/8/   !plotter width in inches
      Integer it/0/   !chart type 0 = 1/2 from plot edge
c                     !          1 = 0 " from plot edge
      Integer ip/2/   !2=multipen plotter with 1" offset
      Integer iz/0/   !0=run in immediate mode
      INTEGER NEWPEN/999/ !999 FOR PLOT10,-3 FOR CALCOMP
      INTEGER*2 BUFFER(IBUFSIZ) !ELEMENTS 9-16 OF FIRST RECORD CONTAIN
C                       !IYR,IMO,IDAY,IHR,IMIN,ISEC,IHSEC,JDAY OF FIRST
C                       !SAMPLE OF EVENT TRACE
      INTEGER IYR(MAXNTRC)
      INTEGER IMO(MAXNTRC)
      INTEGER IDAY(MAXNTRC)
      INTEGER IHR(MAXNTRC)
      INTEGER IMIN(MAXNTRC)
      INTEGER ISEC(MAXNTRC)
      INTEGER IHSEC(MAXNTRC)
      INTEGER JDAY(MAXNTRC)
      INTEGER IDEC/2/ !NUMBER OF DECIMAL PLACES
      BYTE BLK(2*IBUFSIZ)  !BUFFER EQUIVALENT IN BYTES
      EQUIVALENCE (BUFFER(1),BLK(1))
      COMMON /CHARSIZ/AHT,IDEC,AFACTOR
      NAMELIST/LISTIN/FLNAME,XINPLOT,YINPLOT,NSAMPLES,NTRACES,
     +                STRTSAMP,FSVALUE,SAMPLERATE,il,io,ie,
     +                iw,it,ir,iz,NEWPEN,EVTXIN,EVTYIN,PROBXIN,
     +                PROBYIN,FREQMAX,FREQMIN,EVTMAX,EVTMIN,FAC,
     +                SAMESCALE,NCLASSINT,IDEC,NPDFSMPS,AHT,
     +                SCALETRC,AFACTOR
C
C-- READ IN NAMELIST
C
      WRITE(6,*)'TYPE IN FILENAME CONTAINING PDF NAMELIST'
      READ(5,304) FLNAME(1)
      OPEN(UNIT=22,NAME=FLNAME(1),TYPE='OLD')
      ISTAT = 0
      READ(22,NML=LISTIN,IOSTAT=ISTAT)
C
      DO WHILE(ISTAT.EQ.0)
C
C-- READ IN TRACES
C
      GMIN = 100.0
      GMAX = -100.0
      FMIN = 100.0
      FMAX = -100.0
      IDEV = 78
      DO I=1,NTRACES
        OPEN(   UNIT = IDEV,
     +          NAME = FLNAME(I),
     +          BLOCKSIZE = 2*IBUFSIZ,
     +          RECL = IBUFSIZ/2,
     +          FORM = 'UNFORMATTED',
     +          ACCESS = 'DIRECT',
     +          TYPE = 'OLD')
        ISTAT = 0
        IBLK = 1
        READ(IDEV'IBLK,IOSTAT = ISTAT) BLK
        IF (ISTAT.EQ.0) THEN
          IYR(I) = BUFFER(9)
```

```
- CONTINUED -
      PROGRAM PDF


          IMO(I) = BUFFER(10)
          IDAY(I) = BUFFER(11)
          IHR(I) = BUFFER(12)
          IMIN(I)= BUFFER(13)
          ISEC(I) = BUFFER(14)
          IHSEC(I) = BUFFER(15)
          JDAY(I) = BUFFER(16)
          J = 0
          KK = 0
          IBLK = IBLK + 1
          READ(IDEV'IBLK,IOSTAT = ISTAT) BLK
          DO WHILE(ISTAT.EQ.0.AND.J.LT.MAXLEN)
            DO L=1,IBUFSIZ
              K = J + L
              IF(K.GE.STRTSAMP(I).AND.KK.LT.MAXLEN) THEN
                KK = KK + 1
                TRACE(KK,I) = BUFFER(L)*SCALETRC(I)
                IF (KK.LE.NPDFSMPS2) THEN
                  GMIN = ABS(TRACE(KK,I))
                  GMAX = MAX(GMAX,GMIN)
                END IF
              END IF
            END DO
            J = J + IBUFSIZ
            IBLK = IBLK + 1
            READ(IDEV'IBLK,IOSTAT = ISTAT) BLK
          END DO !WHILE(ISTAT.EQ.0.AND.KK.LT.MAXLEN)
        END IF
        CLOSE(UNIT=IDEV)
        END DO
C
C--  DEFINE LIMITS
C
        GMIN = -GMAX
        IF (EVTMAX.GT.EVTMIN) THEN
           GMIN = EVTMIN
           GMAX = EVTMAX
        END IF
        IF (SAMESCALE) THEN
          EVTMAX = GMAX
          EVTMIN = GMIN
        END IF
C
C--  INITIALIZE PROBABILITY DENSITY CLASS INTERVALS TO ZERO
C
        DO I=1,NCLASSINT
          DO J=1,NTRACES
            PDNOISE(I,J) = 0.0
            PDSIGNAL(I,J) = 0.0
          END DO
        END DO
C
C-- CALCULATE CLASS INTERVAL USING GREATEST MINIMUM AND
C-- GREATEST MAXIMUM VELOCITY AMPLITUDES
C-- FOR THE FOUR EVENT TRACES PLOTTED
C
        CLASSINT = (GMAX - GMIN)/FLOAT(NCLASSINT)
        FCVALUE = GMIN + CLASSINT/2.
C
C--  CALCULATE PROBABILITY DENSITY DISTRIBUTION FOR NOISE SAMPLE 1-NPDFSMPS
C
```

```
- CONTINUED -
      PROGRAM PDF


      DO J=1,NTRACES
        DO I=1,NPDFSMPS
          K=1
          CLASS = .FALSE.
          DO WHILE(.NOT.CLASS.AND.K.LE.NCLASSINT)
            IF (TRACE(I,J).GT.(K*CLASSINT+GMIN)) THEN
              K = K + 1
            ELSE
              PONOISE(K,J) = PONOISE(K,J) + 1.0
              CLASS = .TRUE.
            END IF
          END DO !WHILE(.NOT.CLASS)
        END DO
        DO I=1,NCLASSINT
          PONOISE(I,J) = PONOISE(I,J)/FLOAT(NPDFSMPS) !RELATIVE FREQUENCY
          FMAX = MAX(FMAX,PONOISE(I,J))
        END DO
      END DO
C
C-- CALCULATE PROBABILITY DENSITY DISTRIBUTION FOR SIGNAL+NOISE
C-- NPDFSMPS+1 TO 2*NPDFSMPS
C
      NPDFSMPS2 = 2*NPDFSMPS
      DO J=1,NTRACES
        DO I=NPDFSMPS+1,NPDFSMPS2
          K=1
          CLASS = .FALSE.
          DO WHILE(.NOT.CLASS.AND.K.LE.NCLASSINT)
            IF (TRACE(I,J).GT.(K*CLASSINT+GMIN)) THEN
              K = K + 1
            ELSE
              POSIGNAL(K,J) = POSIGNAL(K,J) + 1.0
              CLASS = .TRUE.
            END IF
          END DO !WHILE(.NOT.CLASS)
        END DO
        DO I = 1,NCLASSINT
          POSIGNAL(I,J) = POSIGNAL(I,J)/FLOAT(NPDFSMPS) !RELATIVE FREQUENCY
          FMAX = MAX(FMAX,POSIGNAL(I,J))
        END DO
      END DO
      IF (FREQMAX.LT.FREQMIN) THEN
        FREQMAX = FMAX
        FREQMIN = FMIN
      END IF
C
C-- SET STATUS TO 0 AND THEN TRY TO READ ANOTHER NAMELIST
C
      ISTAT = 0
      READ(22,NML=LISTIN,IOSTAT=ISTAT)
      END DO !WHILE(ISTAT.EQ.0)
384   FORMAT(A16)
      END
```

```
      SUBROUTINE POLR_ArBURG(X,N,COEF,IP)
C
C—      Modified from Gray-Woodward ARMA spectral analysis
C—    package for the IBM PC by o.hayward  1-28-86
C—      This subroutine computes the Burg coefficients as
C—    described by Kay and Marple, (1982).
C
        Parameter (MaxOrder=50)
        Parameter (MaxPts=10000)
        Integer         N                   !number of input pts
        Real               X(N)             !time series inputs
        Real            R(MaxOrder)
        Real            C(MaxOrder+1)
        Real            S(MaxOrder+1)
        Real            Coef(IP)
        Real            AT(MaxOrder+1,2)
C
        DIMENSION Q1(maxpts),Q2(maxpts),P1(maxpts),P2(maxpts)
C
        If(N.gt.MaxPts) then
              Write(6,1) N
1             Format(1h0,'Number of input points exceeds maximum')
              Write(11,1) N
              Stop 'Polr_ArBURG —— error 1'
        End If
C
C—      CREATE A ZERO MEAN
C
        SUM=0.0
        DO  I=1,N
              SUM=SUM+X(I)
        End Do
        XBAR=SUM/N
C
        I0=0
C
C—      INITIALIZE EQUATIONS————————————————————————————
C
        IEND=N-1
        DO J=1,IEND
                    P1(J)=X(J+1)-XBAR
                  Q1(J)=X(J)-XBAR
        End Do
             TMP=0
             IEND=N-1
             DO  J=2,IEND
                 TMP=TMP+(X(J)-XBAR)**2
        End Do
             S(1+0)=(X(1)-XBAR)**2+(X(N)-XBAR)**2+2*TMP
             TMP=0
             IEND=N-1
             DO  J=1,IEND
                TMP=TMP+P1(J)*Q1(J)
        End Do
             R(1+0)=TMP
             C(1+0)=2*(R(1+0)/S(1+0))
             IEND=N-2
             DO  J=1,IEND
                     P2(J)=P1(J+1)-C(1+0)*Q1(J+1)
                   Q2(J)=Q1(J)-C(1+0)*P1(J)
        End do
             T=(1+C(1+0)**2)*S(1+0)-4*C(1+0)*R(1+0)
             S(1+1)=T-(Q1(N-0-1)-C(1+0)*P1(N-0-1))**2-(P1(1)-C(1+0)*Q1(1))**2
             DO  N1=1,IP
                     IEND=N-2
```

```
- CONTINUED -
      SUBROUTINE POLR_A-BURG(X,N,COEF,IP)


                        DO IK=1,IEND
                              P1(IK)=P2(IK)
                            Q1(IK)=Q2(IK)
                    End do
                          TMP=0
                          IEND=N-N1-1
                          DO  K=1,IEND
                             TMP=TMP+P1(K)*Q1(K)
                    End do
                          R(1+N1)=TMP
                          TMP=0
                          IEND=N-N1-1
                          DO  K=1,IEND
                             TMP=TMP+(P1(K)**2+Q1(K)**2)
                     End Do
                     S(1+N1)=TMP
                          C(1+N1)=2*(R(1+N1)/S(1+N1))
                          IEND=N-N1-2
                          DO  J=1,IEND
                                P2(J)=P1(J+1)-C(1+N1)*Q1(J+1)
                                   Q2(J)=Q1(J)-C(1+N1)*P1(J)
                     End do
                          T=(1+C(1+N1)**2)*S(1+N1)-4*C(1+N1)*R(1+N1)
                          T1=T-(Q1(N-N1-1)-C(1+N1)*P1(N-N1-1))**2
                       S(1+N1+1)=T1-(P1(1)-C(1+N1)*Q1(1))**2
            End Do
C
C     ----------NOW CALCULATE THE A'S----------
C
                  DO  KI=1,IP
                      AT(KI,2)=1
            End do
                  DO  IORDER=1,IP
                        DO KI=1,IORDER
                           AT(KI,1)=AT(KI,2)
                     End do
                          N1=IORDER-1
                          IEND=N1+1
                          DO  K=1,IEND
                                 IT=N1+1
                                 IF(IT.EQ.K)AFIRST=0
                                 IF(IT.NE.K)AFIRST=AT(1+K,1)
                                 IT1=N1+1-K
                                 IF(IT1.EQ.IT)ASECOND=0
                                 IF(IT1.NE.IT)ASECOND=AT(1+N1+1-K,1)
                             AT(1+K,2)=AFIRST-C(1+N1)*ASECOND
                      End do
                End do
                      DO IK=1,IP
                            COEF(IK)=-AT(IK+1,2)
                 End do
                      RETURN
                      END
```

```
      SUBROUTINE RANKFREQ(N,DATA,RANK,FREQ,RANKMAX)
C
C—       This subroutine computes the rank and frequency
C—    of occurrence for each data point in an array of N
C—    data values.
C
      REAL DATA(N) !CONTAINS DATA
      REAL RANK(N) !CONTAINS RANK
      REAL FREQ(N) !CONTAINS FREQUENCY
      REAL RANKMAX
C
C—    INITIALLY GIVE ALL N DATA POINTS A RANK OF 1.0
C—                          AND A FREQUENCY OF 0.0
C
      DO I=1,N
        RANK(I) = 1.0       !INITIALIZE RANK
        FREQ(I) = 0.0       !INITIALIZE FREQUENCY
      END DO
C
C—    CALCULATE RANK OF DATA VALUE
C—              AND
C—    CALCULATE FREQUENCY OF DATA VALUE
C
      DO I=1,N
        DO J=1,N
          IF (DATA(I).GT.DATA(J)) THEN
            RANK(I) = RANK(I) + 1.0        !INCREASE RANK OF DATA
          END IF
          IF (DATA(I).EQ.DATA(J)) THEN
            FREQ(I) = FREQ(I) + 1.0        !INCREASE FREQUENCY OF DATA
          END IF
        END DO
      END DO
C
C—    ADJUST RANK OF DATA ACCORDING TO FREQUENCY
C
      DO I=1,N
        RANK(I) = RANK(I) + (FREQ(I)-1.0)/2.0
        RANKMAX = MAX(RANK(I),RANKMAX)
      END DO
C
C—    RETURN RANKS AND FREQUENCIES
C
      RETURN
      END
```

```
      SUBROUTINE RANKTEST(N,XDATA,YDATA,K,TEST,ACCEPT)
C
C--- SUBROUTINE TO PERFORM RANK SUM TEST
C--- MOODY,GRAYBILL & BOES
C
      REAL XDATA(N)
      REAL YDATA(N)
      INTEGER N !NUMBER OF SAMPLES IN RUN TEST
      INTEGER K !ACCEPT OR REJECT CRITERIA
      REAL Z(200,3) !WORK ARRAY FOR ORDERING SAMPLES
      LOGICAL ACCEPT
C
C--- COMPUTE RANK SUM TEST FOR WINDOWS OF SIZE N
C
      N2 = 2*N
      DO I=1,N
        Z(I,1) = ABS(XDATA(I))
        Z(I+N,1) = ABS(YDATA(I))
      END DO
      CALL RANKFREQ(N2,Z(1,1),Z(1,2),Z(1,3),RANKMAX)
      TY = 0.0
      DO I=1,N
        J = I + N
        TY = TY + Z(J,2)
      END DO
C
        C1 = FLOAT( N2 + 1)
        C2 = FLOAT(N*N)
C
        EXV = FLOAT(N)*C1/2.                    !EXPECTED VALUE OF Ty
C
        VAR = C2*C1/12.                         !VARIANCE OF Ty
C
        TEST = ABS(TY - EXV)
C
        IF (TEST.GE.FLOAT(K)) THEN
          ACCEPT = .FALSE.                      !REJECT THE NULL HYPOTHESIS
        ELSE
          ACCEPT = .TRUE.                       !ACCEPT THE NULL HYPOTHESIS
        END IF
      RETURN
      END
```

```
      SUBROUTINE RANK2700(NSAMPLES,AMPTRC,TRC,N,MEAN,INC,TEST,SEGLEN,
     +                    PATTERN,IST,RANGE,RMAX,RMIN,NRANK,RANK)
C
C--       This subroutine computes the rank sum test as described
C--   in the Introduction to the Theory of Statistics, Mood, Graybill
C--   and Boes, McGraw-Hill, 3rd Edition, 1974.  The observations,
C--   x(I), I=1,N, are taken from the representative background noise
C--   assumed to be present in the first 2.5 seconds of the event
C--   trace.  The second group of observations, y(I), I=1,N, is
C--   chosen from a window of N samples moved incrementally along
C--   the event trace for each excution of the rank sum test.
C--       The rank sum test statistic is computed for each window
C--   of observations, y(I), I=1,N, and the representative noise
C--   observations, x(I), I=1,N.  Detection occurs when the rank
C--   sum of the y(I) ranks exceeds the threshold for procable
C--   noise.  The automatic first arrival pick is the first
C--   zero crossing preceding the first modified slope value that
C--   exceeds the maximum modified slope value of the representative
C--   noise samples, x(I), I=1,N, occurring in the first detection
C--   window.
C
      REAL TEST
      REAL RMAX
      REAL RMIN
      REAL PATTERN(1)      !NULL HYPOTHESIS = 1.0 // ALTERNATIVE = 2.0
      REAL TRC(1)          !ARRAY CONTAINING FEATURE OF SIGNAL TO RANK
      REAL AMPTRC(1)     !ARRAY CONTAINING AMPLITUDES OF SIGNAL POINTS
      REAL SEGLEN(1)                          !LENGTH OF PATTERN SEGMENT
      REAL MEAN                          !EXPECTED VALUE OF RANK SUM TEST
      REAL RANGE                                !RANK SUM RANGE OF VALUES
      INTEGER NSAMPLES          !NUMBER OF OBSERVATIONS IN EVENT TRACE
      INTEGER NRANK      !NUMBER OF RANK SUM VALUES COMPUTED FOR TRACE
      INTEGER INC                  !INCREMENT WINDOW MOVES DOWN TRACE
      INTEGER IST                              !FIRST ARRIVAL PICK INDEX
      INTEGER N  !NUMBER OF SAMPLES REFERENCE BACKGROUND NOISE WINDOW
      REAL T(300,3)        !WORK ARRAY TO RANK  NOISE & SIGNAL WINDOWS
      REAL RANK(1)                        !SUMATION  TY OF RANKS OF SIGNAL
      LOGICAL FOUND/.FALSE./
      LOGICAL SECOND/.FALSE./
      LOGICAL FIRST/.TRUE./
C
C--   COMPUTE RANK SUM TEST OVER TRACE
C
      N2 = 2*N
      RMAX = MEAN
      RMIN = MEAN
      ENMAX = 0.0        !EVENT NOISE MAXIMUM MODIFIED SLOPE MAGNITUDE
C
C--   STORE REFERENCE BACKGROUND NOISE IN WORK VECTOR
C--   FIND EVENT NOISE MAXIMUM
C
      DO I=1,N
        L = I-1
        PATTERN(NSAMPLES-L) = 1.0
        SEGLEN(NSAMPLES-L) = 1.0
        PATTERN(I) = 1.0
        SEGLEN(I) = 1.0
        T(I,1) = ABS(TRC(I*2-1))
        T(I+N,1) = ABS(TRC(I*2))
        ENMAX = MAX(T(I,1),ENMAX)
        ENMAX = MAX(T(I+N,1),ENMAX)
      END DO
      ENMAX = ENMAX*1.01           !THRESHOLD FOR FIRST ARRIVAL PICKER
C
C--   COMPUTE RANK SUM FOR A WINDOW OF LENGHT N COMPARED
```

```
- CONTINUED -
      SUBROUTINE RANK2700(NSAMPLES,AMPTRC,TRC,N,MEAN,INC,TEST,SEGLEN,


C--  WITH THE REFERENCE BACKGROUND NOISE WINDOW OF LENGHT N
C
        IR = 0
C
C--  SLIDE THE WINDOW DOWN THE TRACE IN INCREMENTS = INC
C
        DO I=1,(NSAMPLES-N),INC
          IR = IR + 1
          DO J=1,N
            JJ = J + (I-1)
            T(J+N,1) = ABS(TRC(JJ))
          END DO !J=1,N
          CALL RANKFREQ(N2,T(1,1),T(1,2),T(1,3),RANKMAX)
          TY = 0.0
          DO J=1,N
            TY = TY + T(J+N,2)
          END DO
          RMAX = MAX(TY,RMAX)                    !RANK SUM MAXIMUM VALUE
          RMIN = MIN(TY,RMIN)                    !RANK SUM MINIMUM VALUE
          RANK(IR) = TY                        !RANK SUM OF THE IR-th WINDOW
        END DO !I
      NRANK = IR
      RANGE = RMAX - RMIN          !SIGNAL AND NOISE RANK SUM INTERVAL
C
C-- NOW DETERMINE THRESHOLD = 2700 + RMIN,OR.0.75*(RMAX-RMIN) + RMIN
C
      IF ((RMAX-RMIN).LT.3600.) THEN   !LOW SIGNAL TO NOISE RANK SUMS
        TEST = (RMAX-RMIN)*0.75 + RMIN
      ELSE
        TEST = 2700. + RMIN
      END IF
C
C-- FIND SIGNAL
C
      FIRST = .TRUE.                !LOOKING FOR FIRST DETECTION WINDOW
      DO I=1,NRANK
        K = (I-1)*INC + 1
        IF (RANK(I).GT.TEST) THEN  !PROBABLE SIGNAL PRESENT IN WINDOW
          DO L=K,(K+(INC-1))
            PATTERN(L) = 2.0                                 !REJECT H0
            SEGLEN(L) = 1.0
          END DO
          L = K
          DO WHILE (FIRST.AND.(L.LT.(K+(N-1))))
            IST = L
            IF (ABS(TRC(L)).GT.ENMAX) THEN
              MM = L - 1
              DO WHILE (FIRST.AND.(MM.GE.1))
                IST = MM
                IF (AMPTRC(MM+1)*AMPTRC(MM).LT.0.0) THEN
                  FIRST = .FALSE.            !FOUND IST=ZERO CROSSING
                ELSE
                  MM = MM - 1      !CONTINUE LOOKING FOR ZERO CROSSING
                END IF
              END DO !WHILE
            ELSE
              L = L + 1
              END IF
          END DO !WHILE
          IF (FIRST) THEN       !OBSERVATIONS IN WINDOW NOT .GT. NOISE
              MM = L - 1
```

```
- CONTINUED -
      SUBROUTINE RANK2700(NSAMPLES,AMPTRC,TRC,N,MEAN,INC,TEST,SEGLEN,


            DO WHILE (FIRST.AND.(MM.GE.1))  !PICK 1ST ZERO CROSSING
              IST = MM                      !BEFORE END OF WINDOW
              IF (AMPTRC(MM+1)*AMPTRC(MM).LT.0.0) THEN
                FIRST = .FALSE.             !FOUND IST=ZERO CROSSING
              ELSE
                MM = MM - 1     !CONTINUE LOOKING FOR ZERO CROSSING
              END IF
            END DO !WHILE
          END IF
        ELSE
          DO L=K,(K+(INC-1))
            PATTERN(L) = 1.0                          !ACCEPT H0
            SEGLEN(L) = 1.0
          END DO
        END IF
      END DO !I
      RETURN
      END
```

```
      SUBROUTINE RUNEXP(N,XDATA,YDATA,IZ0,NRUNS,EXV,VAR)
C
C--       This subroutine calculates the run test statistic
C--   for two arrays of data, x(i), i=1,N and y(i), i=1,N.
C--   The threshold, z0, for the number of runs below which we
C--   reject the null hypothesis, F(x) = F(y), is provided as
C--   input to the subroutine.  It is calculated outside the
C--   subroutine using the normal distribution and a specified
C--   alpha level.  The algorithm is based on the description of
C--   the run test given in the Introduction to the Theory of
C--   Statistics, Mood, Graybill and Boes, McGraw-Hill, 3rd Edition,
C--   1974.
C
      REAL XDATA(N)
      REAL YDATA(N)
      REAL EXV                        !EXPECTED VALUE OF NUMBER OF RUNS
      REAL VAR                        !VARIANCE OF NUMBER OF RUNS
      INTEGER N                       !NUMBER OF SAMPLES IN RUN TEST
      INTEGER IZ0                     !ACCEPT OR REJECT CRITERIA
      REAL Z(200,2)                   !WORK ARRAY FOR ORDERING SAMPLES
C
C--   COMPUTE RUN TEST OVER TRACE
C
      N2 = 2*N
      DO I=1,N
        Z(I,1) = ABS(XDATA(I))
        Z(I,2) = 1.0
        Z(I+N,1) = ABS(YDATA(I))
        Z(I+N,2) = -1.0
      END DO
C
C--   ORDER COMBINED, X(I) AND Y(I), DATA INTO ASCENDING ORDER
C
      DO I=1,N2-1
        DO J=I+1,N2
          IF (Z(J,1).LT.Z(I,1)) THEN
            TEMP = Z(I,1)
            Z(I,1) = Z(J,1)
            Z(J,1) = TEMP
            TEMP = Z(I,2)
            Z(I,2) = Z(J,2)
            Z(J,2) = TEMP
          END IF
        END DO
      END DO
C
C--   COUNT THE NUMBER OF RUNS
C
      ZSIGN = Z(1,2)
      NRUNS = 1
      DO I=2,N2
          IF ((ZSIGN*Z(I,2)).LT.0.0) THEN
            ZSIGN = Z(I,2)
            NRUNS = NRUNS + 1
          END IF
      END DO !!
C
C--   COMPUTE EXPECTED VALUE AND VARIANCE OF THE NUMBER OF RUNS
C--   ASSUMING THE NULL HYPOTHESIS IS TRUE
C
        C1 = FLOAT(2*N*N)
        C2 = FLOAT(N2)
        EXV = C1/C2 + 1.
        VAR = (C1*(C1-C2))/(C2**2*(C2-1.))
      RETURN
      END
```

```
      SUBROUTINE SLOPE(NSAMPLES,TRC,S)
C
C--       This subroutine computes the integrated slope of
C--   a seismic signal for discrete segments of the signal
C--   with continuous slope direction.
C--   Kathleen A. Alden, March 16, 1986.
C
      REAL S(1)                          !MODIFIED SLOPE OF OBSERVATION
      REAL TRC(1)          !TRACE CONTAINING SEISMIC SIGNAL OBSERVATIONS
      INTEGER NSAMPLES                 !NUMBER OF OBSERVATIONS IN TRACE
C
C-- ASSUME SAMPLE MEAN OF TRACE INPUT IS ZERO
C
C
C-- COMPUTE SEISMIC TRACE MODIFIED SLOPE
C
      S(1) = TRC(2) - TRC(1)                        !SLOPE OF 1ST SAMPLE
      DO I =2,NSAMPLES - 1
        S(I) = ((TRC(I+1)-TRC(I))+(TRC(I)-TRC(I-1)))/2.      !Ith SLOPE
C
        IF (S(I)*S(I-1).GT.0.0) THEN    !SLOPE DIRECTION IS CONTINUOUS
          S(I) = S(I) + S(I-1)                          !INTEGRATE SLOPE
        END IF
      END DO
      S(NSAMPLES) = TRC(NSAMPLES) - TRC(NSAMPLES-1) !SLOPE LAST SAMPLE
      RETURN
      END
```

```
      SUBROUTINE SIGNEXP(N,XDATA,YDATA,K,SN,EXV,TEST)
C
C--      This subroutine calculates the sign test statistic
C--   for the absolute value of two arrays of data, x(I), I=1,N and
C--   y(I), I=1,N.  The threshold, k, which must be less than the
C--   test statistic to reject the null hypothesis, F(x) = F(y), is
C--   provided as input to the subroutine.  It is calculated outside
C--   the subroutine using the normal distribution and a specified
C--   alpha level.  The algorithm is based on the description of
C--   the sign test given in the Introduction to the Theory of
C--   Statistics, Mood, Graybill and Boes, McGraw-Hill, 3rd Edition,
C--   1974.
C
      REAL XDATA(N)
      REAL YDATA(N)
      INTEGER K                          !THRESHOLD FOR THE TEST STATISTIC
      INTEGER N                          !NUMBER OF SAMPLES IN SIGN TEST
      REAL SN          !SUMATION OF THE POSITIVE SIGNS OF (Y(I) - X(I))
      REAL EXV                           !EXPECTED VALUE OF SUMMATION OF SIGNS
      REAL TEST                          !ABSOLUTE VALUE OF (SN - EXV)

C
C--   COMPUTE SIGN TEST OVER TRACE
C
        SN = 0.0
        DO I=1,N
          IF (ABS(XDATA(I)).LT.ABS(YDATA(I))) THEN
            SN = SN + 1.0
          END IF
        END DO
C
C--   COMPUTE EXPECTED VALUE OF SUMMATION
C--   AND THE TEST STATISTIC
C
        EXV = FLOAT(N)/2.
        TEST = ABS(SN - EXV)
      RETURN
      END
```

APPENDIX C

Values of w(alpha,M,N)

TABLE C.1 (Continued)

$n = 2$

x	$m = 3$	$m = 4$	$m = 5$	$m = 6$	$m = 7$	$m = 8$	$m = 9$	$m = 10$	$m = 11$
6	.600								
7	.400	.600							
8	.200	.400	.571						
9	.100	.267	.429	.571					
10		.133	.286	.429	.556				
11		.067	.190	.321	.444	.556			
12			.095	.214	.333	.444	.545		
13			.048	.143	.250	.356	.455	.545	
14				.071	.167	.267	.364	.455	.538
15				.036	.111	.200	.291	.379	.462
16					.056	.133	.218	.303	.385
17					.028	.089	.164	.242	.321
18						.044	.109	.182	.256
19						.022	.073	.136	.205
20							.036	.091	.154
21							.018	.061	.115
22								.030	.077
23								.015	.051
24									.026
25									.013

$n = 2$

x	$m = 12$	$m = 13$	$m = 14$	$m = 15$	$m = 16$	$m = 17$	$m = 18$	$m = 19$	$m = 20$
15	.538								
16	.462	.533							
17	.396	.467	.533						
18	.330	.400	.467	.529					
19	.275	.343	.408	.471	.529				
20	.220	.286	.350	.412	.471	.526			
21	.176	.238	.300	.360	.418	.474	.526		
22	.132	.190	.250	.309	.366	.421	.474	.524	
23	.099	.152	.208	.265	.320	.374	.426	.476	.524
24	.066	.114	.167	.221	.275	.327	.379	.429	.476
25	.044	.086	.133	.184	.235	.287	.337	.386	.433
26	.022	.057	.100	.147	.196	.246	.295	.343	.390
27	.011	.038	.075	.118	.163	.211	.258	.305	.351
28		.019	.050	.088	.131	.175	.221	.267	.312
29		.010	.033	.066	.105	.146	.189	.233	.277
30			.017	.044	.078	.117	.158	.200	.242
31			.008	.029	.059	.094	.132	.171	.212
32				.015	.039	.070	.105	.143	.182

TABLE C.1 (Continued)

$n = 2$

x	$m = 12$	$m = 13$	$m = 14$	$m = 15$	$m = 16$	$m = 17$	$m = 18$	$m = 19$	$m = 20$
33				.007	.026	.053	.084	.119	.156
34					.013	.035	.063	.095	.130
35					.007	.023	.047	.076	.108
36						.012	.032	.057	.087
37						.006	.021	.043	.069
38							.011	.029	.052
39							.005	.019	.039
40								.010	.026
41								.005	.017
42									.009
43									.004

$n = 3$

x	$m = 3$	$m = 4$	$m = 5$	$m = 6$	$m = 7$	$m = 8$	$m = 9$	$m = 10$	$m = 11$
11	.500								
12	.350	.571							
13	.200	.429							
14	.100	.314	.500						
15	.050	.200	.393	.548					
16		.114	.286	.452					
17		.057	.196	.357	.500				
18		.029	.125	.274	.417	.539			
19			.071	.190	.333	.461			
20			.036	.131	.258	.388	.500		
21			.018	.083	.192	.315	.432	.531	
22				.048	.133	.248	.364	.469	
23				.024	.092	.188	.300	.406	.500
24				.012	.058	.139	.241	.346	.442
25					.033	.097	.186	.287	.385
26					.017	.067	.141	.234	.330
27					.008	.042	.105	.185	.277
28						.024	.073	.143	.228
29						.012	.050	.108	.184
30						.006	.032	.080	.146
31							.018	.056	.113
32							.009	.038	.085
33							.005	.024	.063
34								.014	.044
35								.007	.030
36								.003	.019
37									.011
38									.005
39									.003

TABLE C.1 (Continued)

$n = 3$

x	$m = 12$	$m = 13$	$m = 14$	$m = 15$	$m = 16$	$m = 17$	$m = 18$	$m = 19$	$m = 20$
24	.527								
25	.473								
26	.420	.500							
27	.367	.450	.524						
28	.316	.400	.476						
29	.268	.352	.429	.500					
30	.224	.305	.384	.456	.521				
31	.182	.261	.338	.412	.479				
32	.147	.220	.296	.369	.438	.500			
33	.116	.182	.254	.327	.396	.461	.519		
34	.090	.148	.216	.287	.356	.421	.481		
35	.068	.120	.181	.249	.317	.382	.444	.500	
36	.051	.095	.150	.213	.280	.345	.407	.464	.517
37	.035	.073	.122	.180	.244	.308	.370	.429	.483
38	.024	.055	.099	.151	.211	.273	.335	.394	.449
39	.015	.041	.078	.125	.180	.239	.300	.359	.415
40	.009	.029	.060	.102	.152	.208	.267	.325	.382
41	.004	.020	.046	.082	.127	.179	.235	.293	.349
42	.002	.012	.034	.065	.105	.153	.206	.262	.317
43		.007	.024	.050	.086	.129	.178	.232	.286
44		.004	.016	.038	.069	.108	.153	.204	.257
45		.002	.010	.028	.055	.089	.131	.178	.229
46			.006	.020	.042	.073	.111	.154	.202
47			.003	.013	.032	.059	.092	.132	.177
48			.001	.009	.024	.046	.077	.113	.155
49				.005	.017	.036	.062	.095	.134
50				.002	.011	.027	.050	.080	.115
51				.001	.007	.020	.040	.066	.098
52					.004	.014	.031	.054	.083
53					.002	.010	.023	.044	.069
54					.001	.006	.017	.034	.058
55						.004	.012	.027	.047
56						.002	.008	.020	.038
57						.001	.005	.015	.030
58							.003	.010	.023
59							.002	.007	.018
60							.001	.005	.013
61								.003	.009
62								.001	.006
63								.001	.004
64									.002
65									.001
66									.001

TABLE C.1 (Continued)

$n = 4$

x	$m = 4$	$m = 5$	$m = 6$	$m = 7$	$m = 8$	$m = 9$	$m = 10$	$m = 11$
18	.557							
19	.443							
20	.343	.548						
21	.243	.452						
22	.171	.365	.543					
23	.100	.278	.457					
24	.057	.206	.381	.536				
25	.029	.143	.305	.464				
26	.014	.095	.238	.394	.533			
27		.056	.176	.324	.467			
28		.032	.129	.264	.404	.530		
29		.016	.086	.206	.341	.470		
30		.008	.057	.158	.285	.413	.527	
31			.033	.115	.230	.355	.473	
32			.019	.082	.184	.302	.420	.525
33			.010	.055	.141	.252	.367	.475
34			.005	.036	.107	.207	.318	.426
35				.021	.077	.165	.270	.377
36				.012	.055	.130	.227	.330
37				.006	.036	.099	.187	.286
38				.003	.024	.074	.152	.245
39					.014	.053	.120	.206
40					.008	.038	.094	.171
41					.004	.025	.071	.140
42					.002	.017	.053	.113
43						.010	.038	.089
44						.006	.027	.069
45						.003	.018	.052
46						.001	.012	.039
47							.007	.028
48							.004	.020
49							.002	.013
50							.001	.009
51								.005
52								.003
53								.001
54								.001

TABLE C.1 (Continued)

$n = 4$

x	$m = 12$	$m = 13$	$m = 14$	$m = 15$	$m = 16$	$m = 17$	$m = 18$	$m = 19$	$m = 20$
34	.524								
35	.476								
36	.431	.522							
37	.385	.478							
38	.342	.435	.521						
39	.299	.392	.479						
40	.260	.352	.439	.519					
41	.223	.312	.399	.481					
42	.190	.274	.360	.443	.518				
43	.158	.239	.323	.405	.482				
44	.131	.206	.287	.368	.446	.517			
45	.106	.175	.253	.332	.410	.483			
46	.085	.148	.221	.298	.375	.449	.516		
47	.066	.123	.191	.265	.341	.415	.484		
48	.052	.101	.164	.235	.308	.381	.451	.516	
49	.039	.082	.139	.205	.277	.349	.419	.484	
50	.029	.065	.116	.179	.247	.318	.387	.453	.515
51	.021	.051	.096	.154	.219	.287	.356	.422	.485
52	.015	.039	.079	.131	.192	.258	.326	.392	.455
53	.010	.030	.063	.110	.168	.231	.297	.363	.426
54	.007	.022	.051	.092	.145	.205	.269	.334	.397
55	.004	.016	.040	.076	.124	.181	.242	.306	.368
56	.002	.011	.031	.062	.106	.158	.217	.279	.341
57	.001	.008	.023	.050	.089	.138	.193	.253	.314
58	.001	.005	.017	.040	.074	.119	.171	.228	.288
59		.003	.012	.031	.061	.101	.150	.205	.262
60		.002	.009	.024	.050	.086	.131	.183	.239
61		.001	.006	.018	.040	.072	.113	.162	.216
62		.000	.004	.014	.032	.060	.098	.143	.194
63			.002	.010	.025	.049	.083	.125	.174
64			.001	.007	.019	.040	.070	.109	.155
65			.001	.005	.015	.032	.059	.094	.137
66			.000	.003	.011	.026	.049	.081	.120
67				.002	.008	.020	.040	.069	.105
68				.001	.006	.016	.033	.058	.091
69				.001	.004	.012	.027	.049	.079
70				.000	.002	.009	.021	.041	.067
71					.001	.006	.017	.033	.057
72					.001	.005	.013	.027	.048
73					.000	.003	.010	.022	.041
74					.000	.002	.007	.018	.034
75						.001	.005	.014	.028
76						.001	.004	.011	.023
77						.000	.002	.008	.018

TABLE C.1 (Continued)

$n = 4$

x	$m = 12$	$m = 13$	$m = 14$	$m = 15$	$m = 16$	$m = 17$	$m = 18$	$m = 19$	$m = 20$
78						.000	.002	.006	.015
79							.001	.004	.011
80							.001	.003	.009
81							.000	.002	.007
82							.000	.001	.005
83								.001	.004
84								.000	.003
85								.000	.002
86								.000	.001
87									.001
88									.000
89									.000
90									.000

$n = 5$

x	$m = 5$	$m = 6$	$m = 7$	$m = 8$	$m = 9$	$m = 10$
28	.500					
29	.421					
30	.345	.535				
31	.274	.465				
32	.210	.396				
33	.155	.331	.500			
34	.111	.268	.438			
35	.075	.214	.378	.528		
36	.048	.165	.319	.472		
37	.028	.123	.265	.416		
38	.016	.089	.216	.362	.500	
39	.008	.063	.172	.311	.449	
40	.004	.041	.134	.262	.399	.523
41		.026	.101	.218	.350	.477
42		.015	.074	.177	.303	.430
43		.009	.053	.142	.259	.384
44		.004	.037	.111	.219	.339
45		.002	.024	.085	.182	.297
46			.015	.064	.149	.257
47			.009	.047	.120	.220
48			.005	.033	.095	.185
49			.003	.023	.073	.155
50			.001	.015	.056	.127
51				.009	.041	.103
52				.005	.030	.082

TABLE C.1 (Continued)

$n = 5$

x	$m = 5$	$m = 6$	$m = 7$	$m = 8$	$m = 9$	$m = 10$
53				.003	.021	.065
54				.002	.014	.050
55				.001	.009	.038
56					.006	.028
57					.003	.020
58					.002	.014
59					.001	.010
60					.000	.006
61						.004
62						.002
63						.001
64						.001
65						.000

$n = 6$

x	$m = 6$	$m = 7$	$m = 8$	$m = 9$	$m = 10$
39	.531				
40	.469				
41	.409				
42	.350	.527			
43	.294	.473			
44	.242	.418			
45	.197	.365	.525		
46	.155	.314	.475		
47	.120	.267	.426		
48	.090	.223	.377	.523	
49	.066	.183	.331	.477	
50	.047	.147	.286	.432	
51	.032	.117	.245	.388	.521
52	.021	.090	.207	.344	.479
53	.013	.069	.172	.303	.437
54	.008	.051	.141	.264	.396
55	.004	.037	.114	.228	.356
56	.002	.026	.091	.194	.318
57	.001	.017	.071	.164	.281
58		.011	.054	.136	.246
59		.007	.041	.112	.214
60		.004	.030	.091	.184
61		.002	.021	.072	.157
62		.001	.015	.057	.132
63		.001	.010	.044	.110

TABLE C.1 (Continued)

$n = 6$

x	$m = 6$	$m = 7$	$m = 8$	$m = 9$	$m = 10$
64			.006	.033	.090
65			.004	.025	.074
66			.002	.018	.059
67			.001	.013	.047
68			.001	.009	.036
69			.000	.006	.028
70				.004	.021
71				.002	.016
72				.001	.011
73				.001	.008
74				.000	.005
75				.000	.004
76					.002
77					.001
78					.001
79					.000
80					.000
81					.000

$n = 7$

x	$m = 7$	$m = 8$	$m = 9$	$m = 10$
53	.500			
54	.451			
55	.402			
56	.355	.522		
57	.310	.478		
58	.267	.433		
59	.228	.389		
60	.191	.347	.500	
61	.159	.306	.459	
62	.130	.268	.419	
63	.104	.232	.379	.519
64	.082	.198	.340	.481
65	.064	.168	.303	.443
66	.049	.140	.268	.406
67	.036	.116	.235	.370
68	.027	.095	.204	.335
69	.019	.076	.176	.300
70	.013	.060	.150	.268
71	.009	.047	.126	.237
72	.006	.036	.105	.209

TABLE C.1 (Continued)

	$n = 7$			
x	$m = 7$	$m = 8$	$m = 9$	$m = 10$
73	.003	.027	.087	.182
74	.002	.020	.071	.157
75	.001	.014	.057	.135
76	.001	.010	.045	.115
77	.000	.007	.036	.097
78		.005	.027	.081
79		.003	.021	.067
80		.002	.016	.054
81		.001	.011	.044
82		.001	.008	.035
83		.000	.006	.028
84		.000	.004	.022
85			.003	.017
86			.002	.012
87			.001	.009
88			.001	.007
89			.000	.005
90			.000	.003
91			.000	.002
92				.002
93				.001
94				.001
95				.000
96				.000
97				.000
98				.000

	$n = 8$		
x	$m = 8$	$m = 9$	$m = 10$
68	.520		
69	.480		
70	.439		
71	.399		
72	.360	.519	
73	.323	.481	
74	.287	.444	
75	.253	.407	
76	.221	.371	.517
77	.191	.336	.483
78	.164	.303	.448
79	.139	.271	.414

	$n = 8$		
x	$m = 8$	$m = 9$	$m = 10$
80	.117	.240	.381
81	.097	.212	.348
82	.080	.185	.317
83	.065	.161	.286
84	.052	.138	.257
85	.041	.118	.230
86	.032	.100	.204
87	.025	.084	.180
88	.019	.069	.158
89	.014	.057	.137
90	.010	.046	.118
91	.007	.037	.102
92	.005	.030	.086
93	.003	.023	.073
94	.002	.018	.061
95	.001	.014	.051
96	.001	.010	.042
97	.001	.008	.034
98	.000	.006	.027
99	.000	.004	.022
100	.000	.003	.017
101		.002	.013
102		.001	.010
103		.001	.008
104		.000	.006
105		.000	.004
106		.000	.003
107		.000	.002
108		.000	.002
109			.001
110			.001
111			.000
112			.000
113			.000
114			.000
115			.000
116			.000

TABLE C.1 (Continued)

$n = 9$		
x	$m = 9$	$m = 10$
86	.500	
87	.466	
88	.432	
89	.398	
90	.365	.516
91	.333	.484
92	.302	.452
93	.273	.421
94	.245	.390
95	.218	.360
96	.193	.330
97	.170	.302
98	.149	.274
99	.129	.248
100	.111	.223
101	.095	.200
102	.081	.178
103	.068	.158
104	.057	.139
105	.047	.121
106	.039	.106
107	.031	.091
108	.025	.078
109	.020	.067
110	.016	.056
111	.012	.047
112	.009	.039
113	.007	.033
114	.005	.027
115	.004	.022
116	.003	.017
117	.002	.014
118	.001	.011
119	.001	.009
120	.001	.007
121	.000	.005

$n = 9$		
x	$m = 9$	$m = 10$
122	.000	.004
123	.000	.003
124	.000	.002
125	.000	.001
126	.000	.001
127		.001
128		.000
129		.000
130		.000
131		.000
132		.000
133		.000
134		.000
135		.000

$n = 10$	
x	$m = 10$
105	.515
106	.485
107	.456
108	.427
109	.398
110	.370
111	.342
112	.315
113	.289
114	.264
115	.241
116	.218
117	.197
118	.176
119	.157
120	.140

$n = 10$	
x	$m = 10$
121	.124
122	.109
123	.095
124	.083
125	.072
126	.062
127	.053
128	.045
129	.038
130	.032
131	.026
132	.022
133	.018
134	.014
135	.012
136	.009
137	.007
138	.006
139	.004
140	.003
141	.003
142	.002
143	.001
144	.001
145	.001
146	.001
147	.000
148	.000
149	.000
150	.000
151	.000
152	.000
153	.000
154	.000
155	.000

Adapted from Table B of *A Nonparametric Introduction to Statistics*, by C. H. Kraft and C. van Eeden, Macmillan, New York, 1968, with the permission of the authors and the publisher.

APPENDIX D

Illustration of the Results of the Automatic Detector and Picker When Run on the Event Traces Recorded by the Four Seismic Stations, Lajitas, Marathon, Shafter and Tres Cuevas for 38 Seismic events

TABLE D.1 Event File Names, Errors (Automatic Minus Analyst Picks in Seconds), and the Range of Rank Sums for the 38 Events Used to Test the RANK2700 Detector

FILE NAME	ERROR IN AUTOMATIC PICK	RANGE OF RANK SUMS
EVENT 1		
L42891418.037	-0.1	4928.5
M42891418.053	0.2	5475.5
S42891418.037	0.0	5057.0
T42891418.034	-0.1	5349.5
EVENT 2		
L42891719.053	1.2	4166.5
M42891719.057	1.7	3826.0
S42891719.025	7.4	4085.5
T42891719.047	1.9	4242.5
EVENT 3		
L42891815.018	0.5	4178.0
M42891815.038	0.6	3481.5
S42891815.018	10.4	3470.5
T42891814.046	1.2	4812.0
EVENT 4		
L42891906.030	-17.5	3068.5
M42891906.042	2.7	3348.5
S42891903.018	-15.1	3361.0
T42891905.008	0.3	3888.0
EVENT 5		
L42892304.039	-19.9	5576.5
M42892304.028	-5.1	4193.5
S42892304.012	-6.3	5496.0
T42892304.016	0.2	5748.0
EVENT 6		
L42892313.003	0.0	4882.5
M42892313.022	-15.3	4768.5
S42892313.016	0.1	5454.0
T42892313.008	0.6	5583.5
EVENT 7		
L42892327.016	-1.8	4615.5
M42892328.007	0.1	3311.5
S42892327.018	-0.8	4896.0
T42892327.012	0.3	5168.0
EVENT 8		
L42900819.051	-0.2	4862.0
M42900819.053	0.1	4579.5
S42900821.023	0.2	4569.5
T42900819.051	-0.1	5564.5
EVENT 9		
L42900136.053	-25.0	4227.5
M42900137.019	12.0	4286.0
S42900136.031	0.1	3581.0
T42900136.021	0.3	4554.5
EVENT 10		
L42901821.016	7.5	4485.5
M42901820.047	0.3	4770.0
S42901821.025	-0.4	4187.0
T42901820.037	-9.1	3292.0
EVENT 11		
L42902054.044	-0.2	5504.0
M42902055.038	0.1	4294.0
S42902054.051	-26.0	6894.0
T42902054.044	0.2	5984.0
EVENT 12		
L42902209.027	3.0	2860.0
M42902210.022	0.7	4052.0
S42902211.000	5.1	2860.0
T42902209.038	0.3	3713.0

TABLE D.1 (Continued)

FILE NAME	ERROR IN AUTOMATIC PICK	RANGE OF RANK SUMS
EVENT 13		
L42902247.013	-0.6	4145.0
M42902246.029	4.4	4954.5
S42902247.016	5.4	2987.0
T42902246.038	0.9	3742.0
EVENT 14		
L42910325.032	1.4	5958.0
M42910325.026	0.7	5548.0
S42910325.016	-22.9	5376.0
T42910325.029	0.6	5643.0
EVENT 15		
L42918922.040	-1.5	5457.0
M42918922.040	0.2	4927.0
S42918922.035	0.1	5062.5
T42918922.040	0.1	5462.0
EVENT 16		
L42911602.007	-33.3	4522.0
M42911602.038	0.9	3788.0
S42911603.000	0.2	4538.5
T42911602.003	0.8	5197.5
EVENT 17		
L42911807.029	0.4	4572.5
M42911807.029	0.4	4144.5
S42911807.026	0.3	4369.0
T42911807.032	-0.3	4579.5
EVENT 18		
L42911819.039	-5.5	3839.5
M42911819.035	-23.9	3895.5
S42911819.030	0.1	3995.5
T42911819.039	0.2	4139.5
EVENT 19		
L42911851.003	-0.6	4626.5
M42911851.051	0.0	3742.0
S42911851.011	-2.4	5646.0
T42911851.007	0.3	5859.5
EVENT 20		
L42911959.017	-0.7	4398.0
M42911959.008	13.4	4199.0
S42911958.058	-6.3	6332.0
T42911958.056	0.3	4692.5
EVENT 21		
L42912140.015	0.4	5738.0
M42912140.040	0.1	5149.0
S42912139.030	18.4	3748.0
T42912140.015	-2.9	5518.5
EVENT 22		
L42912213.057	-0.4	4443.5
M42912214.052	2.1	4867.0
S42912215.201	-23.7	5845.0
T42912213.057	0.1	4814.5
EVENT 23		
L42920528.008	-0.1	5145.5
M42920528.004	-3.4	5799.5
S42920528.001	0.1	4184.0
T42920528.008	-1.2	5536.0
EVENT 24		
L42921429.020	0.5	2295.0
M42921430.014	0.3	4358.0
S42921430.030	-0.2	3994.0
T42921429.018	-0.3	3944.0
EVENT 25		
L42921533.036	0.1	5469.0
M42921533.023	0.1	5871.0
S42921533.026	0.1	5261.5
T42921533.036	-0.4	5751.5

TABLE D.1 (Continued)

FILE NAME	ERROR IN AUTOMATIC PICK	RANGE OF RANK SUMS
EVENT 26		
L42921829.039	0.3	4112.5
M42921838.008	0.0	3958.5
S42921829.023	-2.0	5681.5
T42921829.039	-1.2	4849.5
EVENT 27		
L42921859.031	0.1	3898.0
M42921859.054	-23.6	4645.5
S42921858.056	2.3	3923.5
T42921859.028	0.1	4275.0
* EVENT 28		
L42922157.014	-2.9	5797.5
M42922157.014	-4.9	5198.5
S42922157.014	4.0	9181.5
T42922157.017	0.6	5378.0
* EVENT 29		
L42922304.042	-0.8	5178.0
M42922304.035	-1.6	5818.5
S42922304.039	13.1	4682.5
T42922304.035	1.9	4453.0
* EVENT 30		
L42930148.026	0.1	4853.0
M42930148.029	0.4	5876.5
S42930148.023	0.3	5858.5
T42930148.026	0.1	4648.0
* EVENT 31		
L42931458.014	-21.4	5375.5
M42931449.047	-0.1	5161.0
S42931458.010	-0.3	7872.0
T42931458.014	-1.5	5668.0
EVENT 32		
L42932129.009	-0.1	5495.5
M42932129.031	-0.5	5878.0
S42932129.018	-0.6	6385.5
T42932123.006	0.1	5797.0
EVENT 33		
L42932303.019	0.2	5848.0
M42932303.035	0.2	5869.5
S42932303.035	-1.2	5628.5
T42932303.019	0.0	5323.0
EVENT 34		
L42951908.057	0.3	5912.5
M42951908.052	0.2	5725.0
S42951909.002	-1.1	5251.5
T42951908.057	0.1	5539.5
EVENT 35		
L42962837.016	0.1	3728.5
M42962838.001	0.4	4733.5
S42962238.014	0.8	4264.5
T42962237.016	1.5	3655.0
EVENT 36		
L42970815.046	-1.1	6891.0
M42970815.043	-0.9	6135.5
S42970815.039	0.1	5989.5
T42970815.046	0.0	5751.5
EVENT 37		
L42971753.018	0.0	5272.0
M42971753.030	0.2	5839.5
S42971753.018	0.0	6174.0
T42971752.052	3.3	5585.0
EVENT 38		
L42971952.007	1.2	4583.0
M42971951.000	-1.0	2483.5
S42971950.043	10.1	4355.5
T42971951.000	3.9	3419.5

* Denotes the Events Used as Part of the Training Set.

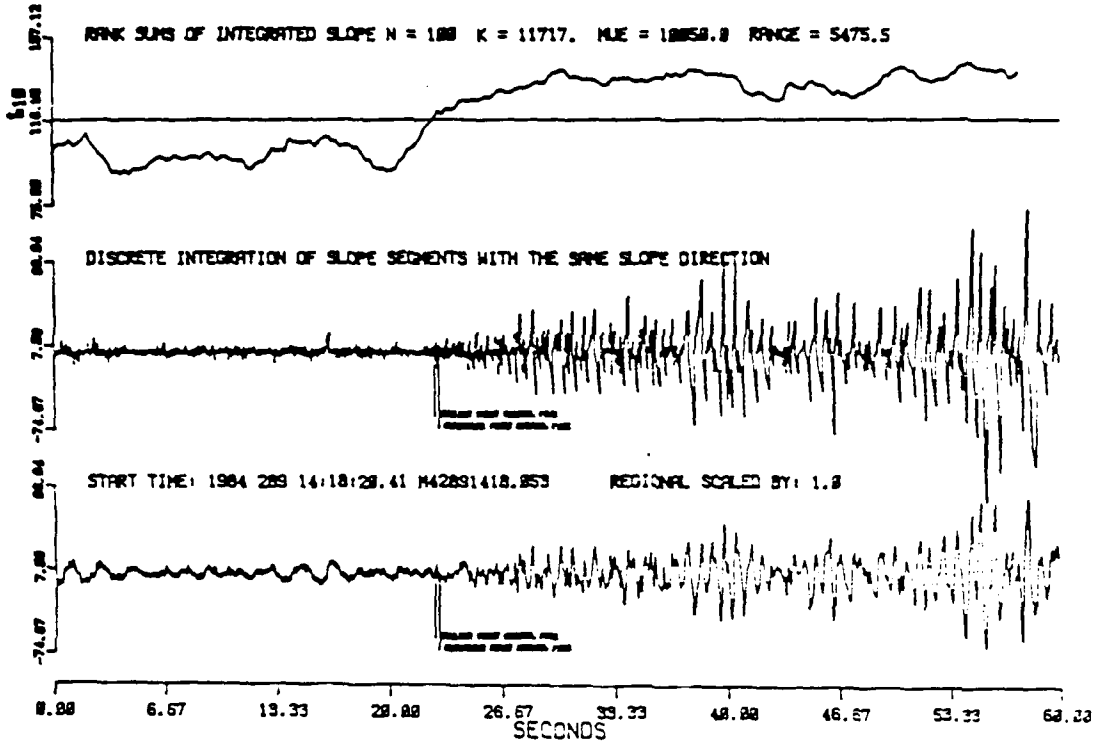

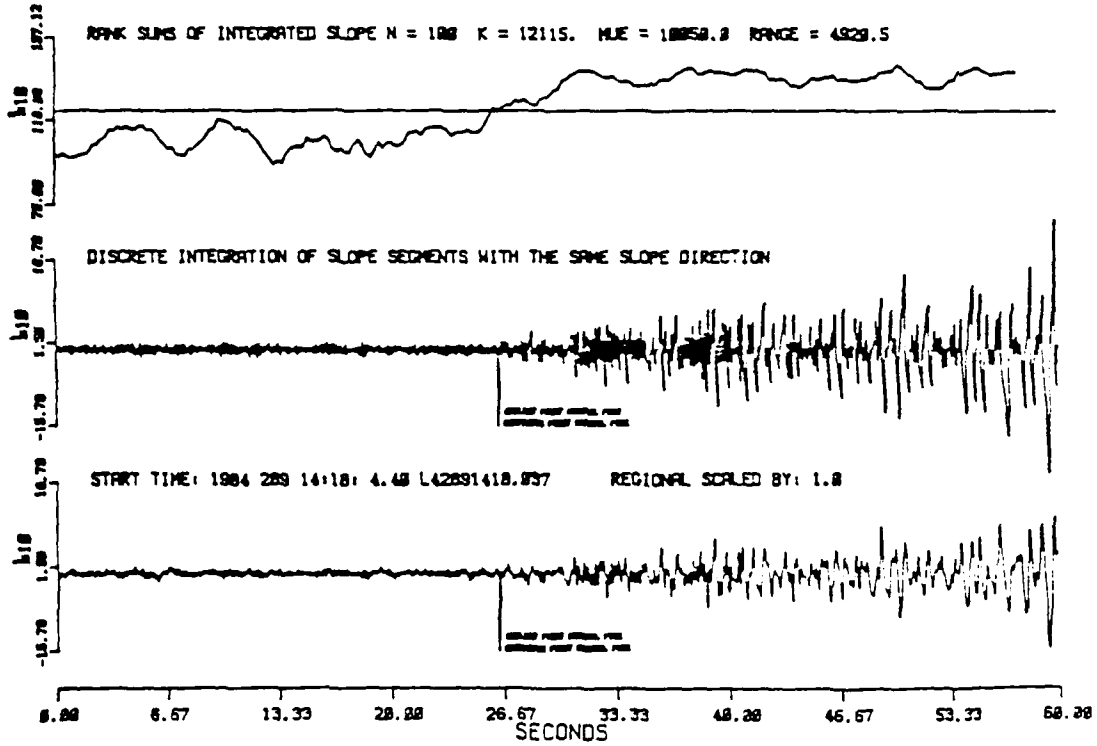

EVENT 1 - Regional (P-Lg) = 2 Minutes

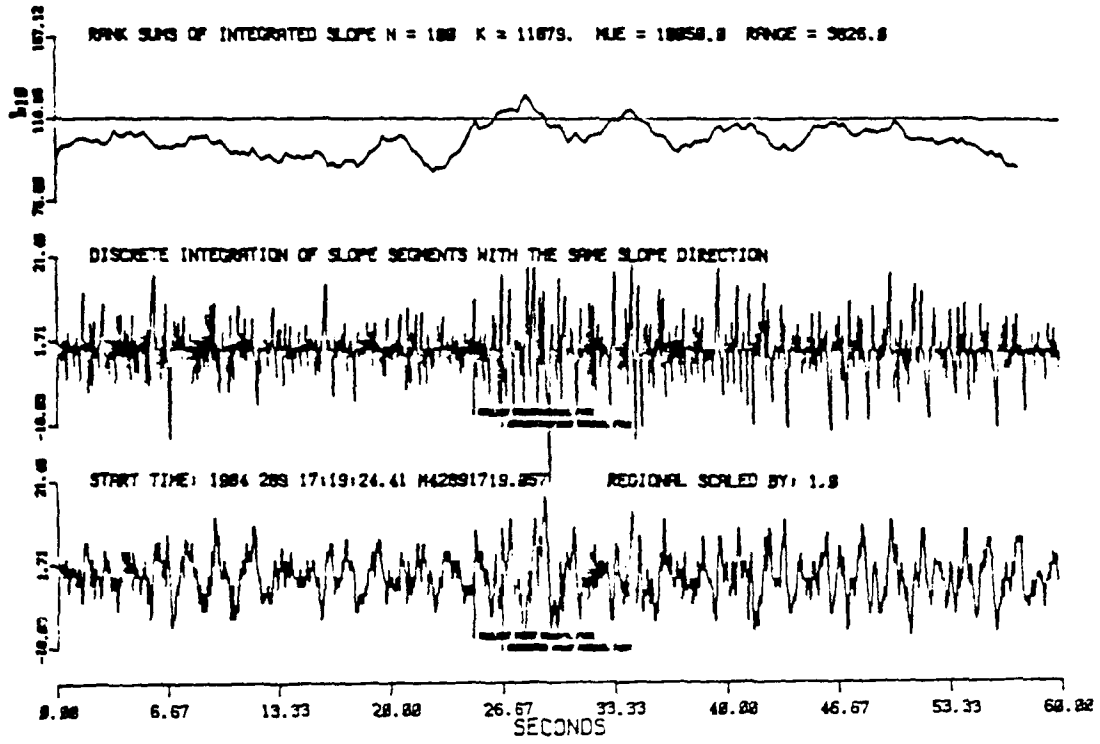

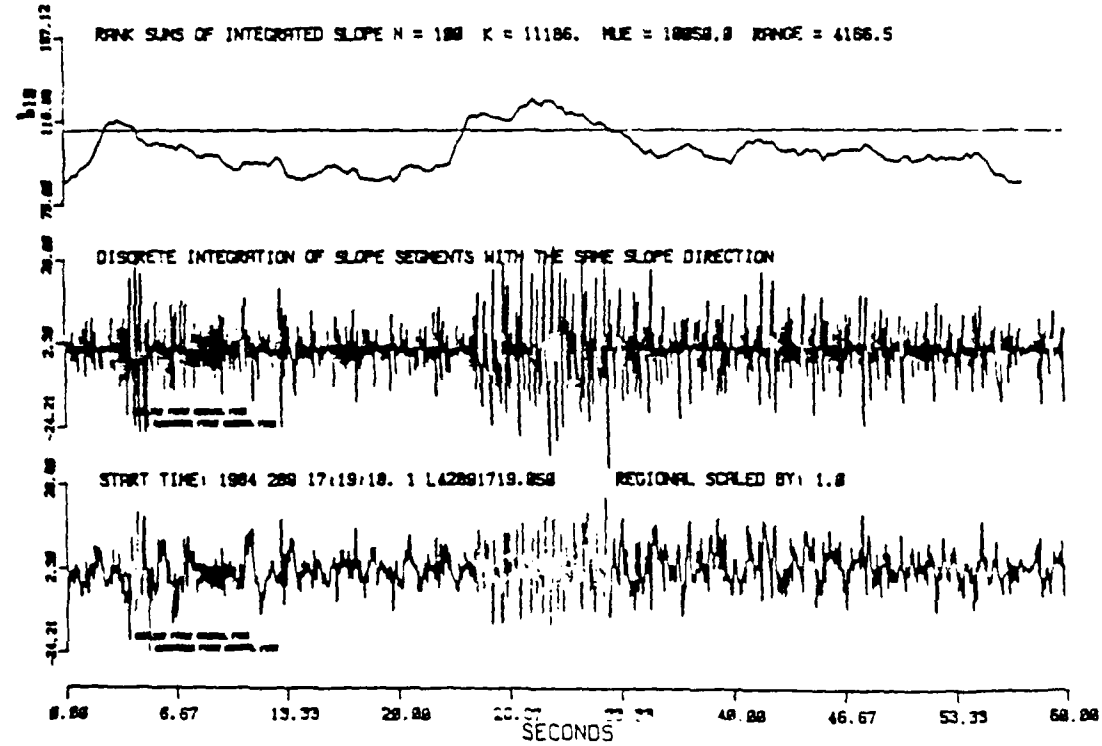

Event 2 Regional (P-Lg) = 20 Seconds

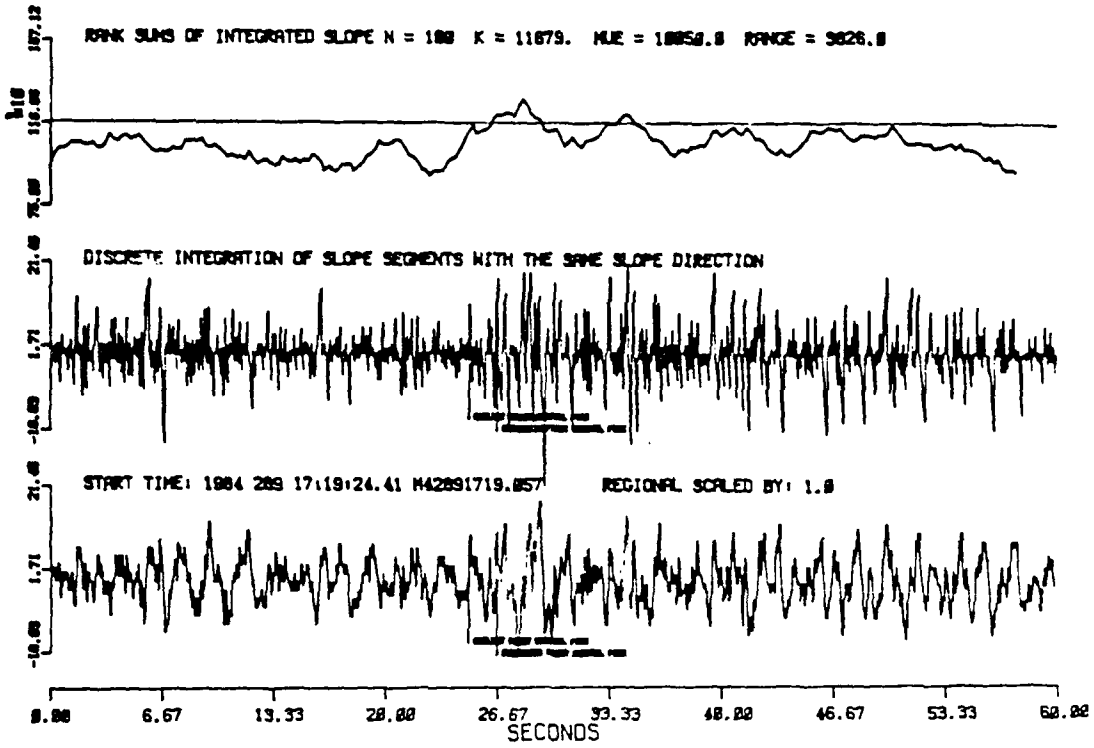

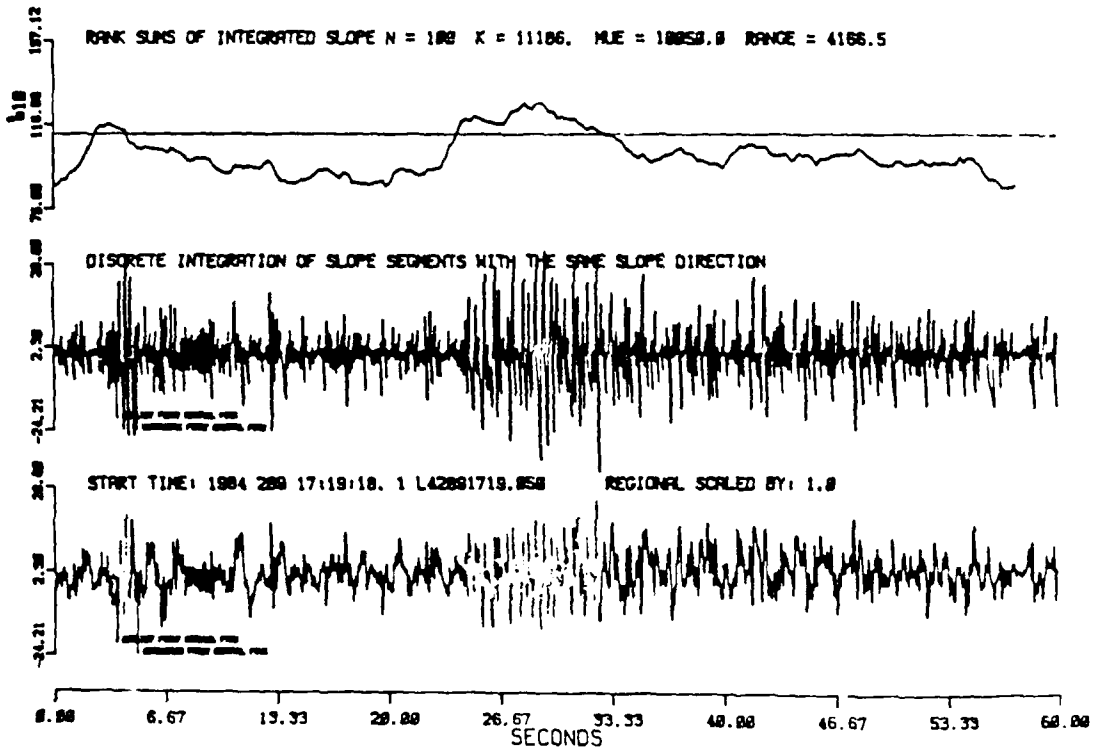

EVENT 2 - Regional (P-Lg) = 20 Seconds

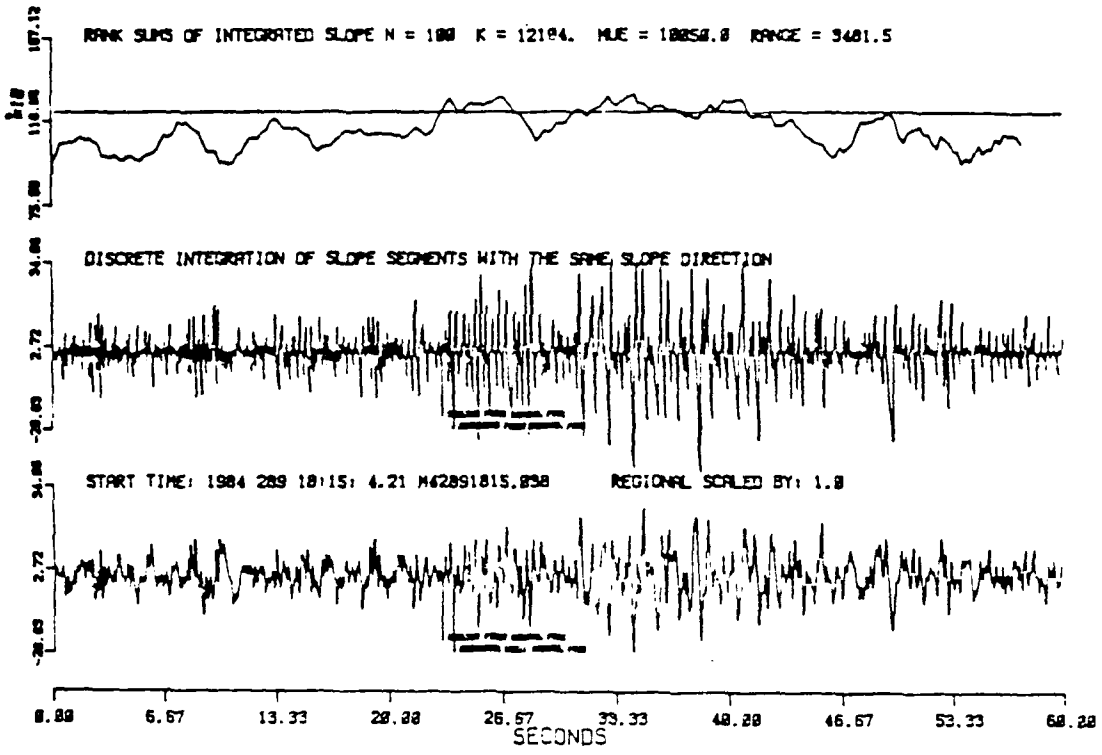

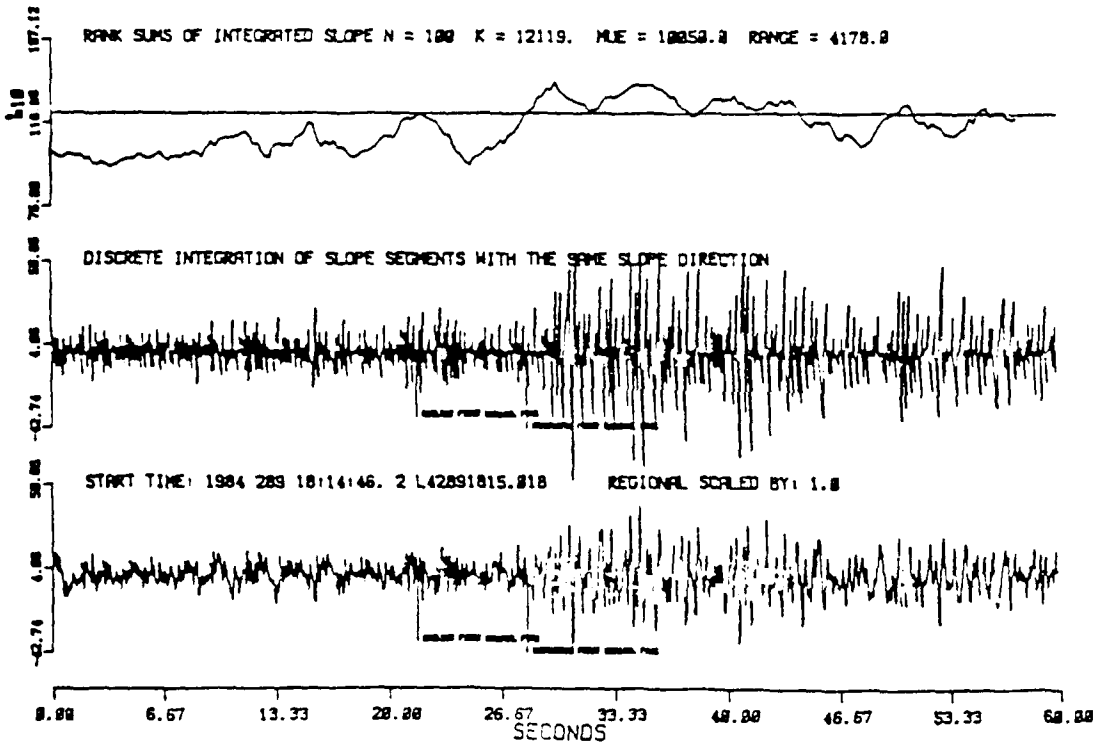

EVENT 3 - Regional (P-Lg) = 1 Minute

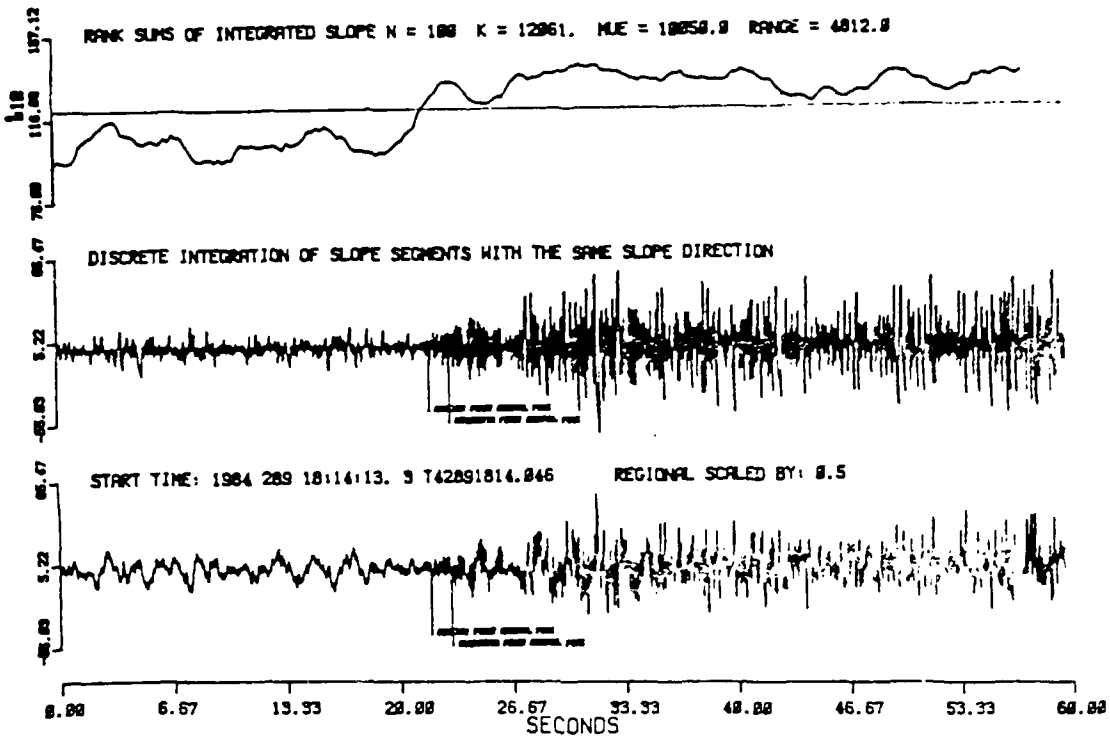
RANK SUMS OF INTEGRATED SLOPE N = 100 K = 12961. MUE = 10050.0 RANGE = 4012.0
DISCRETE INTEGRATION OF SLOPE SEGMENTS WITH THE SAME SLOPE DIRECTION
START TIME: 1984 289 18:14:13. 9 T42891814.046 REGIONAL SCALED BY: 0.5
0.00
6.67
13.33
20.00
26.67
33.33
40.00
46.67
53.33
60.00
SECONDS

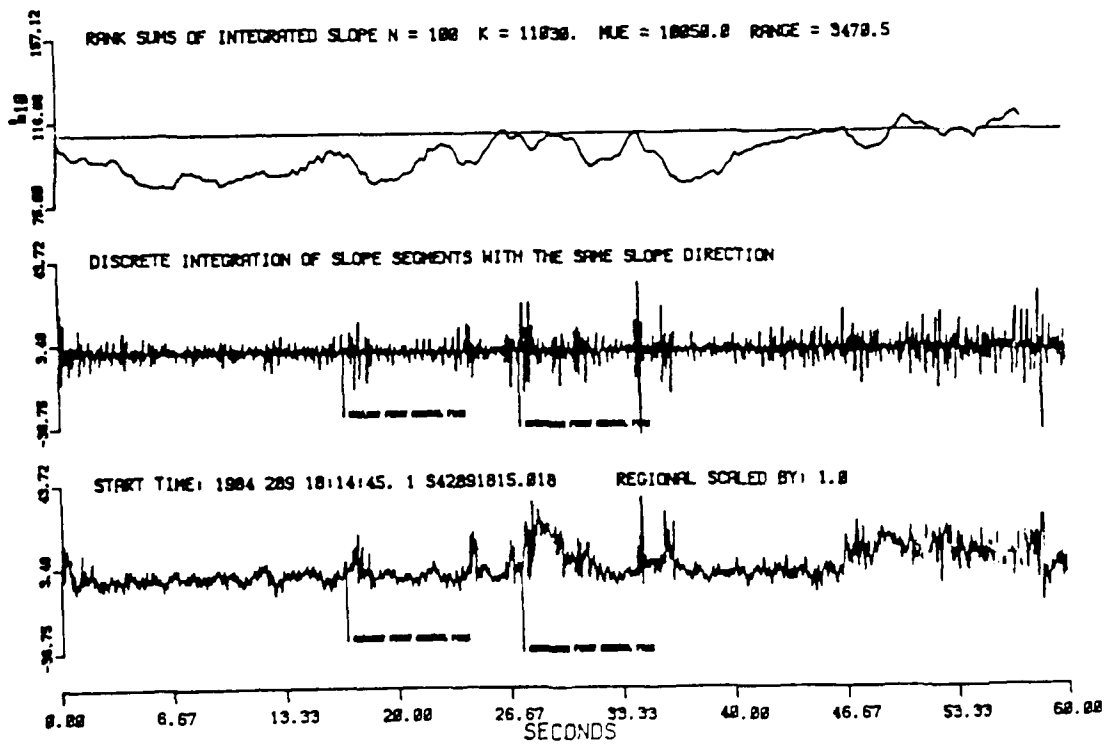
RANK SUMS OF INTEGRATED SLOPE N = 100 K = 11030. MUE = 10050.0 RANGE = 3470.5
DISCRETE INTEGRATION OF SLOPE SEGMENTS WITH THE SAME SLOPE DIRECTION
START TIME: 1984 289 18:14:45. 1 S42891815.010 REGIONAL SCALED BY: 1.0
0.00
6.67
13.33
20.00
26.67
33.33
40.00
46.67
53.33
60.00
SECONDS

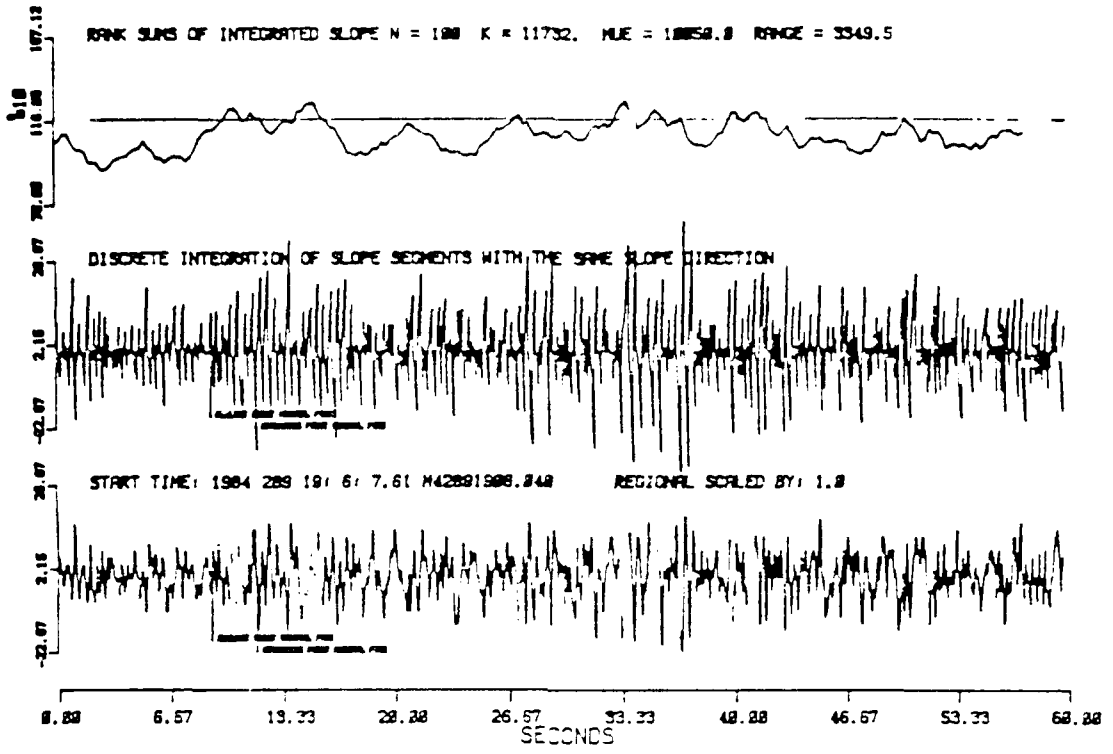

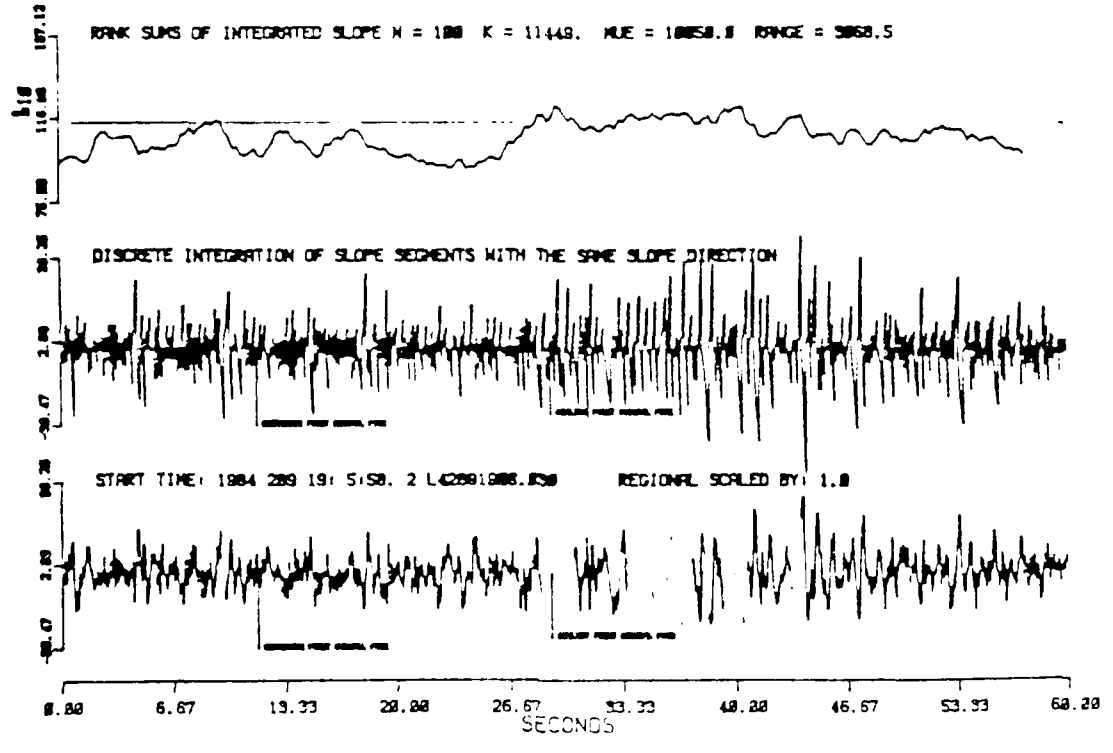

Event 4 - Regional (L - Lg) = 90 Seconds

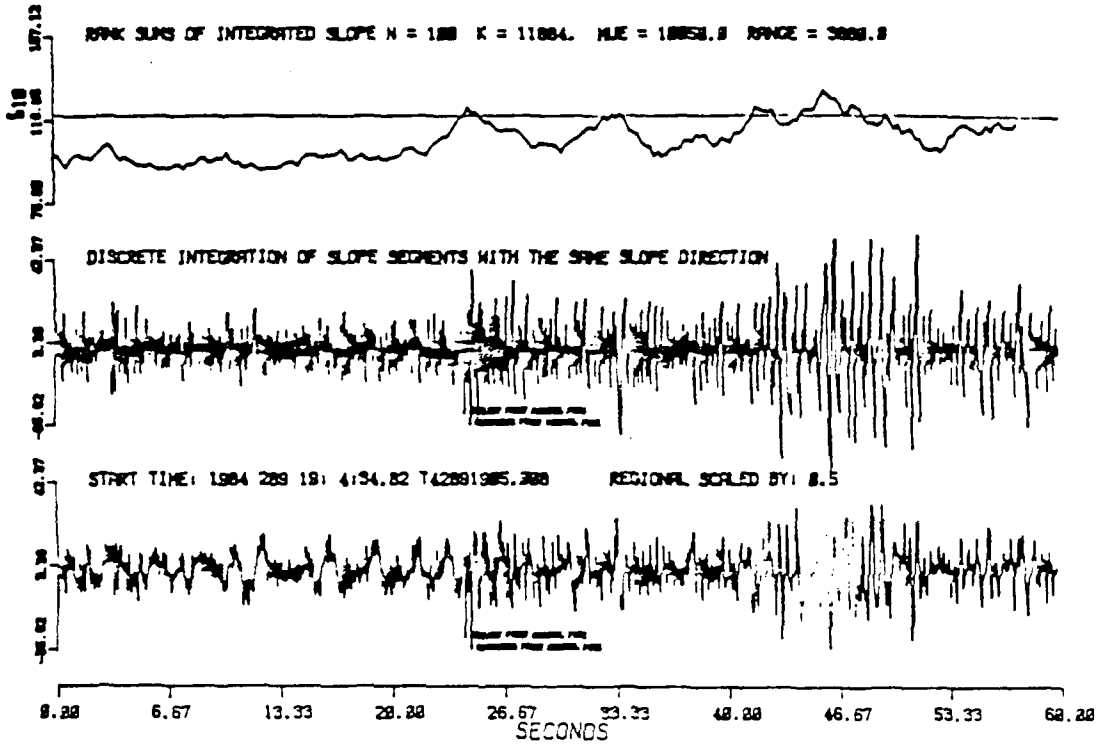
RANK SUMS OF INTEGRATED SLOPE N = 100 K = 11884. MUE = 10050.0 RANGE = 3000.0
DISCRETE INTEGRATION OF SLOPE SEGMENTS WITH THE SAME SLOPE DIRECTION
START TIME: 1984 289 19: 4:54.82 T428891985.300 REGIONAL SCALED BY: 0.5
0.00
6.67
13.33
20.00
26.67
33.33
40.00
46.67
53.33
60.00
SECONDS

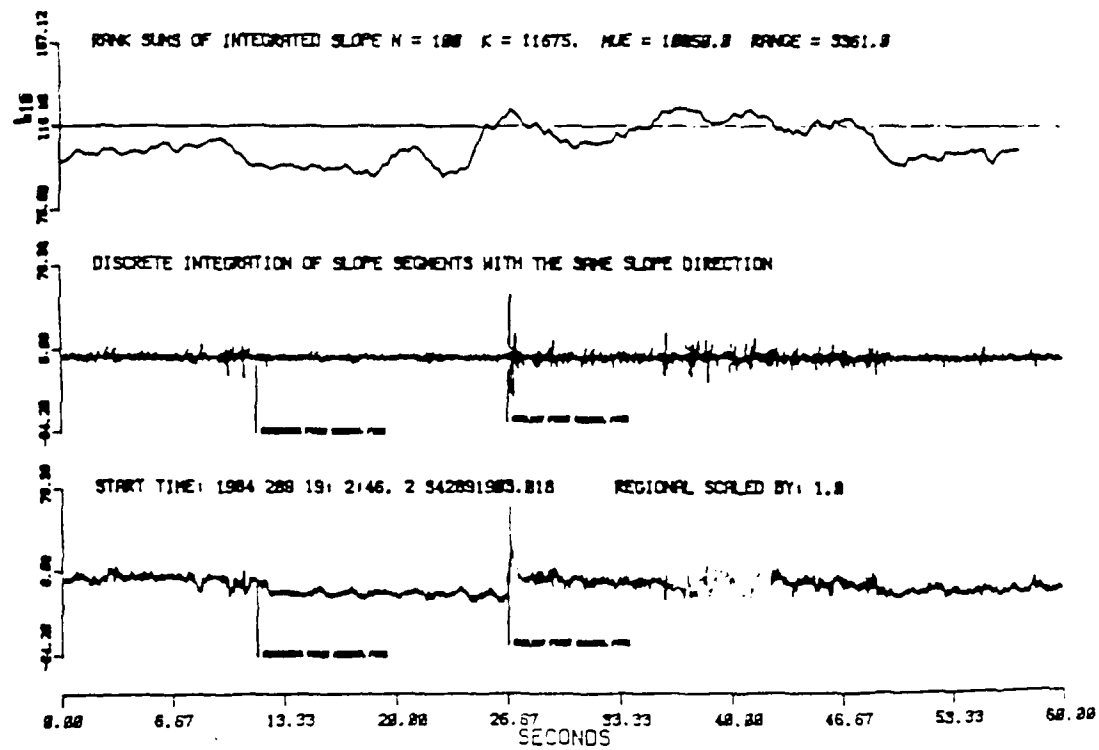
RANK SUMS OF INTEGRATED SLOPE N = 100 K = 11675. MUE = 10050.0 RANGE = 3361.0
DISCRETE INTEGRATION OF SLOPE SEGMENTS WITH THE SAME SLOPE DIRECTION
START TIME: 1984 289 19: 2:46. 2 S428891983.818 REGIONAL SCALED BY: 1.0
0.00
6.67
13.33
20.00
26.67
33.33
40.00
46.67
53.33
60.00
SECONDS

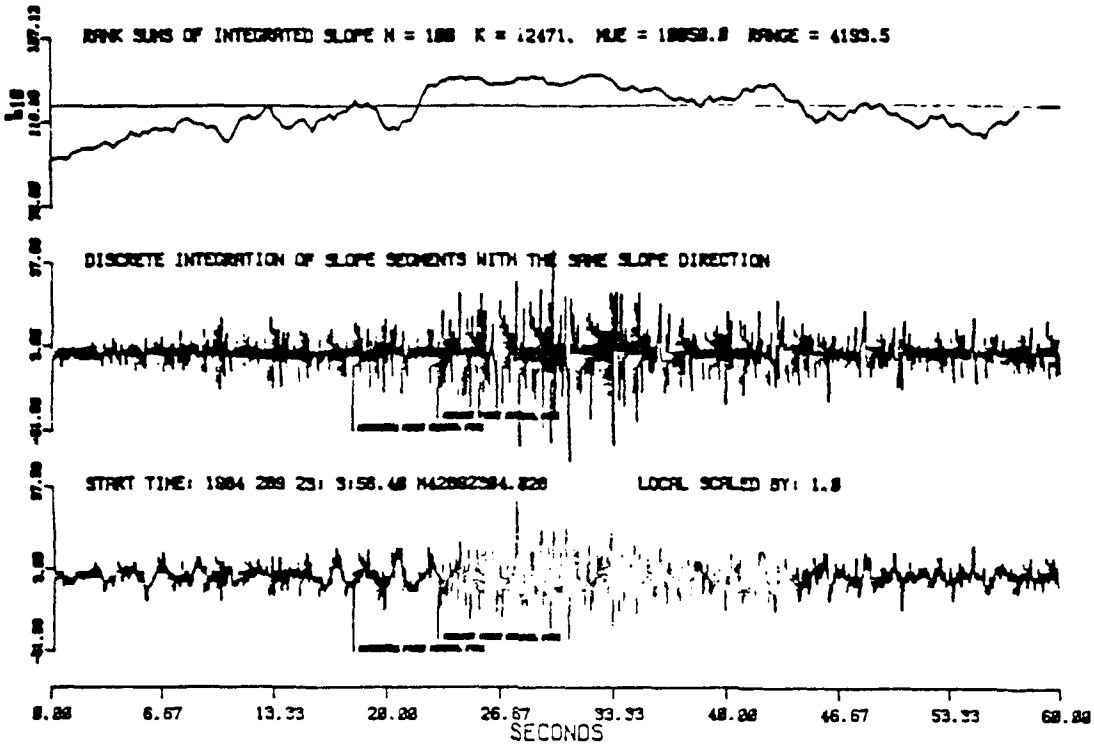

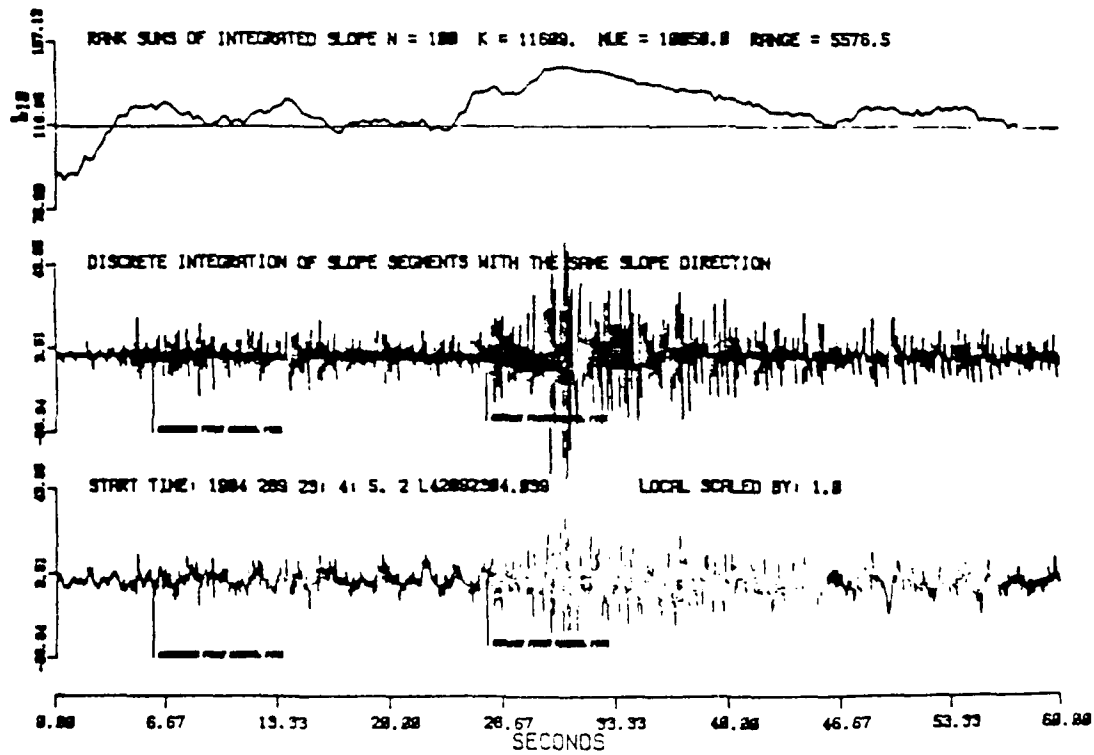

EVENT 5 - Local P Arrival

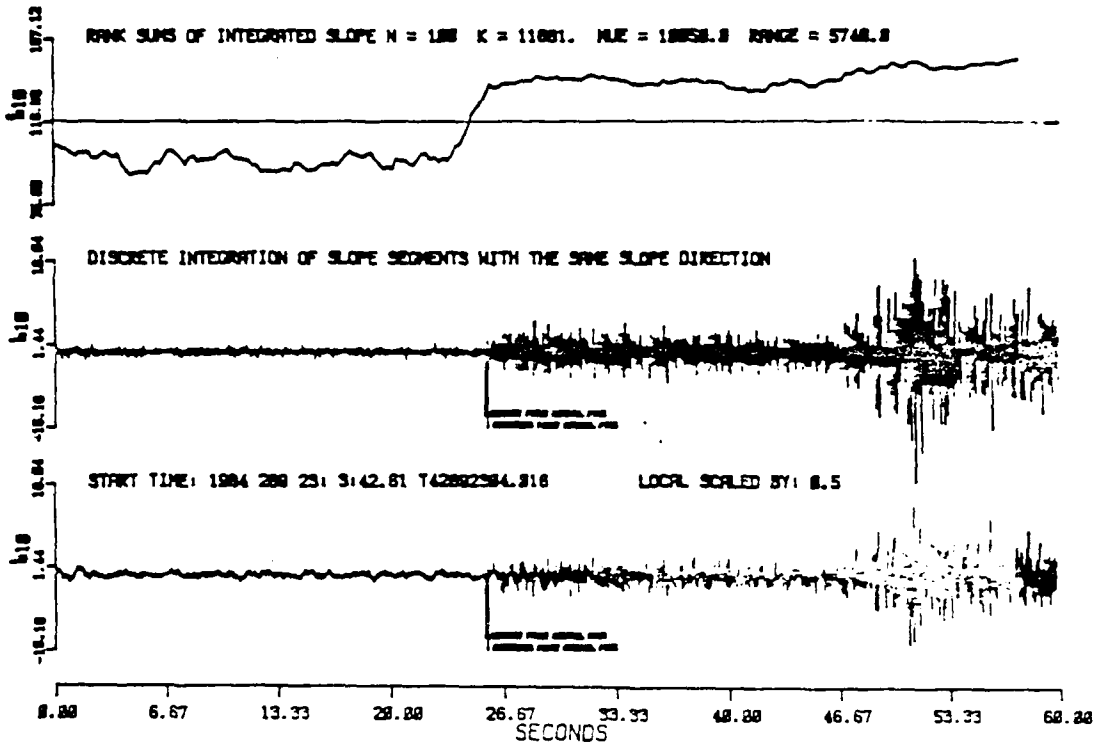
RANK SUMS OF INTEGRATED SLOPE N = 100 K = 11681. MUE = 10050.0 RANGE = 5740.0
DISCRETE INTEGRATION OF SLOPE SEGMENTS WITH THE SAME SLOPE DIRECTION
START TIME: 1984 280 23: 3:42.61 T428892584.816
LOCAL SCALED BY: 8.5
0.00
6.67
13.33
20.00
26.67
33.33
40.00
46.67
53.33
60.00
SECONDS

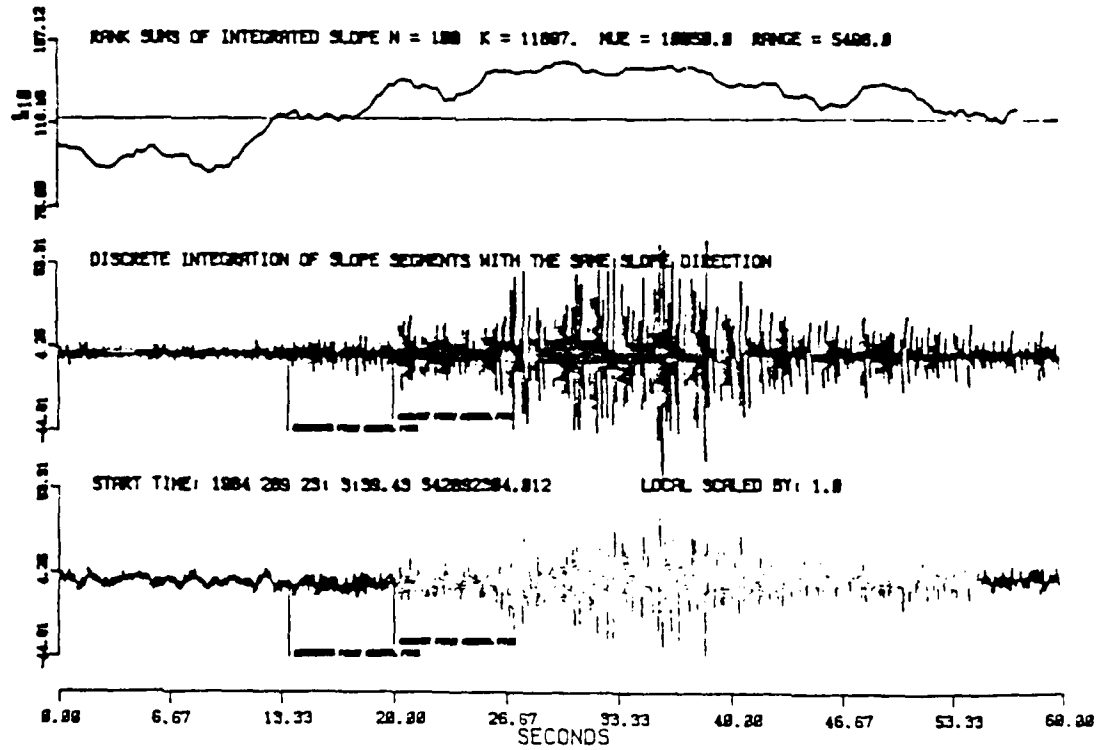
RANK SUMS OF INTEGRATED SLOPE N = 100 K = 11697. MUE = 10050.0 RANGE = 5490.0
DISCRETE INTEGRATION OF SLOPE SEGMENTS WITH THE SAME SLOPE DIRECTION
START TIME: 1984 280 23: 3:50.43 T428892584.812
LOCAL SCALED BY: 1.0
0.00
6.67
13.33
20.00
26.67
33.33
40.00
46.67
53.33
60.00
SECONDS

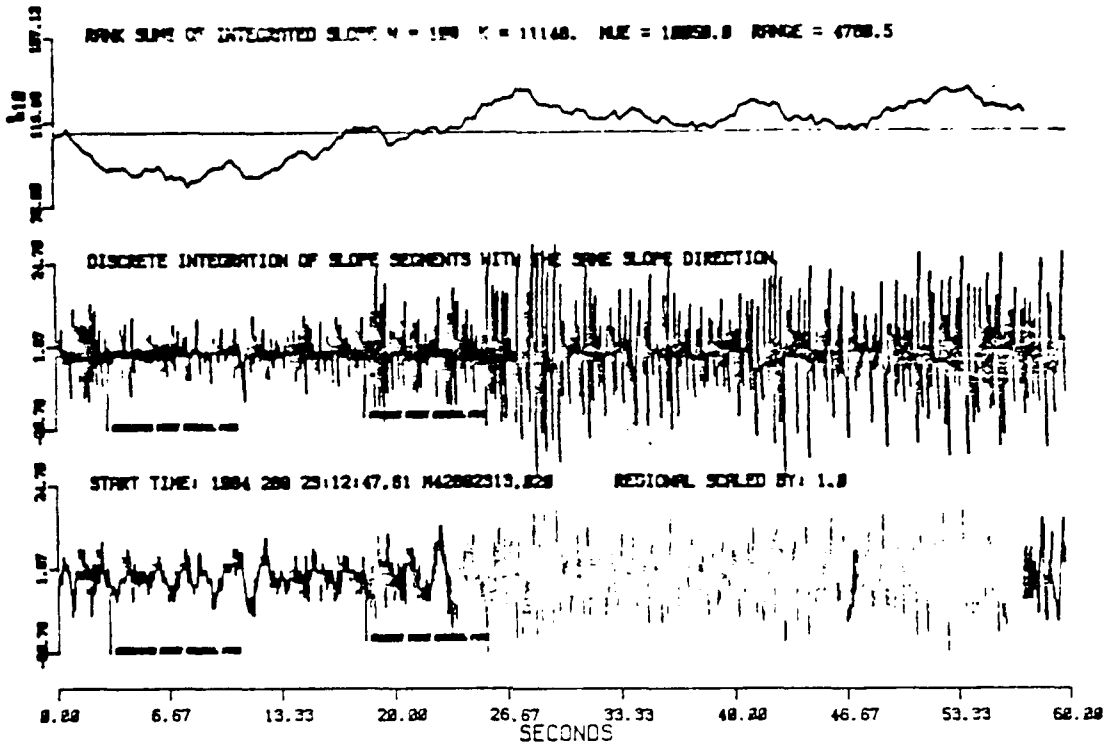

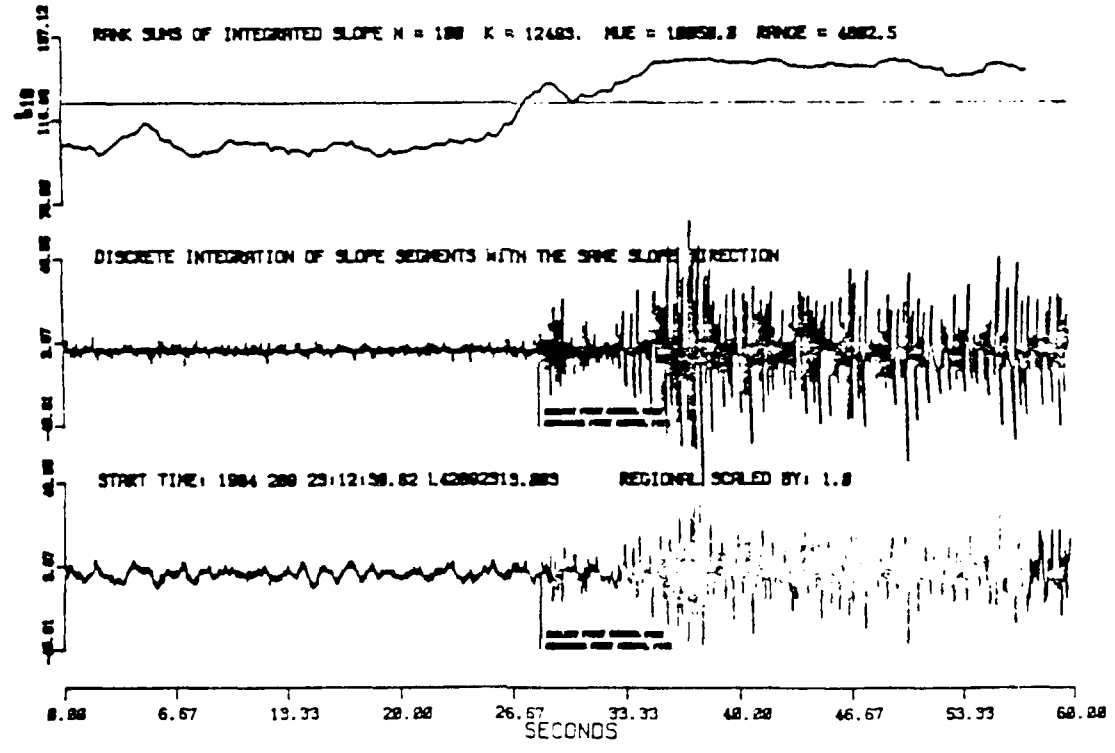

Event 6 - Regional (P - Lg) = 36 Seconds

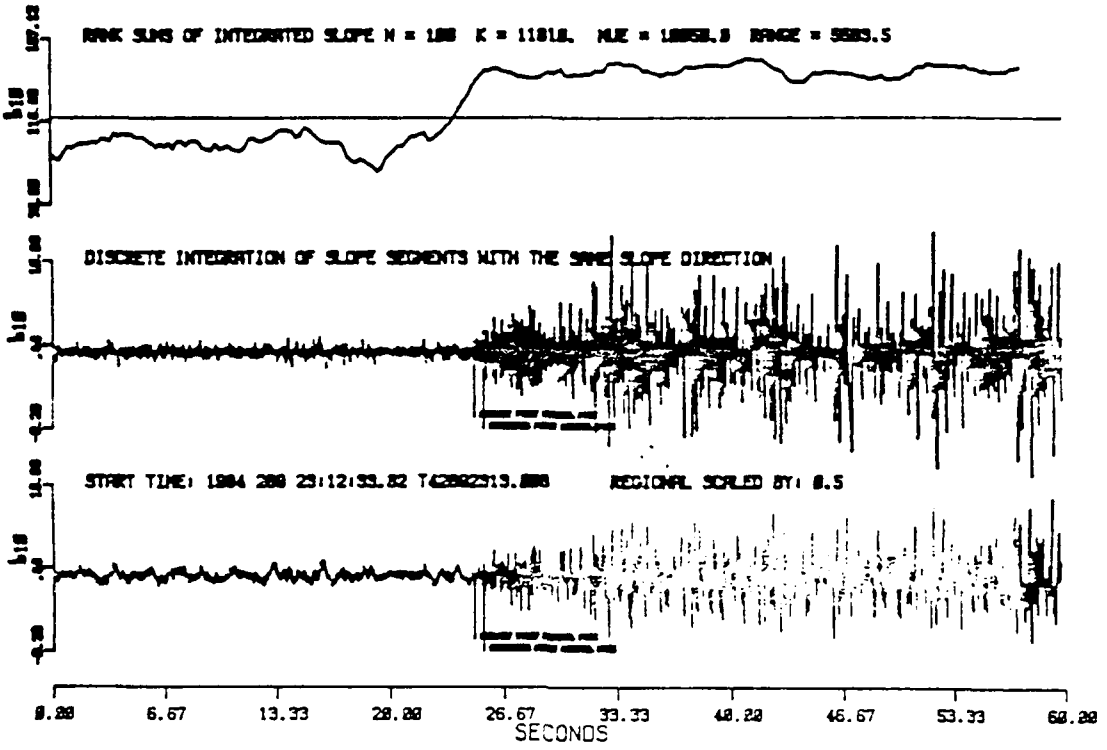
RANK SUMS OF INTEGRATED SLOPE N = 100 K = 11818. MUE = 10050.0 RANGE = 9503.5
DISCRETE INTEGRATION OF SLOPE SEGMENTS WITH THE SAME SLOPE DIRECTION
START TIME: 1984 200 23:12:33.82 T42892313.000 REGIONAL SCALED BY: 0.5
0.00
6.67
13.33
20.00
26.67
33.33
40.00
46.67
53.33
60.00
SECONDS

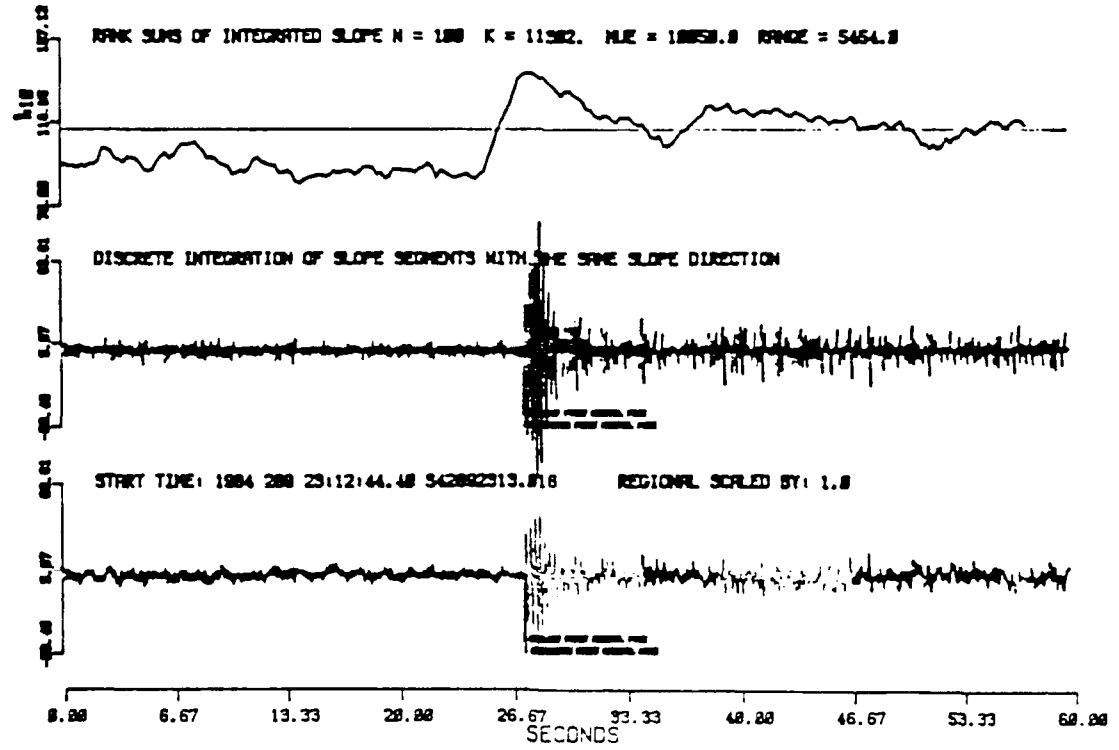
RANK SUMS OF INTEGRATED SLOPE N = 100 K = 11582. MUE = 10050.0 RANGE = 5454.0
DISCRETE INTEGRATION OF SLOPE SEGMENTS WITH THE SAME SLOPE DIRECTION
START TIME: 1984 200 23:12:44.48 T42892313.016 REGIONAL SCALED BY: 1.0
0.00
6.67
13.33
20.00
26.67
33.33
40.00
46.67
53.33
60.00
SECONDS

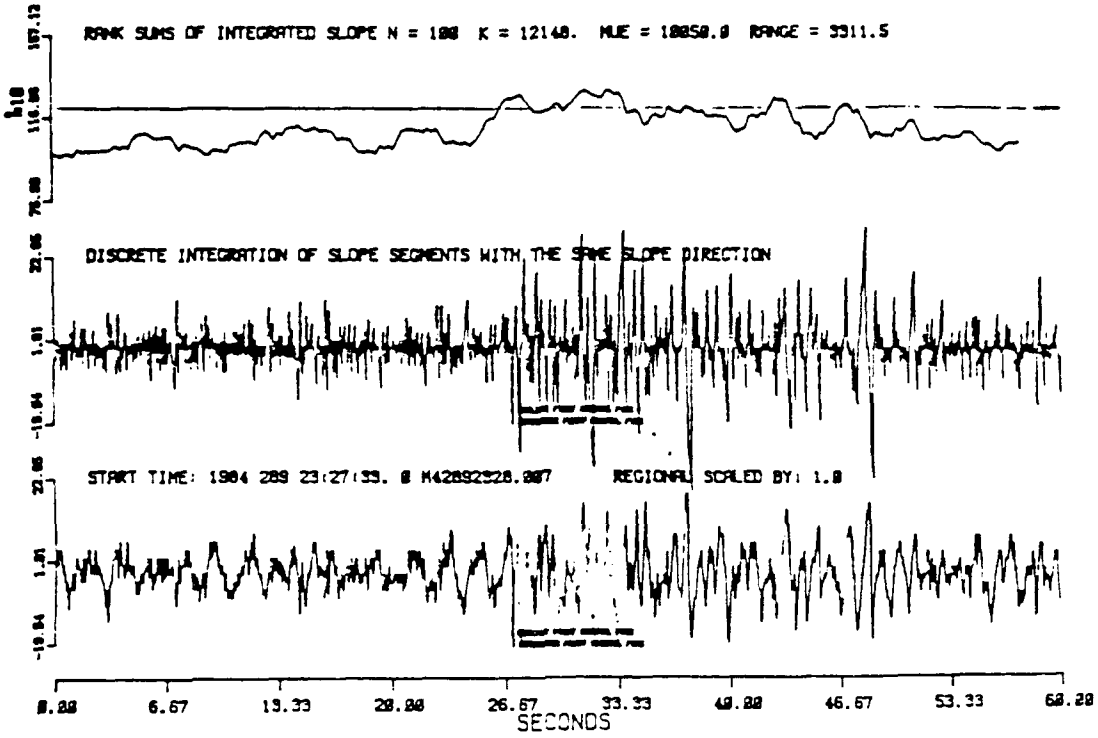

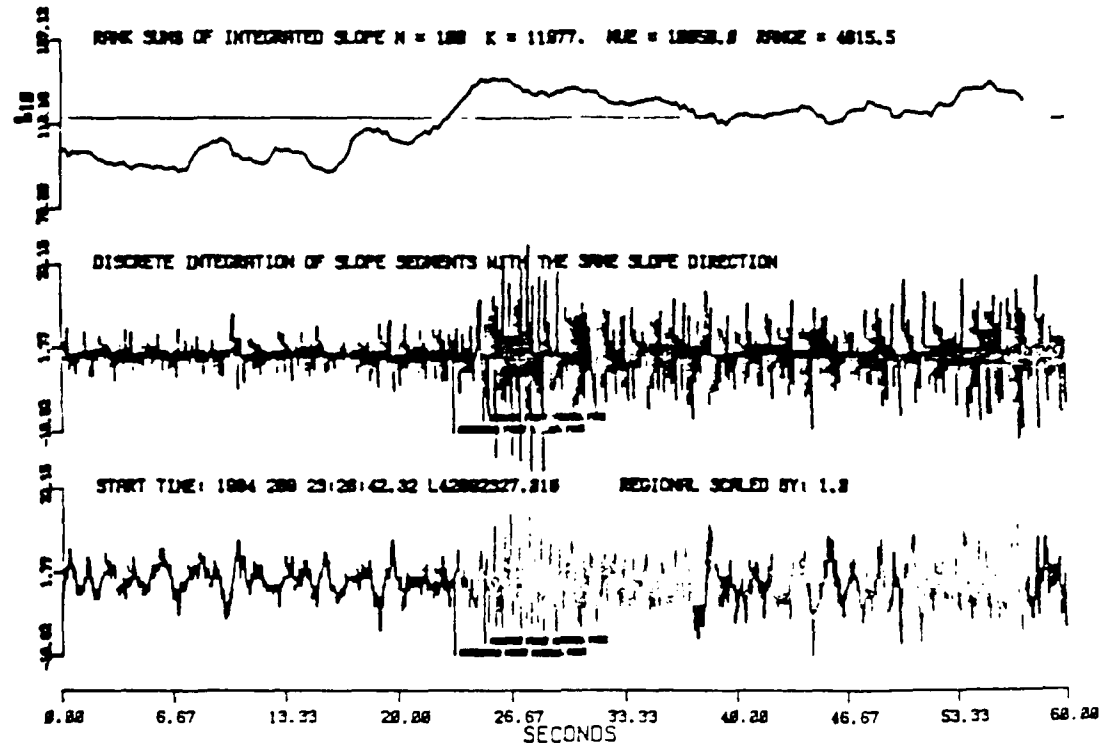

Event 7 - Regional (P - Lg) = 40 Seconds

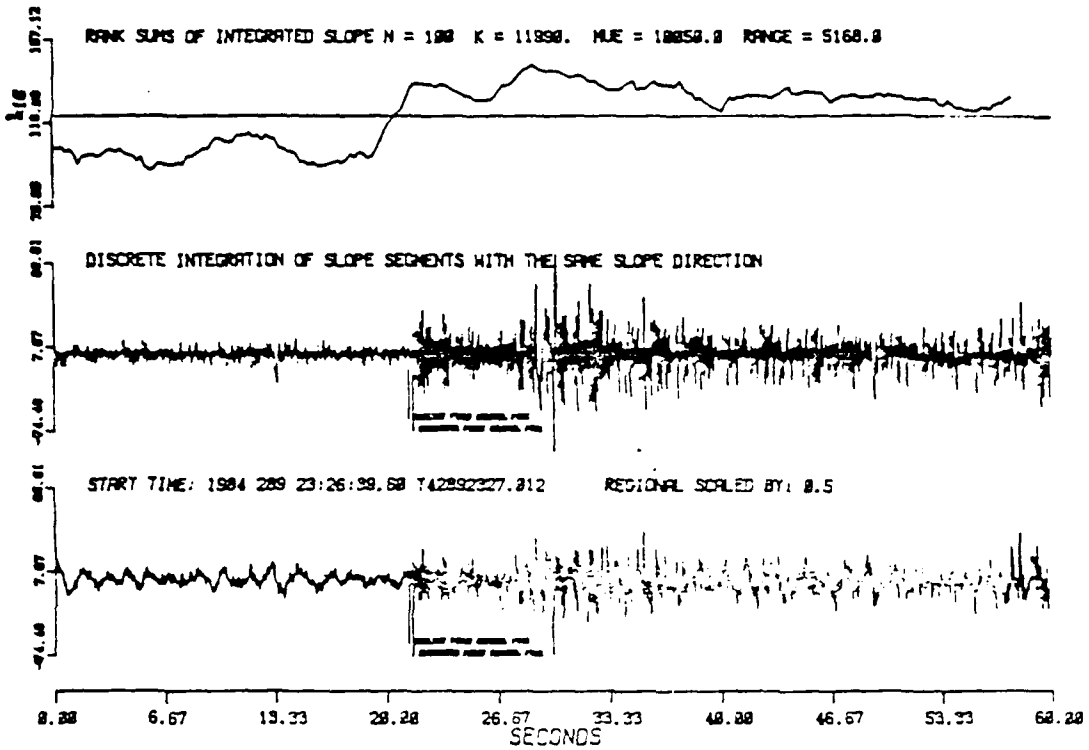
RANK SUMS OF INTEGRATED SLOPE N = 100 K = 11990. MUE = 10050.0 RANGE = 5160.0
DISCRETE INTEGRATION OF SLOPE SEGMENTS WITH THE SAME SLOPE DIRECTION
START TIME: 1984 289 23:26:39.60 T42892327.012 REGIONAL SCALED BY: 0.5
0.00
6.67
13.33
20.00
26.67
33.33
40.00
46.67
53.33
60.00
SECONDS

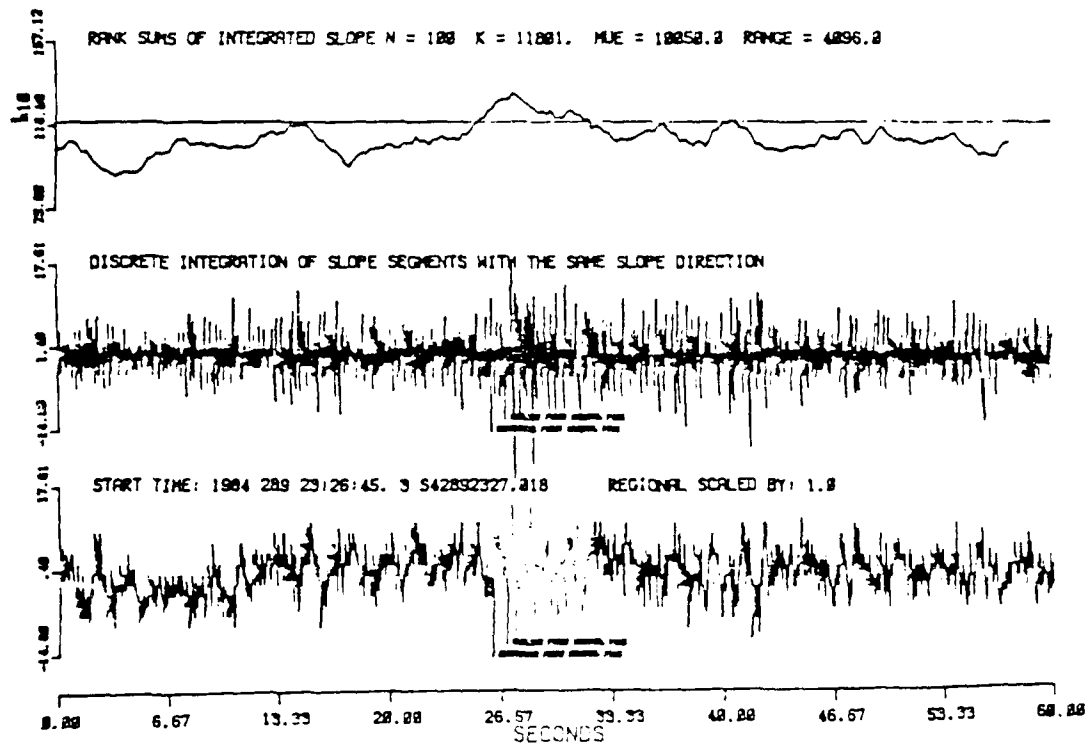
RANK SUMS OF INTEGRATED SLOPE N = 100 K = 11001. MUE = 10050.0 RANGE = 4096.0
DISCRETE INTEGRATION OF SLOPE SEGMENTS WITH THE SAME SLOPE DIRECTION
START TIME: 1984 289 23:26:45. 3 S42892327.018 REGIONAL SCALED BY: 1.0
0.00
6.67
13.33
20.00
26.67
33.33
40.00
46.67
53.33
60.00
SECONDS

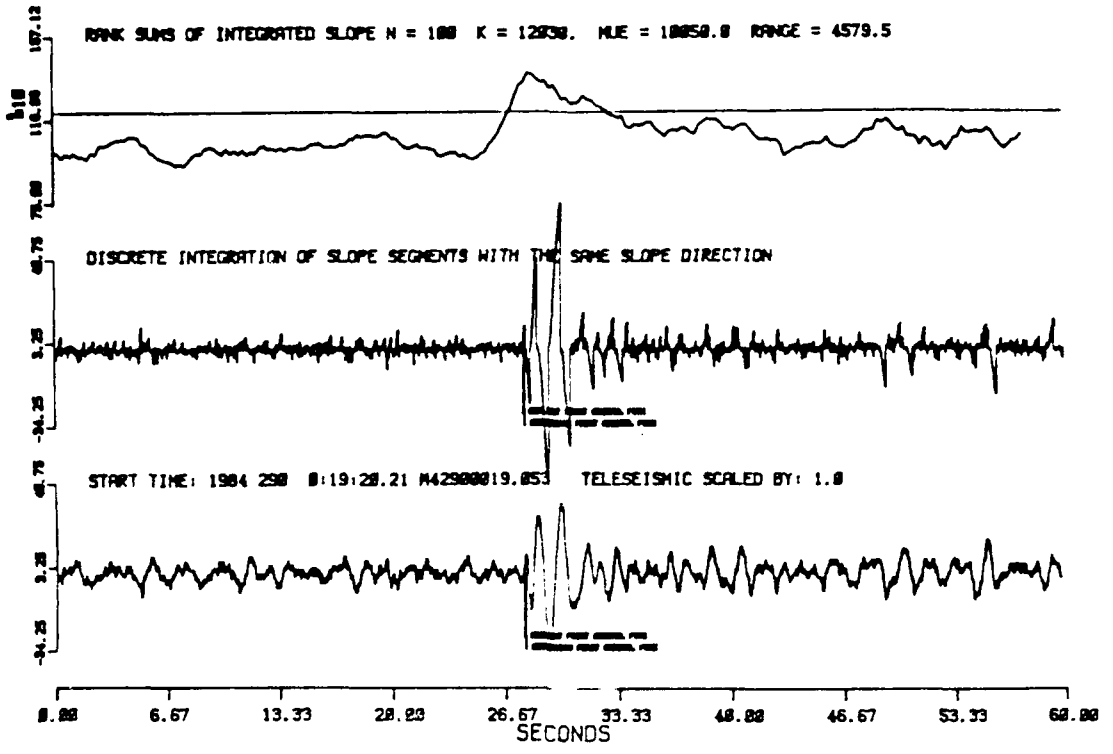

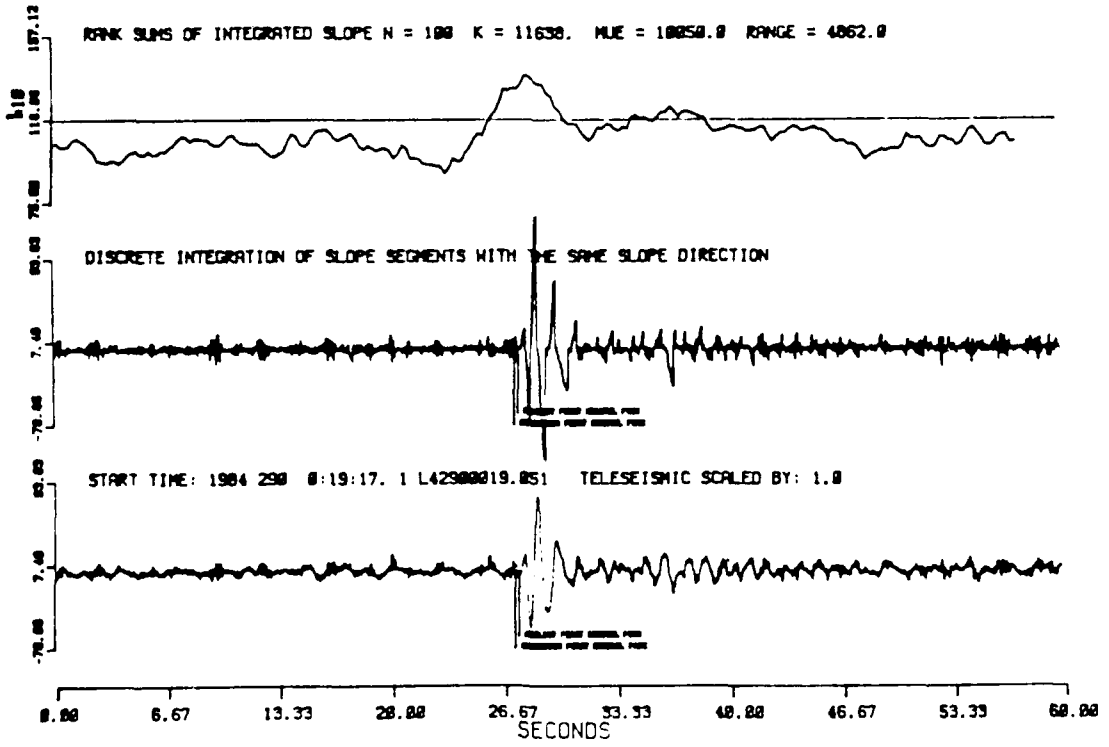

Event 8 - Fiji Islands Region - 19.1S 177.9W - 10/16/84
Origin Time: 00:07:51.3 - Depth: 449 km + 89 M_b: 4.5
Residual Error: -0.0

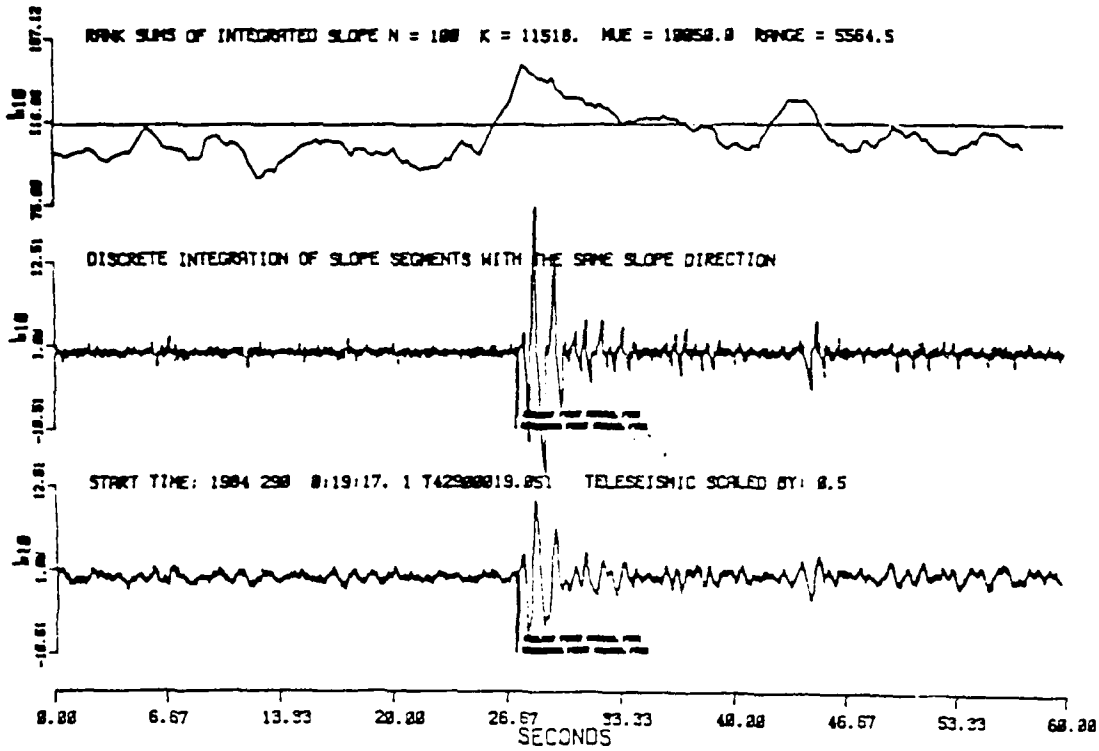
RANK SUMS OF INTEGRATED SLOPE N = 100 K = 11518. MUE = 10050.0 RANGE = 5564.5
DISCRETE INTEGRATION OF SLOPE SEGMENTS WITH THE SAME SLOPE DIRECTION
START TIME: 1984 290 0:19:17. 1 T42900019.051 TELESEISMIC SCALED BY: 0.5
0.00
6.67
13.33
20.00
26.67
33.33
40.00
46.67
53.33
60.00
SECONDS

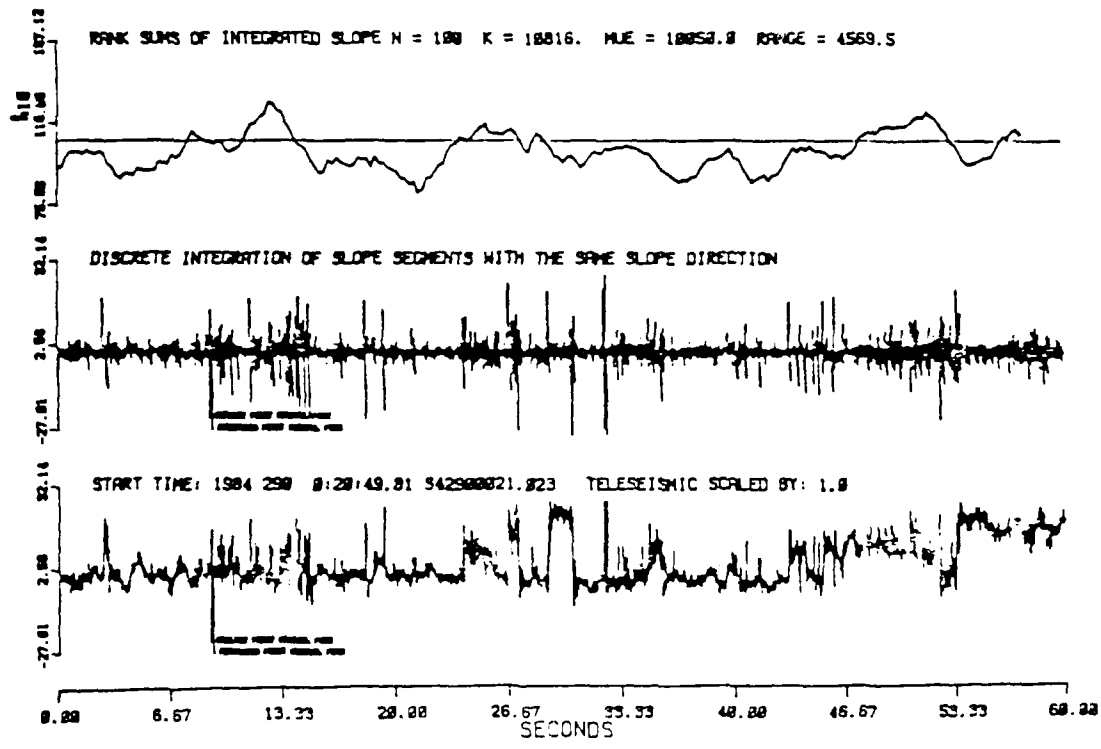
RANK SUMS OF INTEGRATED SLOPE N = 100 K = 10816. MUE = 10050.0 RANGE = 4569.5
DISCRETE INTEGRATION OF SLOPE SEGMENTS WITH THE SAME SLOPE DIRECTION
START TIME: 1984 290 0:20:49.01 T42900021.023 TELESEISMIC SCALED BY: 1.0
0.00
6.67
13.33
20.00
26.67
33.33
40.00
46.67
53.33
60.00
SECONDS

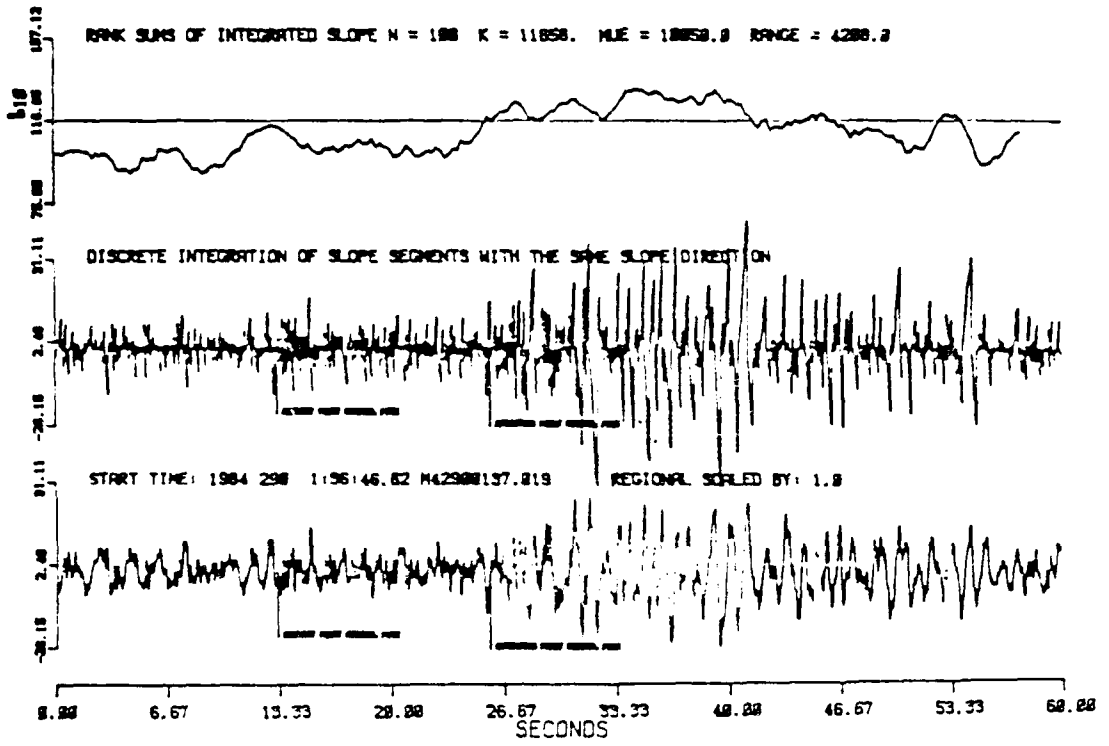

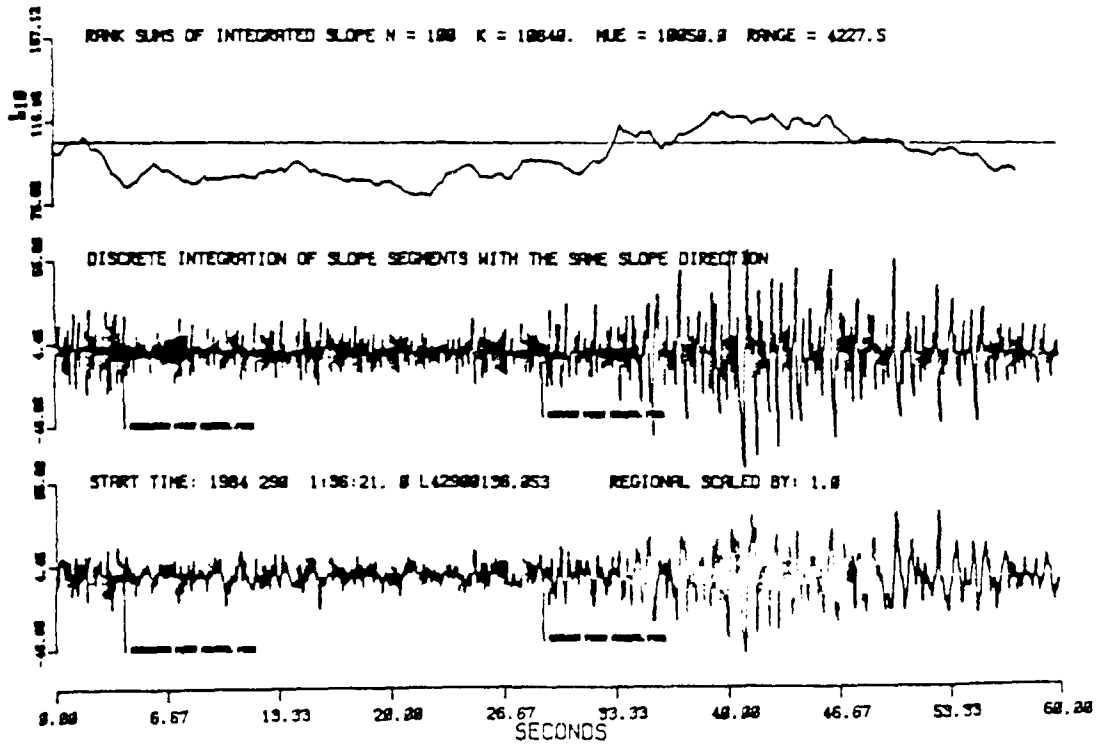

Event 9 - Regional (P - Lg) = 37 Seconds

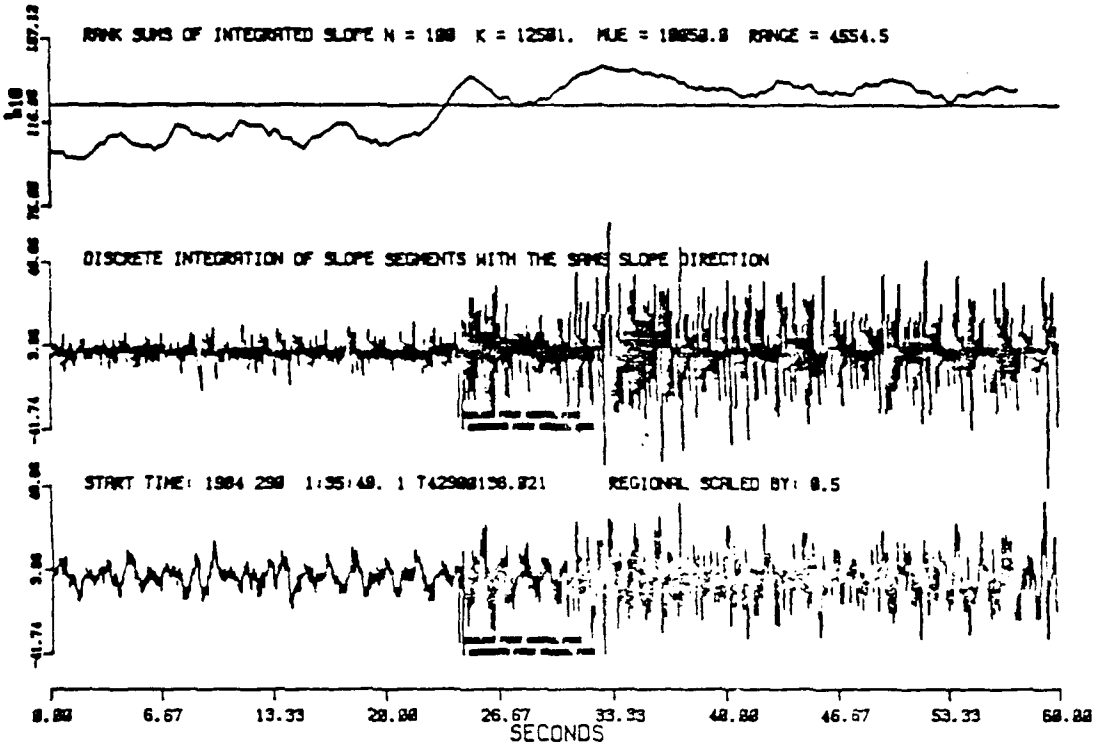
RANK SUMS OF INTEGRATED SLOPE N = 100 K = 12581. MUE = 10050.0 RANGE = 4554.5
DISCRETE INTEGRATION OF SLOPE SEGMENTS WITH THE SAME SLOPE DIRECTION
START TIME: 1984 290 1:35:49. 1 T42900150.021 REGIONAL SCALED BY: 0.5
0.00
6.67
13.33
20.00
26.67
33.33
40.00
46.67
53.33
60.00
SECONDS

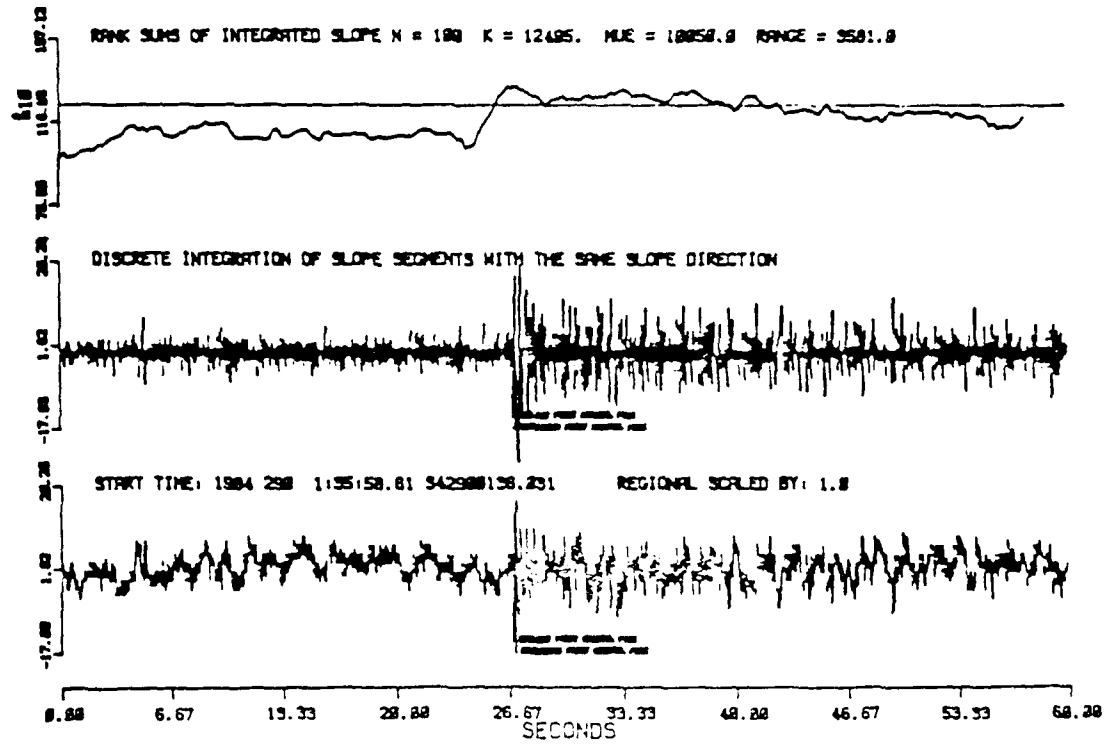
RANK SUMS OF INTEGRATED SLOPE N = 100 K = 12495. MUE = 10050.0 RANGE = 3581.0
DISCRETE INTEGRATION OF SLOPE SEGMENTS WITH THE SAME SLOPE DIRECTION
START TIME: 1984 290 1:35:50.01 T42900150.231 REGIONAL SCALED BY: 1.0
0.00
6.67
13.33
20.00
26.67
33.33
40.00
46.67
53.33
60.00
SECONDS

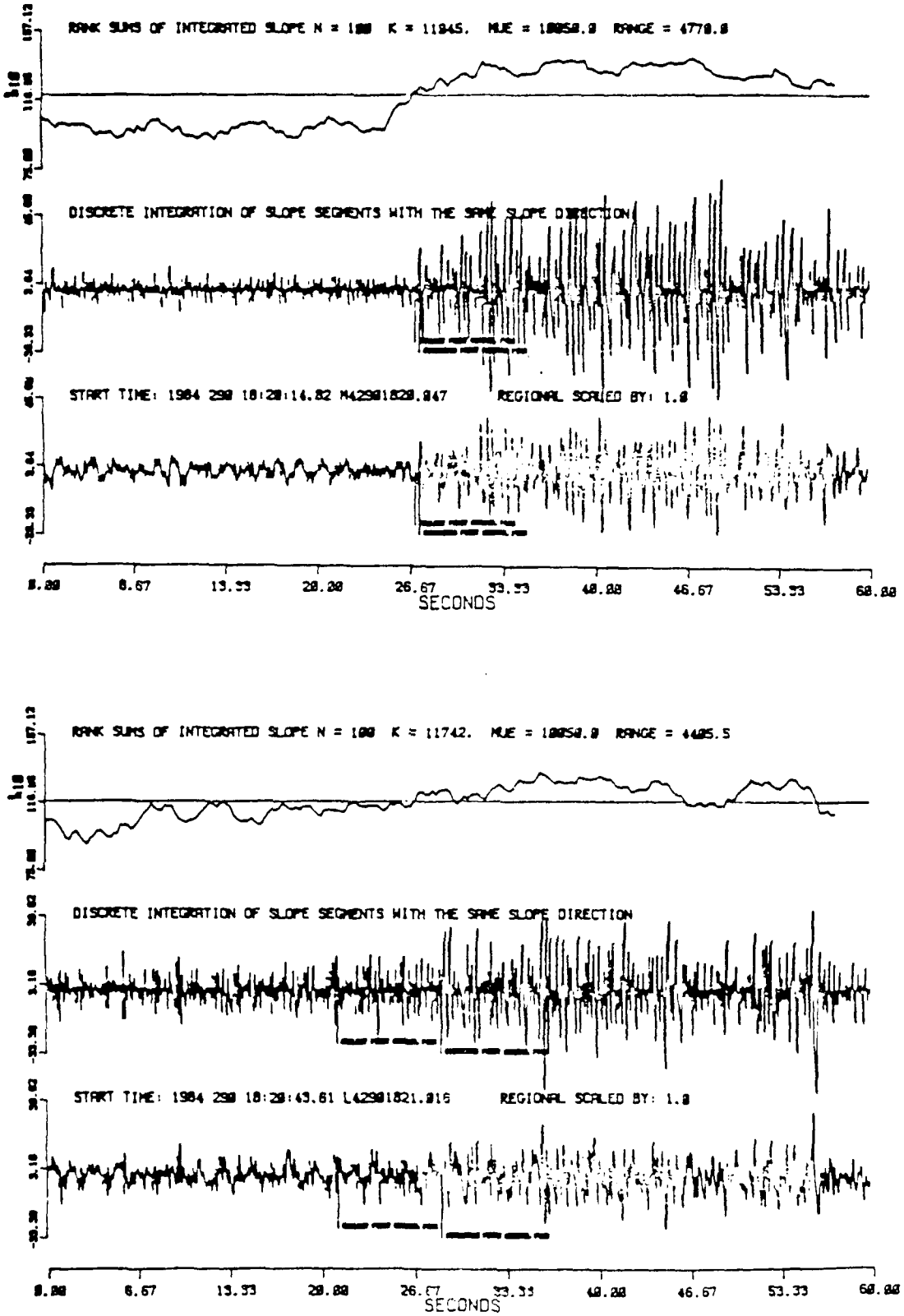

Event 10 - Regional (P - Lg) - 11 Seconds

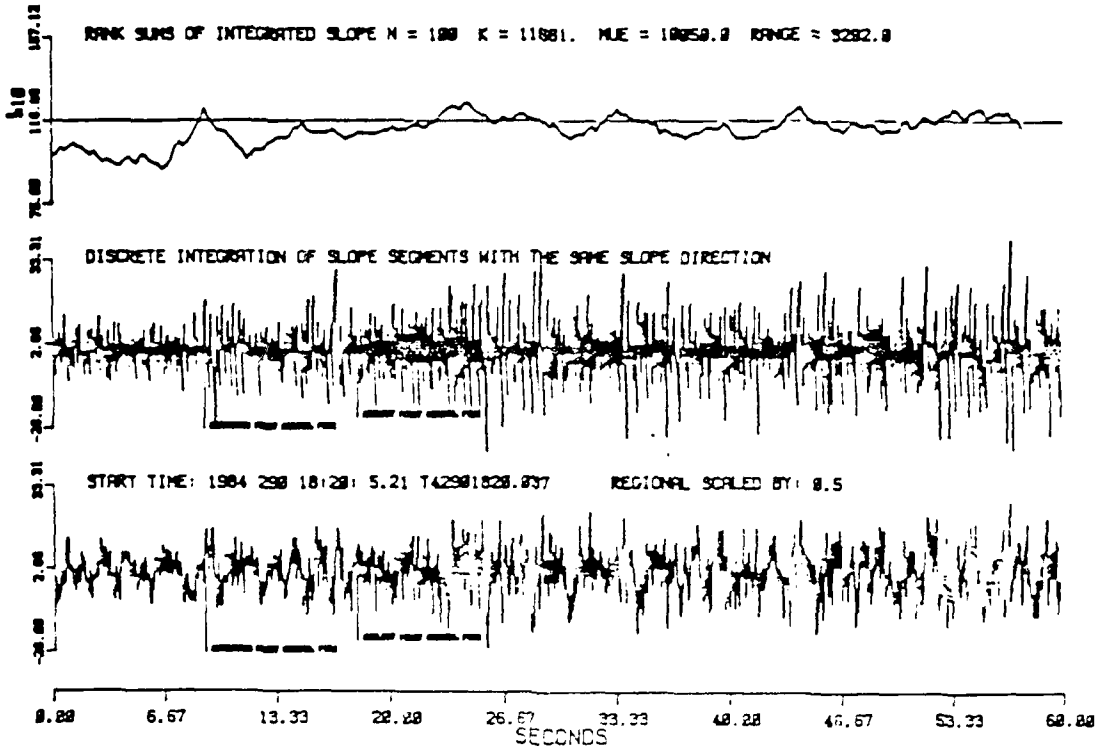
RANK SUMS OF INTEGRATED SLOPE N = 100 K = 11881. MUE = 10050.0 RANGE = 3282.0
DISCRETE INTEGRATION OF SLOPE SEGMENTS WITH THE SAME SLOPE DIRECTION
START TIME: 1984 290 18:20: 5.21 T42901820.897 REGIONAL SCALED BY: 0.5
0.00
6.67
13.33
20.00
26.67
33.33
40.00
46.67
53.33
60.00
SECONDS

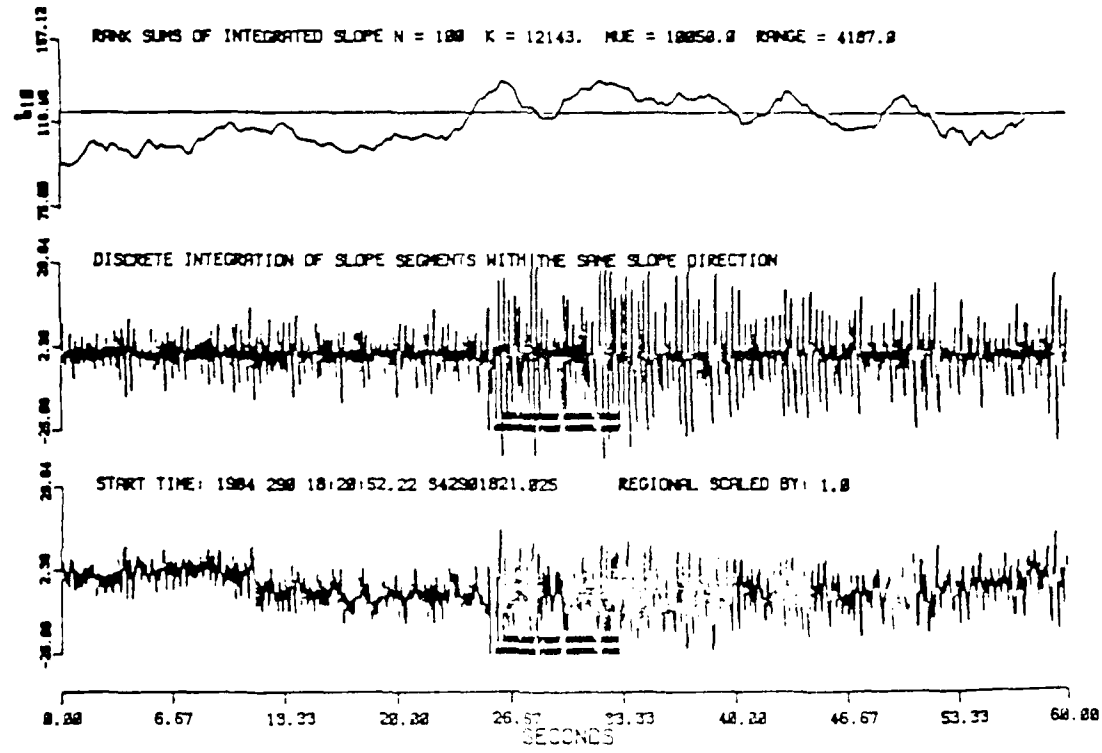
RANK SUMS OF INTEGRATED SLOPE N = 100 K = 12143. MUE = 10050.0 RANGE = 4187.0
DISCRETE INTEGRATION OF SLOPE SEGMENTS WITH THE SAME SLOPE DIRECTION
START TIME: 1984 290 18:20:52.22 S42901821.825 REGIONAL SCALED BY: 1.0
0.00
6.67
13.33
20.00
26.67
33.33
40.00
46.67
53.33
60.00
SECONDS

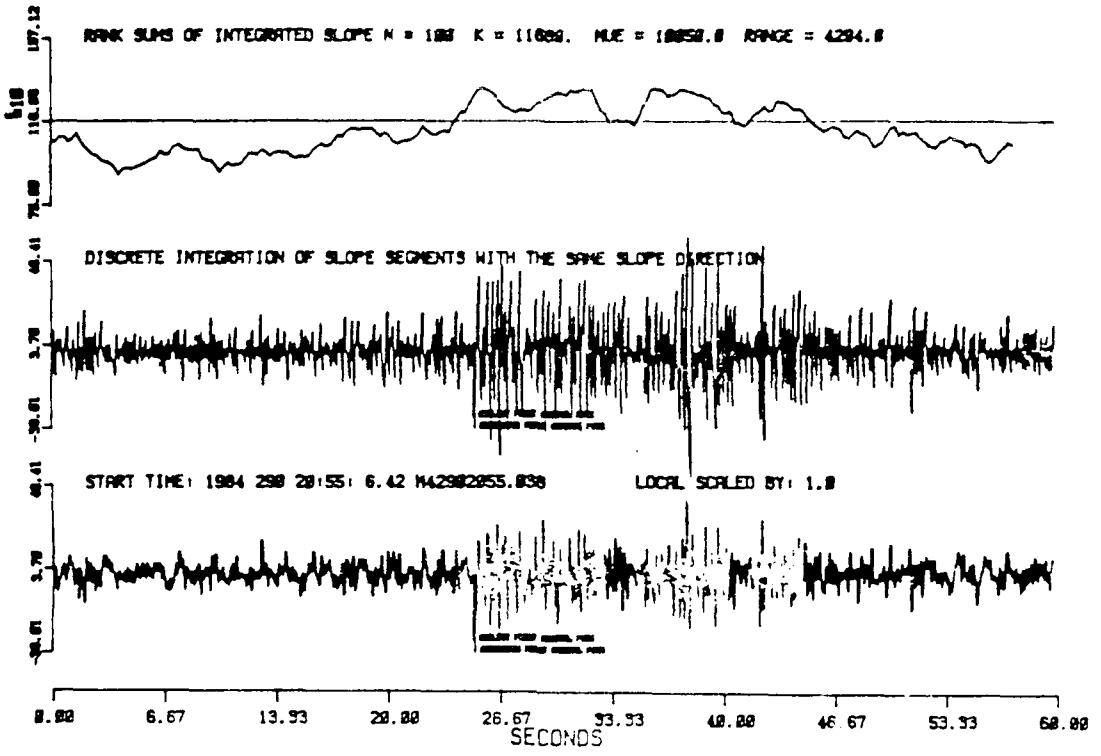

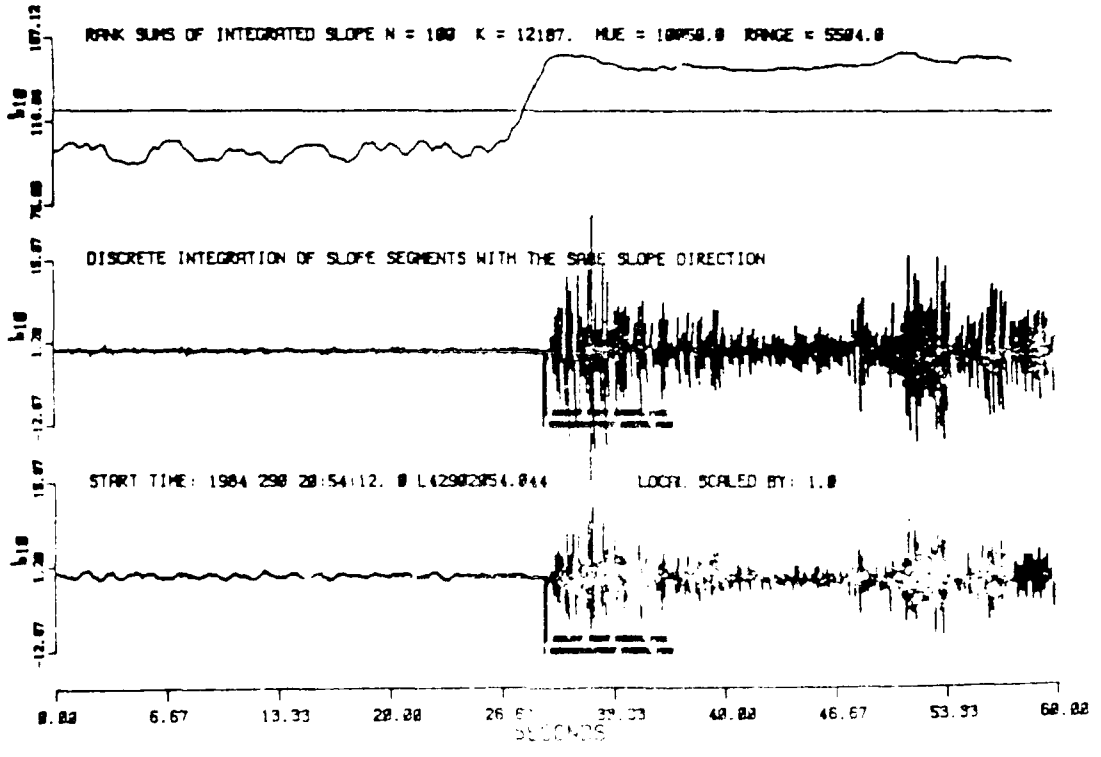

Event 11 - Mexico - October 16, 1984 - Quarry Blast

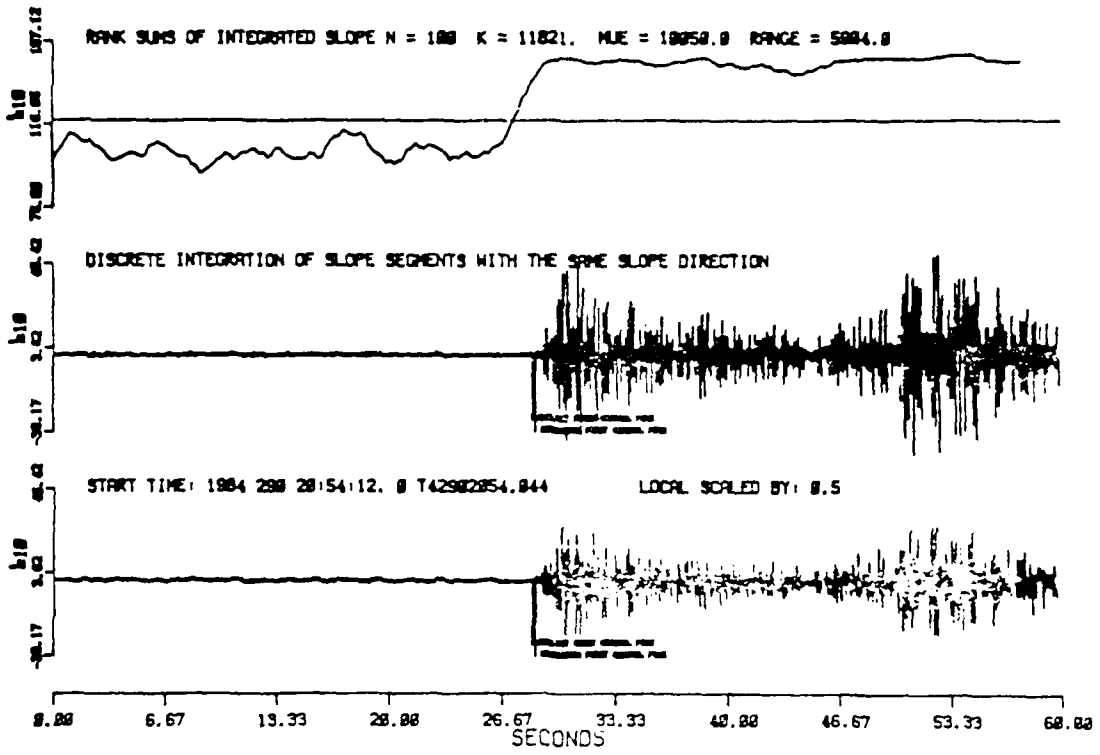
RANK SUMS OF INTEGRATED SLOPE N = 100 K = 11821. MUE = 10050.0 RANGE = 5004.0
DISCRETE INTEGRATION OF SLOPE SEGMENTS WITH THE SAME SLOPE DIRECTION
START TIME: 1984 288 20:54:12. 0 T429002854.844
LOCAL SCALED BY: 0.5
0.00
6.67
13.33
20.00
26.67
33.33
40.00
46.67
53.33
60.00
SECONDS

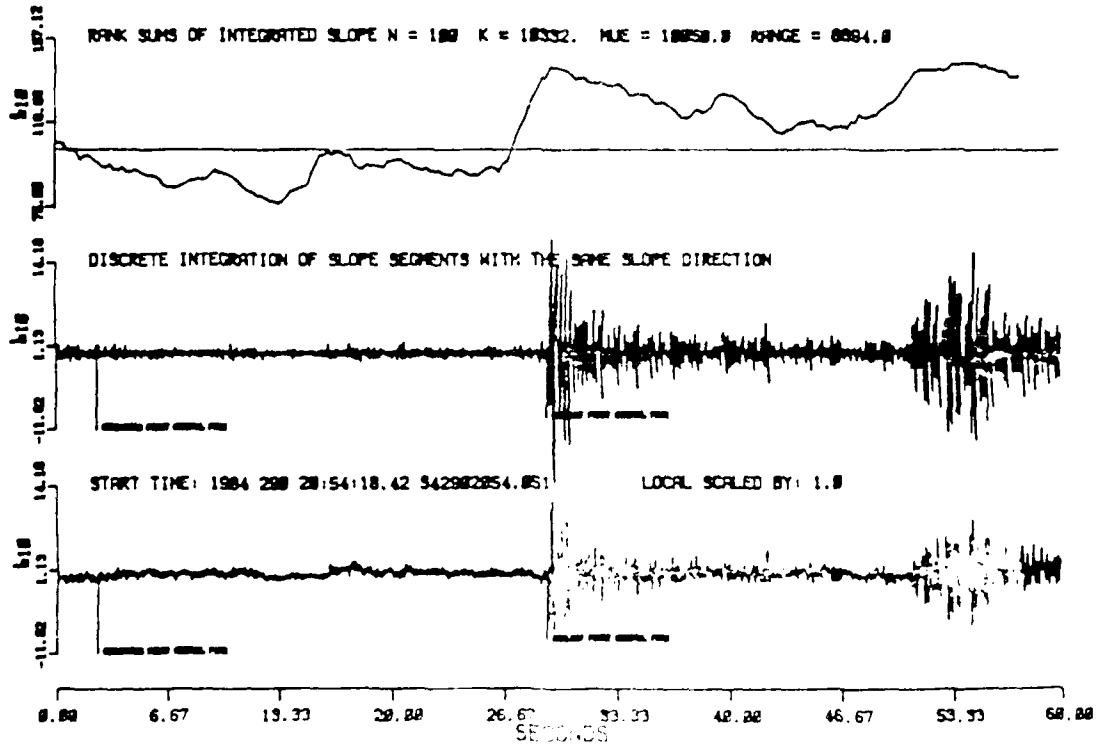
RANK SUMS OF INTEGRATED SLOPE N = 100 K = 10332. MUE = 10050.0 RANGE = 0004.0
DISCRETE INTEGRATION OF SLOPE SEGMENTS WITH THE SAME SLOPE DIRECTION
START TIME: 1984 288 20:54:18.42 T429002854.851
LOCAL SCALED BY: 1.0
0.00
6.67
13.33
20.00
26.67
33.33
40.00
46.67
53.33
60.00
SECONDS

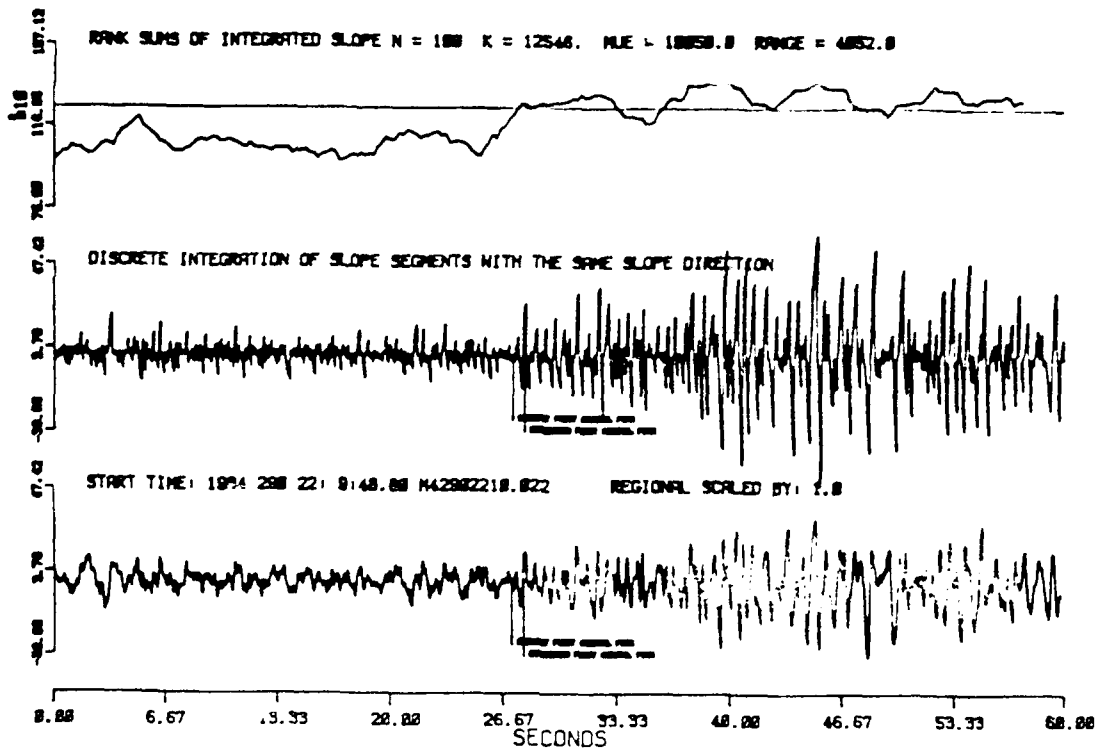

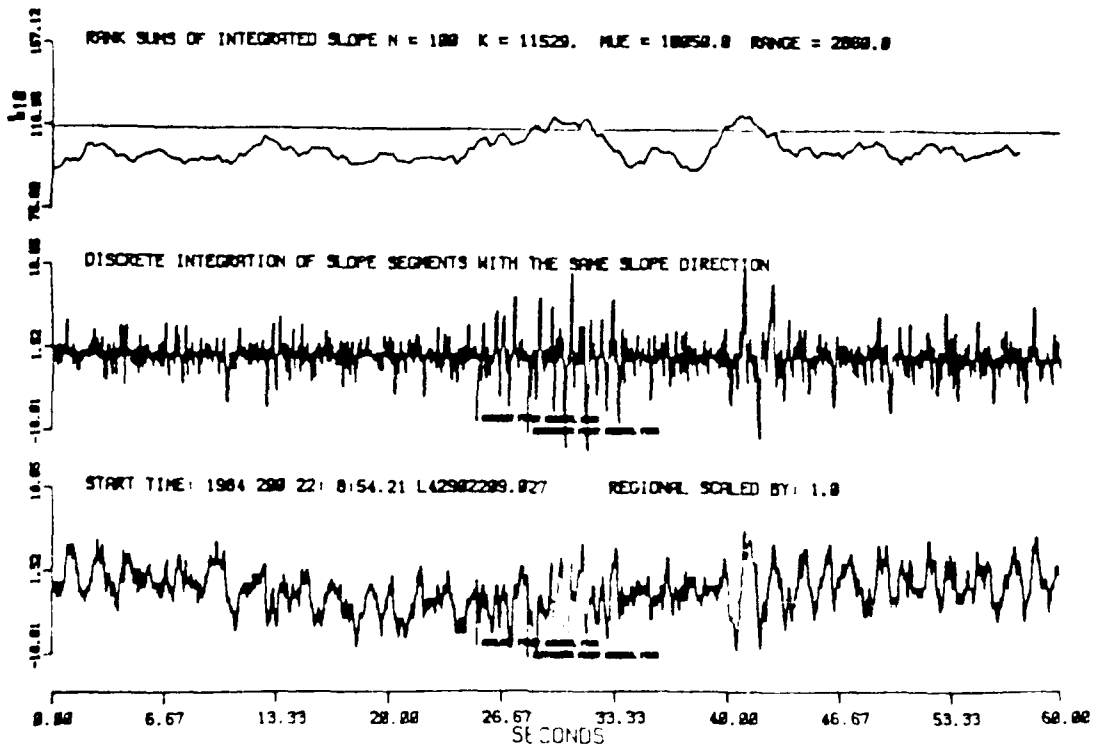

Event 12 - Regional - Probable Lg Arrival

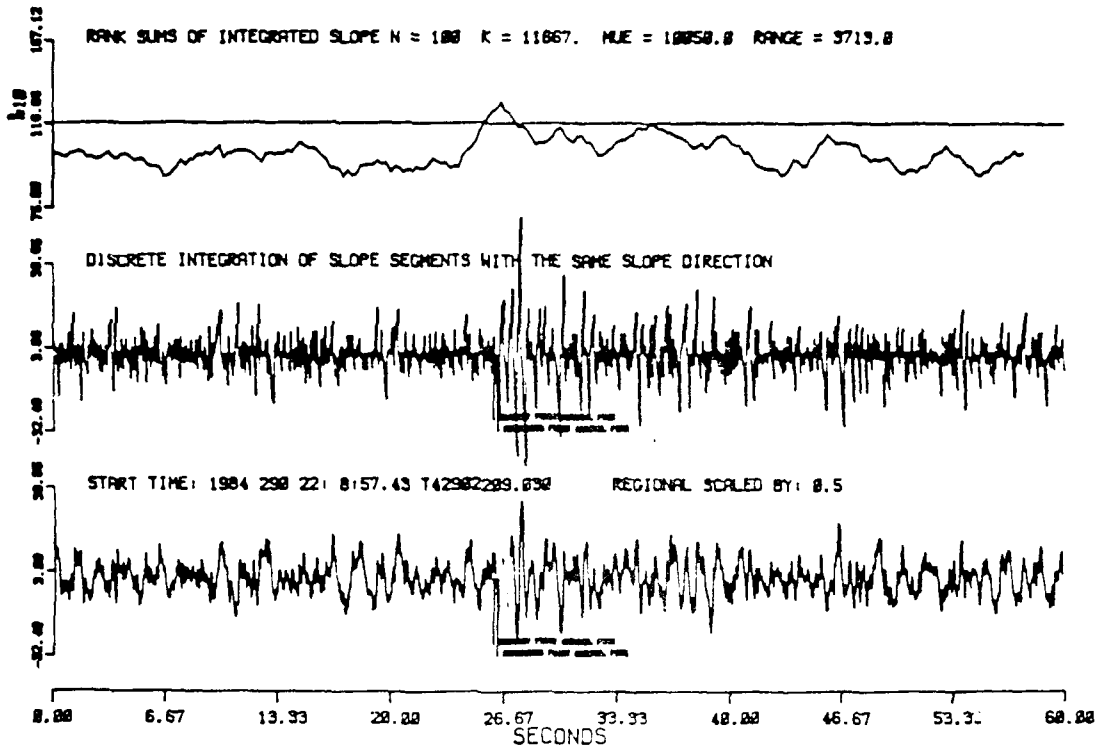
RANK SUMS OF INTEGRATED SLOPE N = 180 K = 11667. MUE = 10050.0 RANGE = 3719.0
DISCRETE INTEGRATION OF SLOPE SEGMENTS WITH THE SAME SLOPE DIRECTION
START TIME: 1984 290 22: 8:57.43 T42982289.030 REGIONAL SCALED BY: 0.5
0.00
6.67
13.33
20.00
26.67
33.33
40.00
46.67
53.33
60.00
SECONDS

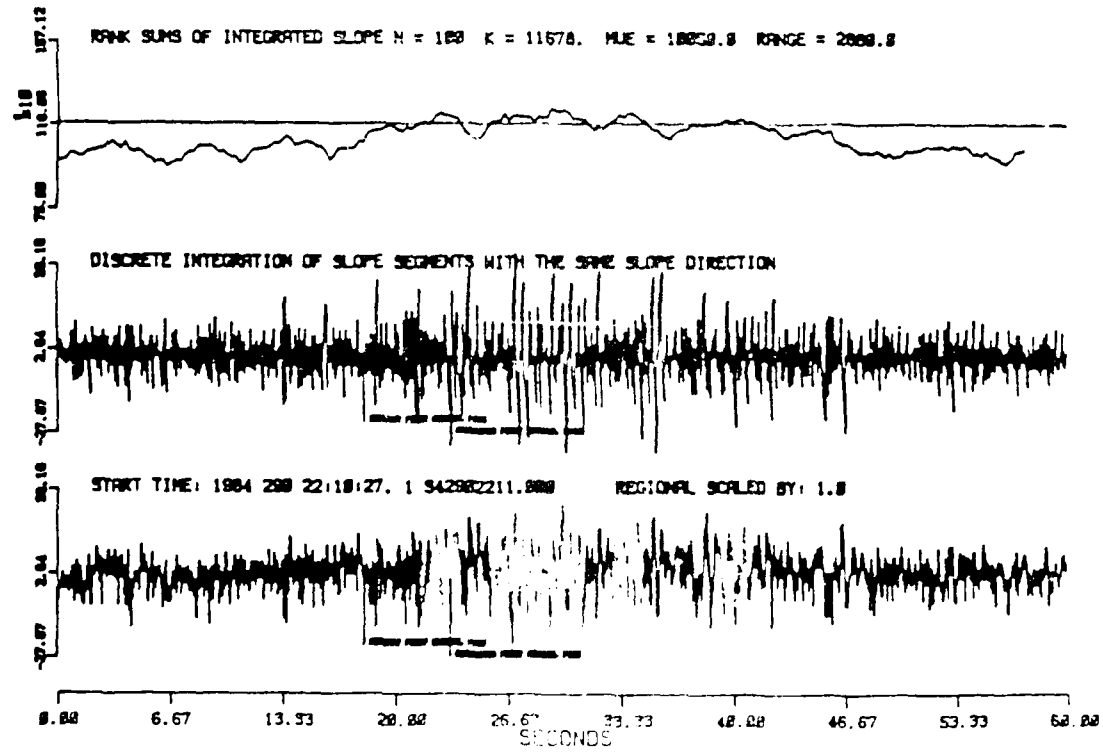
RANK SUMS OF INTEGRATED SLOPE N = 180 K = 11670. MUE = 10050.0 RANGE = 2000.0
DISCRETE INTEGRATION OF SLOPE SEGMENTS WITH THE SAME SLOPE DIRECTION
START TIME: 1984 290 22:10:27. 1 942982211.000 REGIONAL SCALED BY: 1.0
0.00
6.67
13.33
20.00
26.67
33.33
40.00
46.67
53.33
60.00
SECONDS

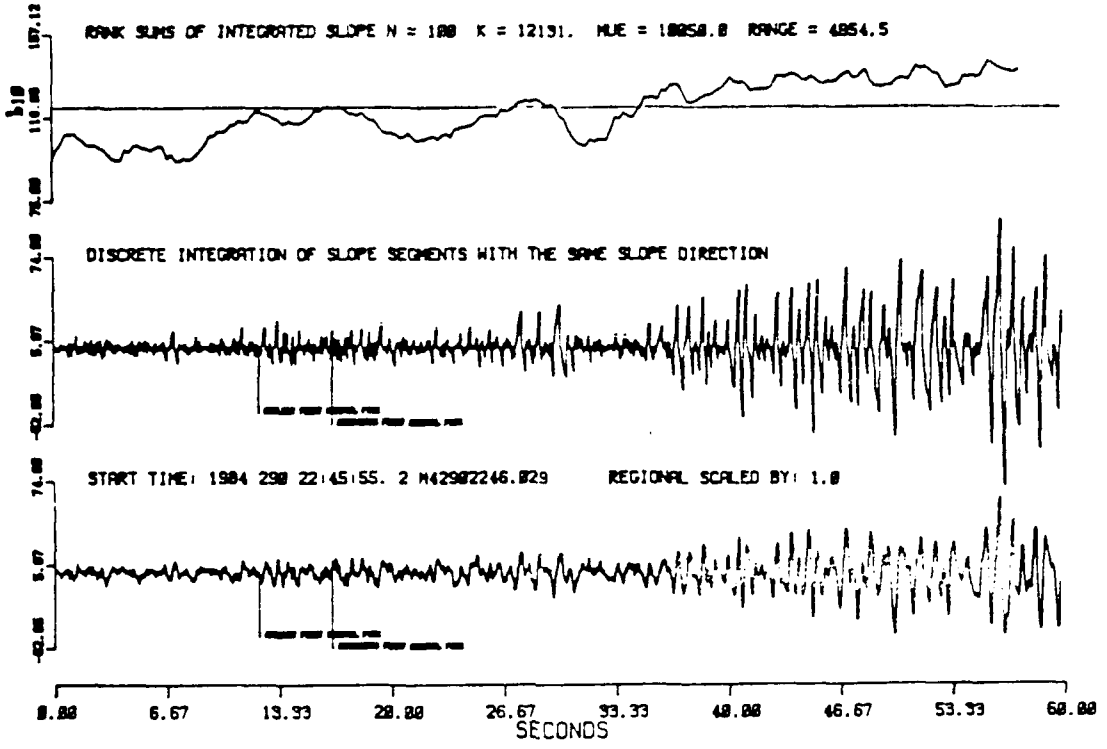

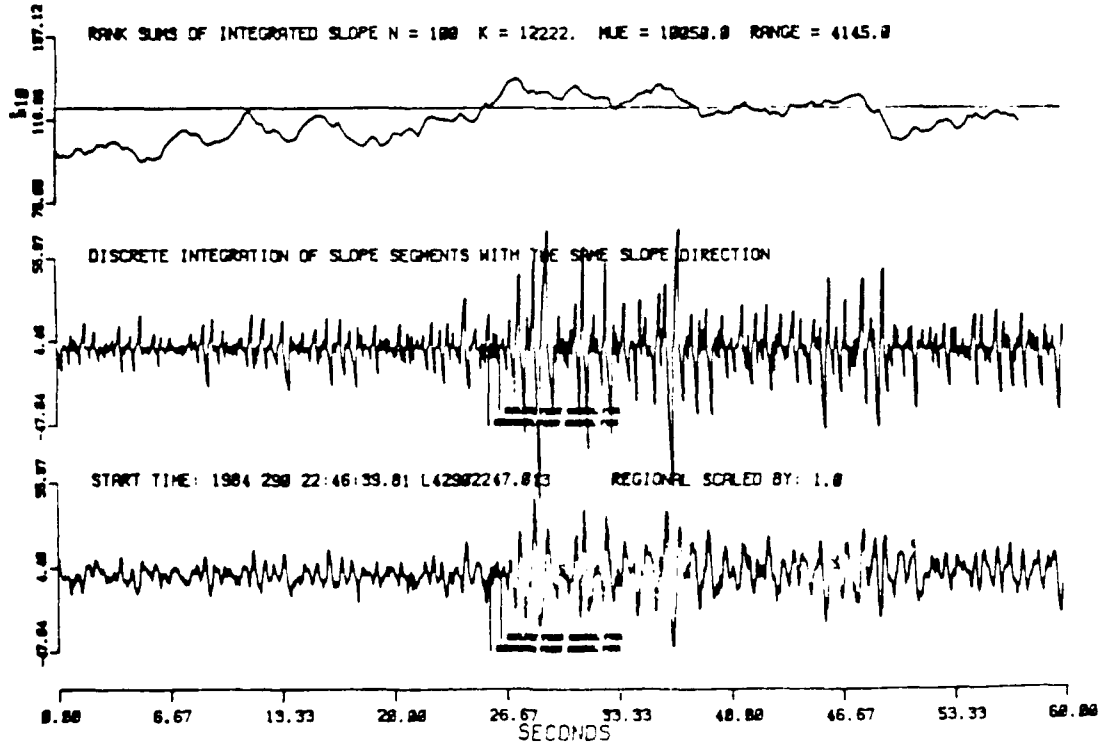

Event 13 - Regional - Probable Lg Arrival

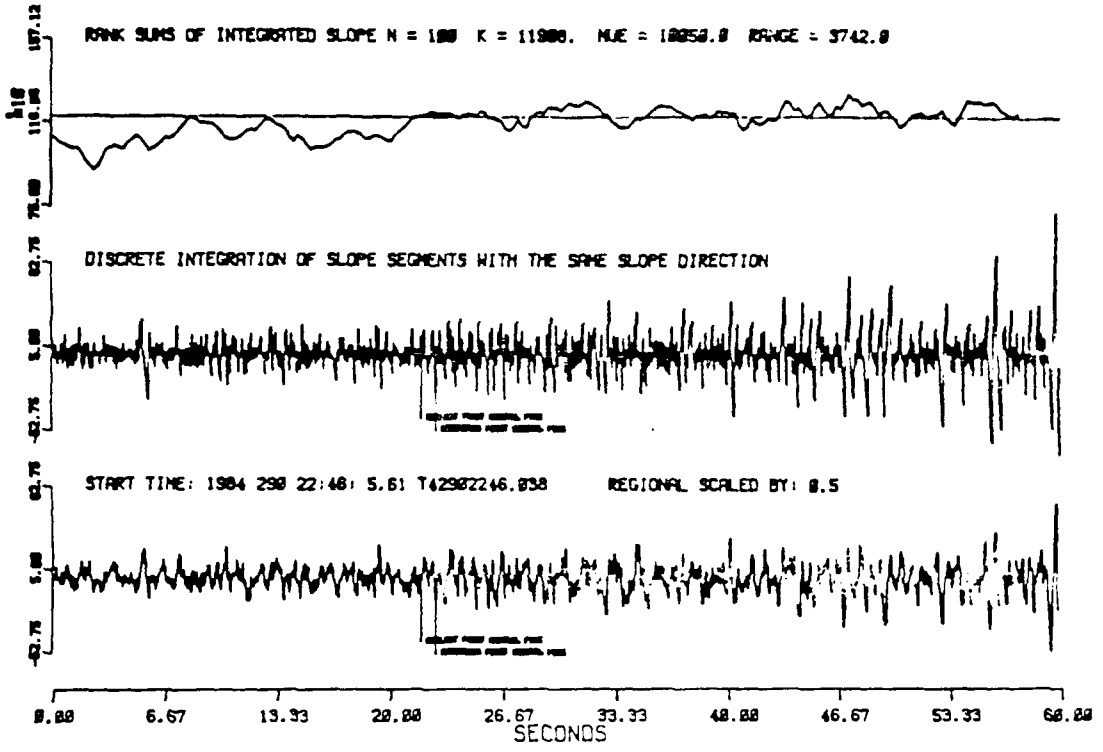
RANK SUMS OF INTEGRATED SLOPE N = 100 K = 11900. MUE = 10050.0 RANGE = 3742.0
DISCRETE INTEGRATION OF SLOPE SEGMENTS WITH THE SAME SLOPE DIRECTION
START TIME: 1984 290 22:46: 5.61 T42902246.038 REGIONAL SCALED BY: 0.5
0.00
6.67
13.33
20.00
26.67
33.33
40.00
46.67
53.33
60.00
SECONDS

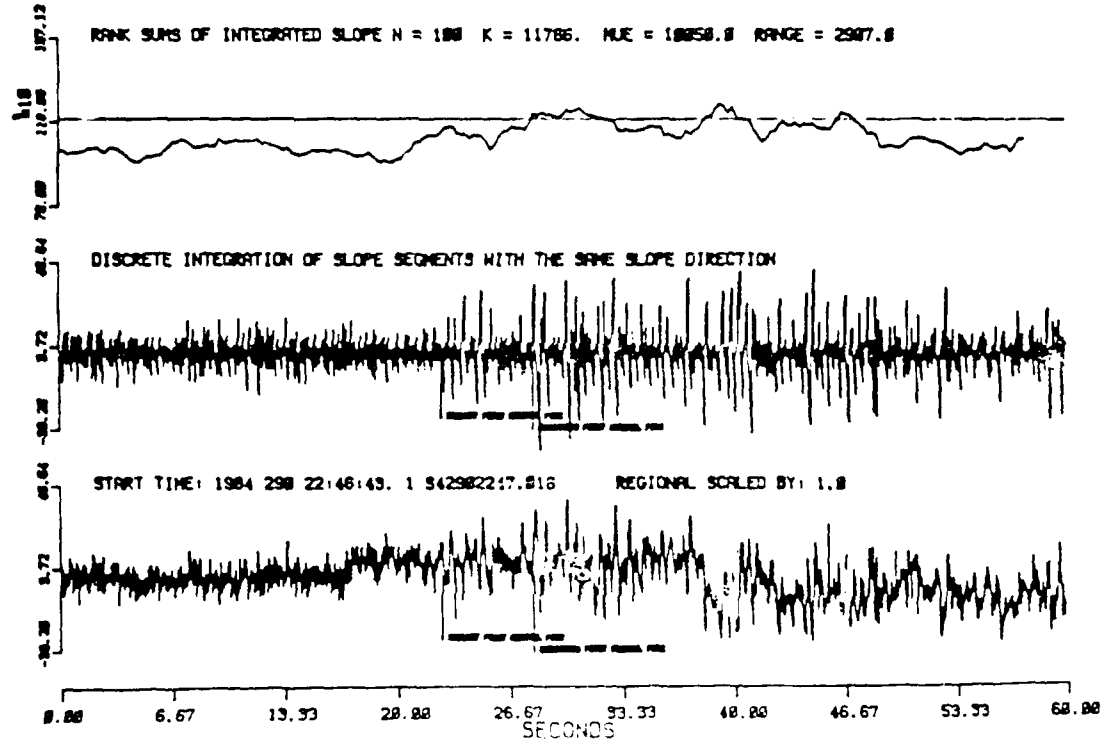
RANK SUMS OF INTEGRATED SLOPE N = 100 K = 11786. MUE = 10050.0 RANGE = 2907.0
DISCRETE INTEGRATION OF SLOPE SEGMENTS WITH THE SAME SLOPE DIRECTION
START TIME: 1984 290 22:46:43. 1 S42902247.016 REGIONAL SCALED BY: 1.0
0.00
6.67
13.33
20.00
26.67
33.33
40.00
46.67
53.33
60.00
SECONDS

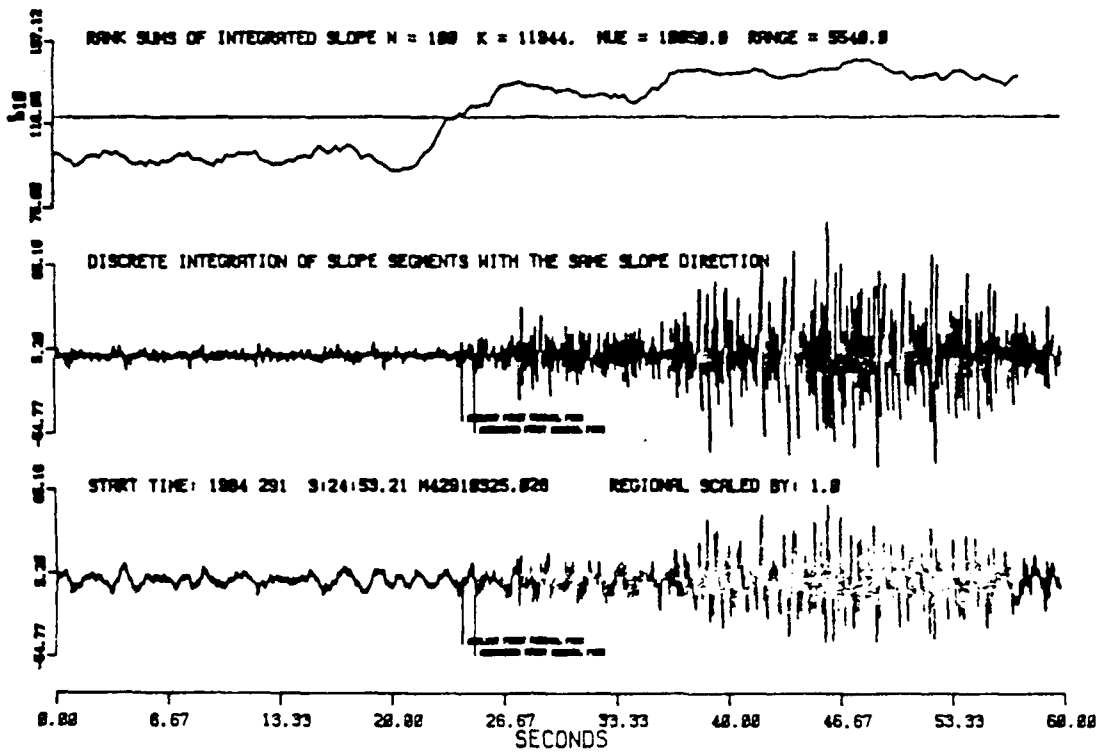

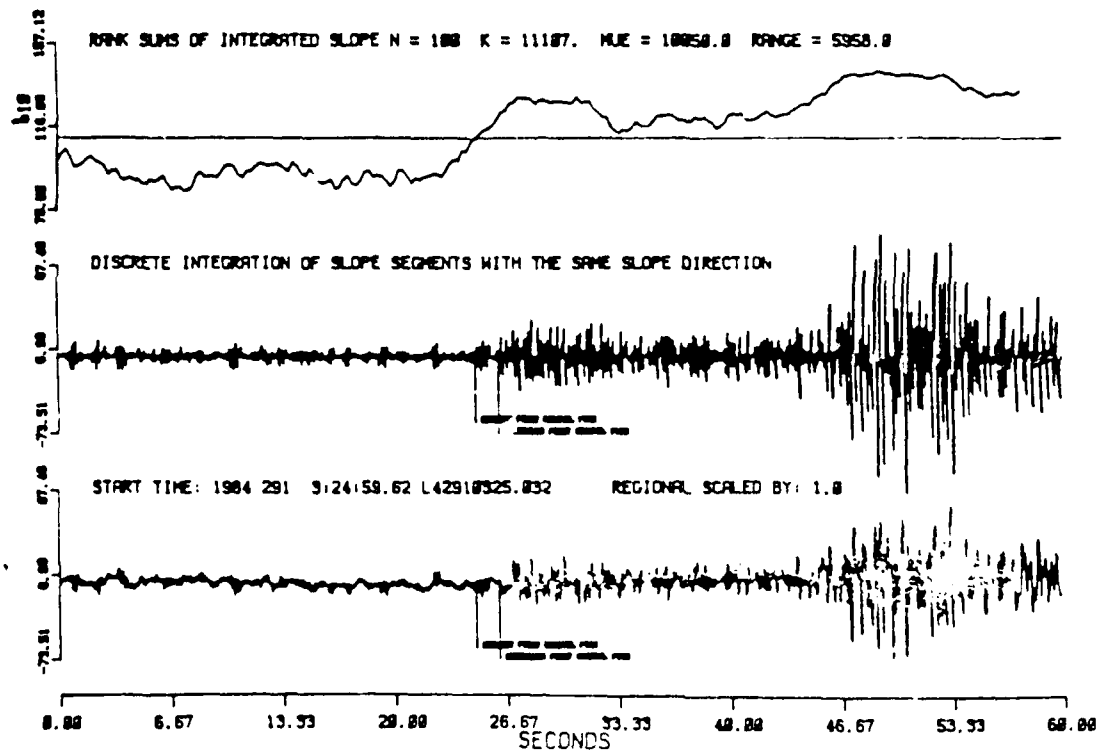

Event 14 - Regional - (P - Lg) = 24 Seconds

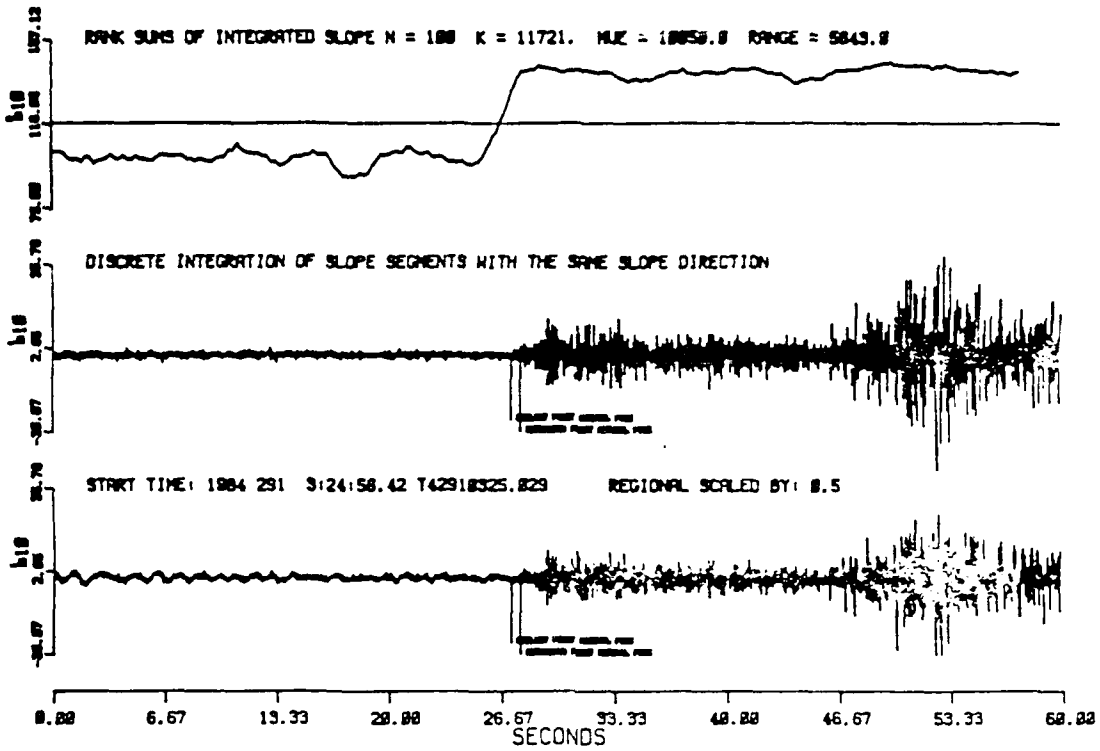
RANK SUMS OF INTEGRATED SLOPE N = 100 K = 11721. MUE = 10050.0 RANGE = 5043.0
DISCRETE INTEGRATION OF SLOPE SEGMENTS WITH THE SAME SLOPE DIRECTION
START TIME: 1984 291 3:24:58.42 T42918325.829 REGIONAL SCALED BY: 0.5
0.00
6.67
13.33
20.00
26.67
33.33
40.00
46.67
53.33
60.00
SECONDS

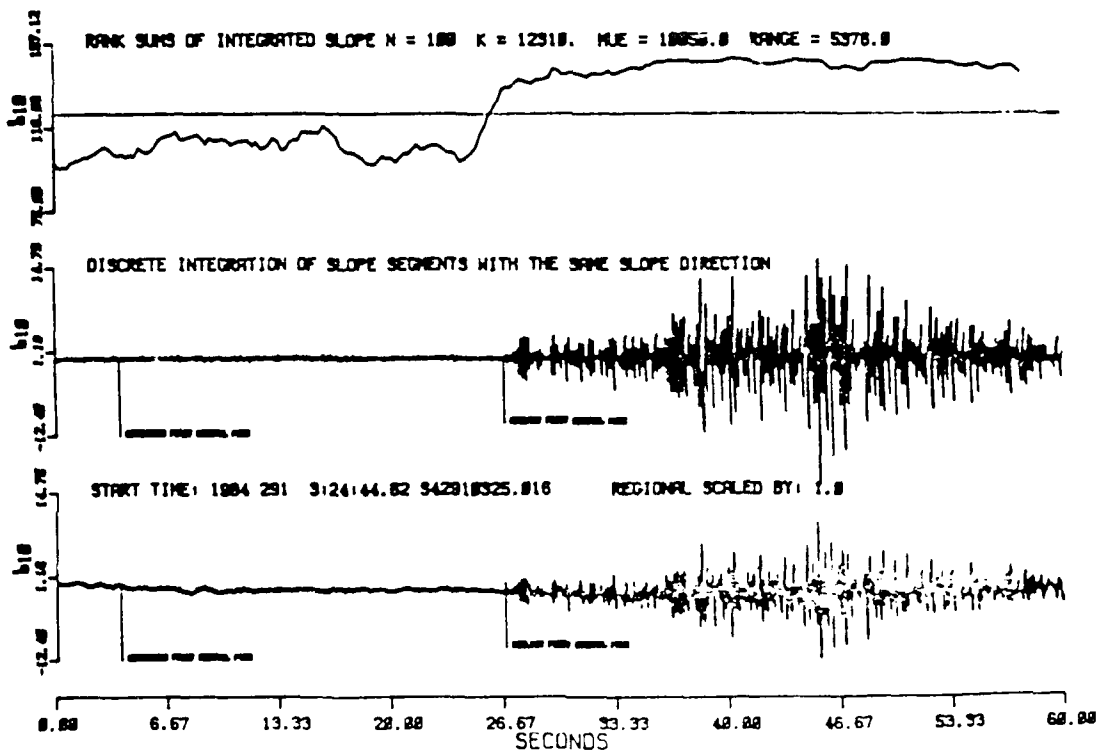
RANK SUMS OF INTEGRATED SLOPE N = 100 K = 12310. MUE = 10050.0 RANGE = 5370.0
DISCRETE INTEGRATION OF SLOPE SEGMENTS WITH THE SAME SLOPE DIRECTION
START TIME: 1984 291 3:24:44.82 T42918325.816 REGIONAL SCALED BY: 1.0
0.00
6.67
13.33
20.00
26.67
33.33
40.00
46.67
53.33
60.00
SECONDS

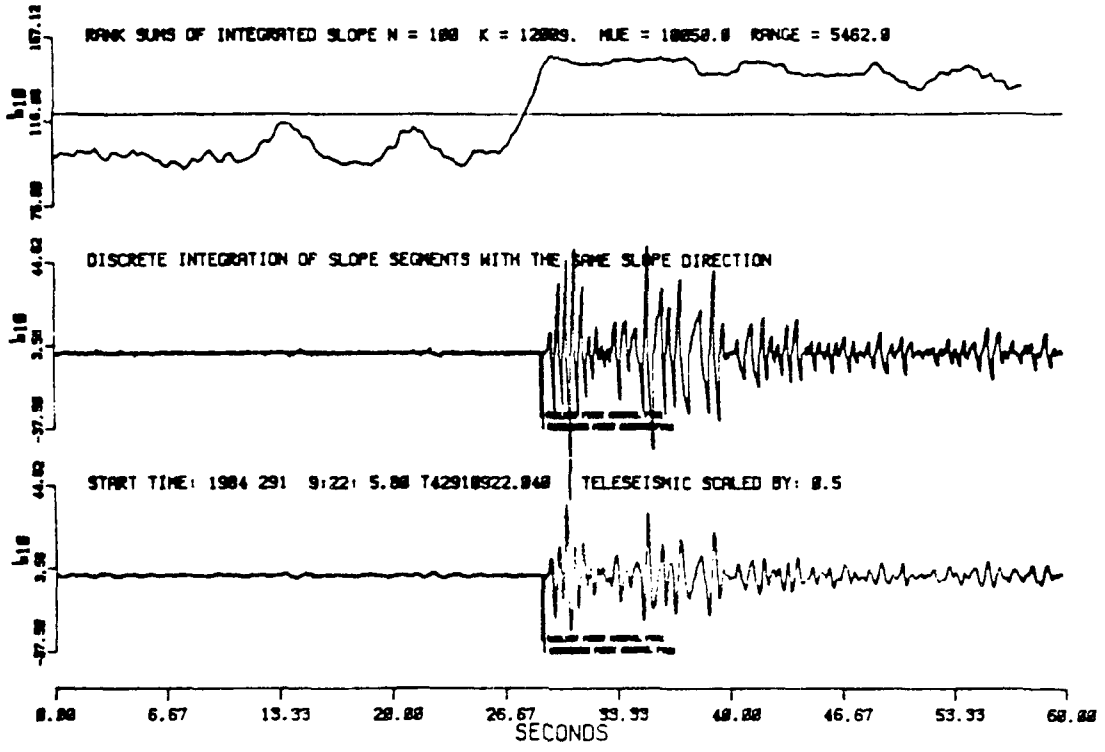

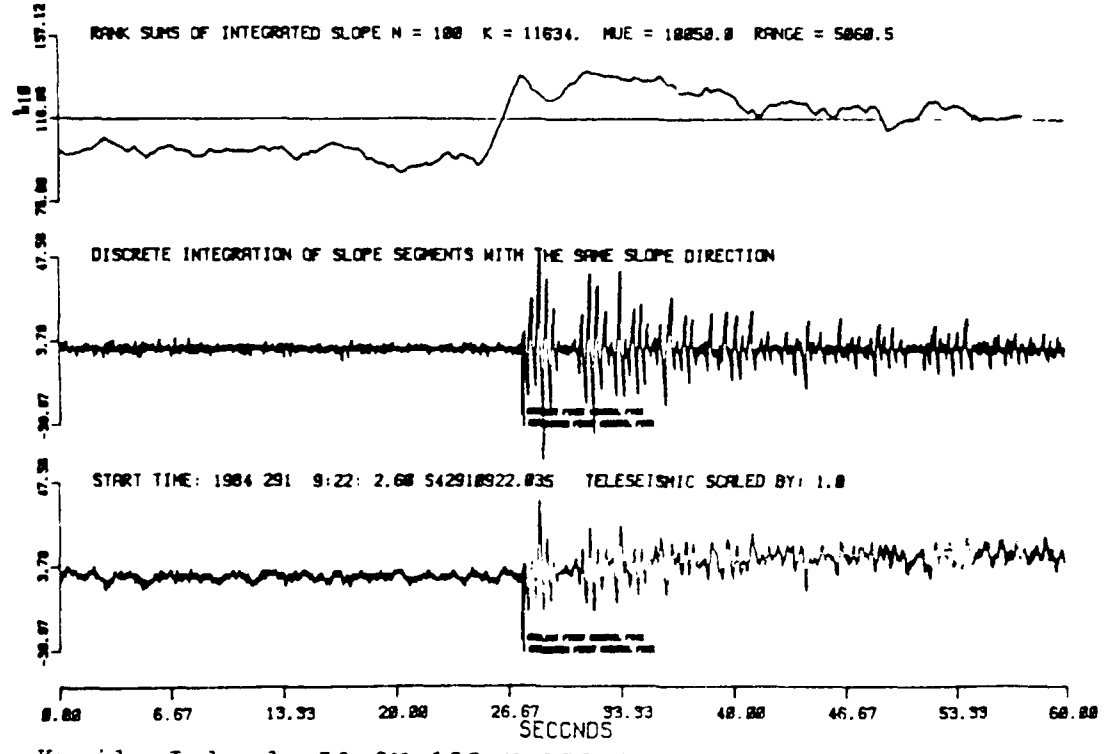

Kurile Islands 50.3N 153.N 153.5E - 10/17/84 Origin Time:09:11:04.8
Origin Time: 09:11:04.8 - Depth 134km+3 M_b: 5.0
Residual Error: - 0.2

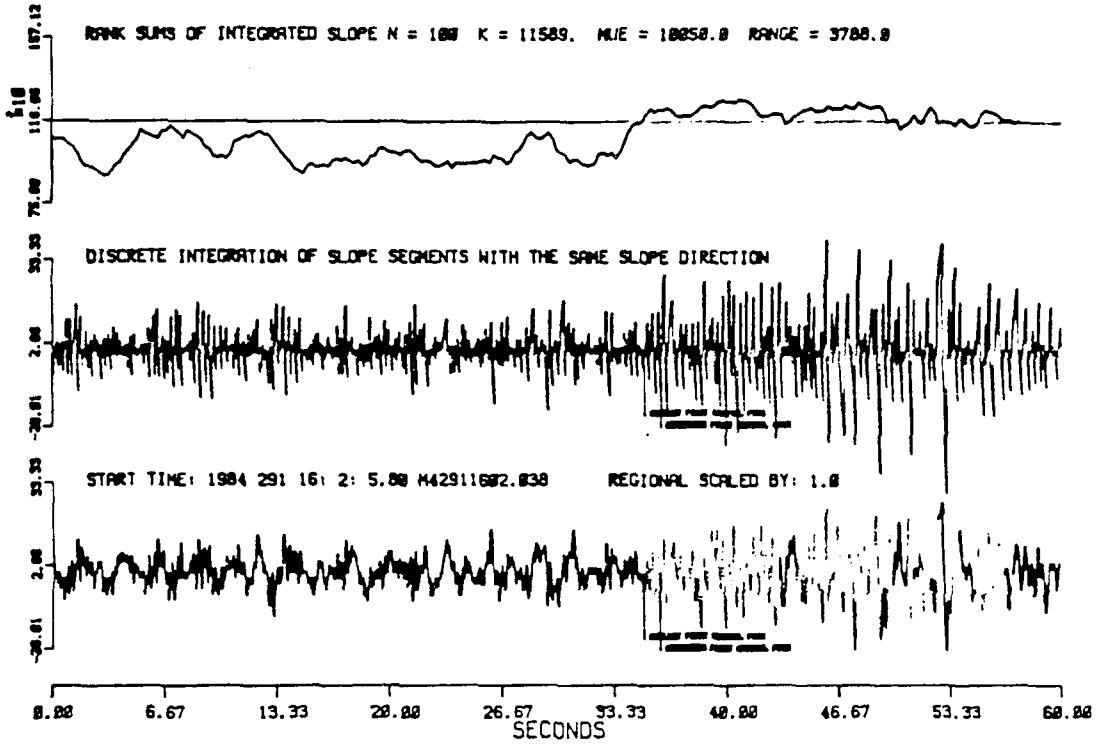

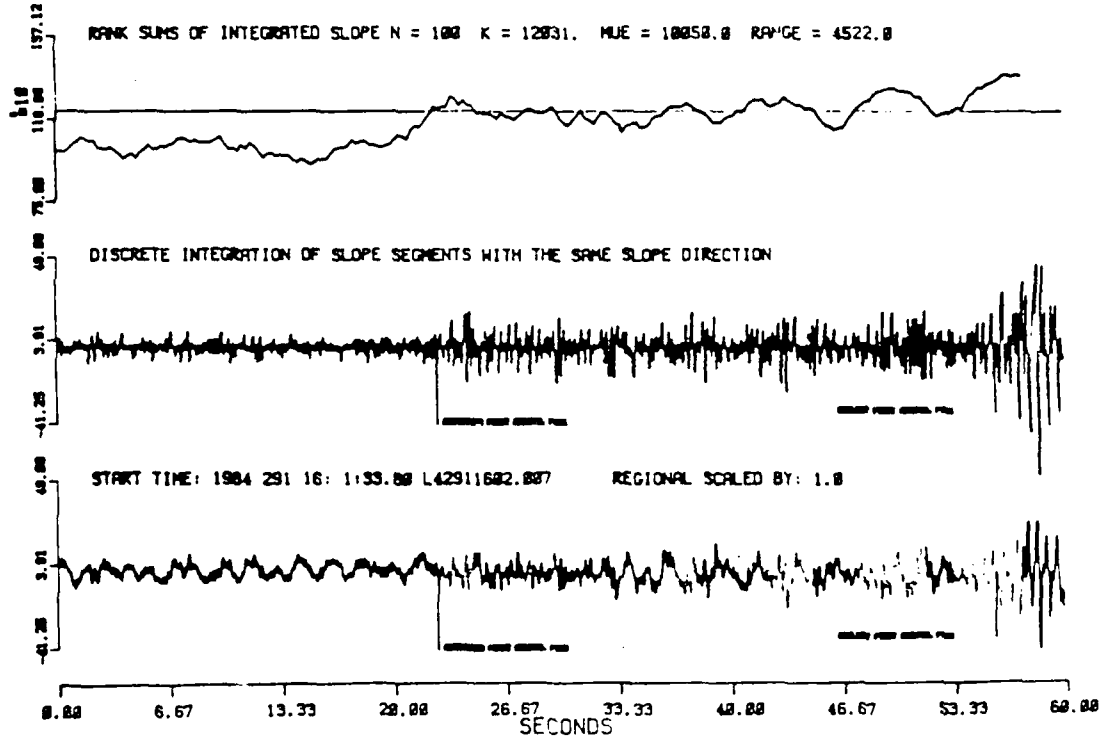

Event 16 - Regional - Probable Lg Arrival

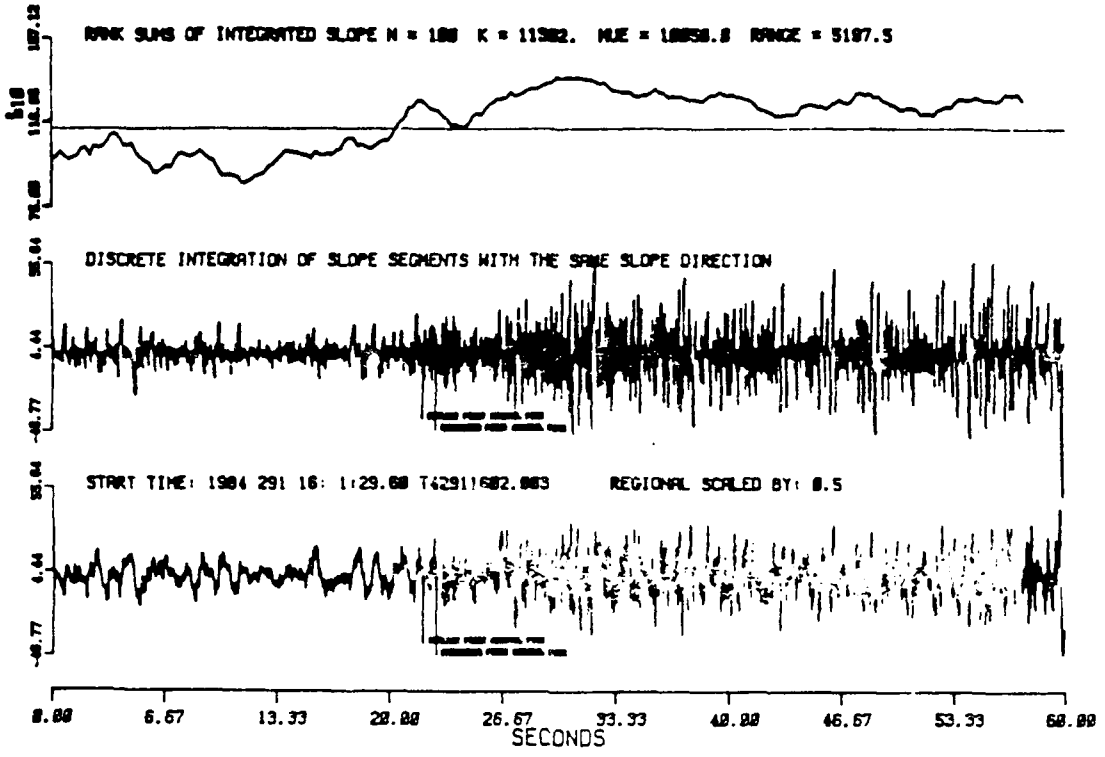
RANK SUMS OF INTEGRATED SLOPE N = 100 K = 11582. MUE = 10050.0 RANGE = 5187.5
DISCRETE INTEGRATION OF SLOPE SEGMENTS WITH THE SAME SLOPE DIRECTION
START TIME: 1984 291 16: 1:29.00 T42911682.003 REGIONAL SCALED BY: 0.5
0.00
6.67
13.33
20.00
26.67
33.33
40.00
46.67
53.33
60.00
SECONDS

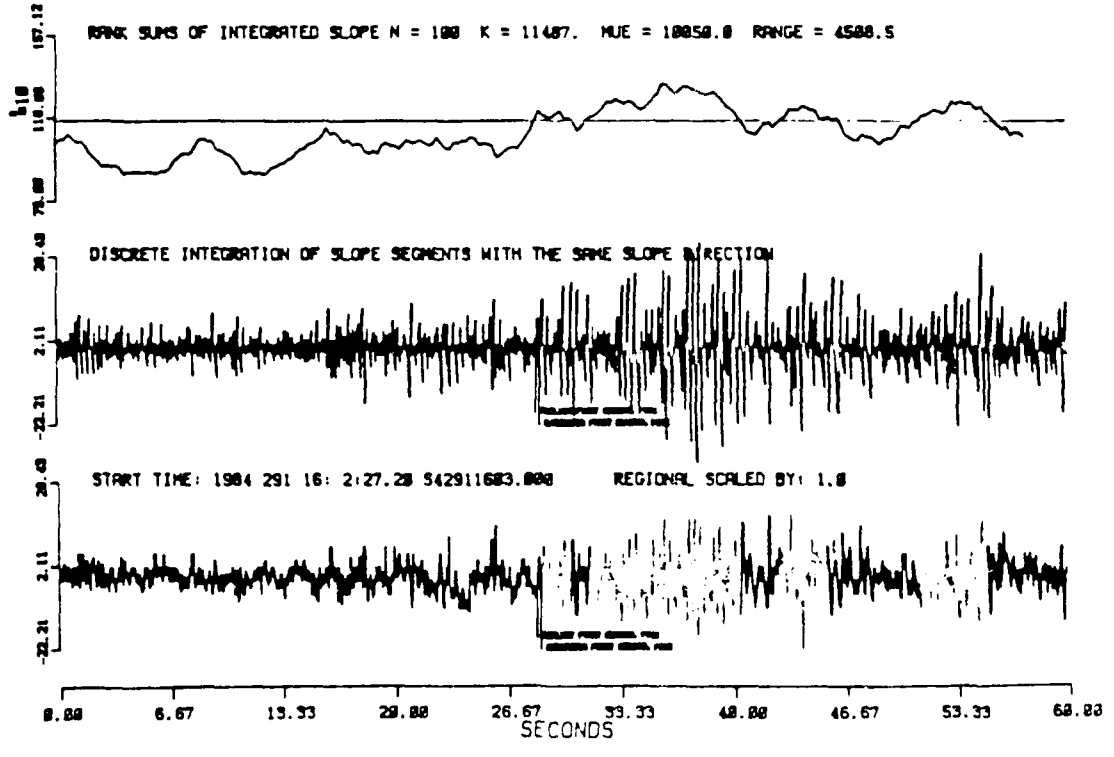
RANK SUMS OF INTEGRATED SLOPE N = 100 K = 11487. MUE = 10050.0 RANGE = 4500.5
DISCRETE INTEGRATION OF SLOPE SEGMENTS WITH THE SAME SLOPE DIRECTION
START TIME: 1984 291 16: 2:27.20 S42911683.000 REGIONAL SCALED BY: 1.0
0.00
6.67
13.33
20.00
26.67
33.33
40.00
46.67
53.33
60.00
SECONDS

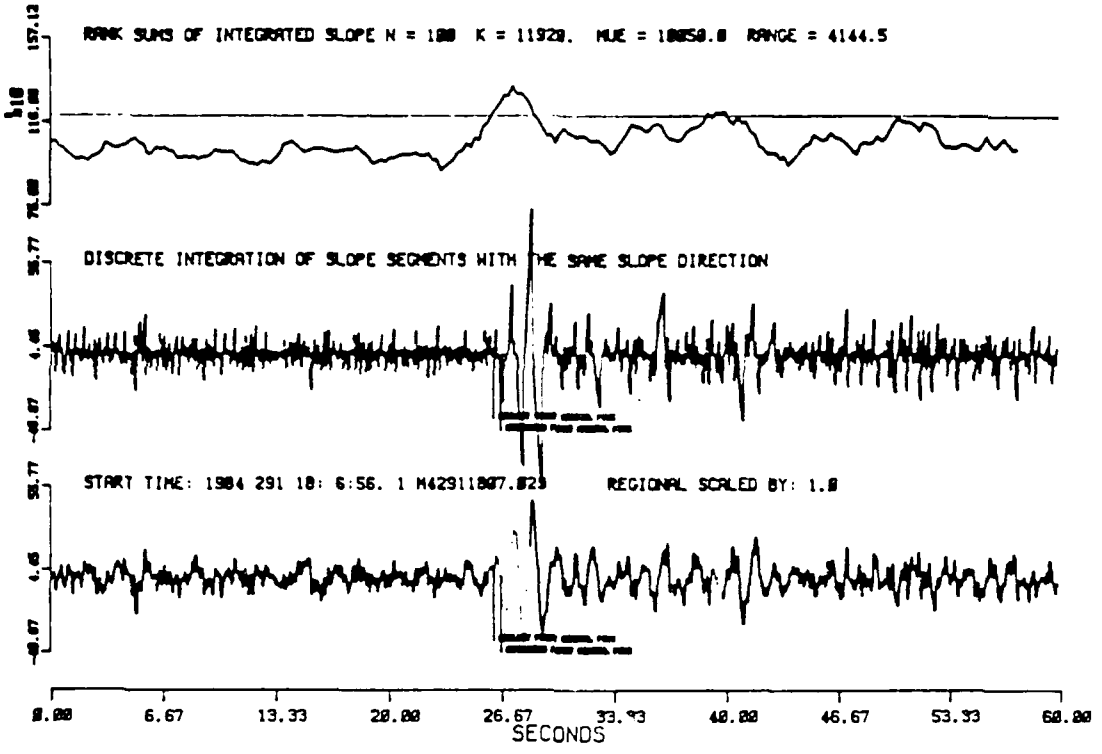

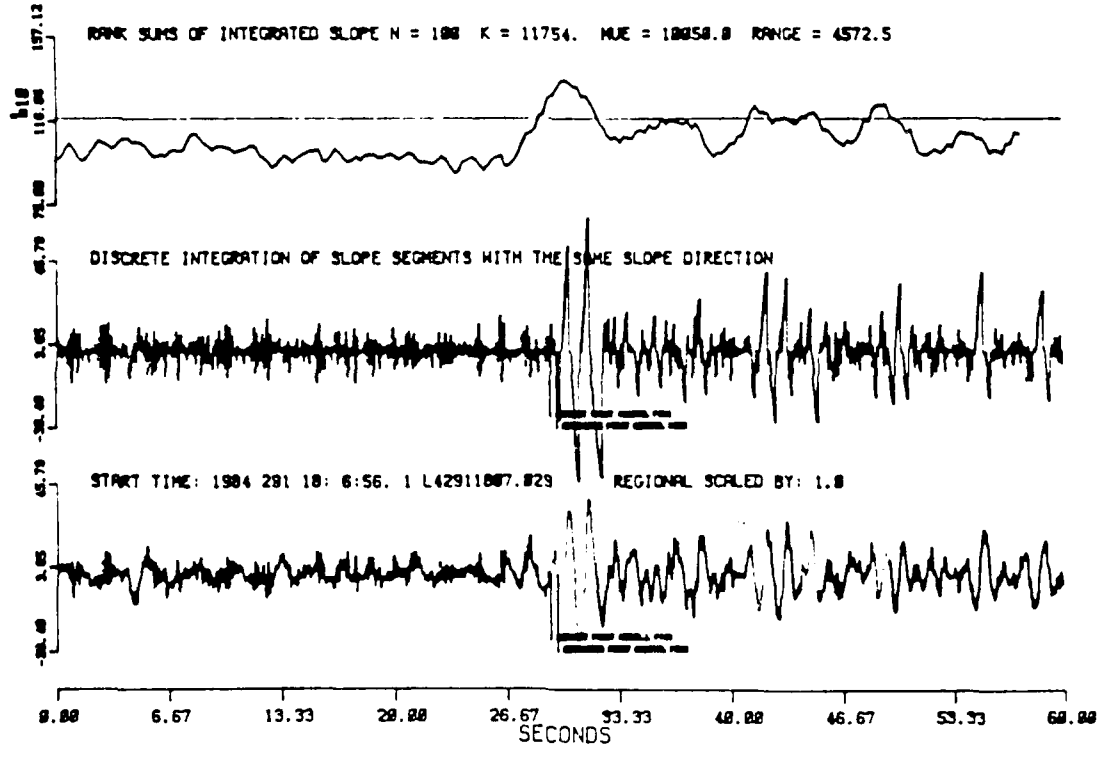

Event 17 - Regional - Probable Lg Arrival

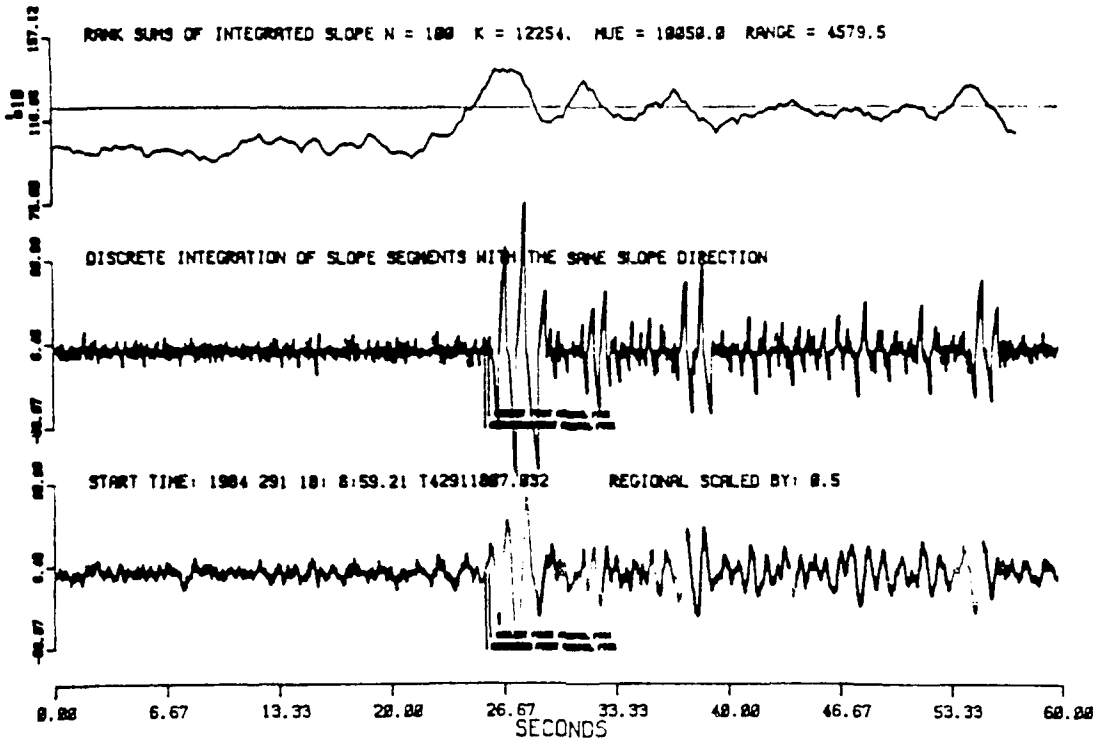
RANK SUMS OF INTEGRATED SLOPE N = 180 K = 12254. MUE = 10050.0 RANGE = 4579.5
DISCRETE INTEGRATION OF SLOPE SEGMENTS WITH THE SAME SLOPE DIRECTION
START TIME: 1984 291 18: 8:59.21 T42911887.832 REGIONAL SCALED BY: 0.5
0.00
6.67
13.33
20.00
26.67
33.33
40.00
46.67
53.33
60.00
SECONDS

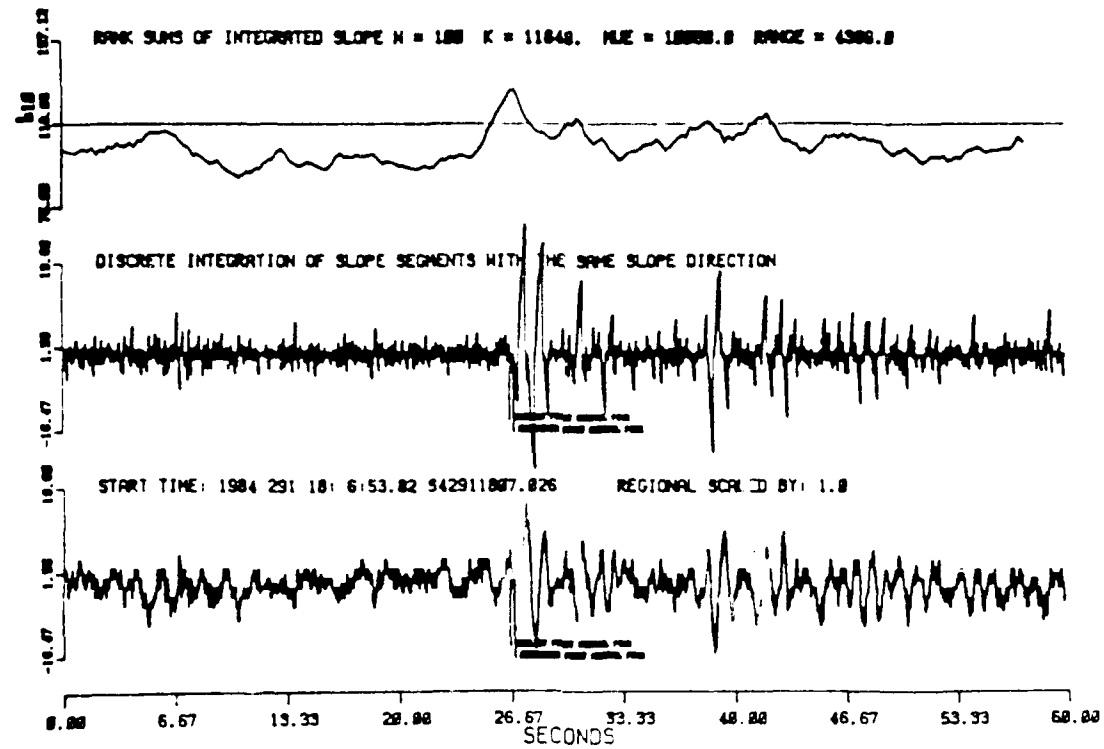
RANK SUMS OF INTEGRATED SLOPE N = 180 K = 11840.
DISCRETE INTEGRATION OF SLOPE SEGMENTS WITH THE SAME SLOPE DIRECTION
START TIME: 1984 291 18: 6:53.82 T42911887.826 REGIONAL SCALED BY: 1.0
0.00
6.67
13.33
20.00
26.67
33.33
40.00
46.67
53.33
60.00
SECONDS

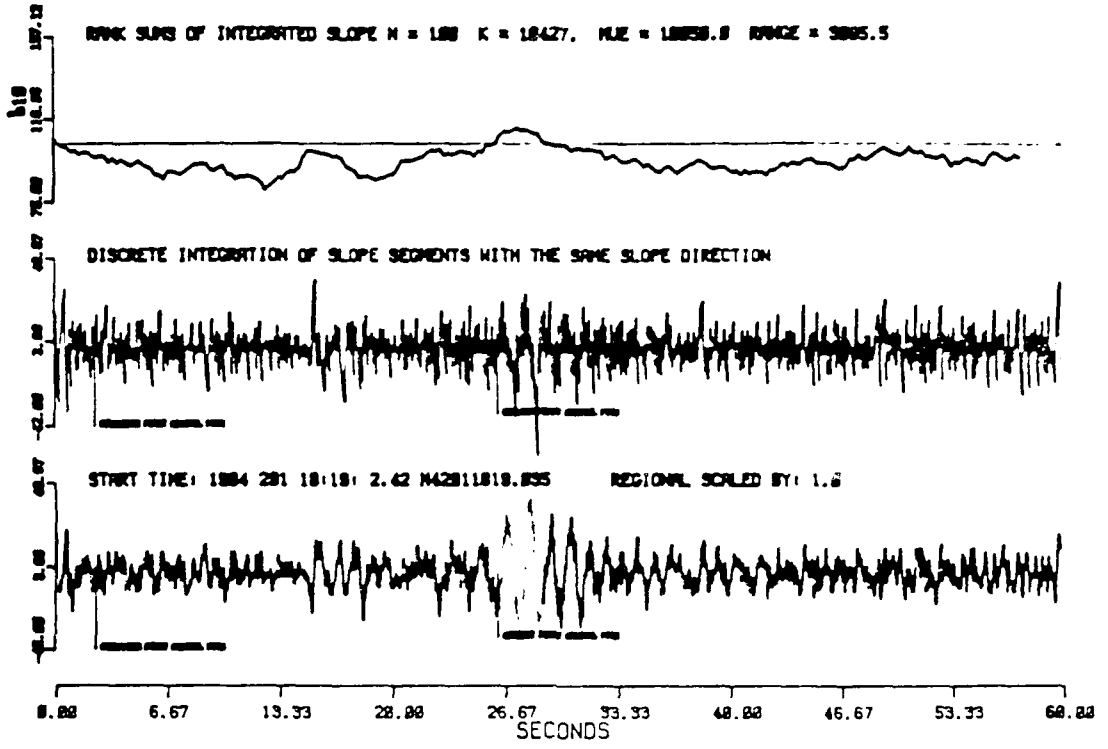

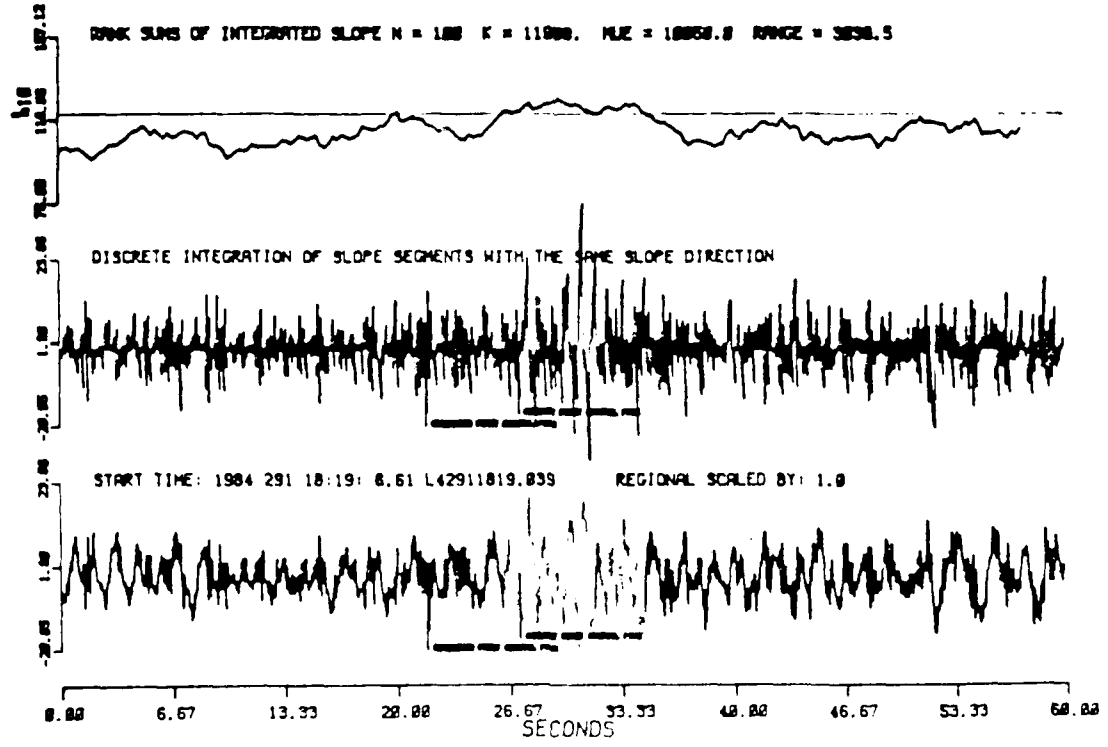

Event 18 - Regional - Probable Lq Arrival

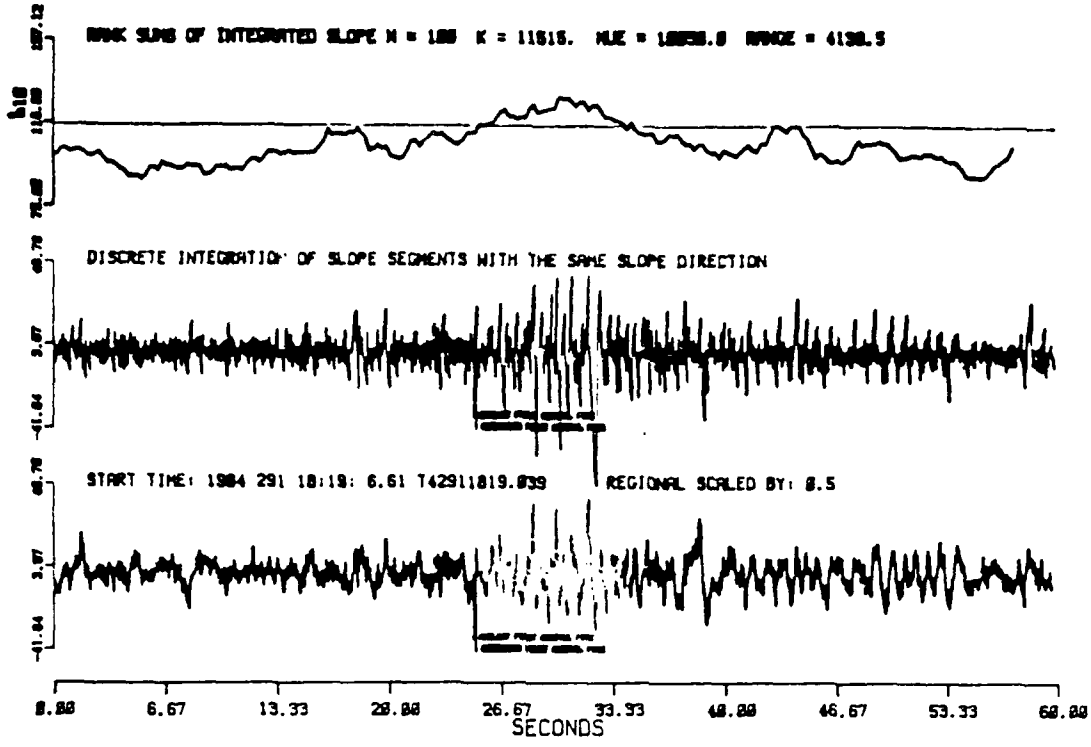
RANK SUMS OF INTEGRATED SLOPE N = 100 K = 11615. MUE = 10050.0 RANGE = 4130.5
DISCRETE INTEGRATION OF SLOPE SEGMENTS WITH THE SAME SLOPE DIRECTION
START TIME: 1984 291 18:19: 6.61 T42911819.039
REGIONAL SCALED BY: 8.5
0.00
6.67
13.33
20.00
26.67
33.33
40.00
46.67
53.33
60.00
SECONDS

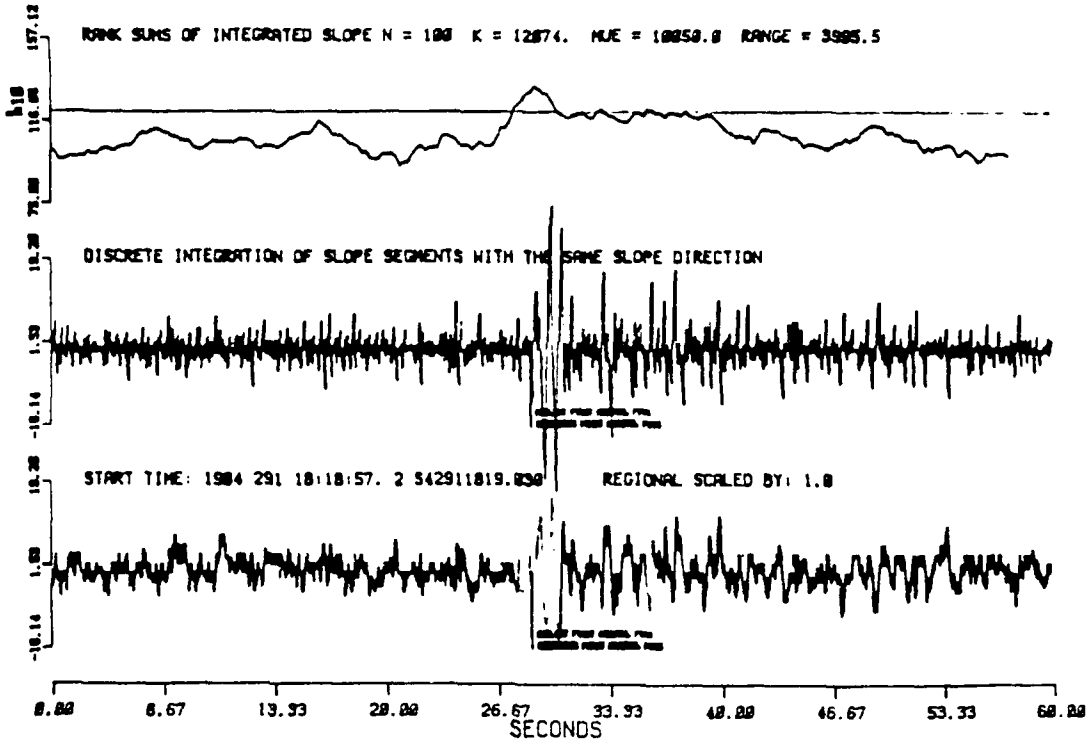
RANK SUMS OF INTEGRATED SLOPE N = 100 K = 12874. MUE = 10050.0 RANGE = 3985.5
DISCRETE INTEGRATION OF SLOPE SEGMENTS WITH THE SAME SLOPE DIRECTION
START TIME: 1984 291 18:18:57. 2 S42911819.039
REGIONAL SCALED BY: 1.0
0.00
6.67
13.33
20.00
26.67
33.33
40.00
46.67
53.33
60.00
SECONDS

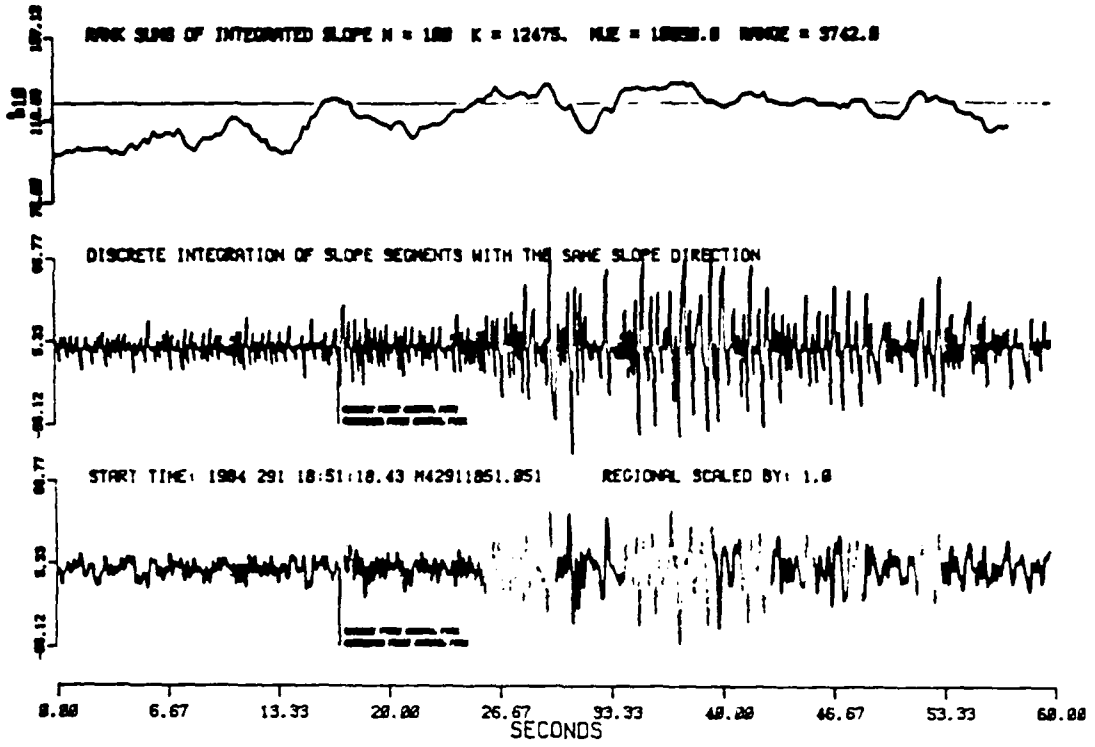
DISCRETE INTEGRATION OF SLOPE SEGMENTS WITH THE SAME SLOPE DIRECTION
START TIME: 1984 291 18:51:18.43 M42911851.051 REGIONAL SCALED BY: 1.0
8.00
6.67
13.33
20.00
26.67
33.33
40.00
46.67
53.33
60.00
SECONDS

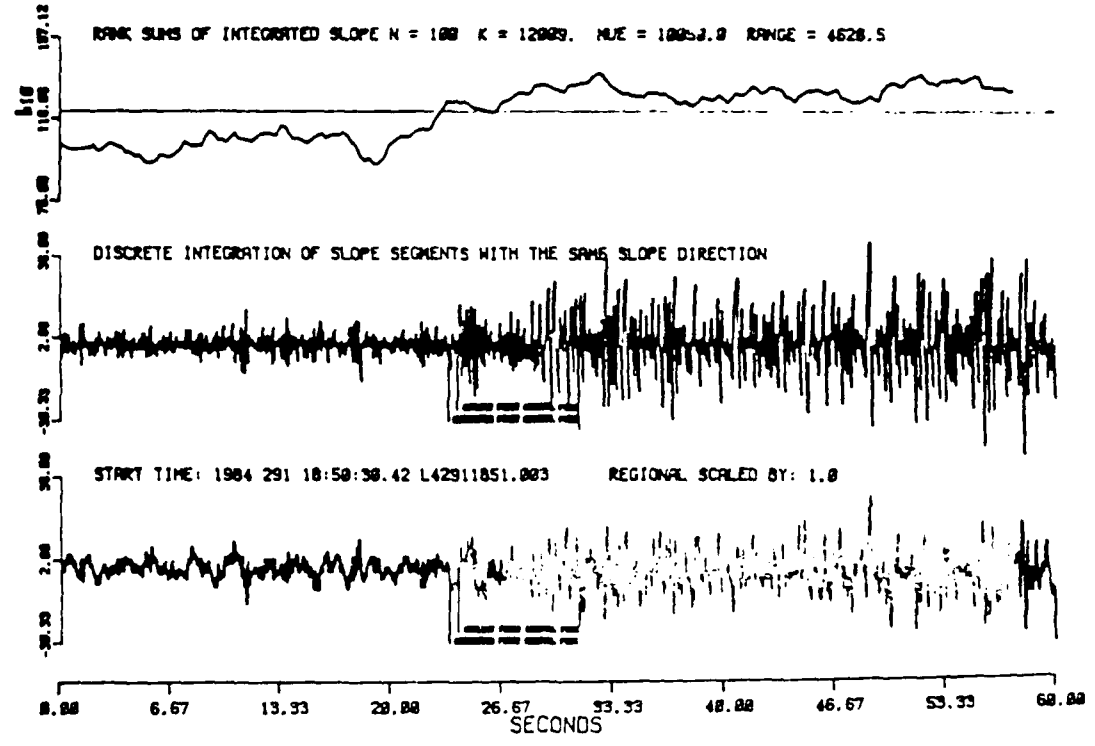
DISCRETE INTEGRATION OF SLOPE SEGMENTS WITH THE SAME SLOPE DIRECTION
START TIME: 1984 291 18:50:38.42 L42911851.003 REGIONAL SCALED BY: 1.0
8.00
6.67
13.33
20.00
26.67
33.33
40.00
46.67
53.33
60.00
SECONDS

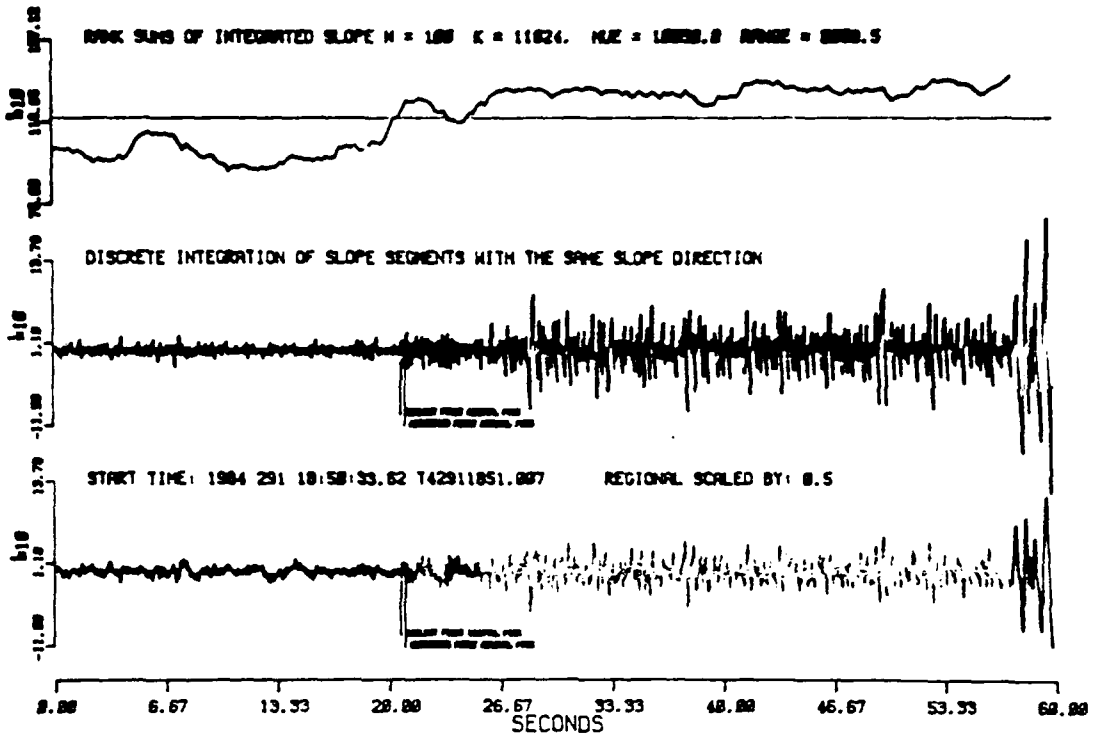
DISCRETE INTEGRATION OF SLOPE SEGMENTS WITH THE SAME SLOPE DIRECTION
START TIME: 1984 291 18:58:33.82 T42911851.007 REGIONAL SCALED BY: 8.5
0.00
6.67
13.33
20.00
26.67
33.33
40.00
46.67
53.33
60.00
SECONDS

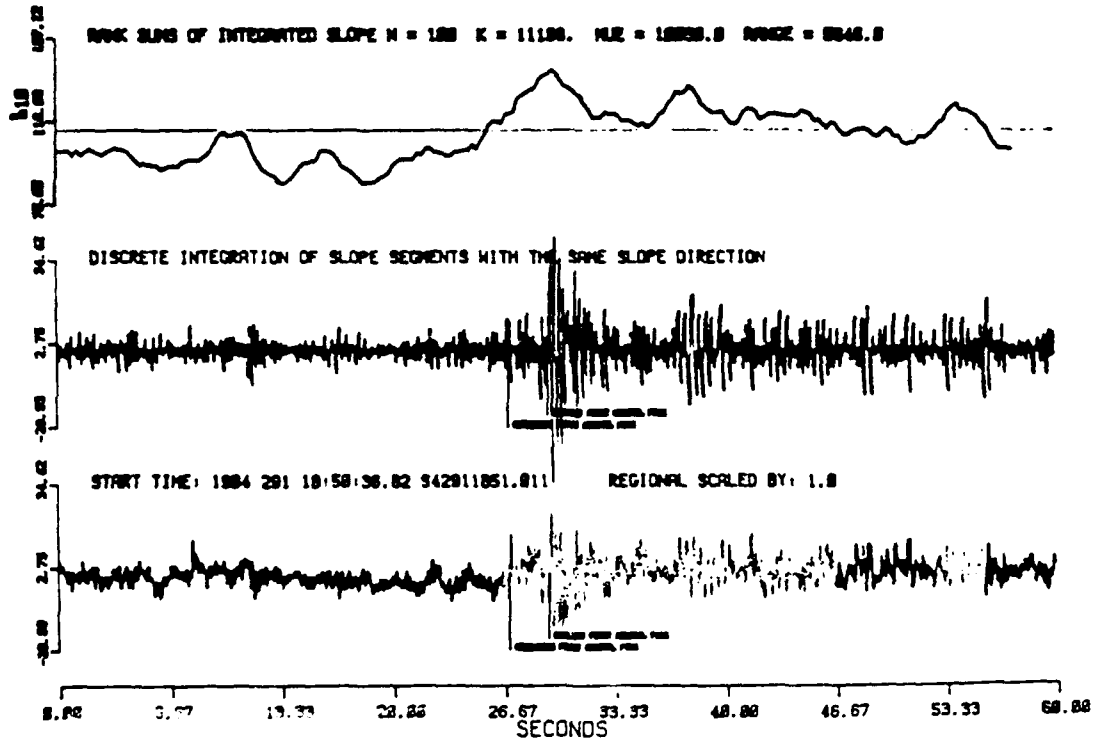
DISCRETE INTEGRATION OF SLOPE SEGMENTS WITH THE SAME SLOPE DIRECTION
START TIME: 1984 291 18:58:36.82 S42911851.011 REGIONAL SCALED BY: 1.0
26.67
33.33
40.00
46.67
53.33
60.00
SECONDS

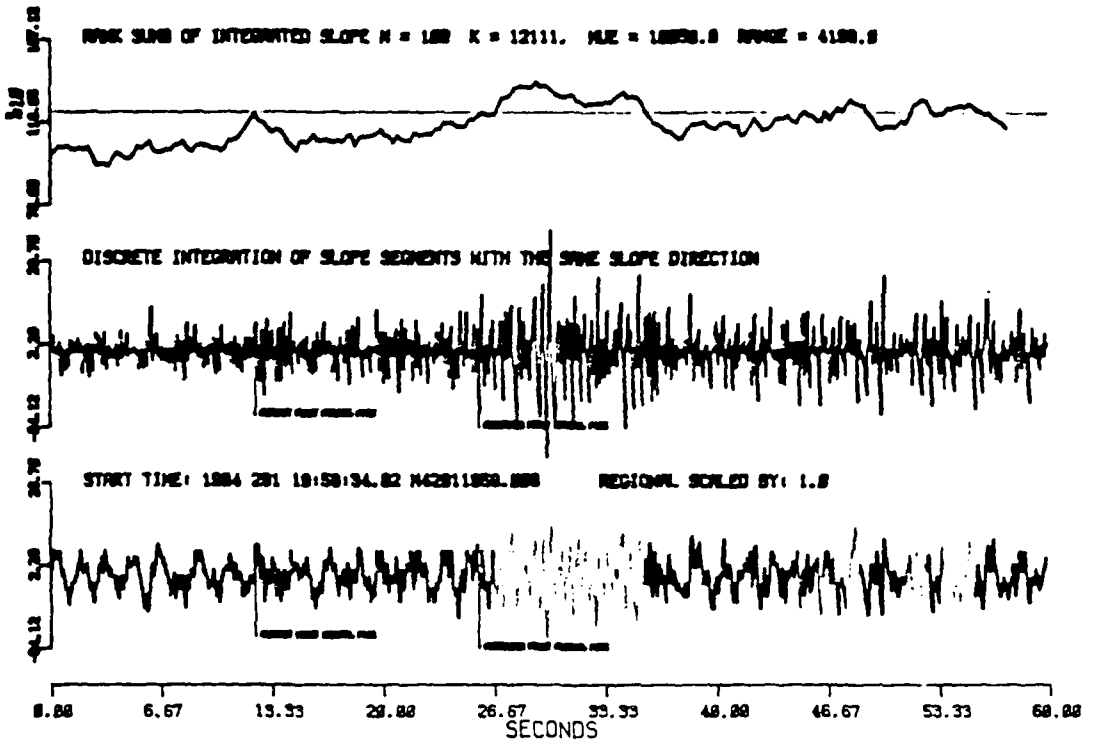

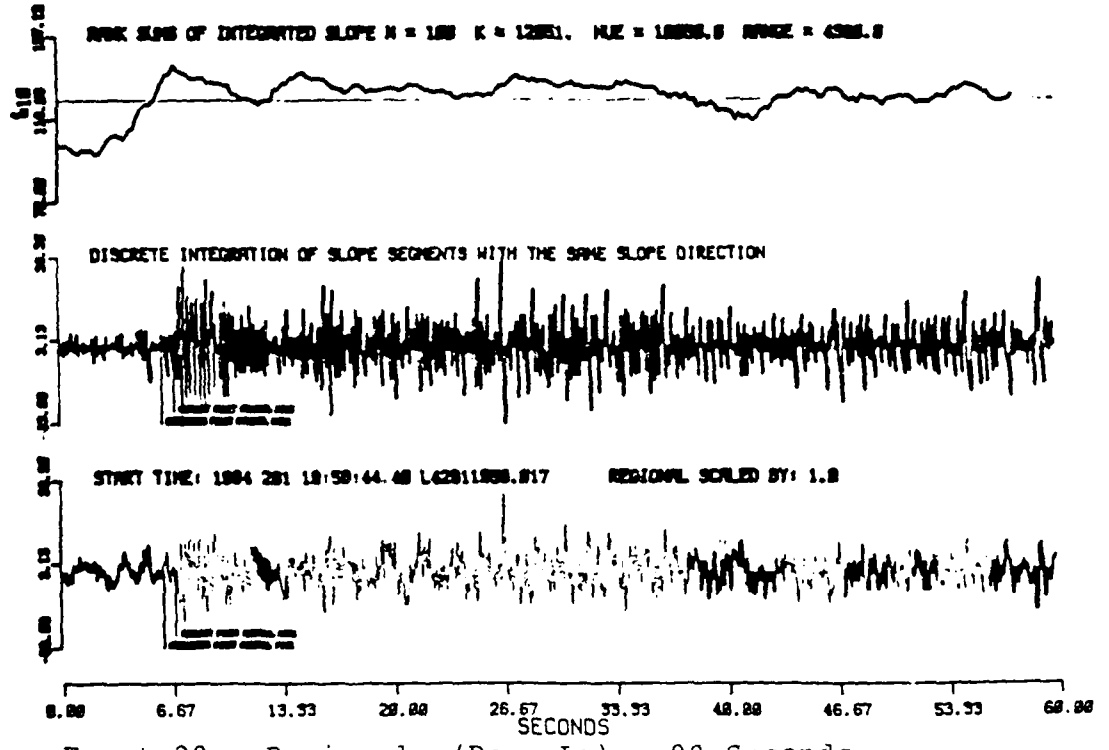

Event 20 - Regional (Pn - Lg) = 90 Seconds

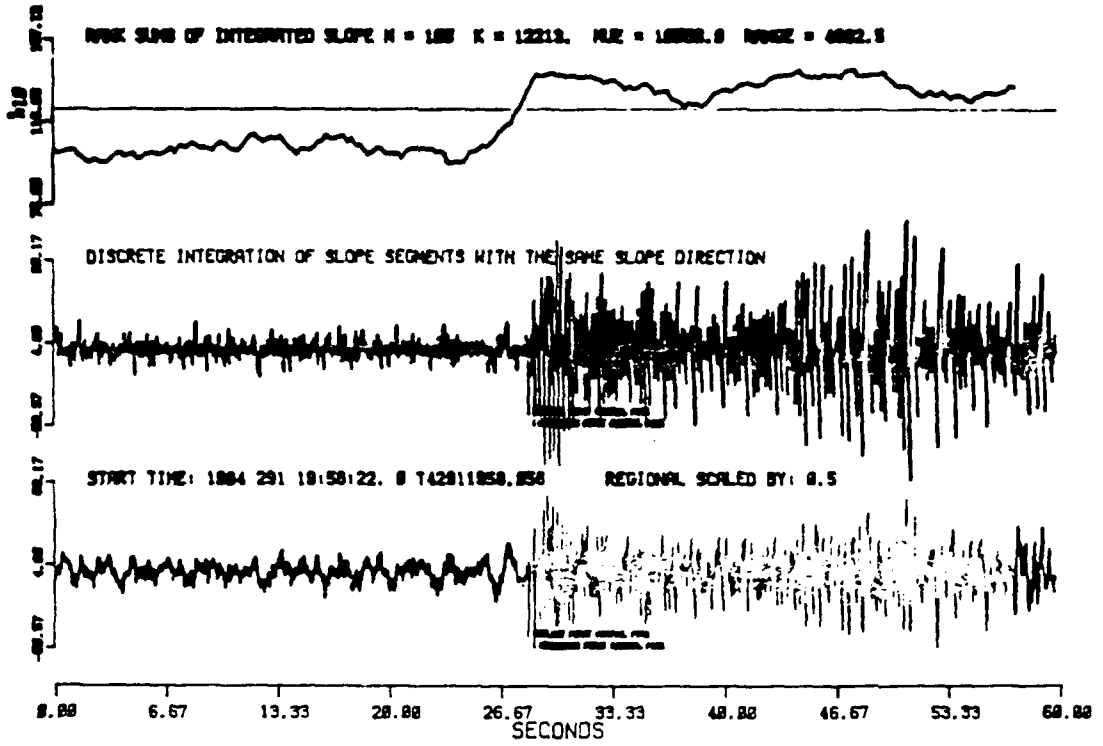

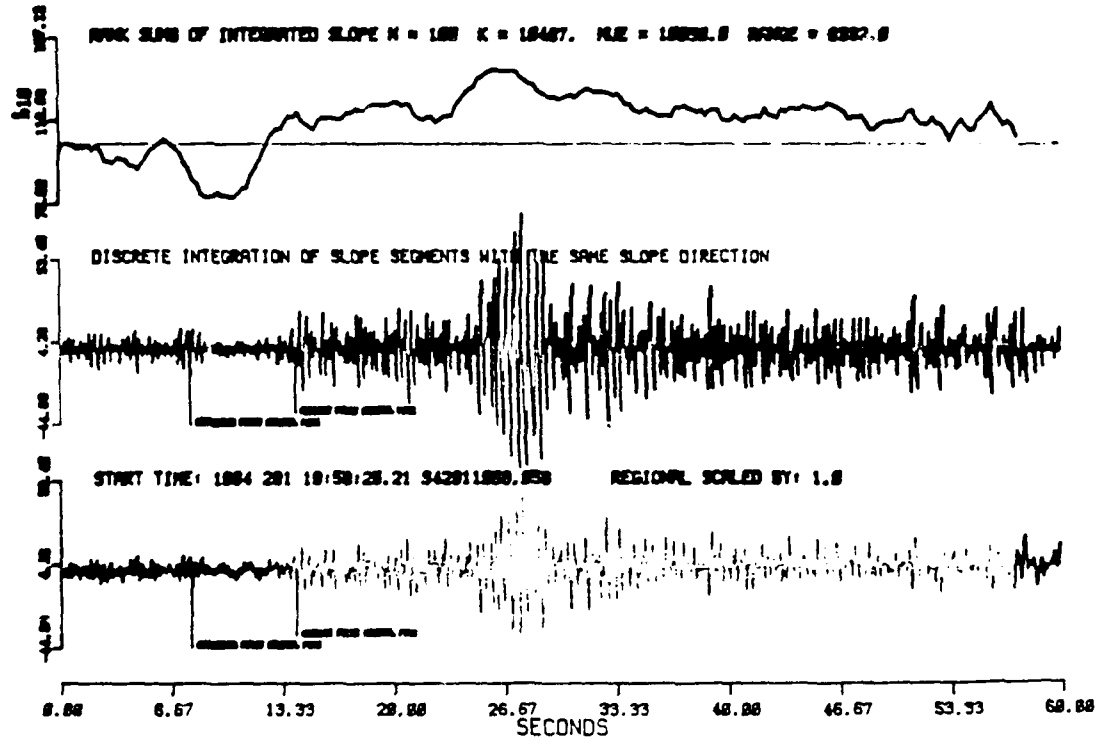

Event 21 - Mexico - October 17, 1984 - Quarry Blast

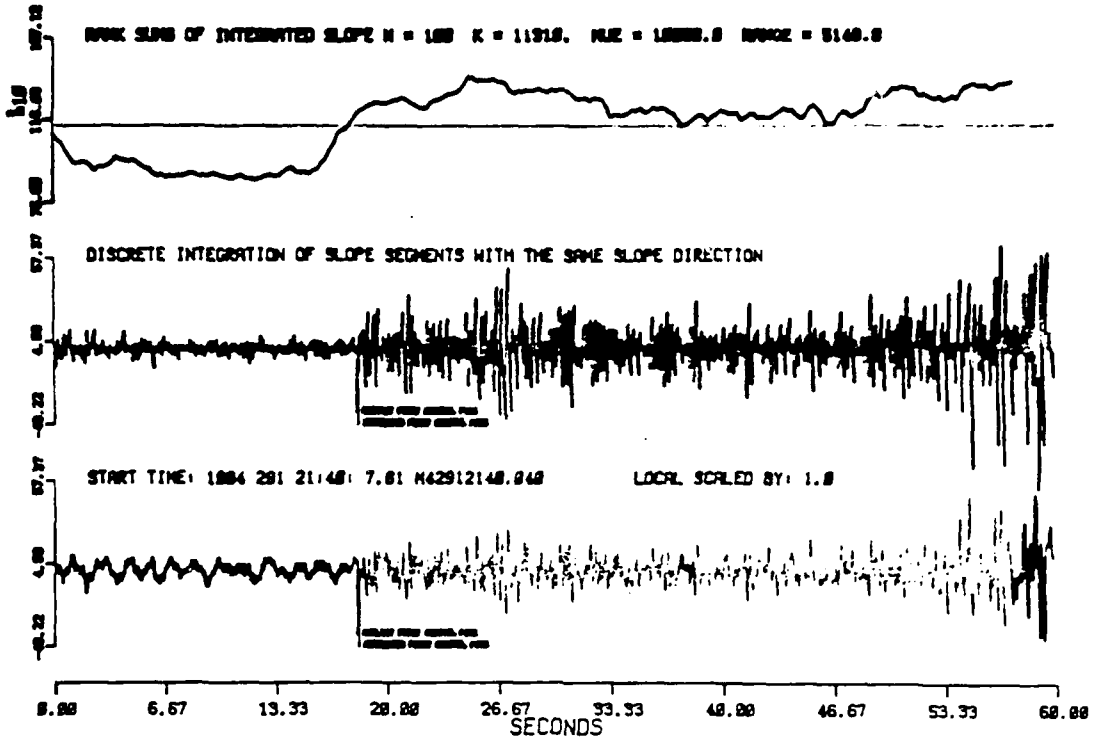
DISCRETE INTEGRATION OF SLOPE SEGMENTS WITH THE SAME SLOPE DIRECTION
START TIME: 1984 291 21:48: 7.81 H42912148.848
LOCAL SCALED BY: 1.8
0.00
6.67
13.33
20.00
26.67
33.33
40.00
46.67
53.33
60.00
SECONDS

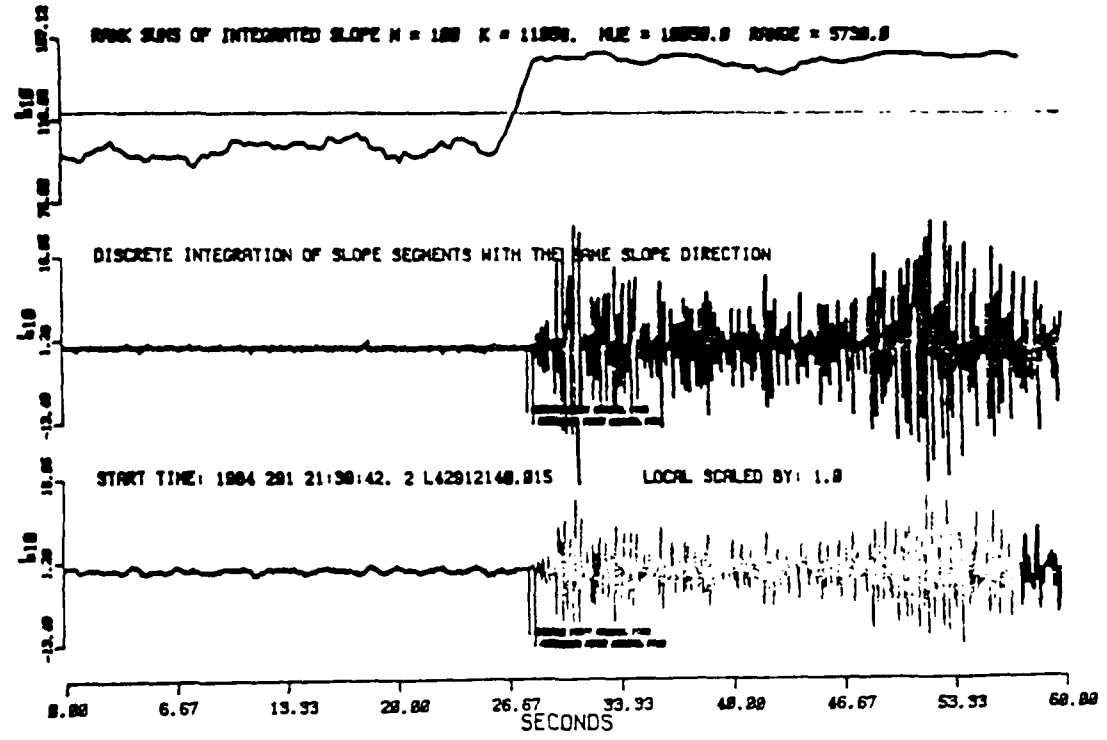
DISCRETE INTEGRATION OF SLOPE SEGMENTS WITH THE SAME SLOPE DIRECTION
START TIME: 1984 291 21:38:42. 2 L42912148.815
LOCAL SCALED BY: 1.8
0.00
6.67
13.33
20.00
26.67
33.33
40.00
46.67
53.33
60.00
SECONDS

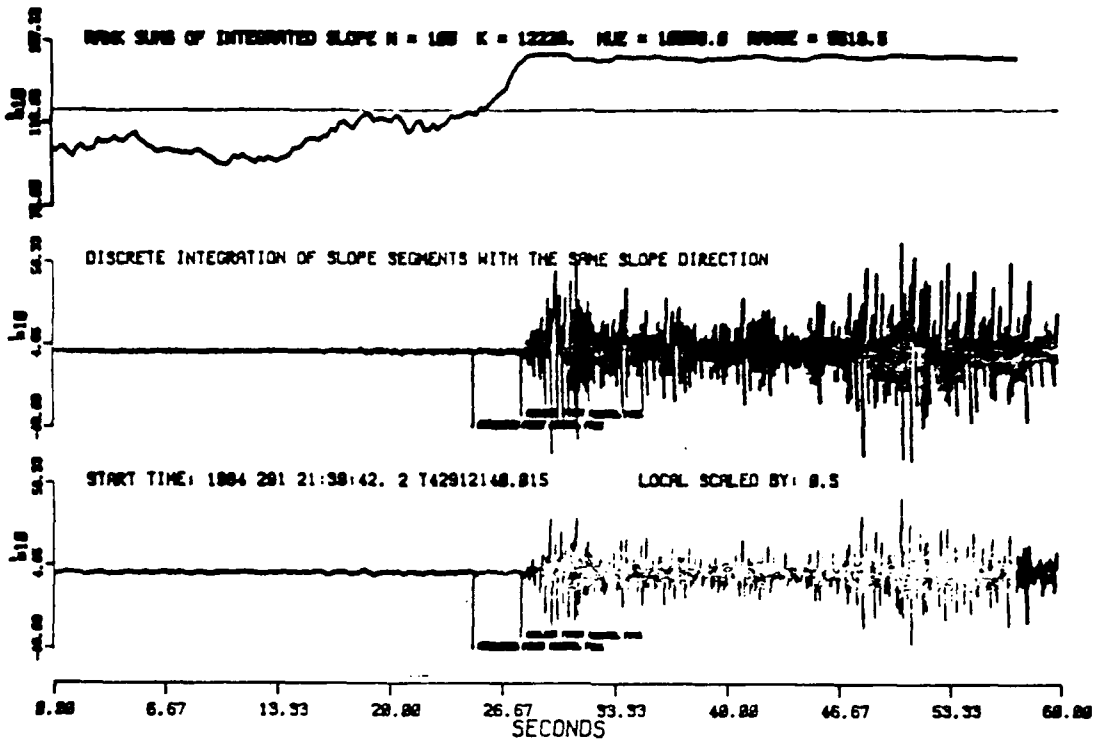
DISCRETE INTEGRATION OF SLOPE SEGMENTS WITH THE SAME SLOPE DIRECTION
START TIME: 1984 281 21:38:42. 2 T42912148.815
LOCAL SCALED BY: 8.5
0.00
6.67
13.33
20.00
26.67
33.33
40.00
46.67
53.33
60.00
SECONDS

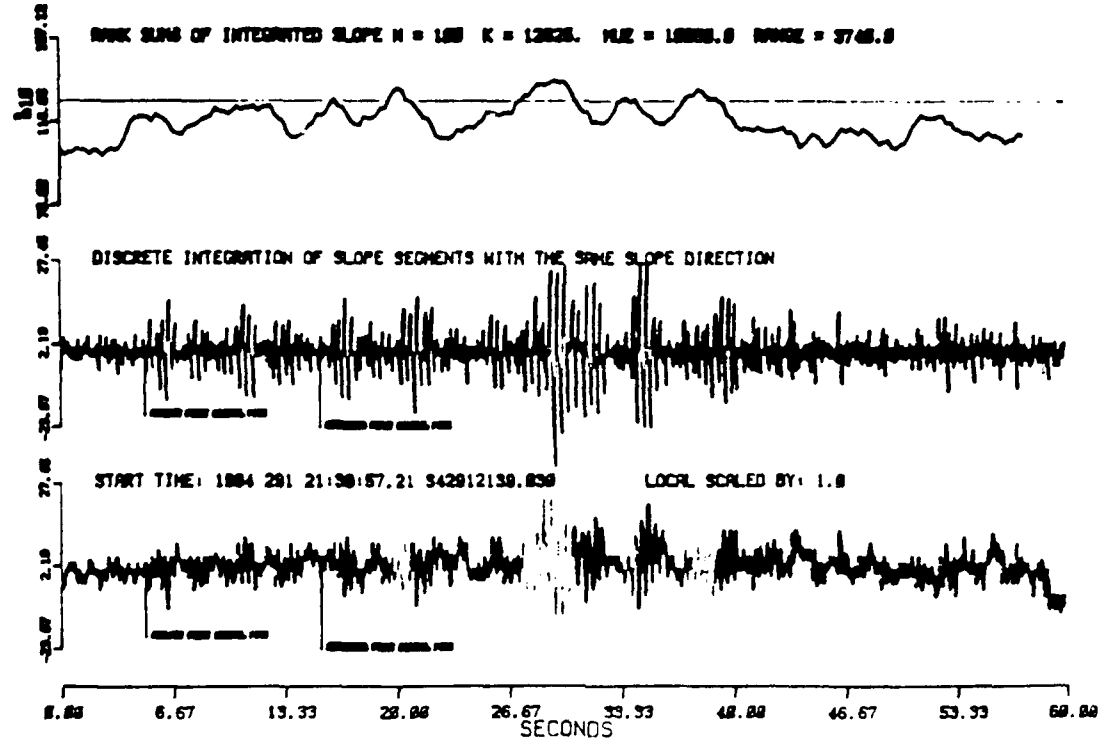
DISCRETE INTEGRATION OF SLOPE SEGMENTS WITH THE SAME SLOPE DIRECTION
START TIME: 1984 281 21:38:57.21 S42912139.859
LOCAL SCALED BY: 1.0
0.00
6.67
13.33
20.00
26.67
33.33
40.00
46.67
53.33
60.00
SECONDS

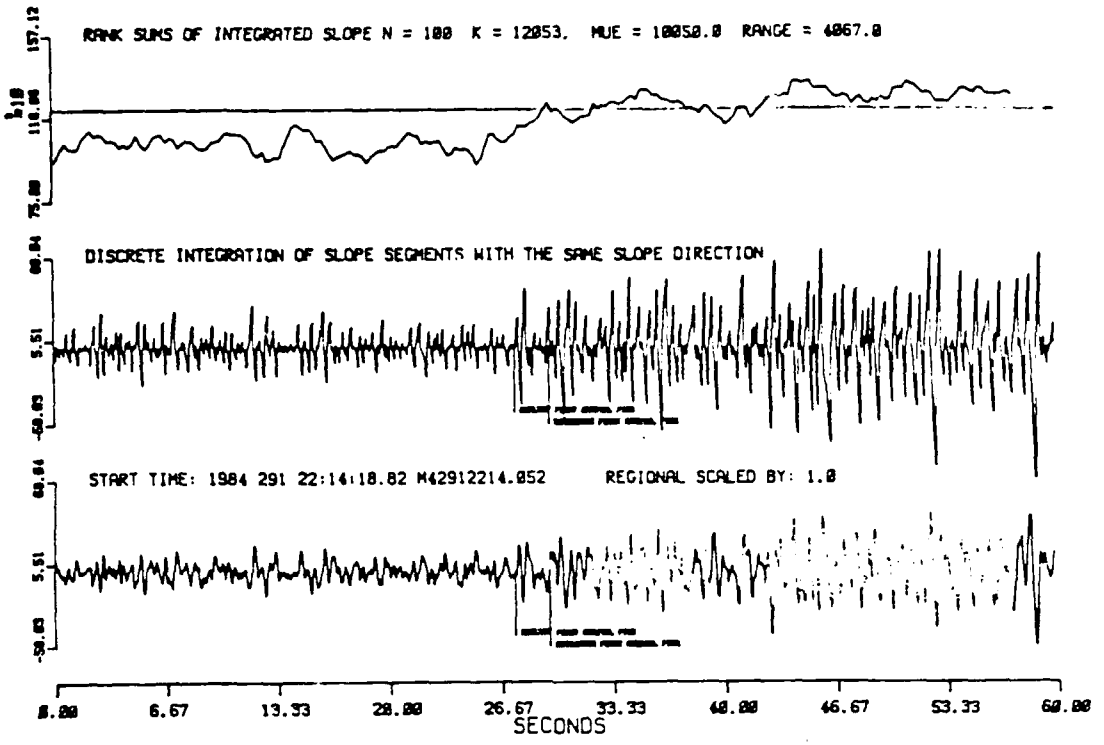

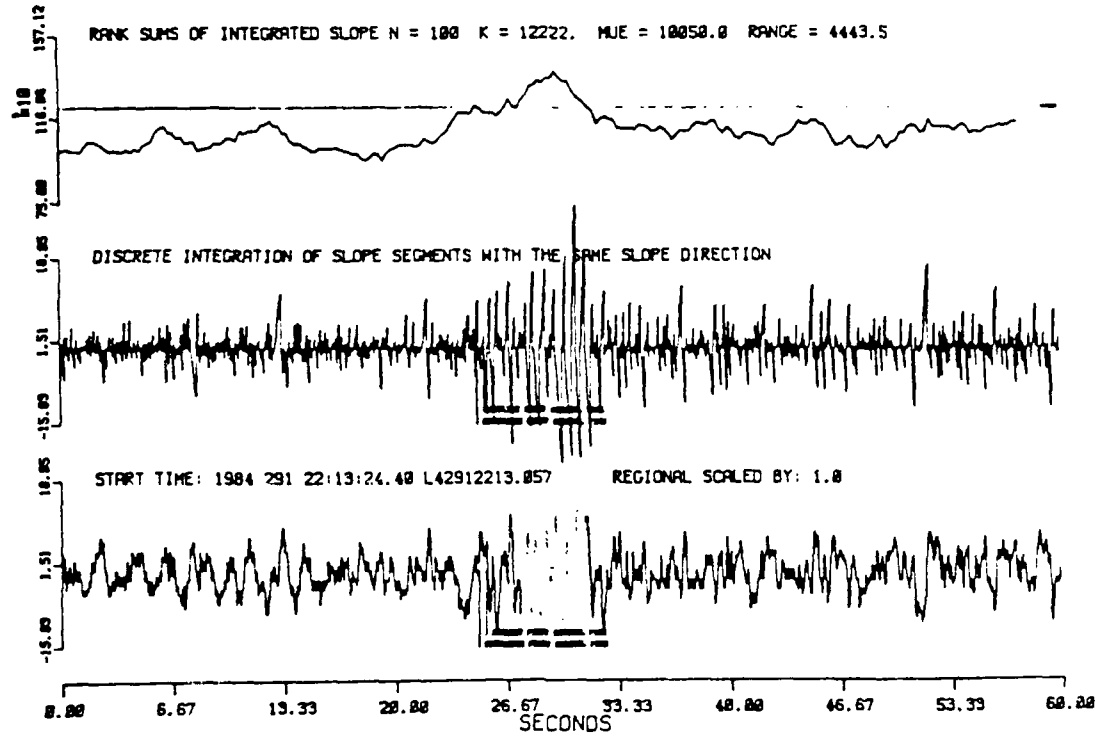

Event 22 - Regional (P - Lg) = 100 seconds

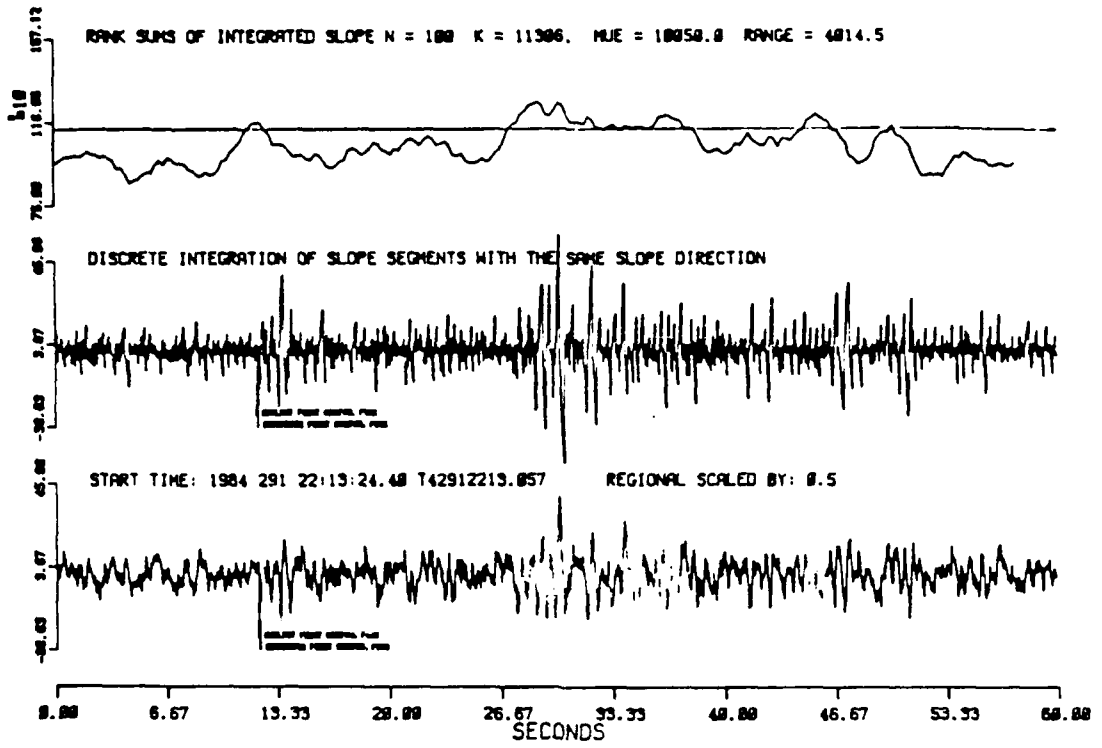
RANK SUMS OF INTEGRATED SLOPE N = 100 K = 11306. MUE = 10050.0 RANGE = 4014.5
DISCRETE INTEGRATION OF SLOPE SEGMENTS WITH THE SAME SLOPE DIRECTION
START TIME: 1984 291 22:13:24.40 T42912213.057 REGIONAL SCALED BY: 0.5
0.00
6.67
13.33
20.00
26.67
33.33
40.00
46.67
53.33
60.00
SECONDS

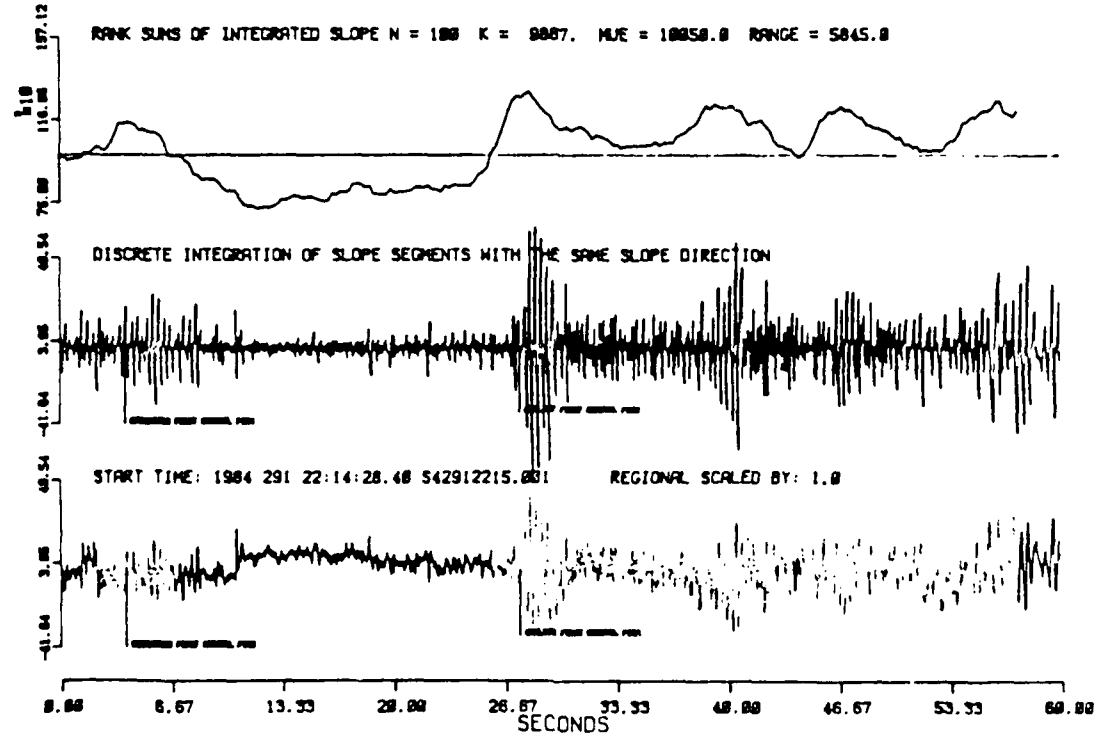
RANK SUMS OF INTEGRATED SLOPE N = 100 K = 9007. MUE = 10050.0 RANGE = 5045.0
DISCRETE INTEGRATION OF SLOPE SEGMENTS WITH THE SAME SLOPE DIRECTION
START TIME: 1984 291 22:14:28.40 S42912215.031 REGIONAL SCALED BY: 1.0
0.00
6.67
13.33
20.00
26.67
33.33
40.00
46.67
53.33
60.00
SECONDS

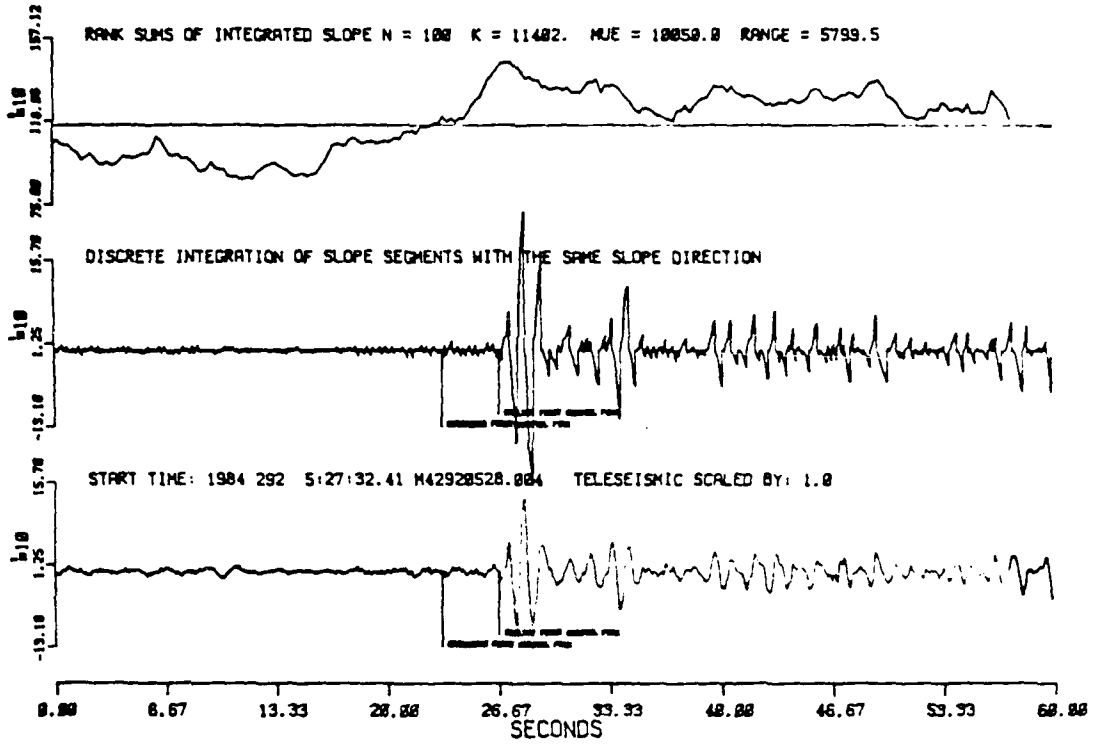

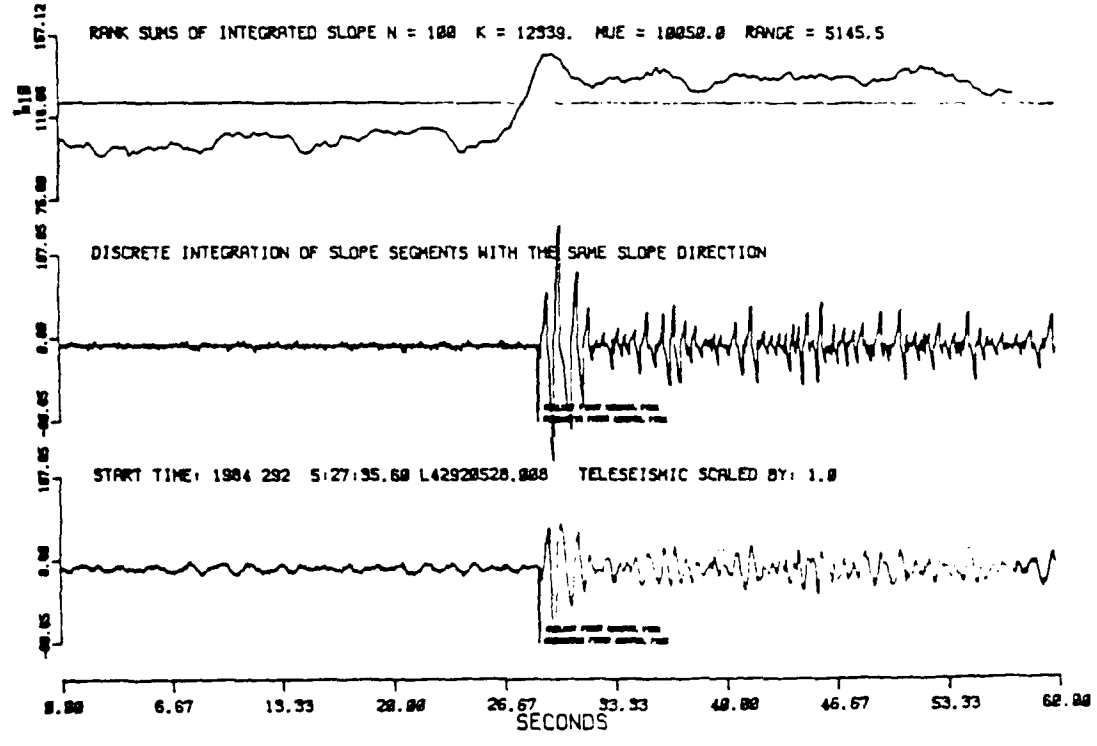

Event 23 - Central Alaska - 63.4N 151.3W 10/18/84
Origin Time: 05:19:53.1 Depth 105 km +7 M_b: 4.3
Residual error: -0.6

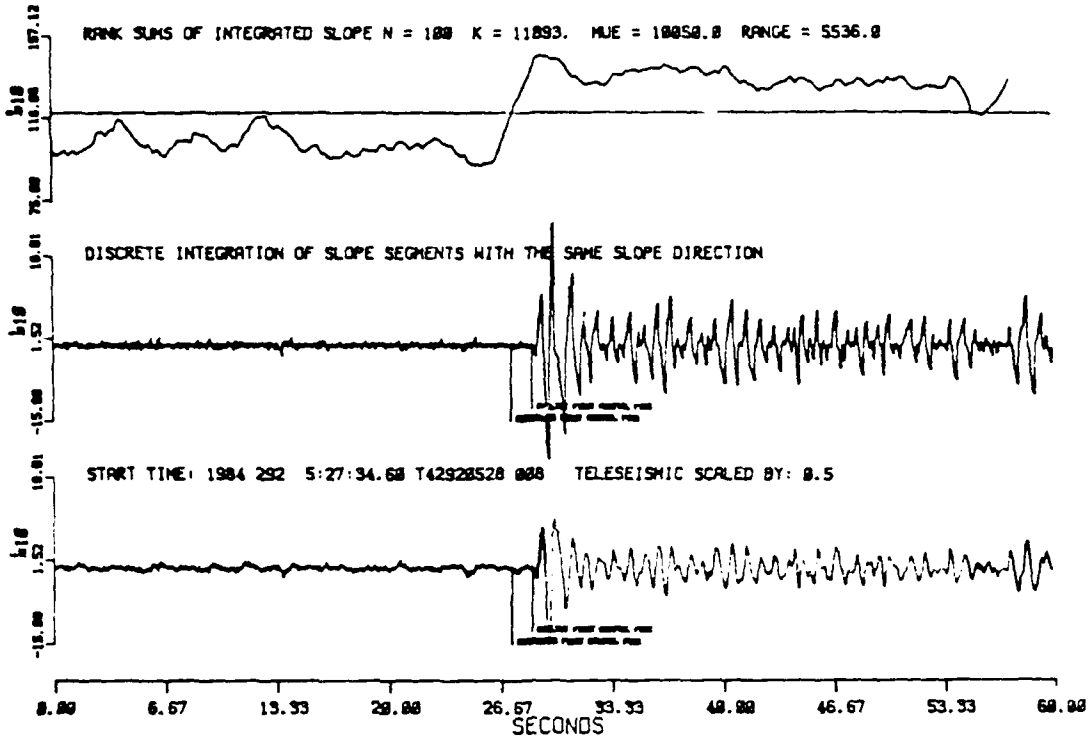
RANK SUMS OF INTEGRATED SLOPE N = 100 K = 11893. MUE = 10050.0 RANGE = 5536.0
DISCRETE INTEGRATION OF SLOPE SEGMENTS WITH THE SAME SLOPE DIRECTION
START TIME: 1984 292 5:27:34.68 T42928528 000 TELESEISMIC SCALED BY: 0.5
0.00
6.67
13.33
20.00
26.67
33.33
40.00
46.67
53.33
60.00
SECONDS

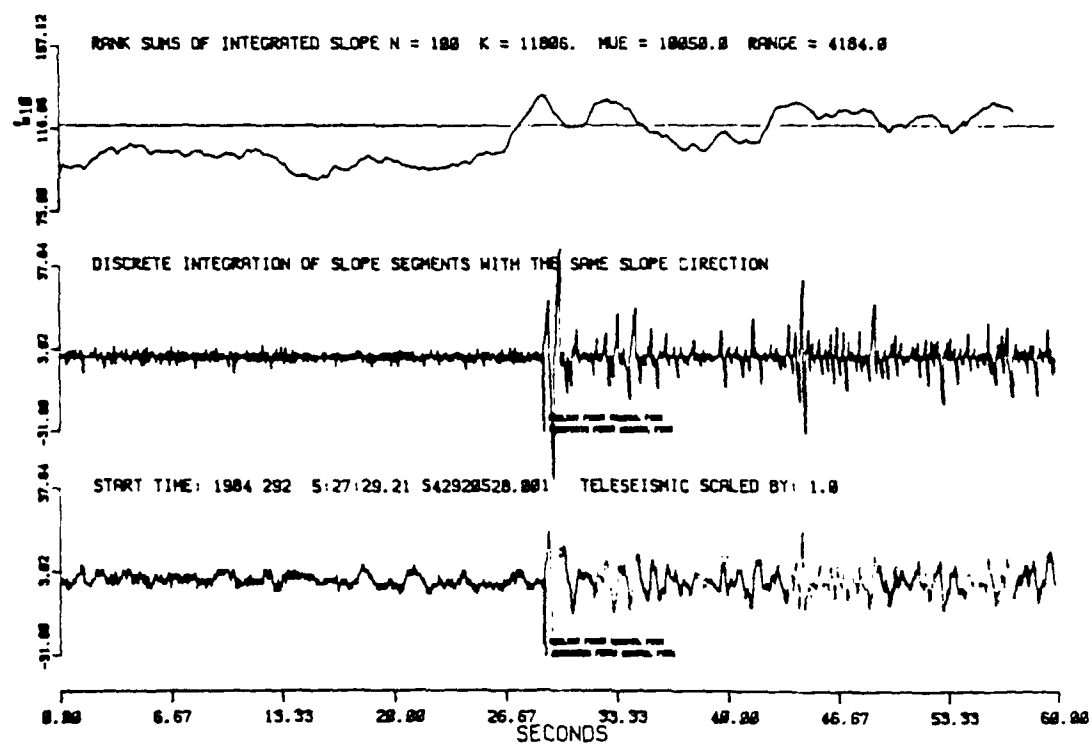
RANK SUMS OF INTEGRATED SLOPE N = 100 K = 11006. MUE = 10050.0 RANGE = 4184.0
DISCRETE INTEGRATION OF SLOPE SEGMENTS WITH THE SAME SLOPE DIRECTION
START TIME: 1984 292 5:27:29.21 S42928528.001 TELESEISMIC SCALED BY: 1.0
0.00
6.67
13.33
20.00
26.67
33.33
40.00
46.67
53.33
60.00
SECONDS

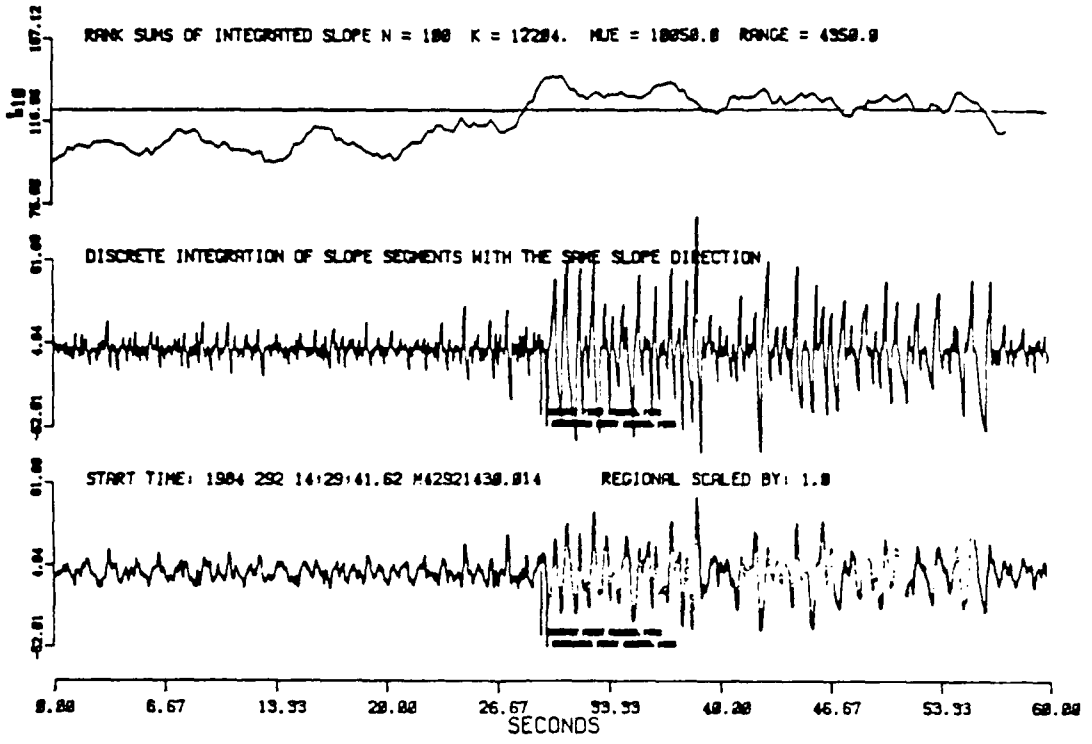

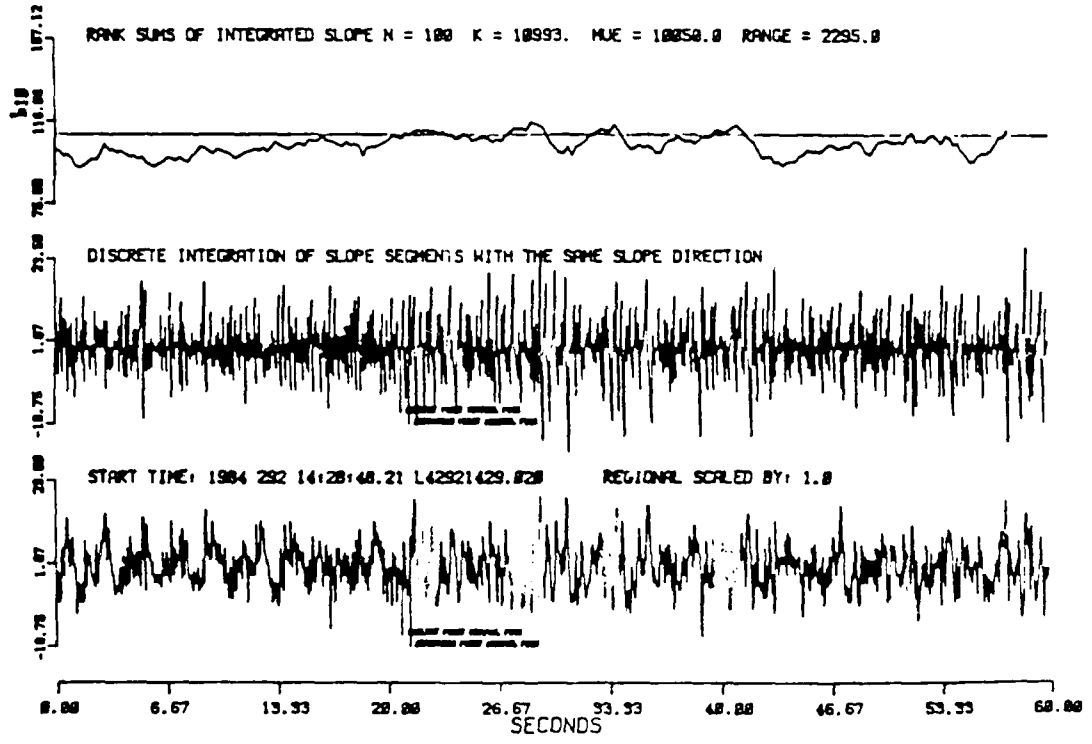

Event 24 - Regional Probable Lg Arrival

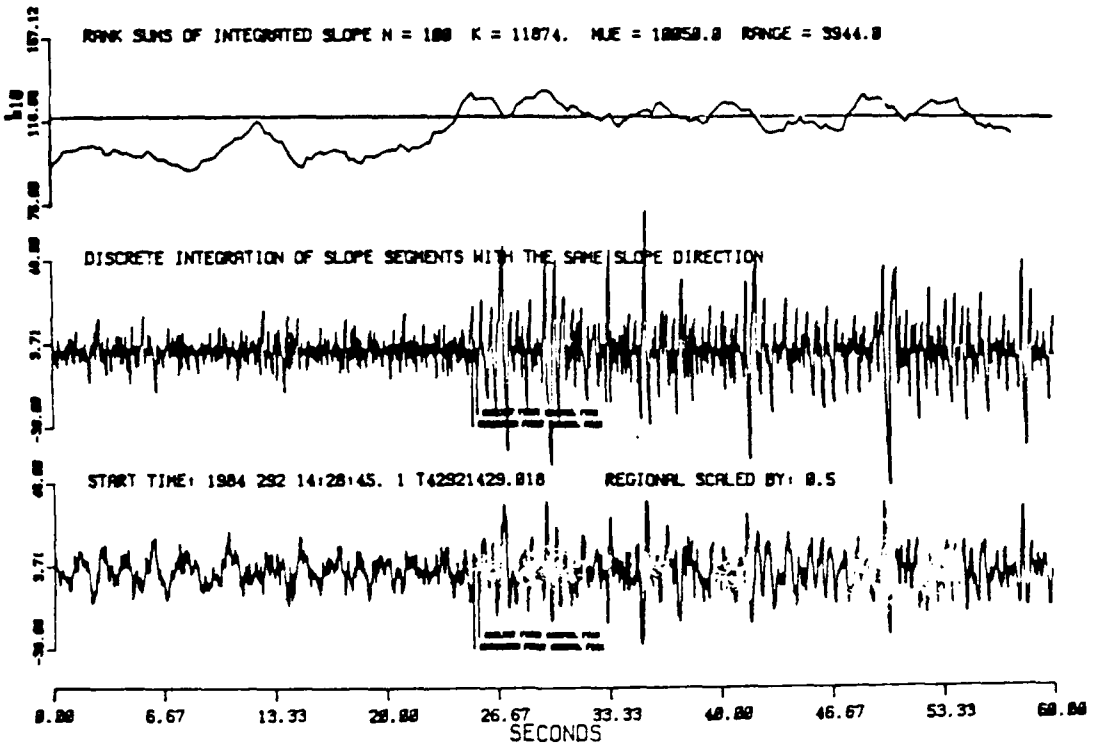
RANK SUMS OF INTEGRATED SLOPE N = 100 K = 11874. MUE = 10050.0 RANGE = 3944.0
DISCRETE INTEGRATION OF SLOPE SEGMENTS WITH THE SAME SLOPE DIRECTION
START TIME: 1984 292 14:28:45. 1 T42921429.010 REGIONAL SCALED BY: 0.5
0.00
6.67
13.33
20.00
26.67
33.33
40.00
46.67
53.33
60.00
SECONDS

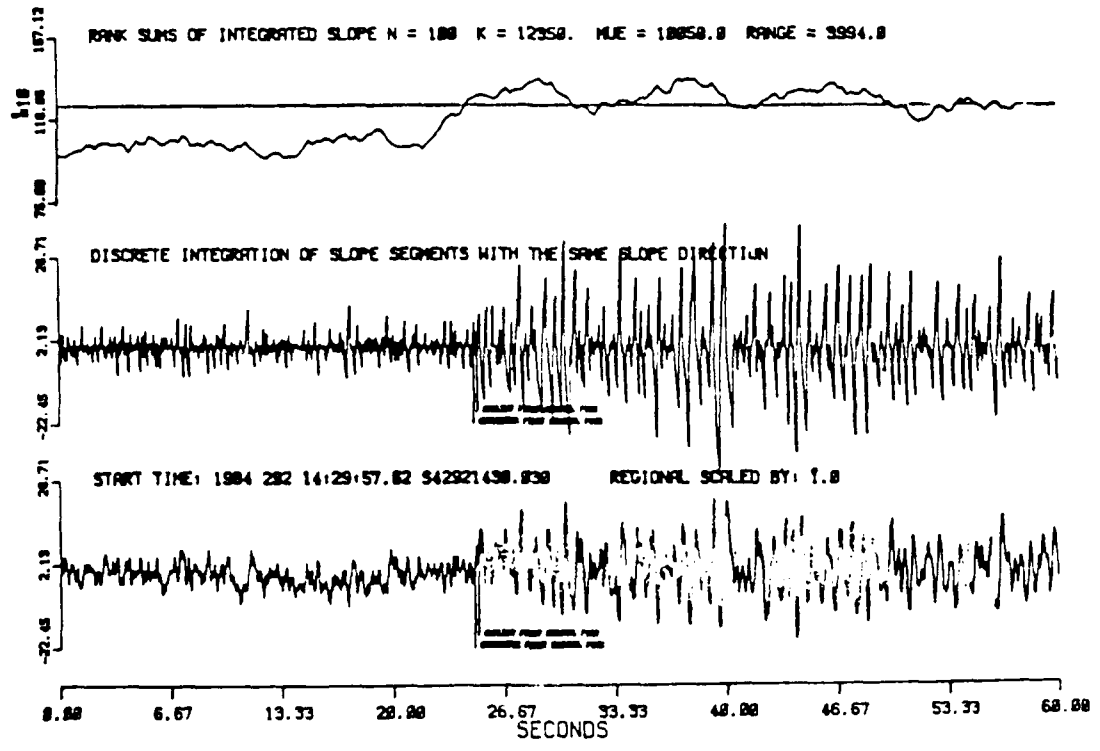
RANK SUMS OF INTEGRATED SLOPE N = 100 K = 12950. MUE = 10050.0 RANGE = 3994.0
DISCRETE INTEGRATION OF SLOPE SEGMENTS WITH THE SAME SLOPE DIRECTION
START TIME: 1984 292 14:29:57.02 S42921430.030 REGIONAL SCALED BY: 1.0
0.00
6.67
13.33
20.00
26.67
33.33
40.00
46.67
53.33
60.00
SECONDS

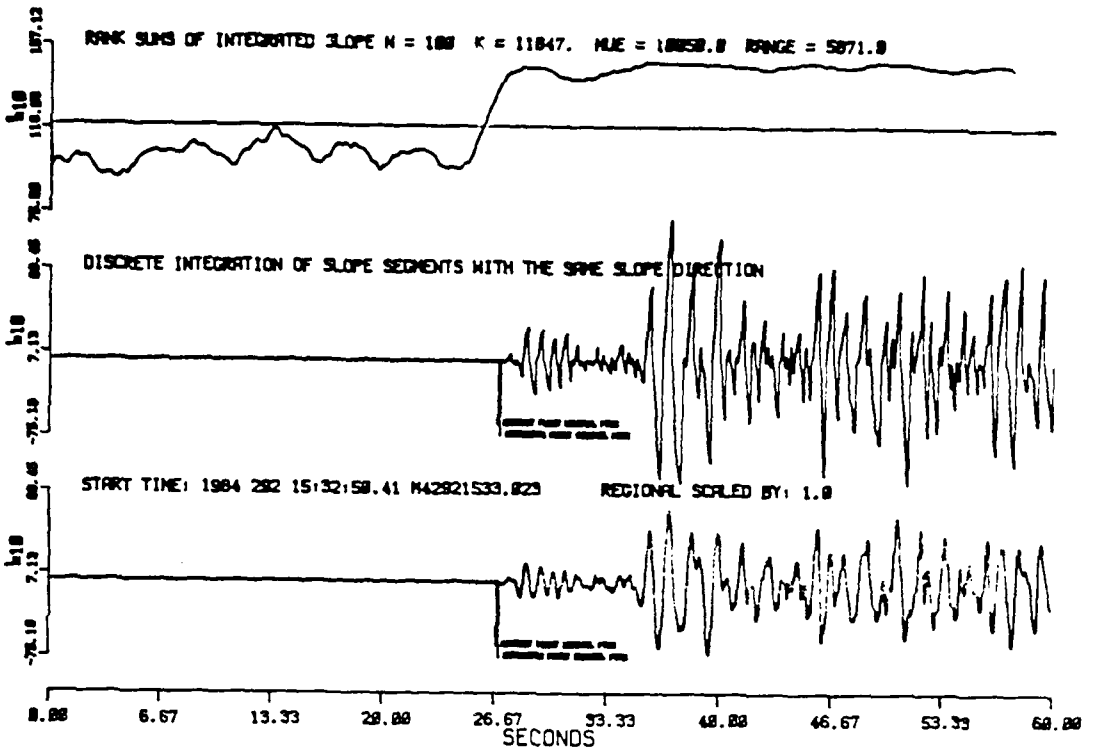

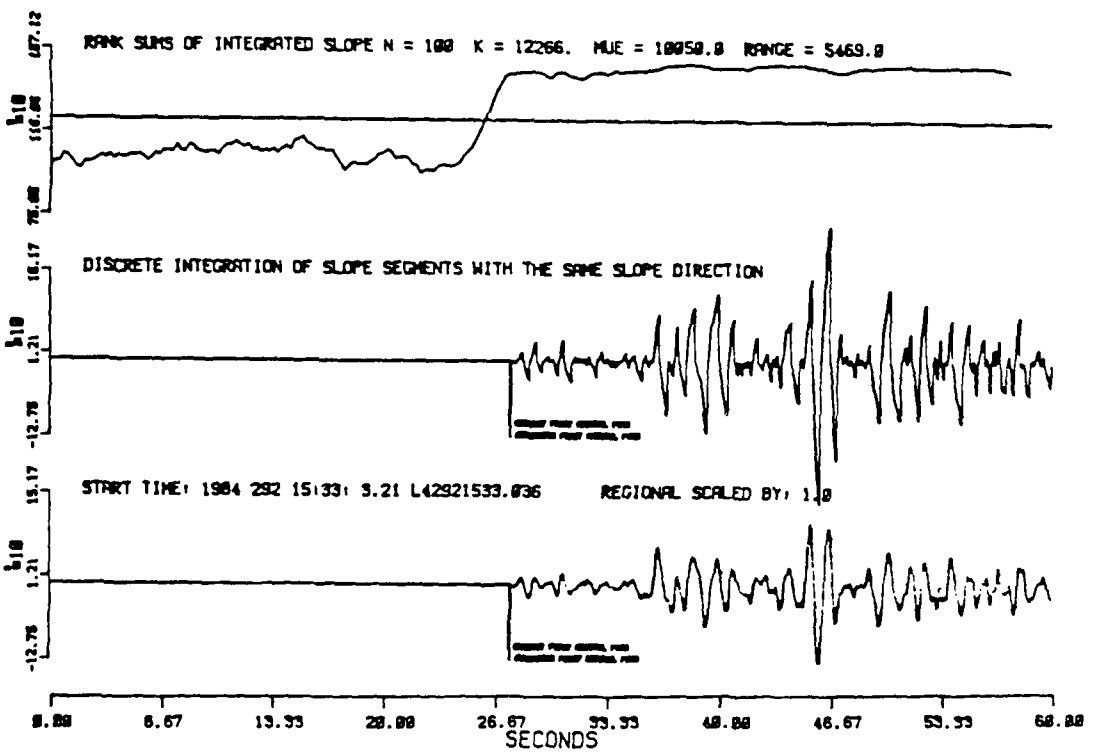

Event 25 Wyoming - 42.4N 105.7W 10/18/84 Origin Time:15:30:21.2
Depth: 18 km + 3 M_b: 4.3 Residual Error: 0.9

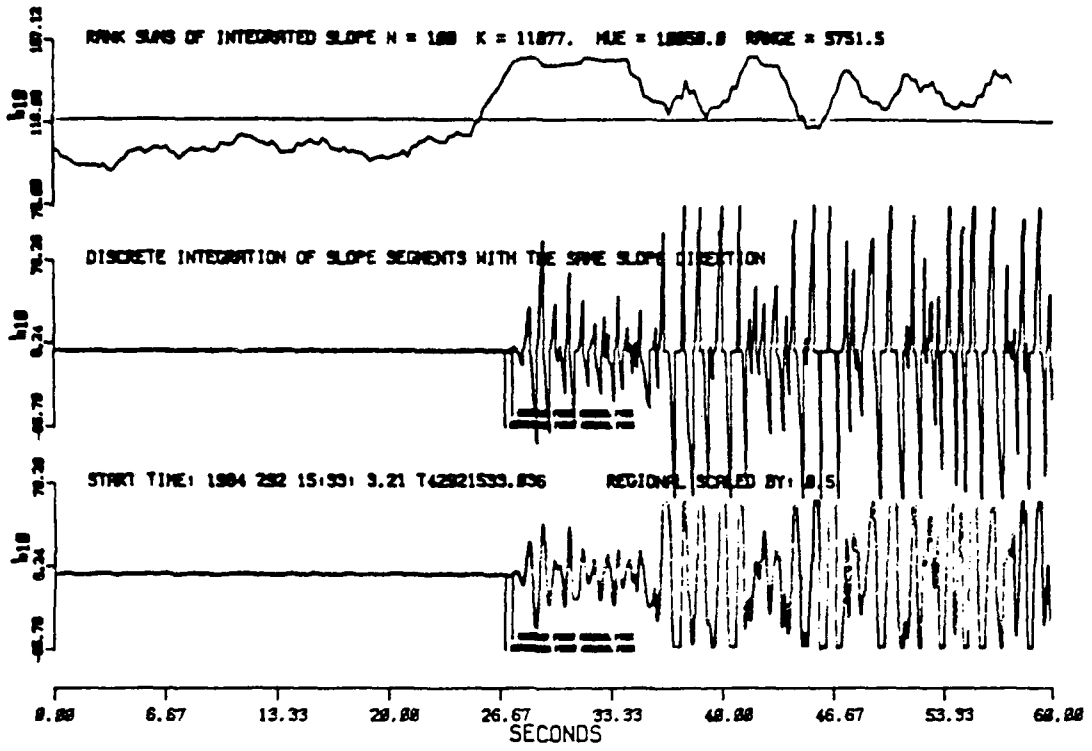
RANK SUMS OF INTEGRATED SLOPE N = 100 K = 11877. MUE = 10050.0 RANGE = 5751.5
DISCRETE INTEGRATION OF SLOPE SEGMENTS WITH THE SAME SLOPE DIRECTION
START TIME: 1984 292 15:33: 3.21 T42821533.836 REGIONAL SCALED BY: 0.5
0.00
6.67
13.33
20.00
26.67
33.33
40.00
46.67
53.33
60.00
SECONDS

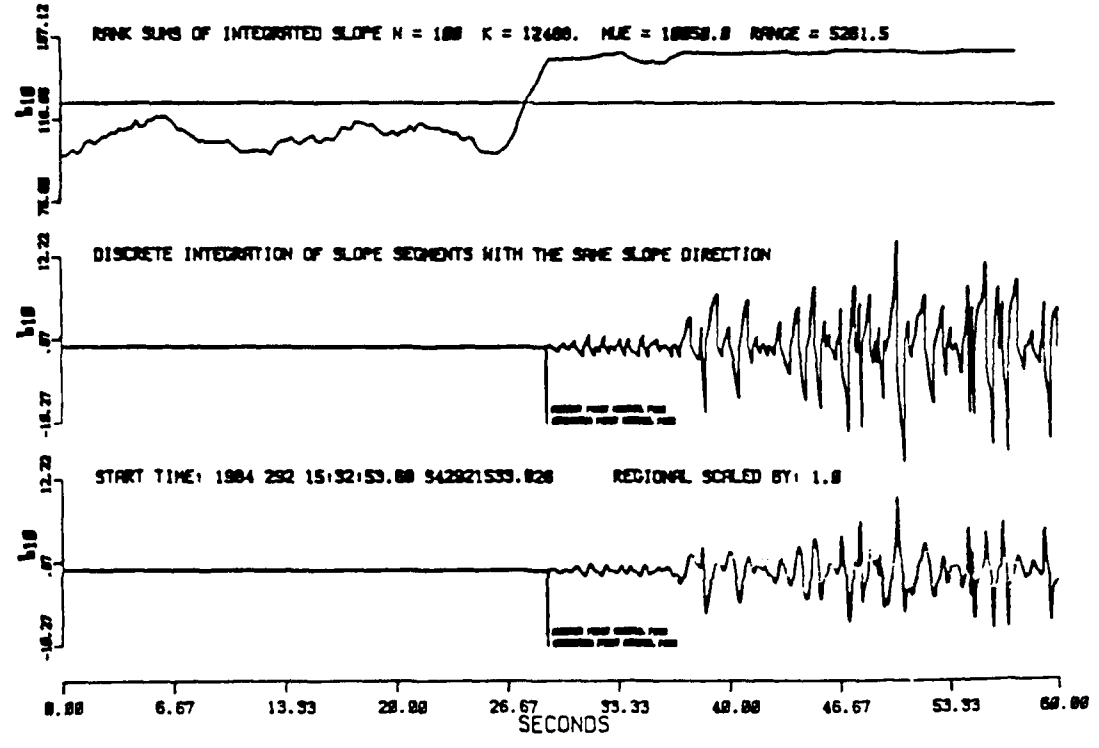
RANK SUMS OF INTEGRATED SLOPE N = 100 K = 12400. MUE = 10050.0 RANGE = 5281.5
DISCRETE INTEGRATION OF SLOPE SEGMENTS WITH THE SAME SLOPE DIRECTION
START TIME: 1984 292 15:32:53.00 842821533.826 REGIONAL SCALED BY: 1.0
0.00
6.67
13.33
20.00
26.67
33.33
40.00
46.67
53.33
60.00
SECONDS

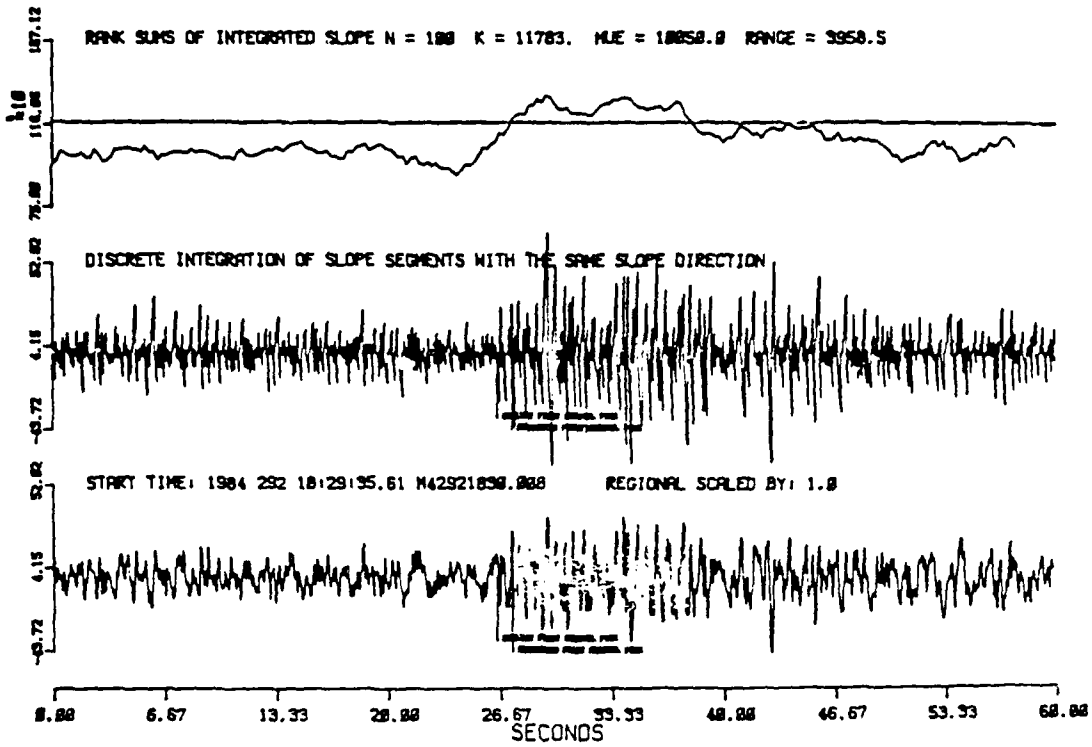

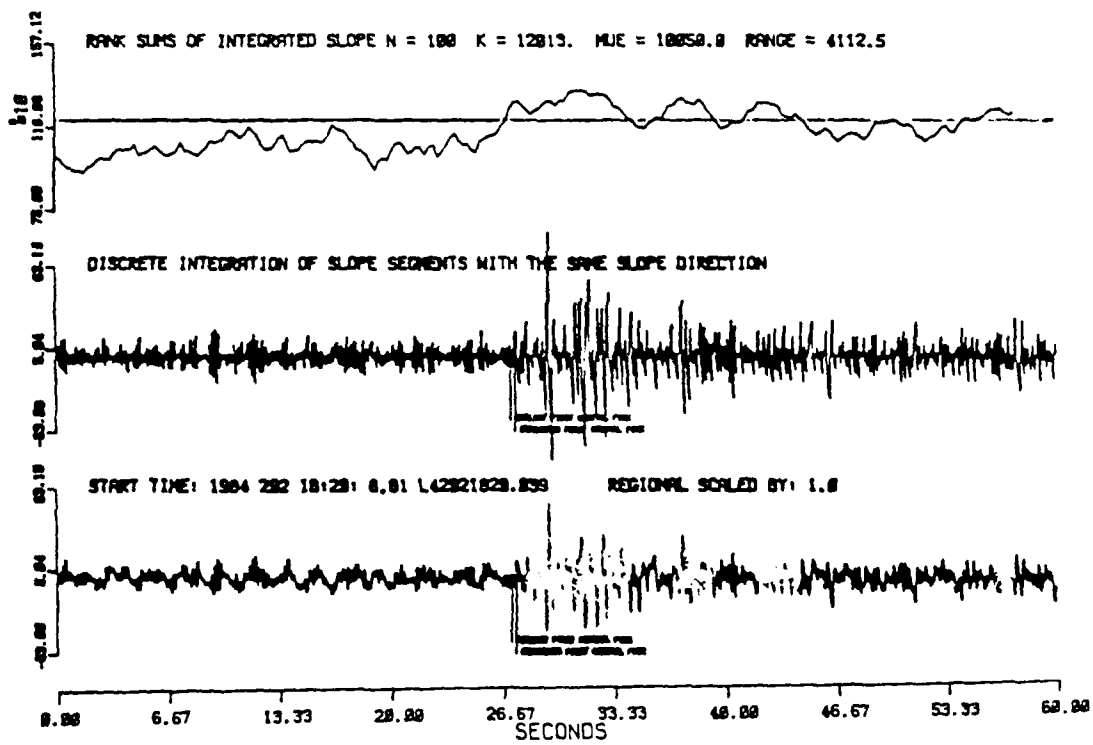

Event 26 - Regional (P - Lg) = 48 seconds

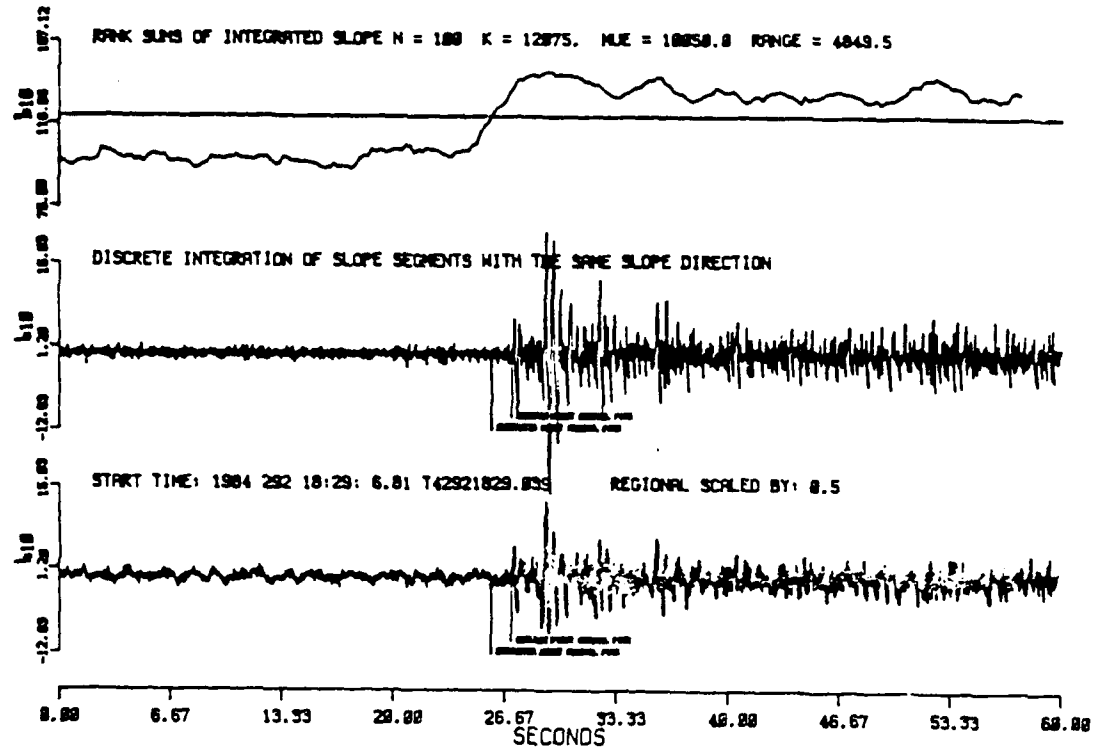
RANK SUMS OF INTEGRATED SLOPE N = 180 K = 12875. MUE = 10050.0 RANGE = 4849.5
DISCRETE INTEGRATION OF SLOPE SEGMENTS WITH THE SAME SLOPE DIRECTION
START TIME: 1984 292 18:29: 6.81 T42921829.835 REGIONAL SCALED BY: 0.5
0.00
6.67
13.33
20.00
26.67
33.33
40.00
46.67
53.33
60.00
SECONDS

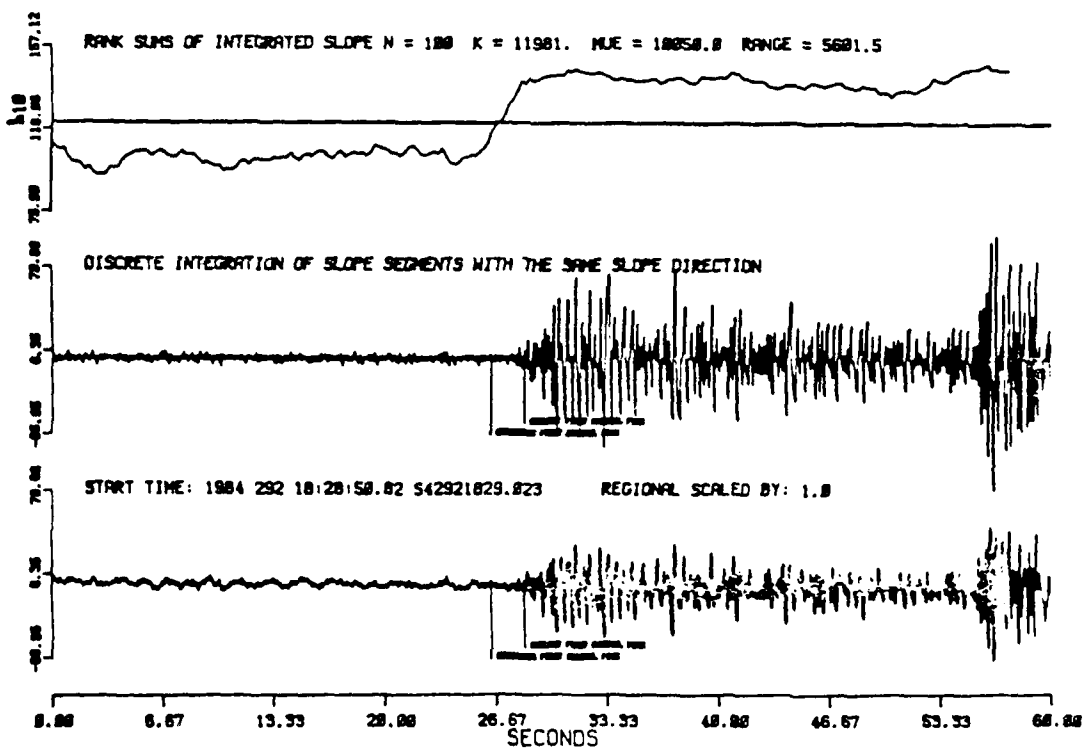
RANK SUMS OF INTEGRATED SLOPE N = 180 K = 11981. MUE = 10050.0 RANGE = 5681.5
DISCRETE INTEGRATION OF SLOPE SEGMENTS WITH THE SAME SLOPE DIRECTION
START TIME: 1984 292 18:28:50.82 S42921829.823 REGIONAL SCALED BY: 1.0
0.00
6.67
13.33
20.00
26.67
33.33
40.00
46.67
53.33
60.00
SECONDS

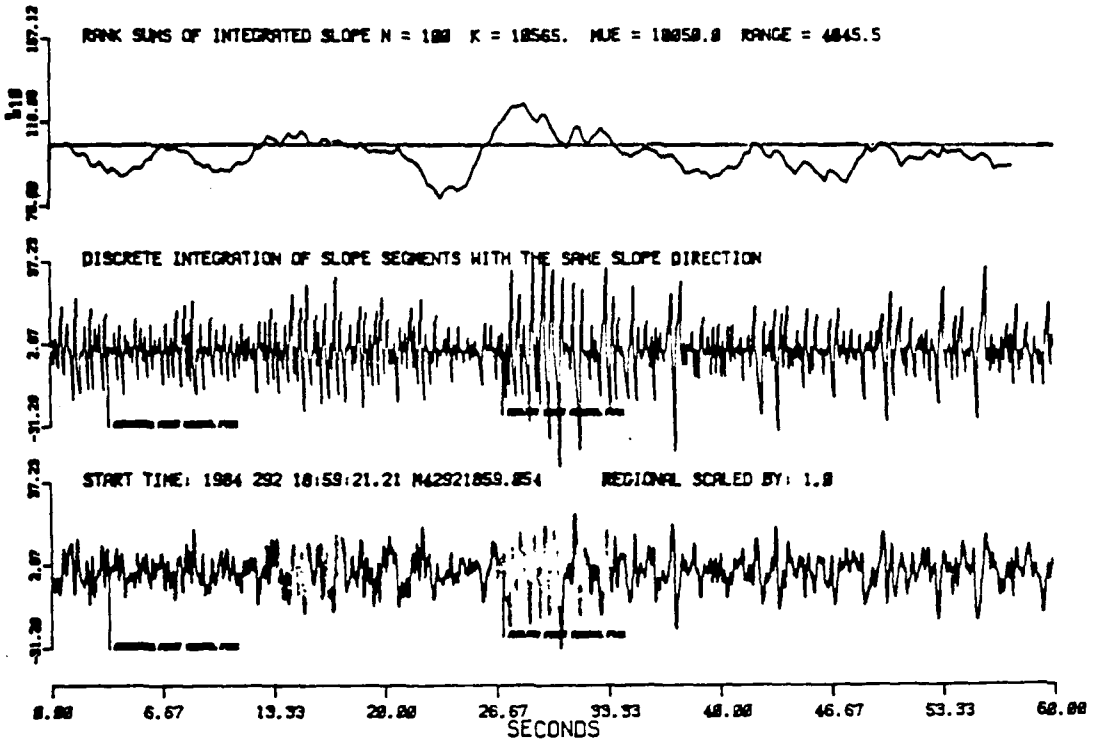

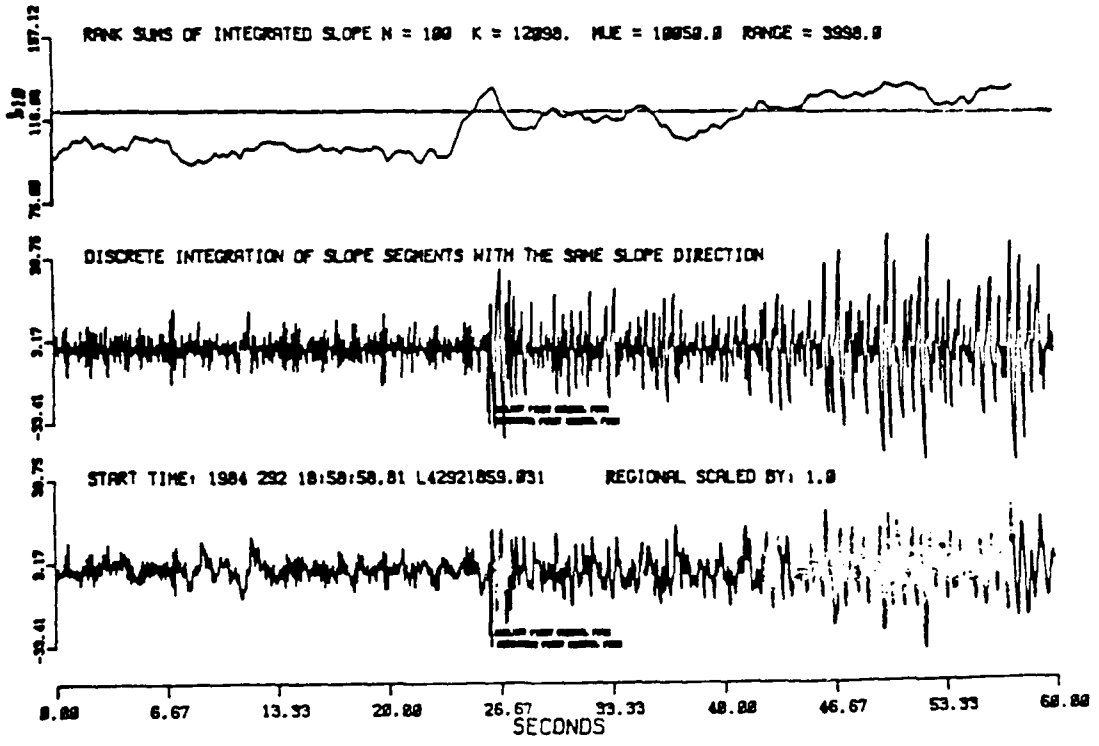

Event 27 - Regional (Pn - Lg) = 95 Seconds

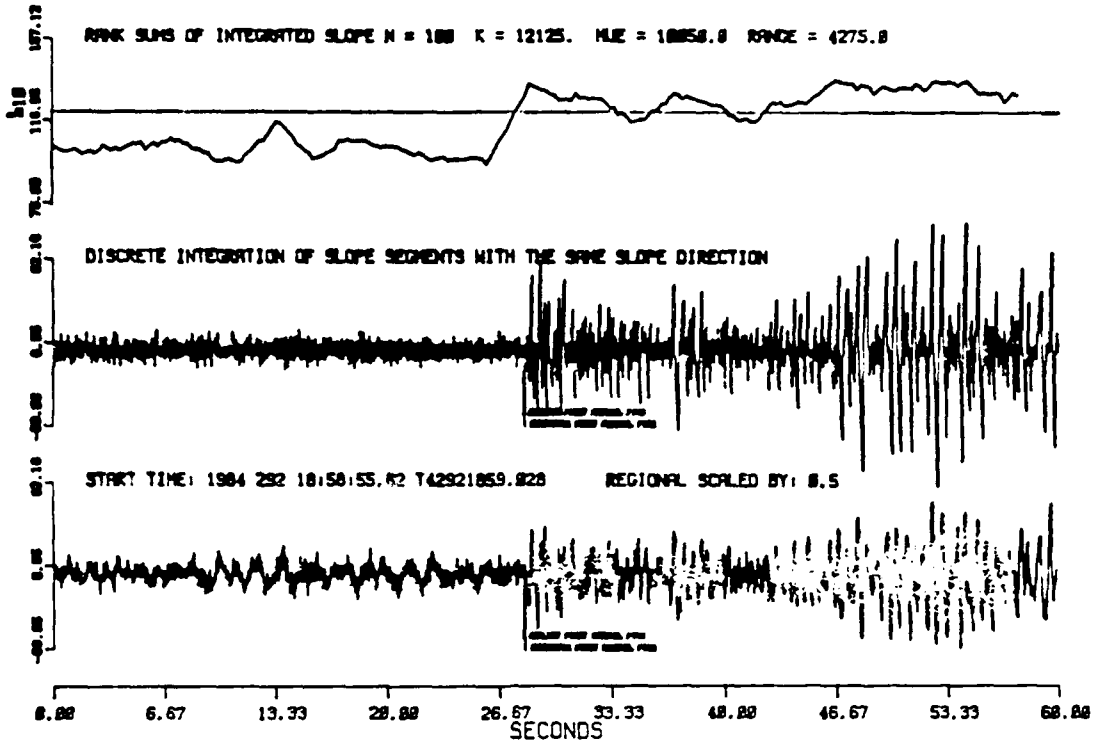
RANK SUMS OF INTEGRATED SLOPE N = 100 K = 12125. MUE = 10050.0 RANGE = 4275.0
DISCRETE INTEGRATION OF SLOPE SEGMENTS WITH THE SAME SLOPE DIRECTION
START TIME: 1984 292 18:58:55.62 T42921859.920 REGIONAL SCALED BY: 0.5
0.00
6.67
13.33
20.00
26.67
33.33
40.00
46.67
53.33
60.00
SECONDS

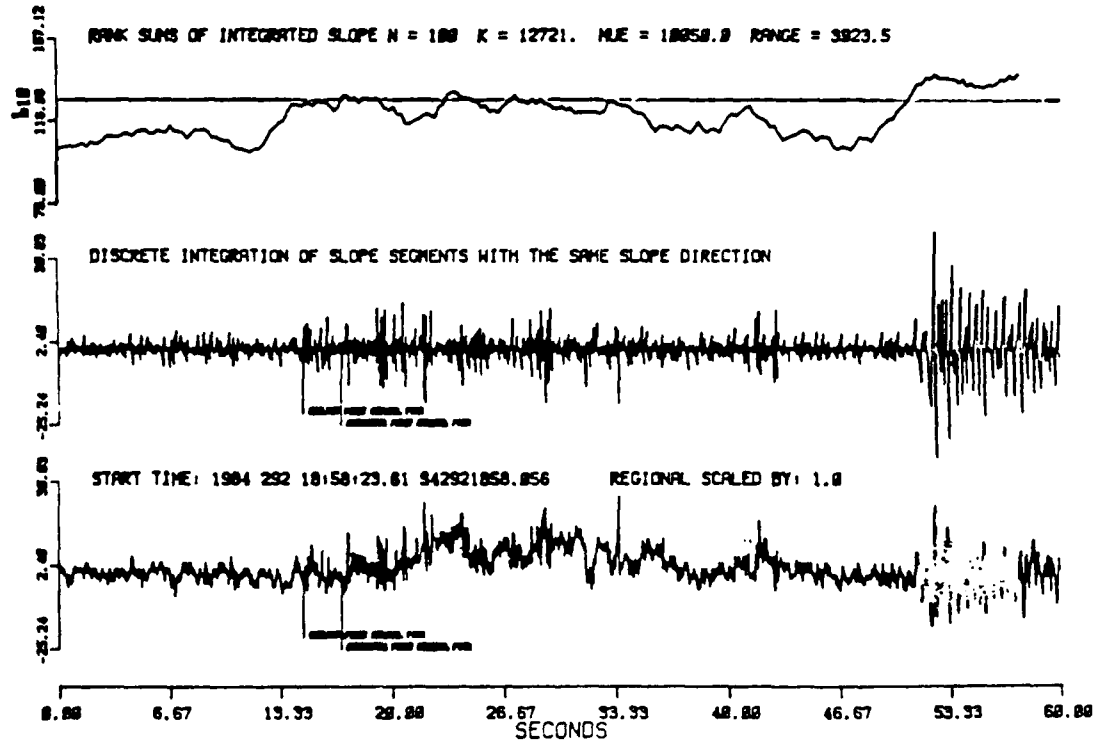
RANK SUMS OF INTEGRATED SLOPE N = 100 K = 12721. MUE = 10050.0 RANGE = 3923.5
DISCRETE INTEGRATION OF SLOPE SEGMENTS WITH THE SAME SLOPE DIRECTION
START TIME: 1984 292 18:58:23.61 S42921858.856 REGIONAL SCALED BY: 1.0
0.00
6.67
13.33
20.00
26.67
33.33
40.00
46.67
53.33
60.00
SECONDS

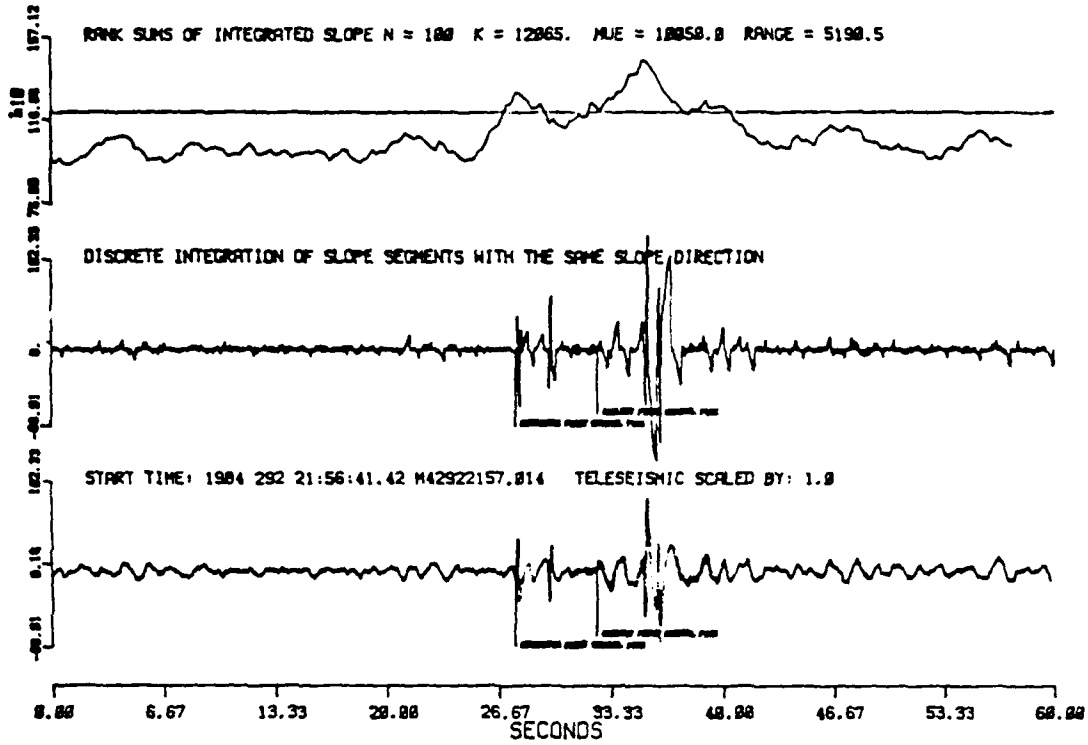

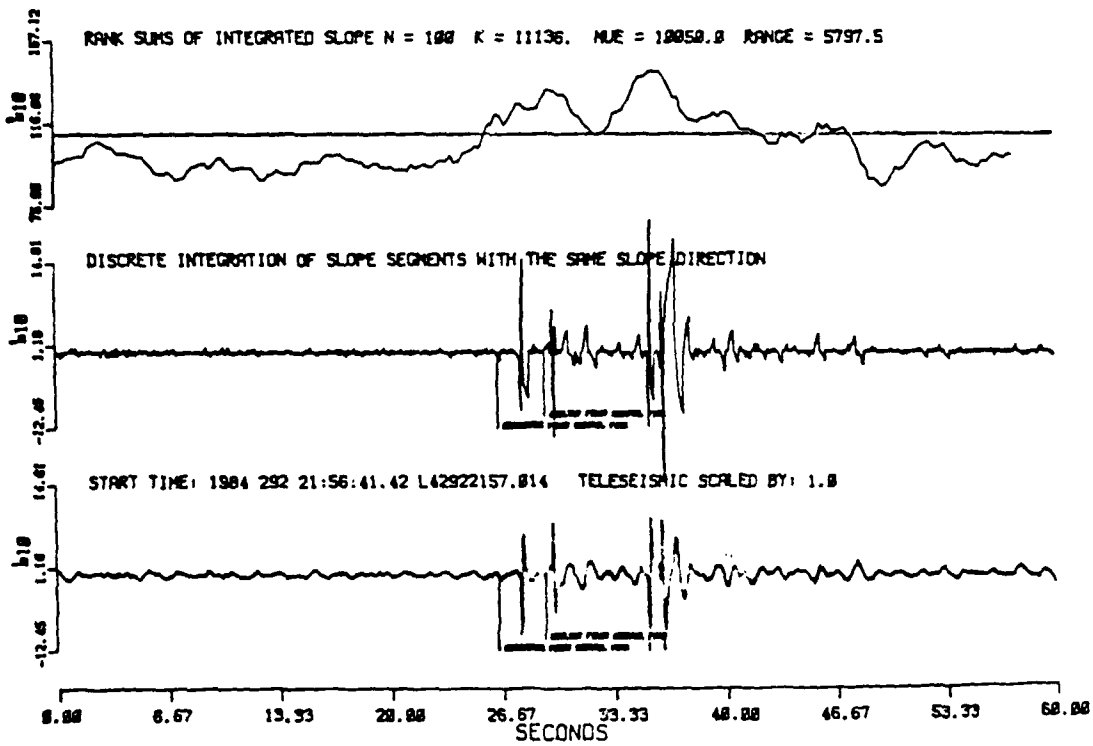

Event 28 Bonin Islands Region 28.1N 139.6E 10/18/84
Origin Time:21:42:38.8 Depth: 529 km + 8 M_b: 4.3
Residual Error: 0.5

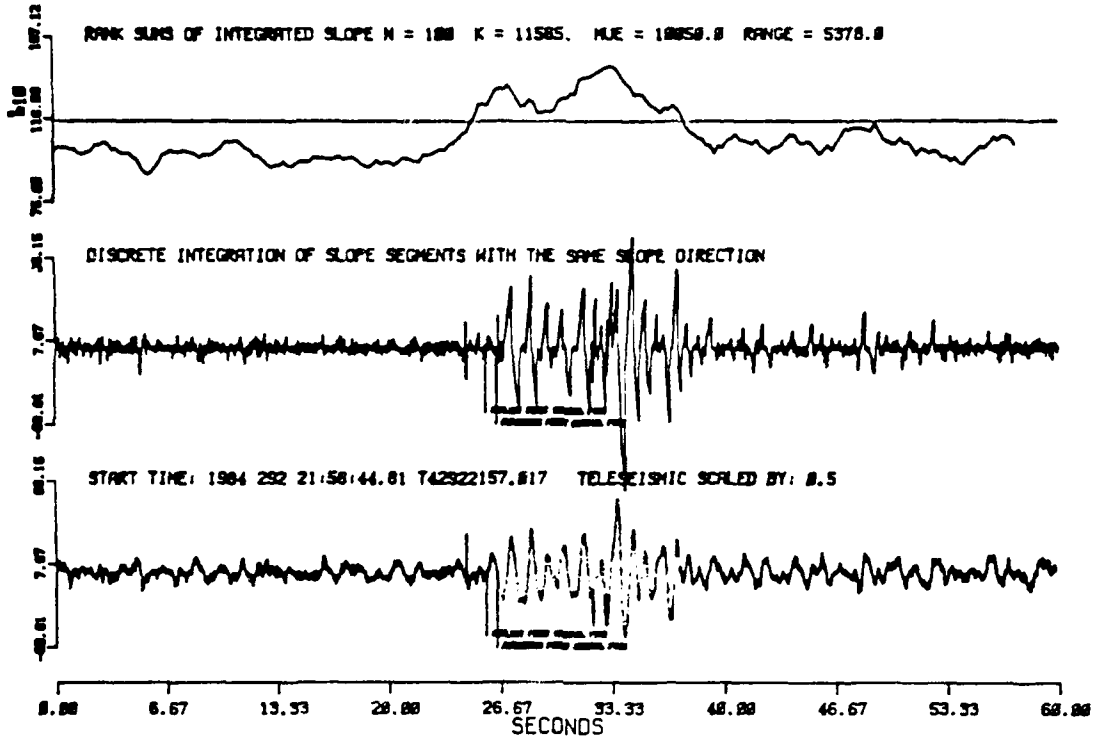
RANK SUMS OF INTEGRATED SLOPE N = 100 K = 11585. MUE = 10050.0 RANGE = 5378.0
DISCRETE INTEGRATION OF SLOPE SEGMENTS WITH THE SAME SLOPE DIRECTION
START TIME: 1984 292 21:50:44.01 T42922157.017 TELESEISMIC SCALED BY: 0.5
0.00
6.67
13.33
20.00
26.67
33.33
40.00
46.67
53.33
60.00
SECONDS

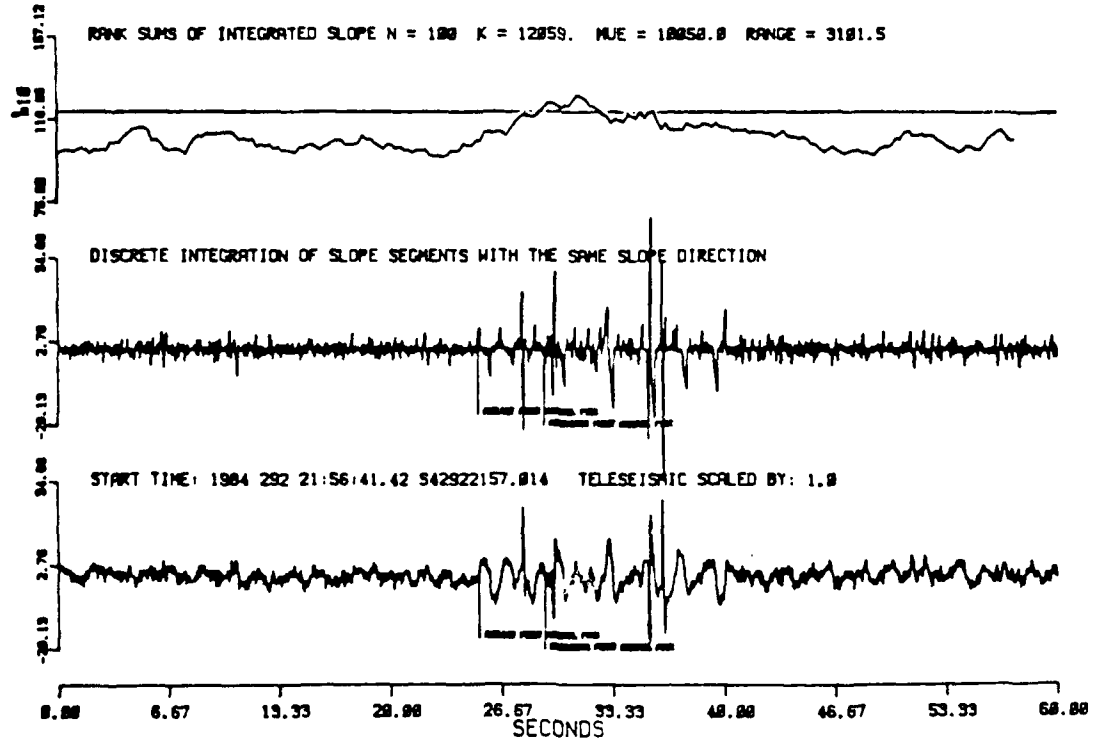
RANK SUMS OF INTEGRATED SLOPE N = 100 K = 12059. MUE = 10050.0 RANGE = 3101.5
DISCRETE INTEGRATION OF SLOPE SEGMENTS WITH THE SAME SLOPE DIRECTION
START TIME: 1984 292 21:56:41.42 S42922157.014 TELESEISMIC SCALED BY: 1.0
0.00
6.67
13.33
20.00
26.67
33.33
40.00
46.67
53.33
60.00
SECONDS

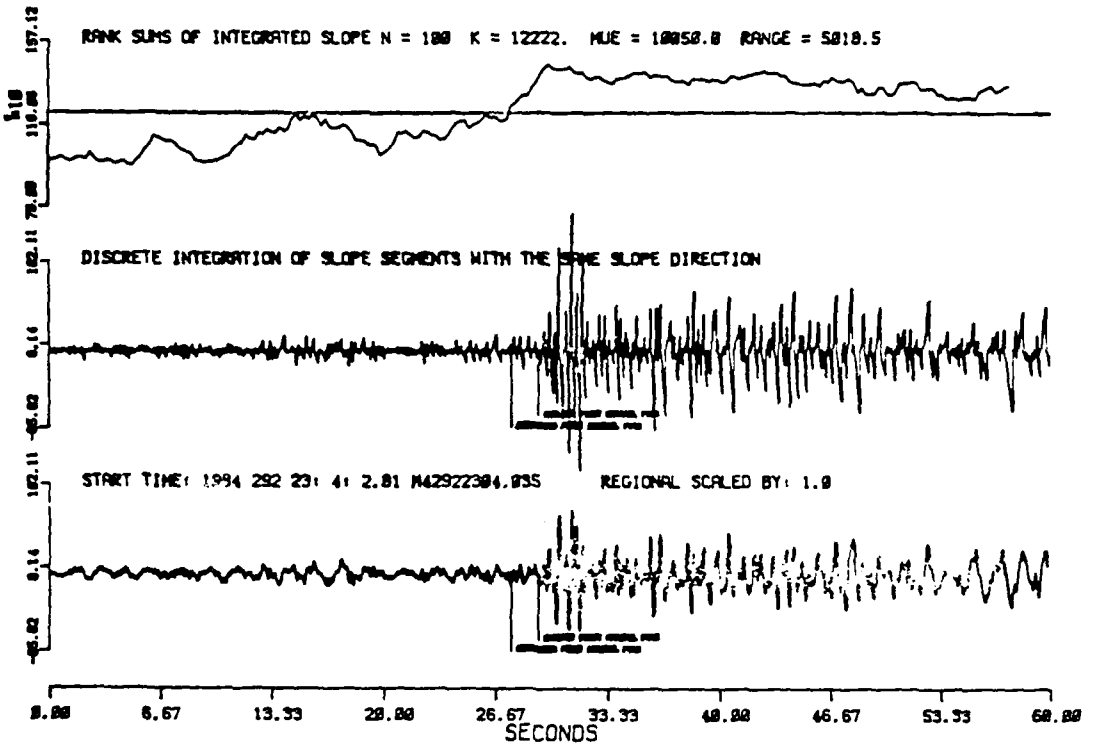

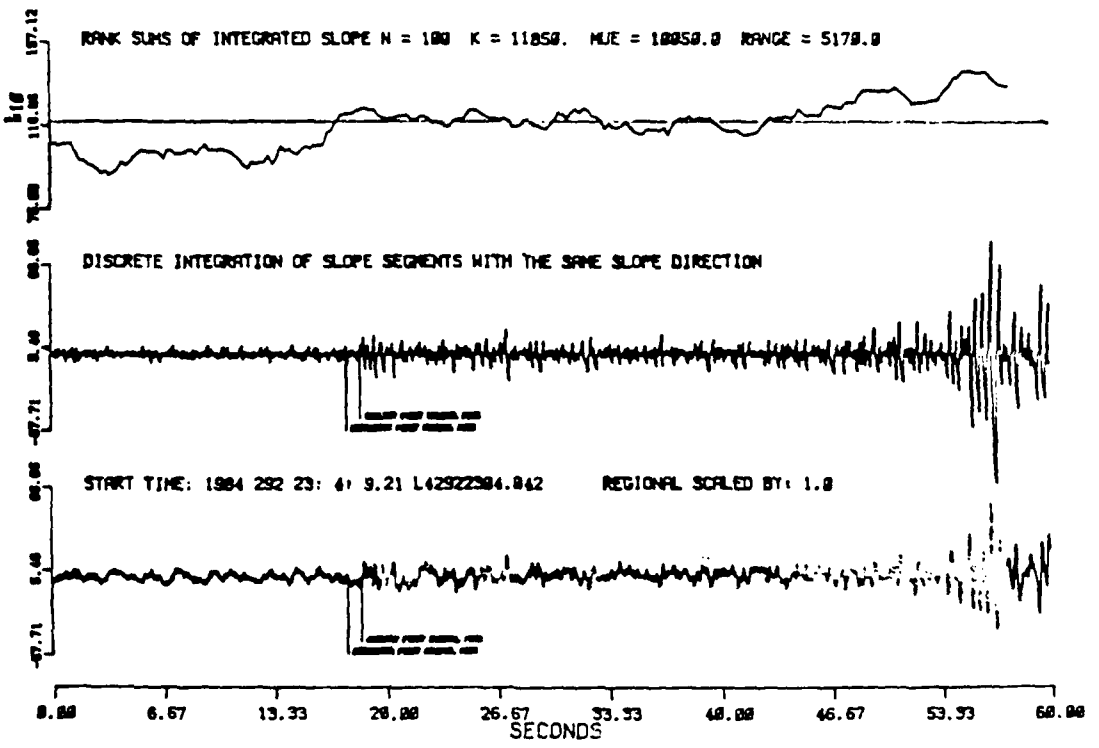

Event 29 - Regional (Pn - Lg) = 37 seconds

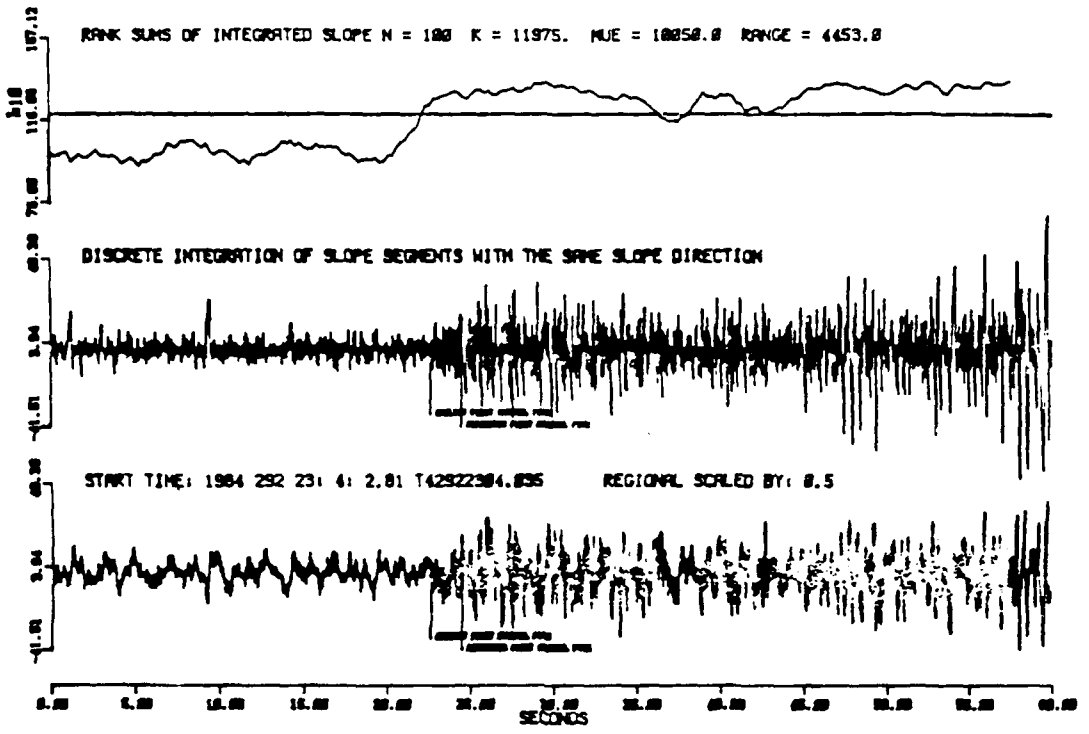
RANK SUMS OF INTEGRATED SLOPE N = 100 K = 11975. MUE = 10050.0 RANGE = 4453.0
DISCRETE INTEGRATION OF SLOPE SEGMENTS WITH THE SAME SLOPE DIRECTION
START TIME: 1984 292 23: 4: 2.81 T42922384.835 REGIONAL SCALED BY: 0.5
SECONDS

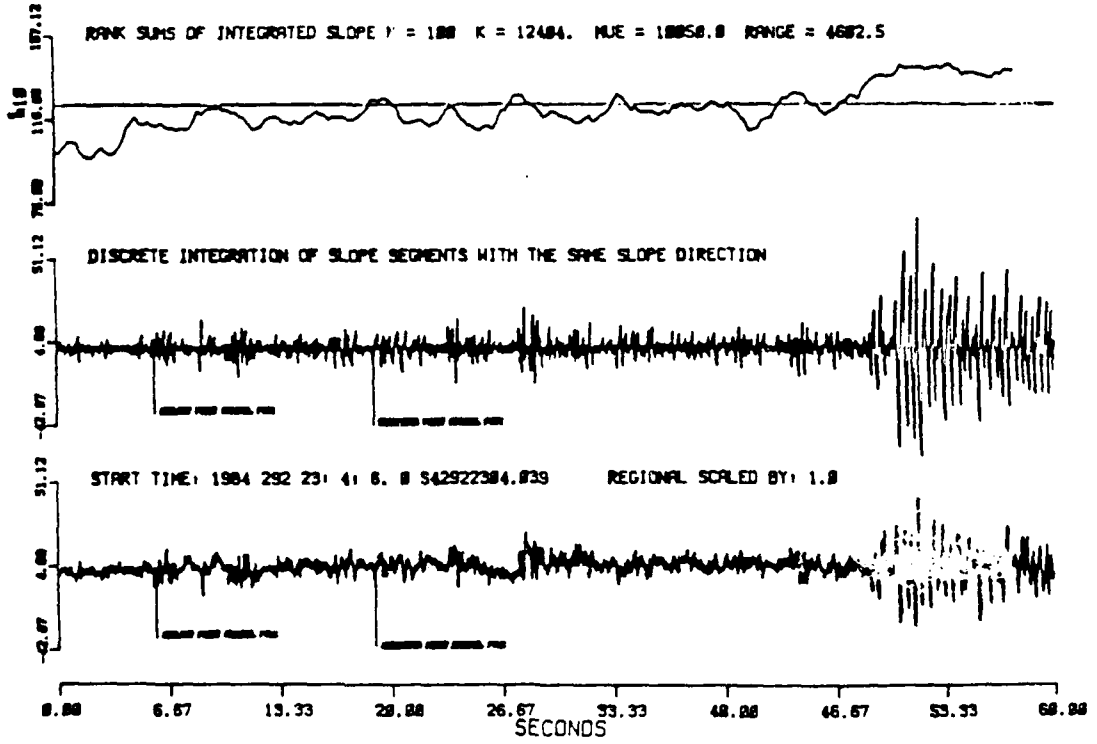
RANK SUMS OF INTEGRATED SLOPE N = 100 K = 12484. MUE = 10050.0 RANGE = 4682.5
DISCRETE INTEGRATION OF SLOPE SEGMENTS WITH THE SAME SLOPE DIRECTION
START TIME: 1984 292 23: 4: 6. 0 S42922384.839 REGIONAL SCALED BY: 1.0
0.00
6.67
13.33
20.00
26.67
33.33
40.00
46.67
53.33
60.00
SECONDS

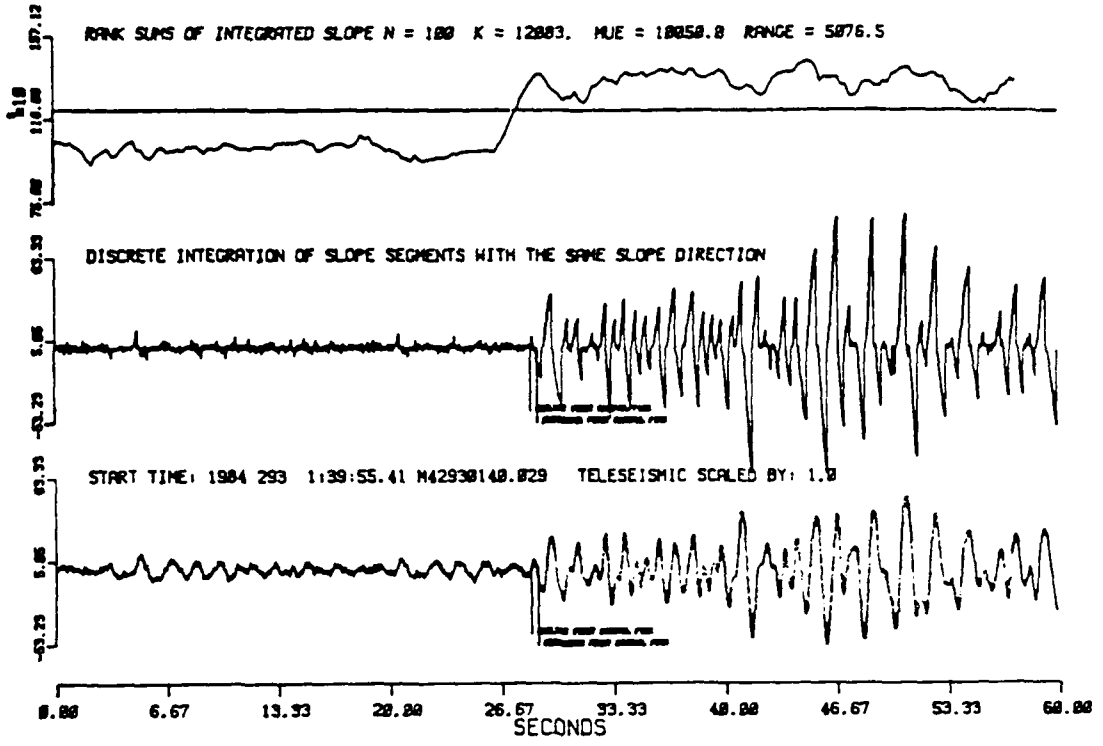

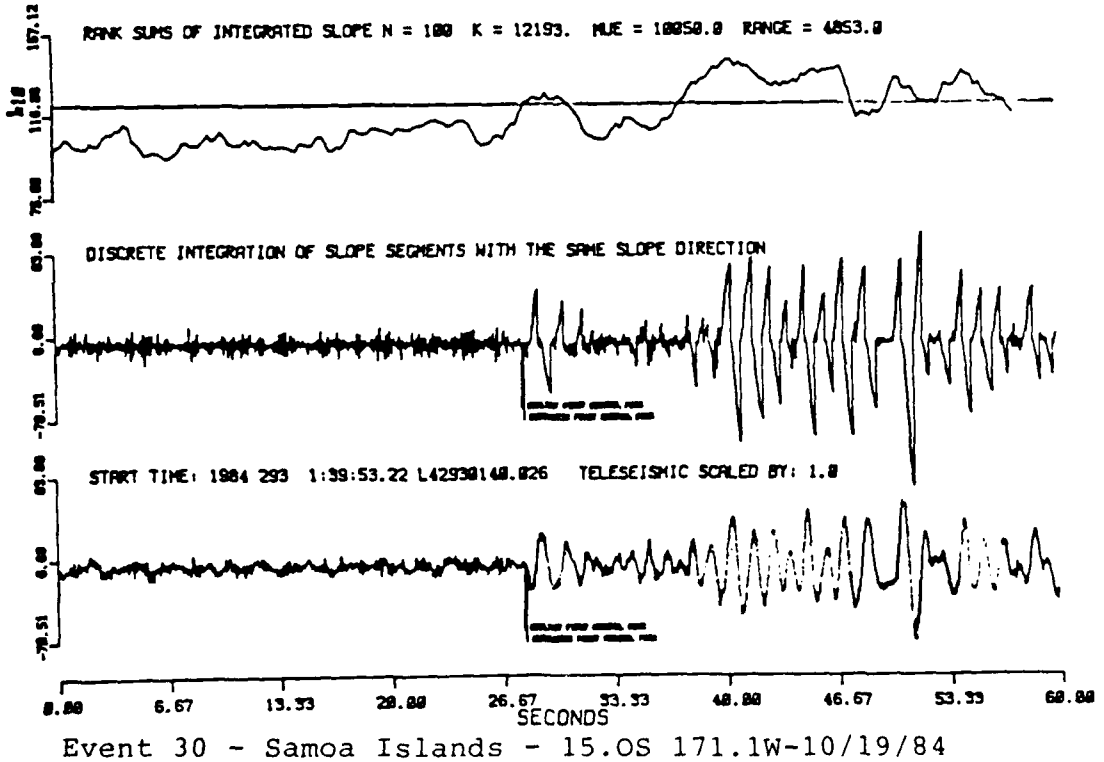

Event 30 - Samoa Islands - 15.0S 171.1W-10/19/84
Origin Time: 01:28:16.3 Depth: 1 km +75 M_b: 4.9
Residual Error: -0.6

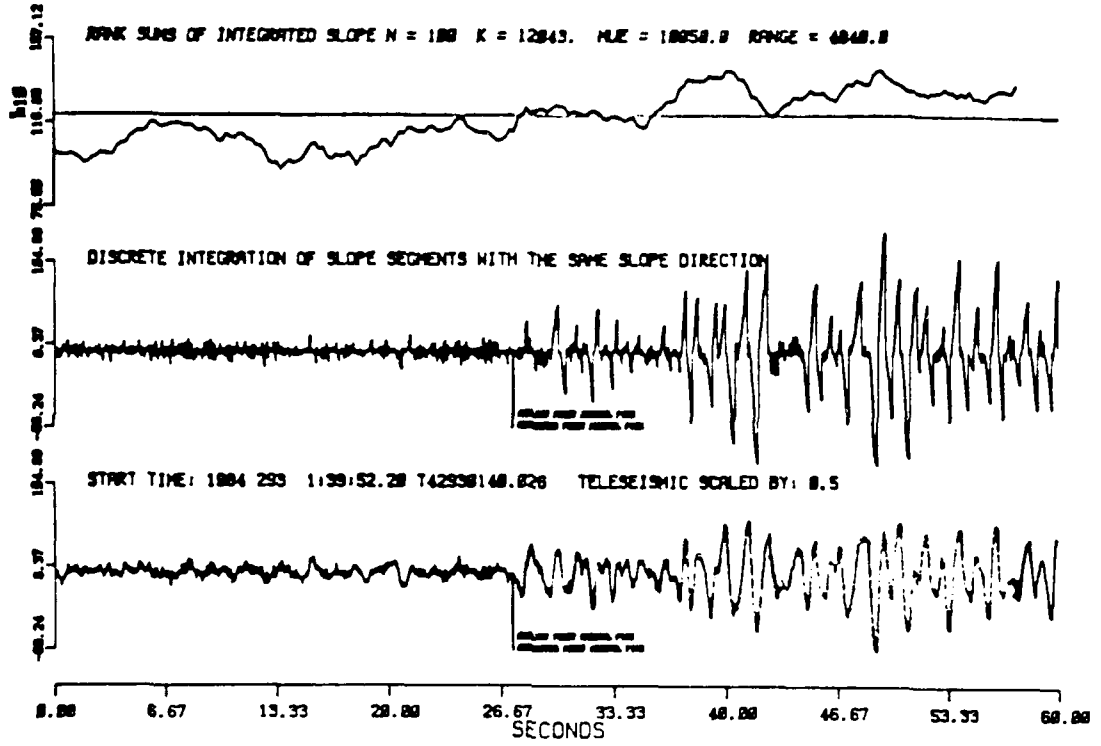
RANK SUMS OF INTEGRATED SLOPE N = 100 K = 12843. MUE = 10050.0 RANGE = 4040.0
DISCRETE INTEGRATION OF SLOPE SEGMENTS WITH THE SAME SLOPE DIRECTION
START TIME: 1984 293 1:39:52.20 T42930140.026 TELESEISMIC SCALED BY: 0.5
0.00
6.67
13.33
20.00
26.67
33.33
40.00
46.67
53.33
60.00
SECONDS

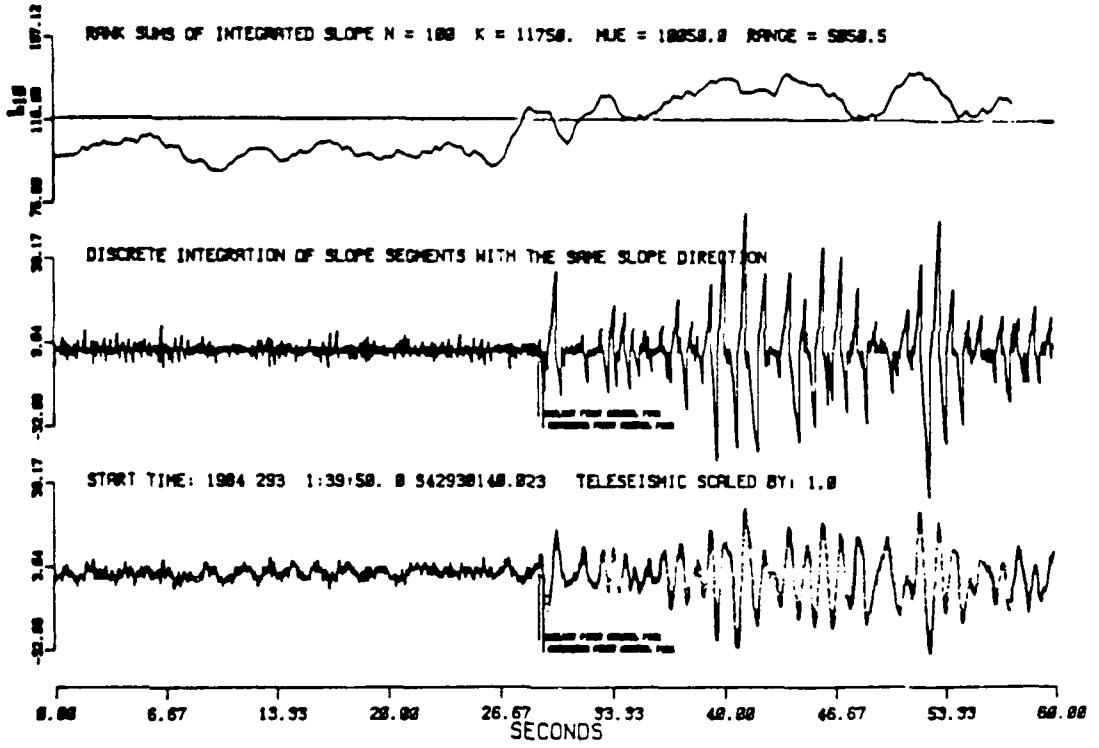
RANK SUMS OF INTEGRATED SLOPE N = 100 K = 11750. MUE = 10050.0 RANGE = 5850.5
DISCRETE INTEGRATION OF SLOPE SEGMENTS WITH THE SAME SLOPE DIRECTION
START TIME: 1984 293 1:39:50. 0 S42930140.023 TELESEISMIC SCALED BY: 1.0
0.00
6.67
13.33
20.00
26.67
33.33
40.00
46.67
53.33
60.00
SECONDS

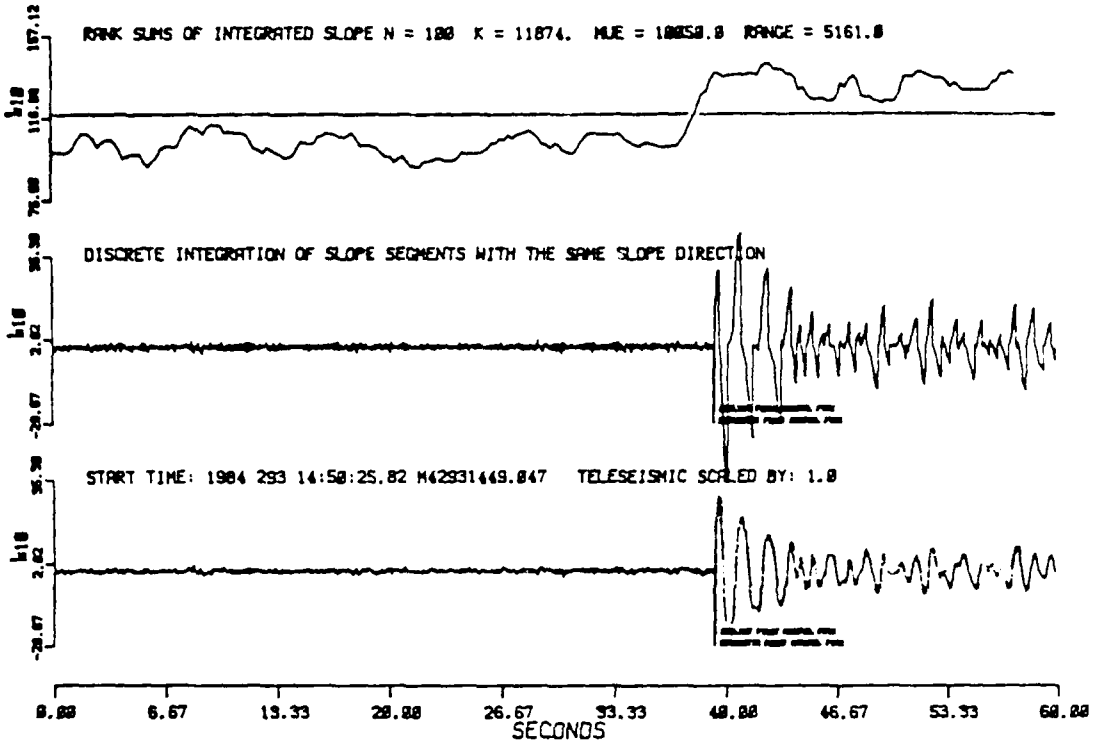

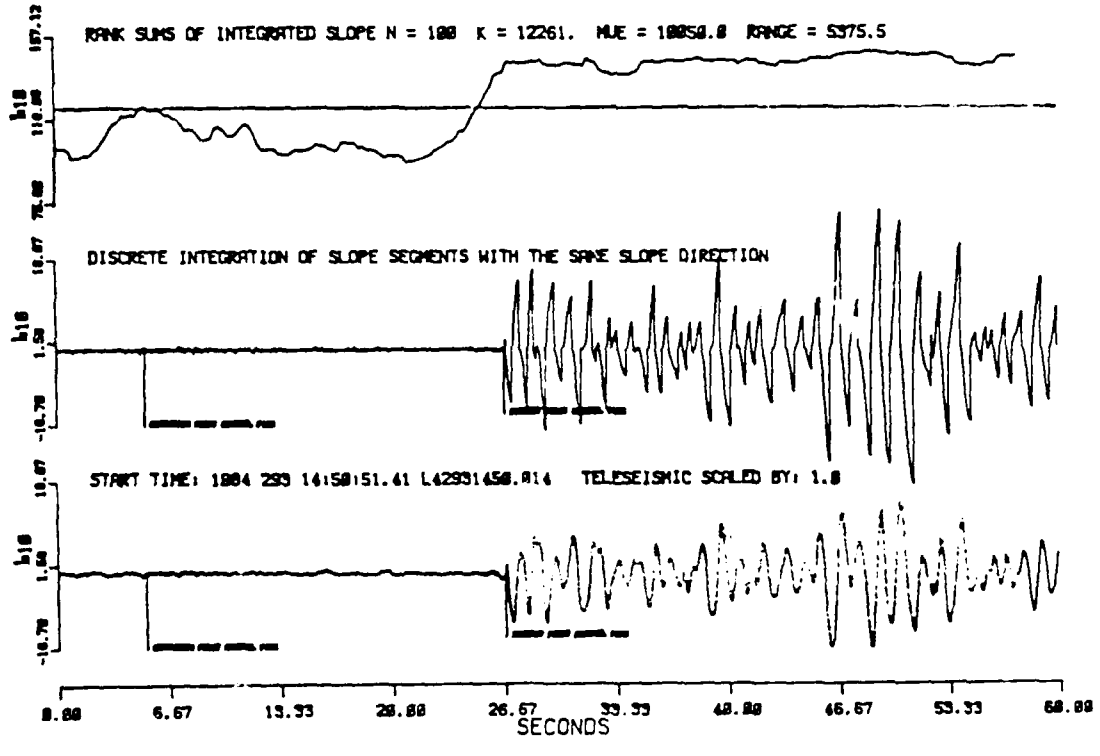

Event 31 - Tonga Islands - 15.7S 173.8W 10/19/84
Origin Time: 14:37:35.6 Depth: 1 km +2 M_b:5.7
Residual Error:1.9

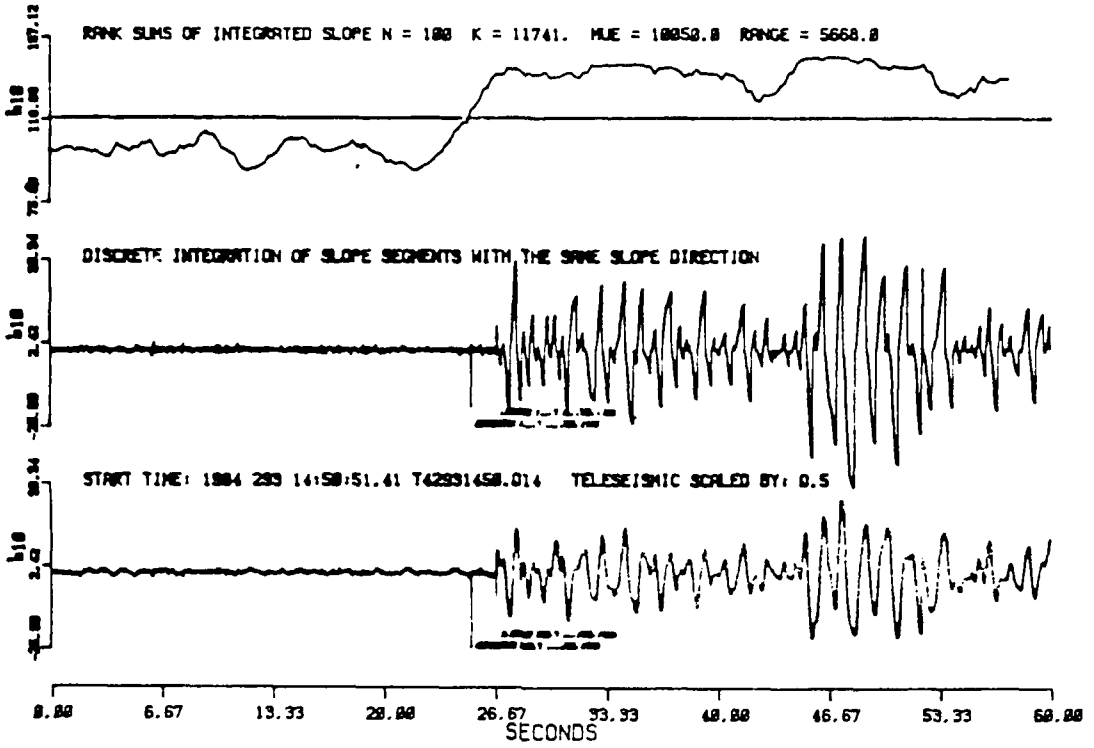
RANK SUMS OF INTEGRATED SLOPE N = 180 K = 11741. MUE = 16050.0 RANGE = 5668.0
DISCRETE INTEGRATION OF SLOPE SEGMENTS WITH THE SAME SLOPE DIRECTION
START TIME: 1984 293 14:50:51.41 T42931450.014 TELESEISMIC SCALED BY: 0.5
0.00
6.67
13.33
20.00
26.67
33.33
40.00
46.67
53.33
60.00
SECONDS

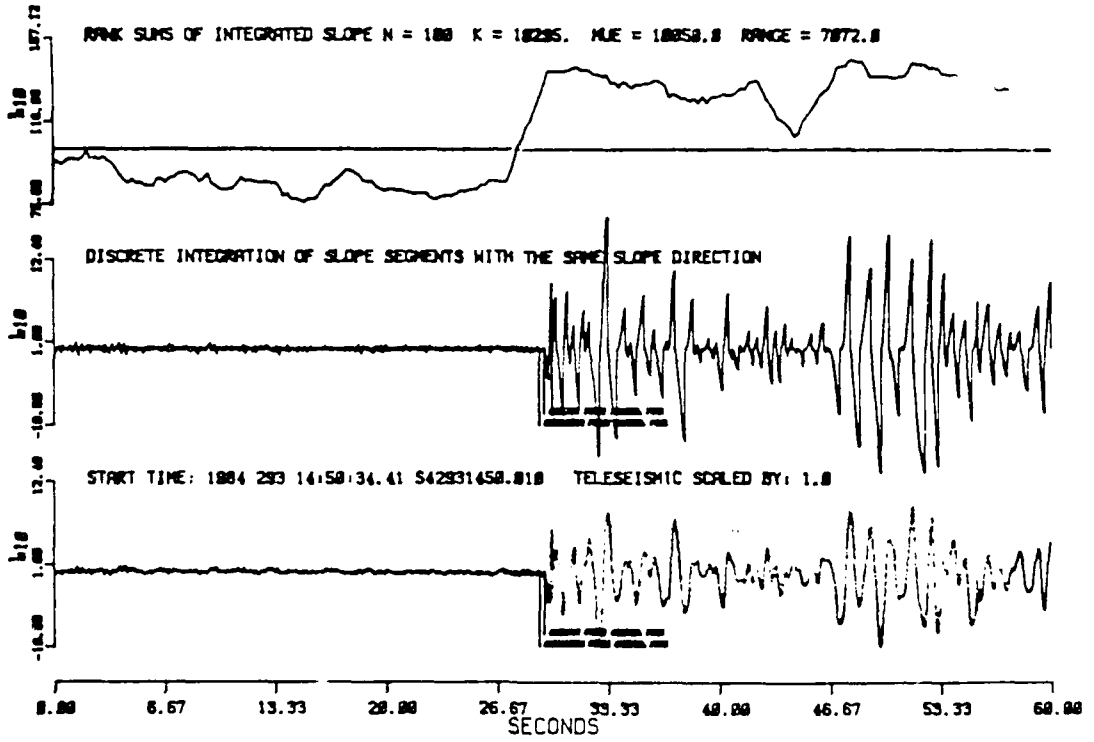
RANK SUMS OF INTEGRATED SLOPE N = 180 K = 10235. MUE = 16050.0 RANGE = 7872.0
DISCRETE INTEGRATION OF SLOPE SEGMENTS WITH THE SAME SLOPE DIRECTION
START TIME: 1984 293 14:50:34.41 S42931450.010 TELESEISMIC SCALED BY: 1.0
0.00
6.67
13.33
20.00
26.67
33.33
40.00
46.67
53.33
60.00
SECONDS

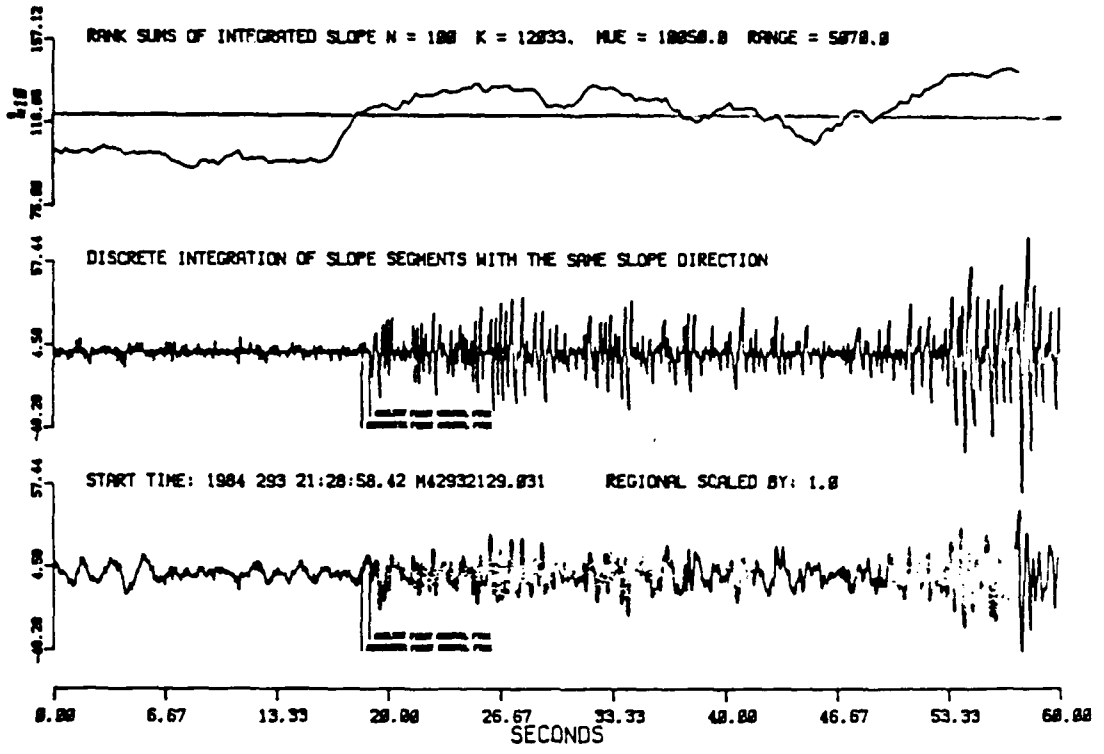

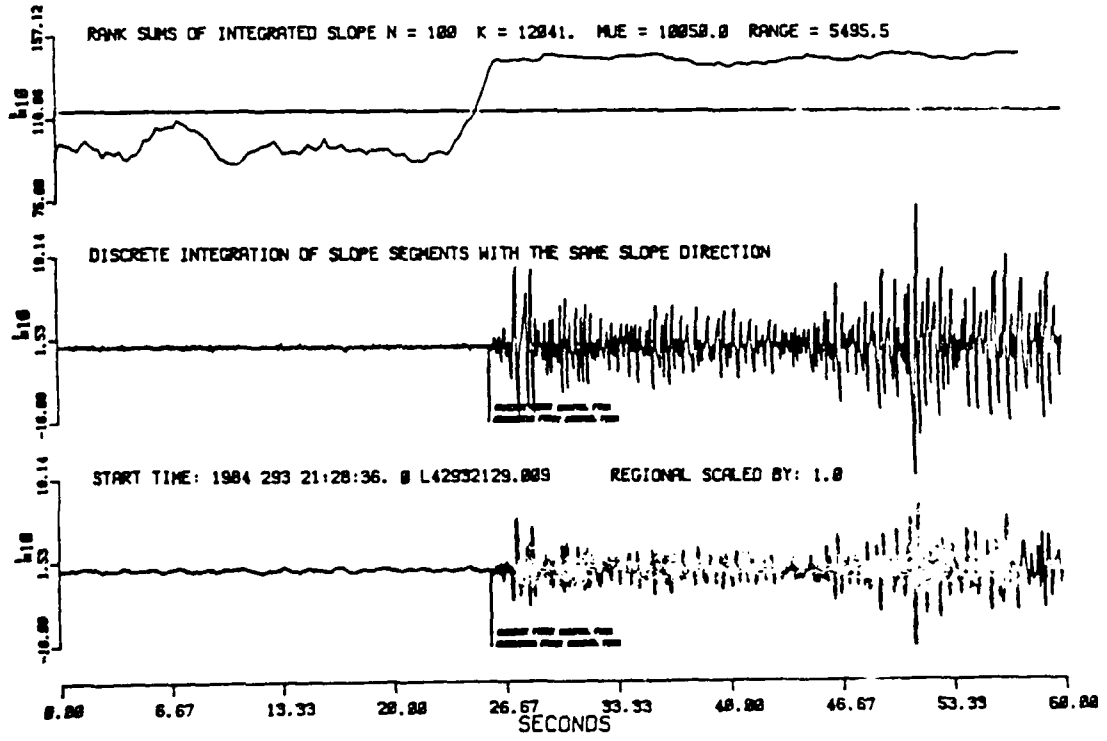

Event 32 - Regional (Pn - Lg) = 21 Seconds

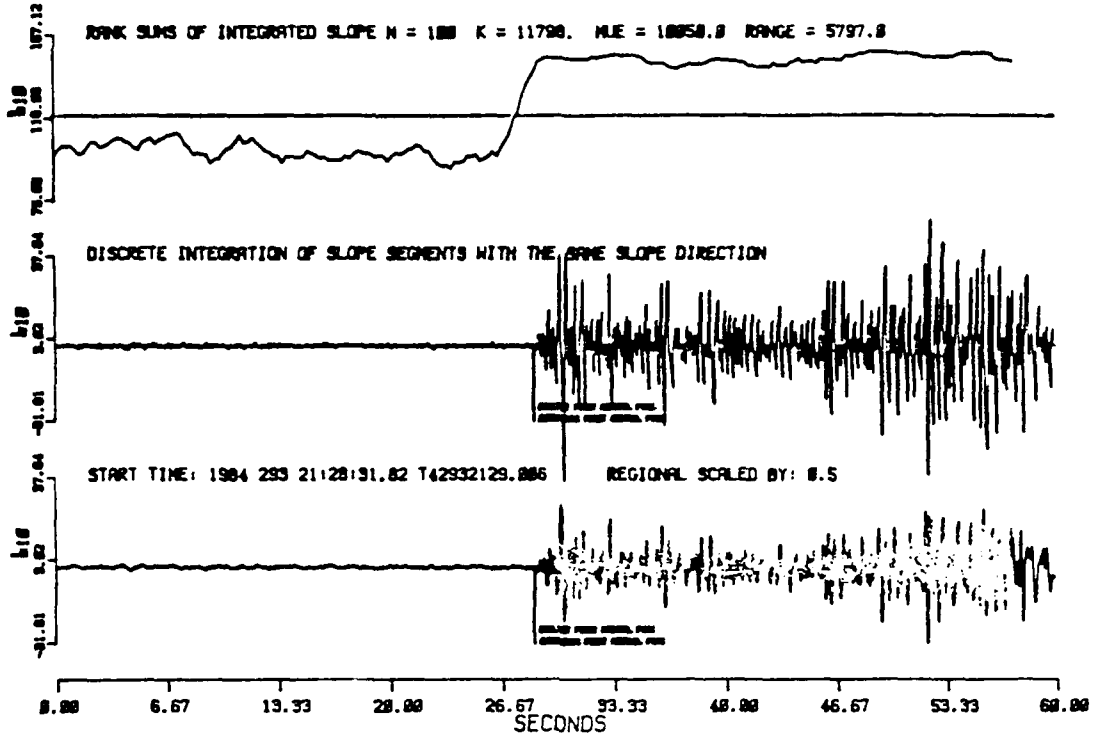
RANK SUMS OF INTEGRATED SLOPE N = 188 K = 11798. MUE = 18858.8 RANGE = 5797.8
DISCRETE INTEGRATION OF SLOPE SEGMENTS WITH THE SAME SLOPE DIRECTION
START TIME: 1984 293 21:28:31.82 T42932129.886 REGIONAL SCALED BY: 8.5
0.00
6.67
13.33
20.00
26.67
33.33
40.00
46.67
53.33
60.00
SECONDS

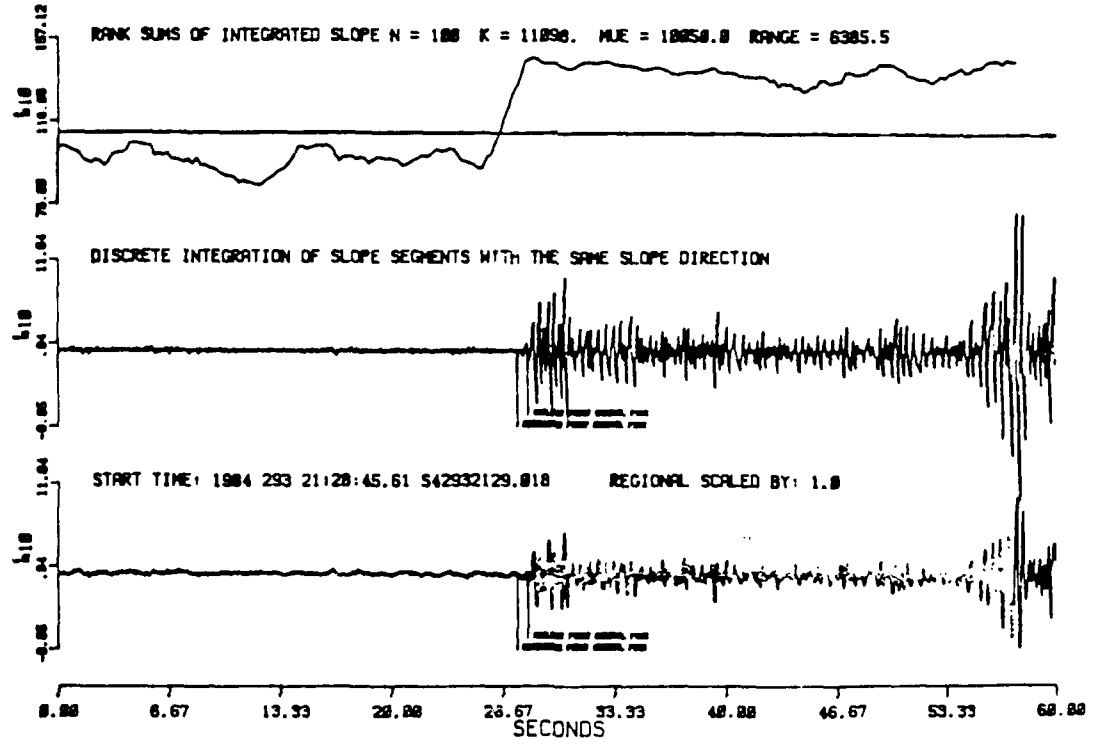
RANK SUMS OF INTEGRATED SLOPE N = 188 K = 11898. MUE = 18858.8 RANGE = 6385.5
DISCRETE INTEGRATION OF SLOPE SEGMENTS WITh THE SAME SLOPE DIRECTION
START TIME: 1984 293 21:28:45.61 S42932129.818 REGIONAL SCALED BY: 1.0
0.00
6.67
13.33
20.00
26.67
33.33
40.00
46.67
53.33
60.00
SECONDS

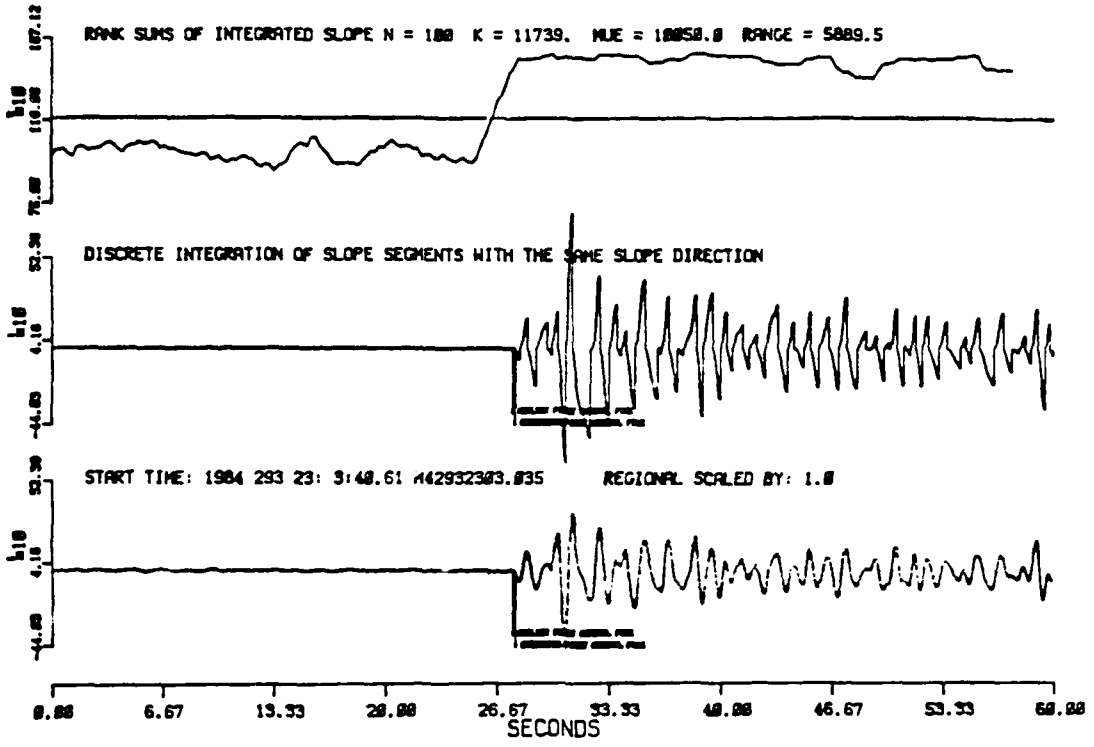

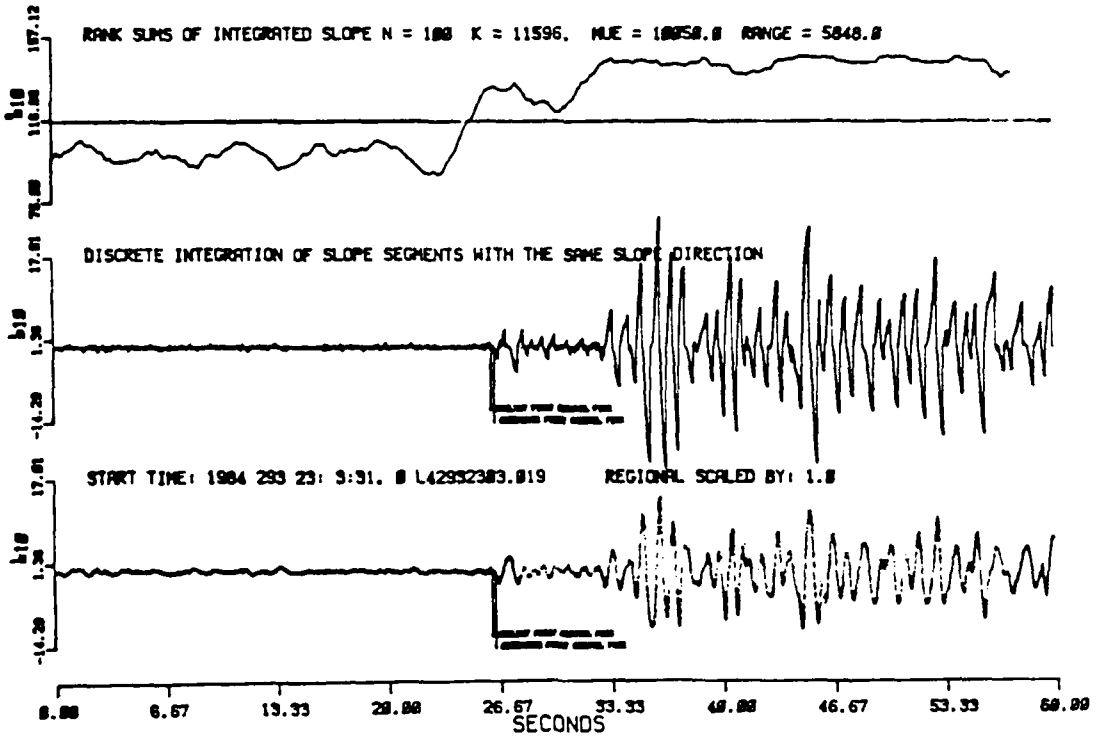

Event 33 - Near Coast of Guerro, Mexiso 16.6N 98.5W 10/19/84
Origin Time: 22:59:57.8 Depth: 25 km + 3 M_b: 4.9
Residual Error: 3.0

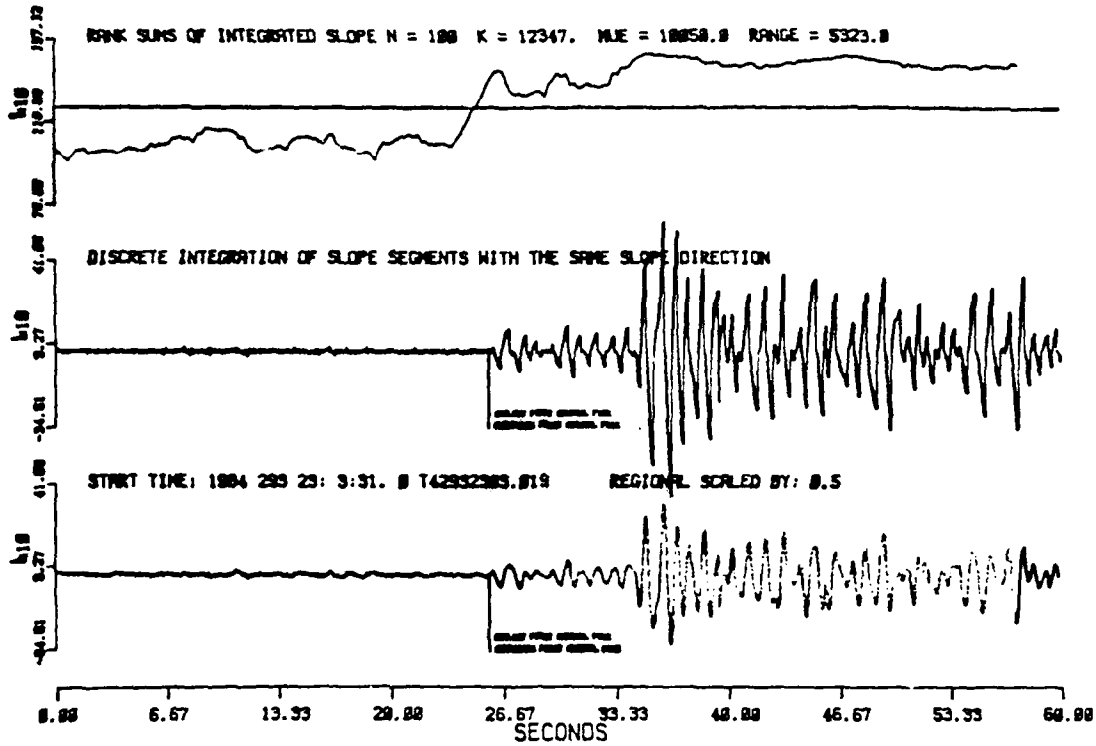
RANK SUMS OF INTEGRATED SLOPE N = 180 K = 12347. MUE = 10050.0 RANGE = 5323.0
DISCRETE INTEGRATION OF SLOPE SEGMENTS WITH THE SAME SLOPE DIRECTION
START TIME: 1984 293 23: 3:31. 0 T42932383.819 REGIONAL SCALED BY: 0.5
0.00
6.67
13.33
20.00
26.67
33.33
40.00
46.67
53.33
60.00
SECONDS

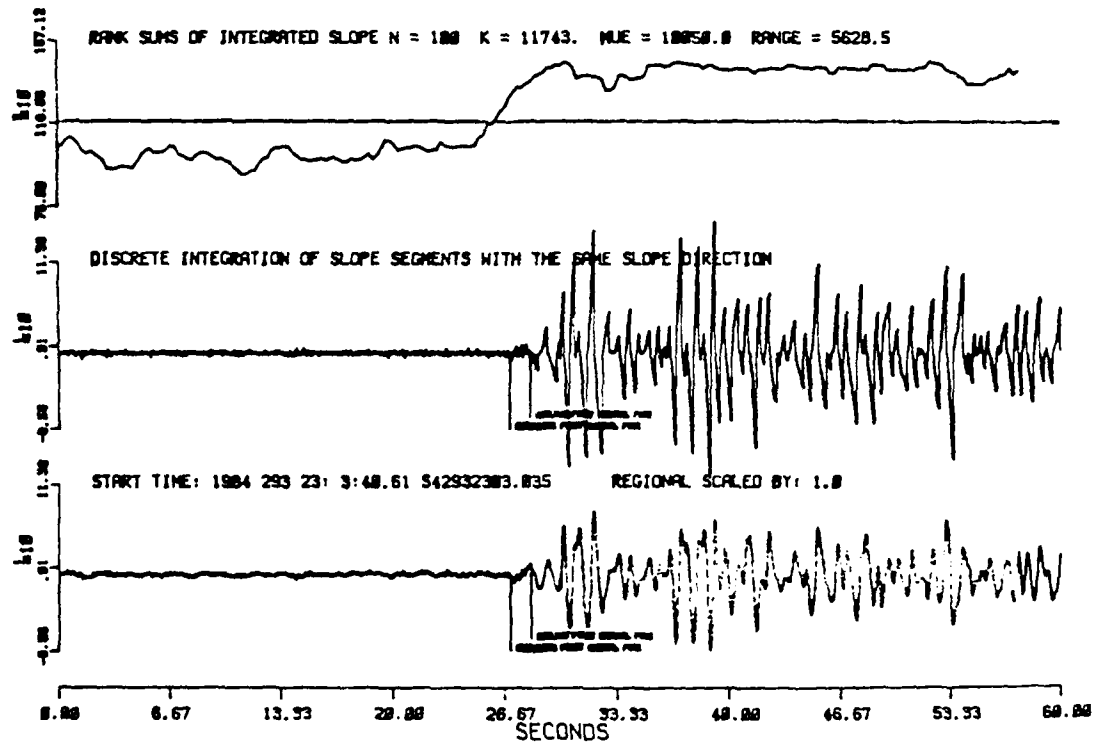
RANK SUMS OF INTEGRATED SLOPE N = 180 K = 11743. MUE = 10050.0 RANGE = 5628.5
DISCRETE INTEGRATION OF SLOPE SEGMENTS WITH THE SAME SLOPE DIRECTION
START TIME: 1984 293 23: 3:40.61 S42932383.835 REGIONAL SCALED BY: 1.0
0.00
6.67
13.33
20.00
26.67
33.33
40.00
46.67
53.33
60.00
SECONDS

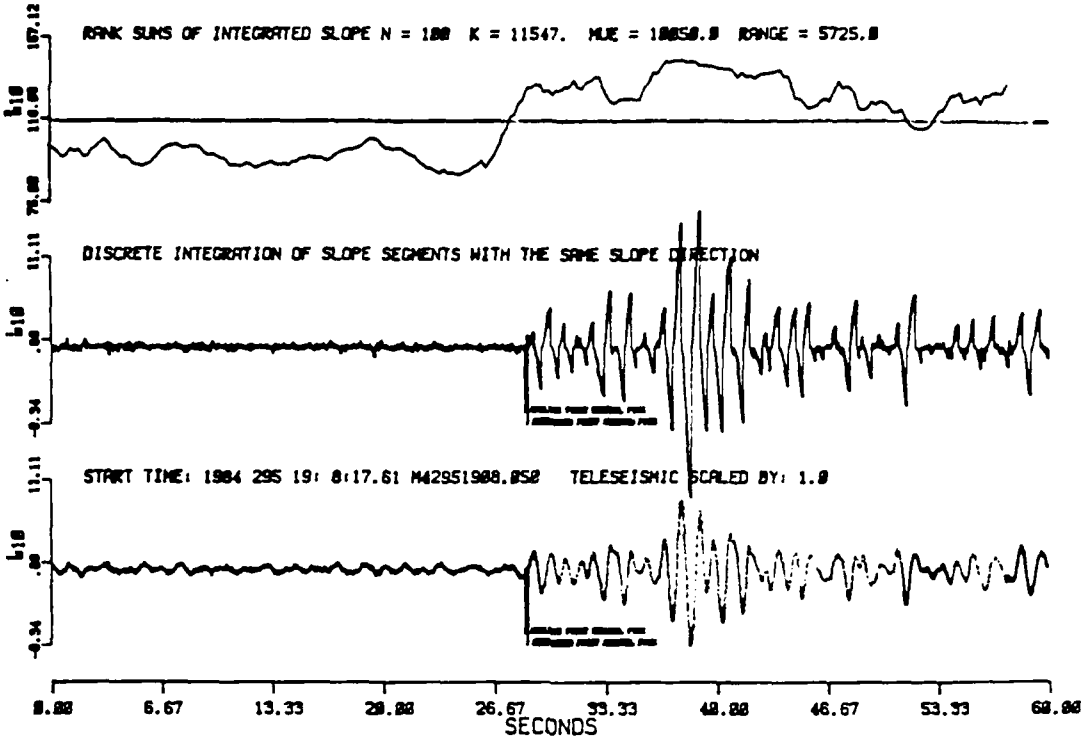

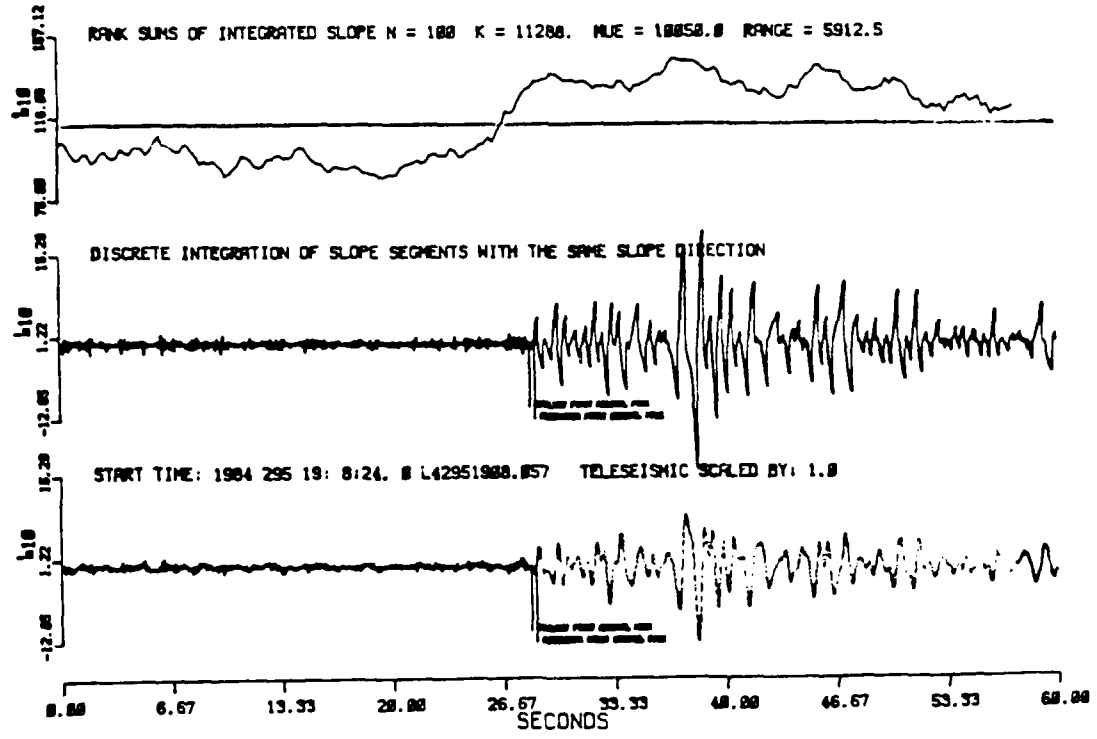

Event 34 - East of Severnoya Zemlya 82.0N 114.2E 10/21/84
Origin Time: 18:57:55.6 Depth: 14km + 4 M_b:4.3
Residual Error: -0.3

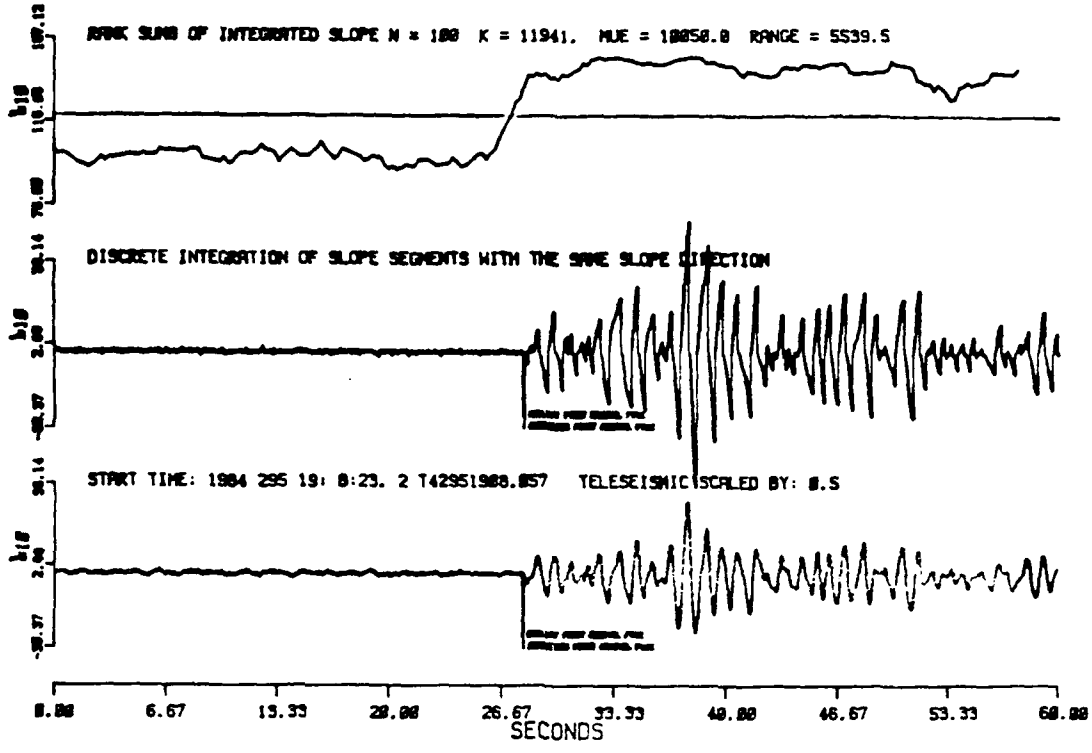
RANK SUMS OF INTEGRATED SLOPE N = 100 K = 11941. MUE = 10050.0 RANGE = 5539.5
DISCRETE INTEGRATION OF SLOPE SEGMENTS WITH THE SAME SLOPE DIRECTION
START TIME: 1984 295 19: 8:23. 2 T42951980.057 TELESEISMIC SCALED BY: 0.5
0.00
6.67
13.33
20.00
26.67
33.33
40.00
46.67
53.33
60.00
SECONDS

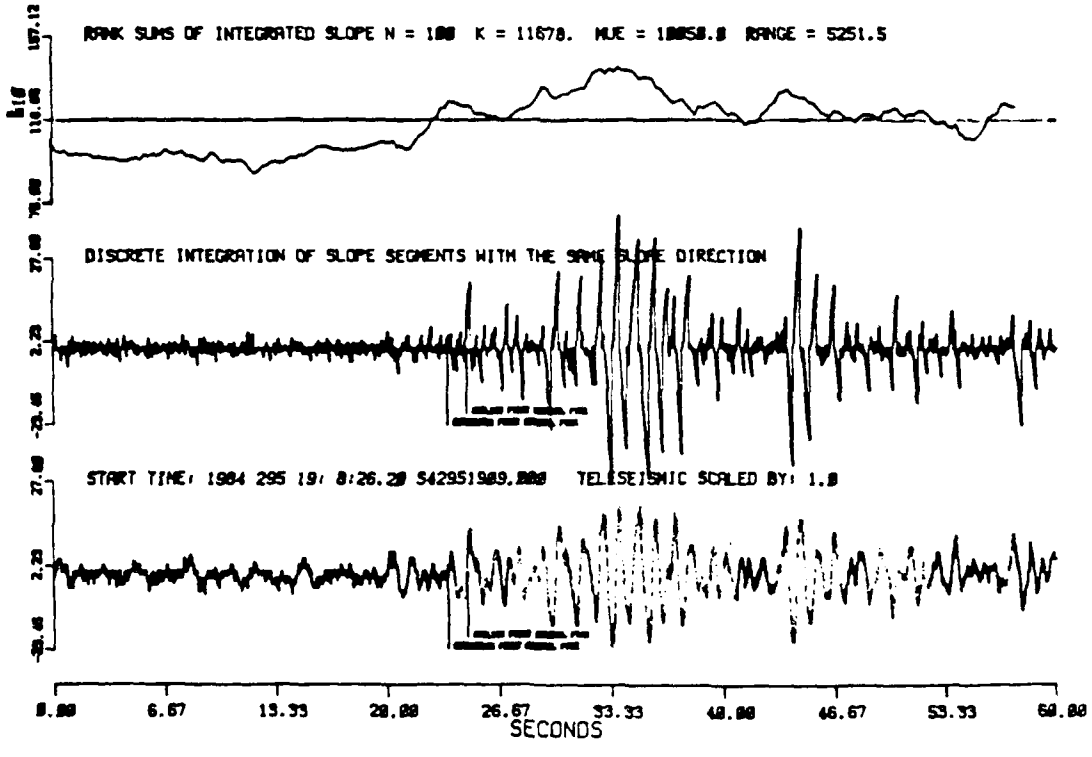
RANK SUMS OF INTEGRATED SLOPE N = 100 K = 11670. MUE = 10050.0 RANGE = 5251.5
DISCRETE INTEGRATION OF SLOPE SEGMENTS WITH THE SAME SLOPE DIRECTION
START TIME: 1984 295 19: 8:26.20 S42951989.000 TELESEISMIC SCALED BY: 1.0
0.00
6.67
13.33
20.00
26.67
33.33
40.00
46.67
53.33
60.00
SECONDS

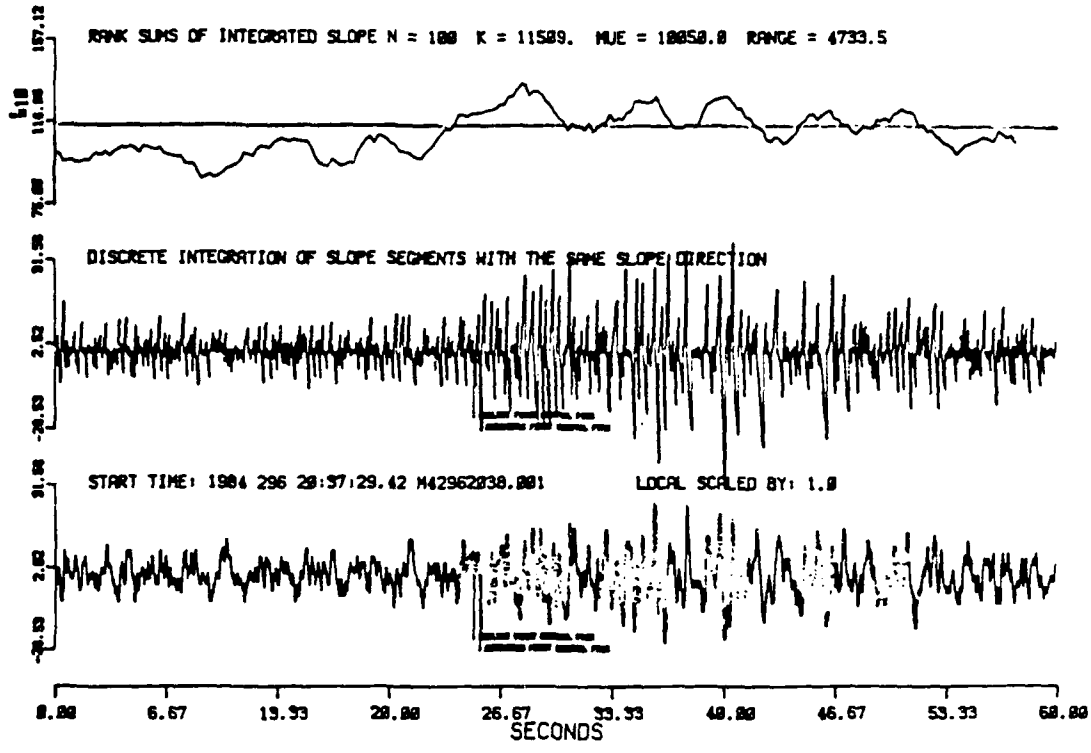

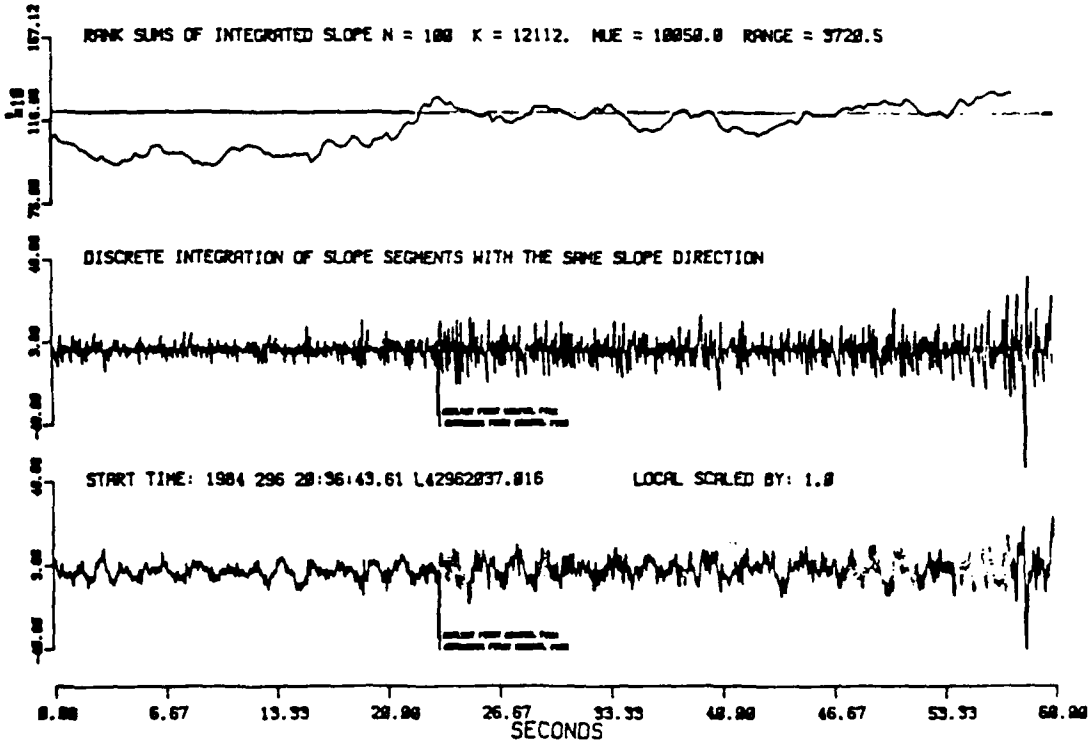

Event 35 Local P Arrival

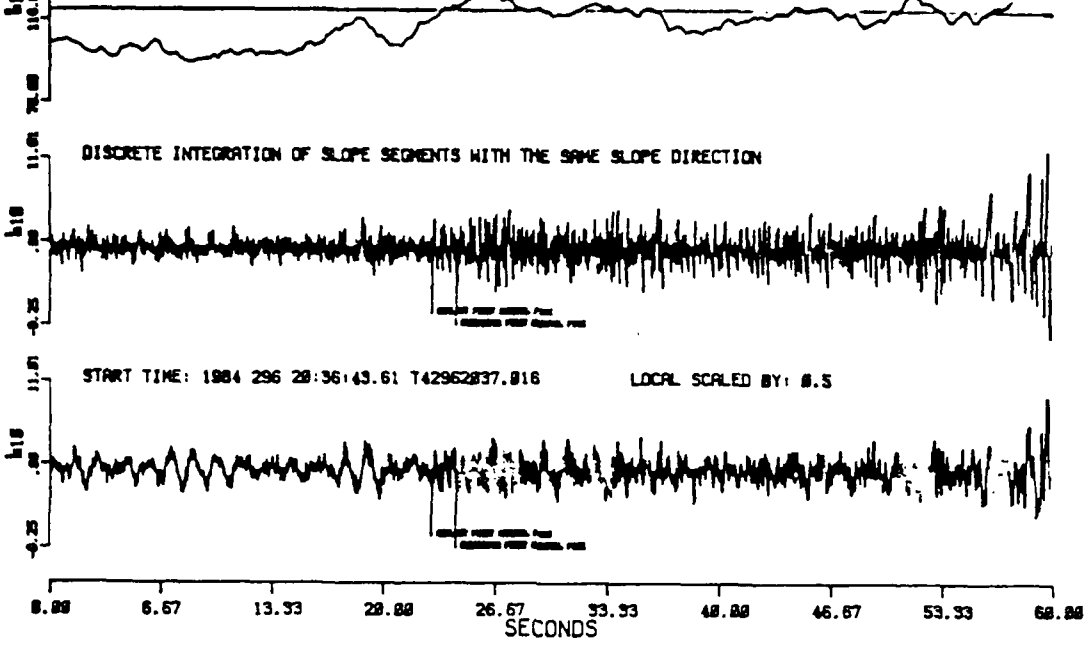
RANK SUMS OF INTEGRATED SLOPE N = 100 K = 12155. MUE = 10050.0 RANGE = 3055.0
DISCRETE INTEGRATION OF SLOPE SEGMENTS WITH THE SAME SLOPE DIRECTION
START TIME: 1984 296 20:36:43.61 T42962037.016 LOCAL SCALED BY: 0.5
0.00
6.67
13.33
20.00
26.67
33.33
40.00
46.67
53.33
60.00
SECONDS

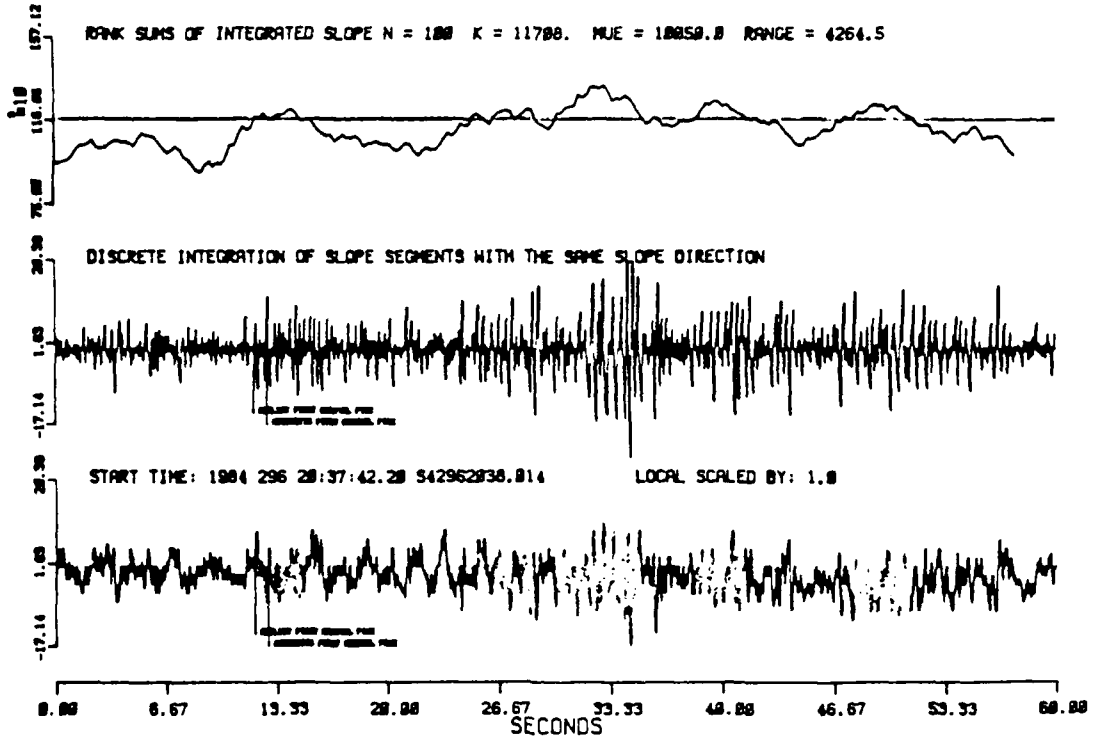
RANK SUMS OF INTEGRATED SLOPE N = 100 K = 11700. MUE = 10050.0 RANGE = 4264.5
DISCRETE INTEGRATION OF SLOPE SEGMENTS WITH THE SAME SLOPE DIRECTION
START TIME: 1984 296 20:37:42.20 S42962038.014 LOCAL SCALED BY: 1.0
0.00
6.67
13.33
20.00
26.67
33.33
40.00
46.67
53.33
60.00
SECONDS

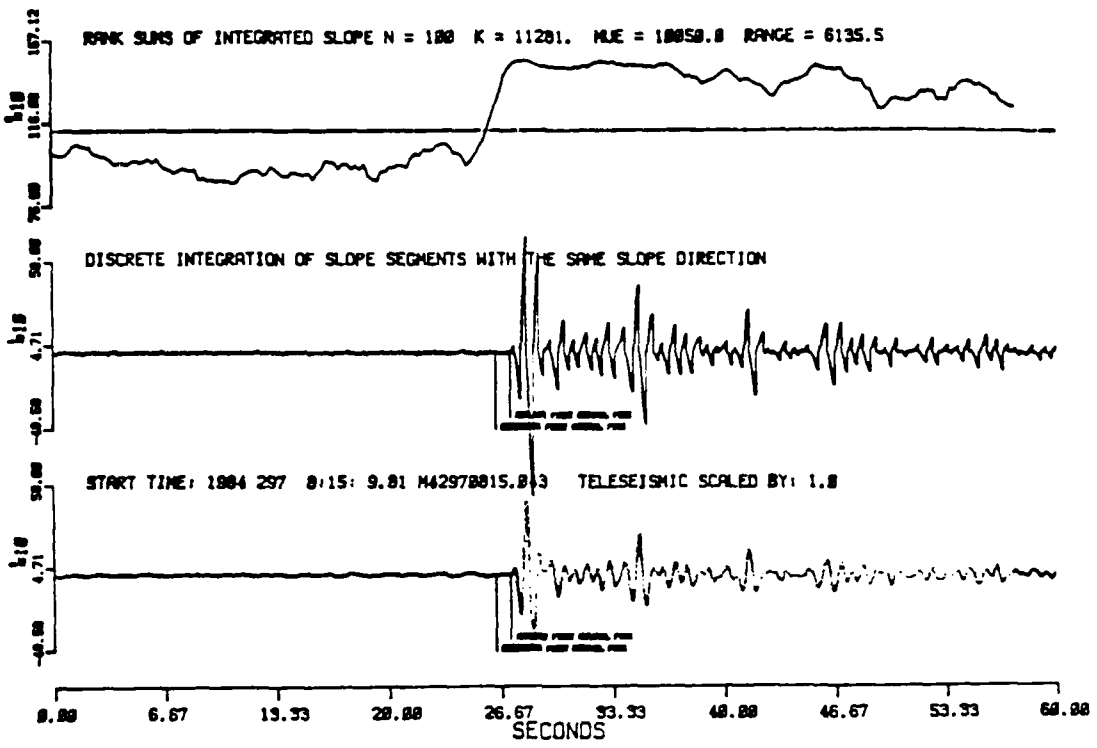

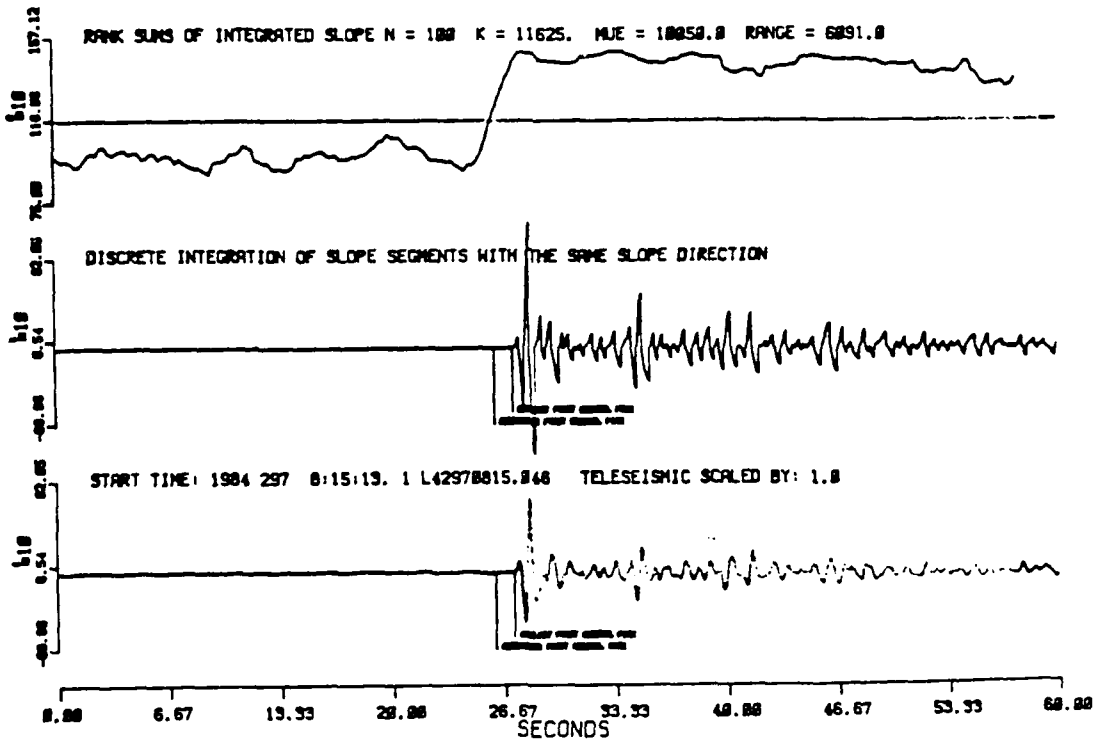

Event 36 Komandorsky Islands Region 55.7N 165.0E 10/23/84
Origin Time: 08:04:46.1 Depth: 20 km +3 M_b:4.8
Residual Error: 0.3

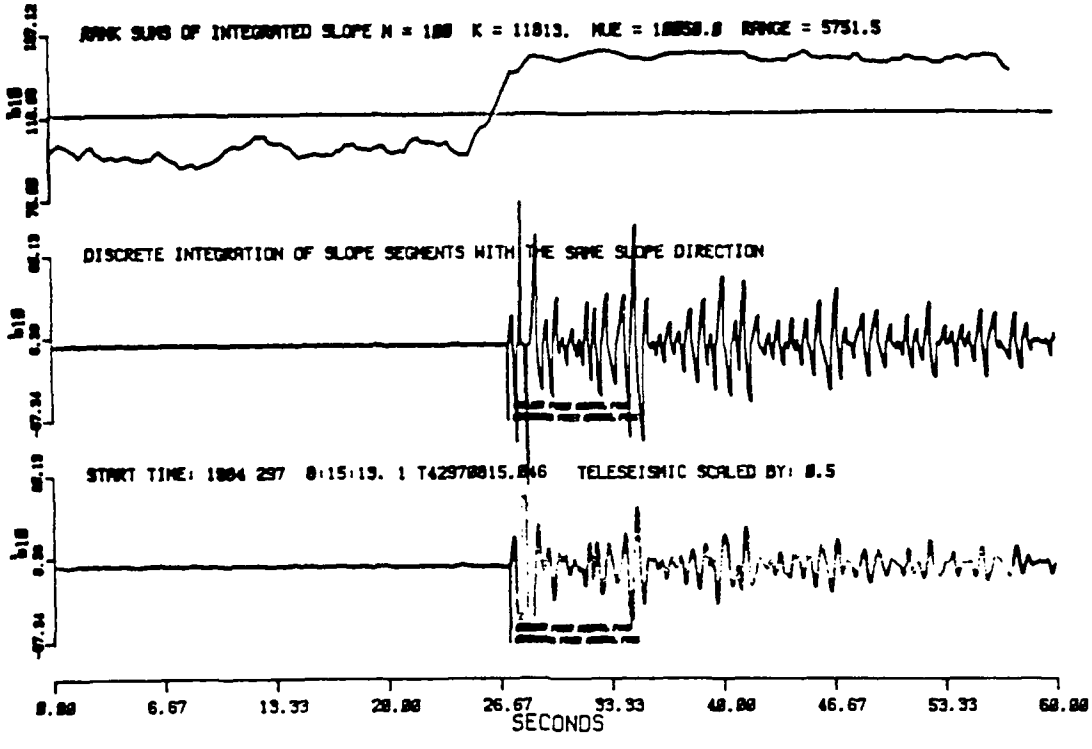
RANK SUMS OF INTEGRATED SLOPE N = 100 K = 11813. MUE = 10050.0 RANGE = 5751.5
DISCRETE INTEGRATION OF SLOPE SEGMENTS WITH THE SAME SLOPE DIRECTION
START TIME: 1984 297 8:15:19. 1 T42978815.046 TELESEISMIC SCALED BY: 0.5
0.00
6.67
13.33
20.00
26.67
33.33
40.00
46.67
53.33
60.00
SECONDS

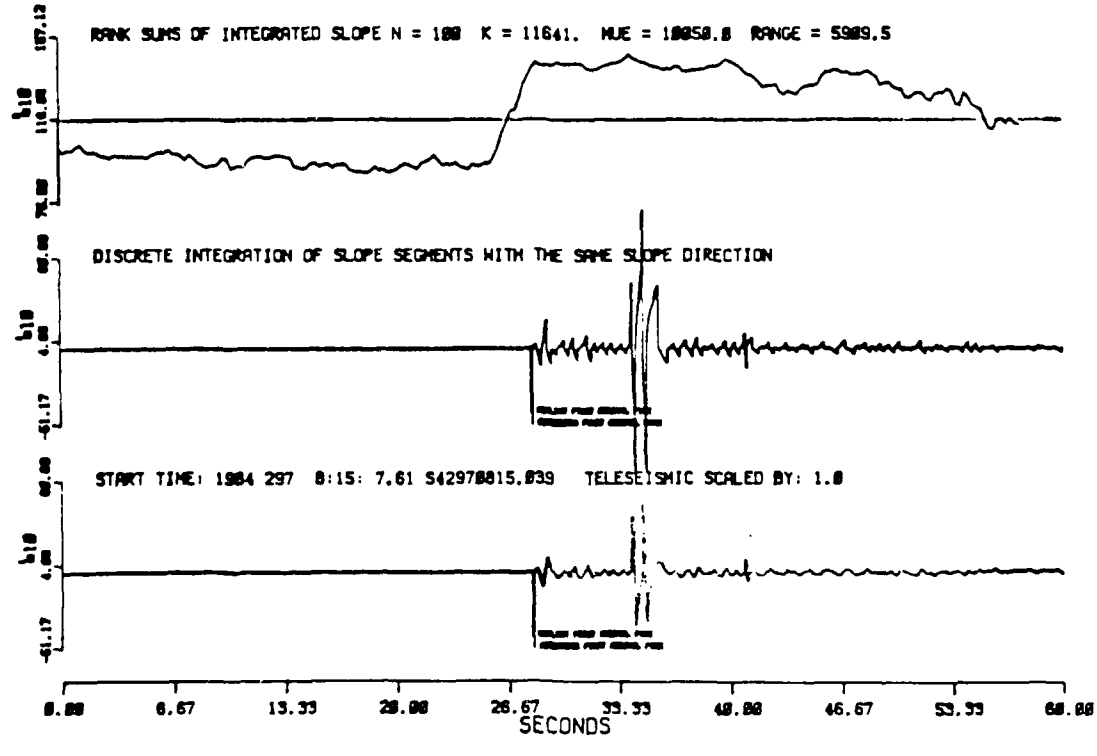
RANK SUMS OF INTEGRATED SLOPE N = 100 K = 11641. MUE = 10050.0 RANGE = 5989.5
DISCRETE INTEGRATION OF SLOPE SEGMENTS WITH THE SAME SLOPE DIRECTION
START TIME: 1984 297 8:15: 7.61 S42978815.039 TELESEISMIC SCALED BY: 1.0
0.00
6.67
13.33
20.00
26.67
33.33
40.00
46.67
53.33
60.00
SECONDS

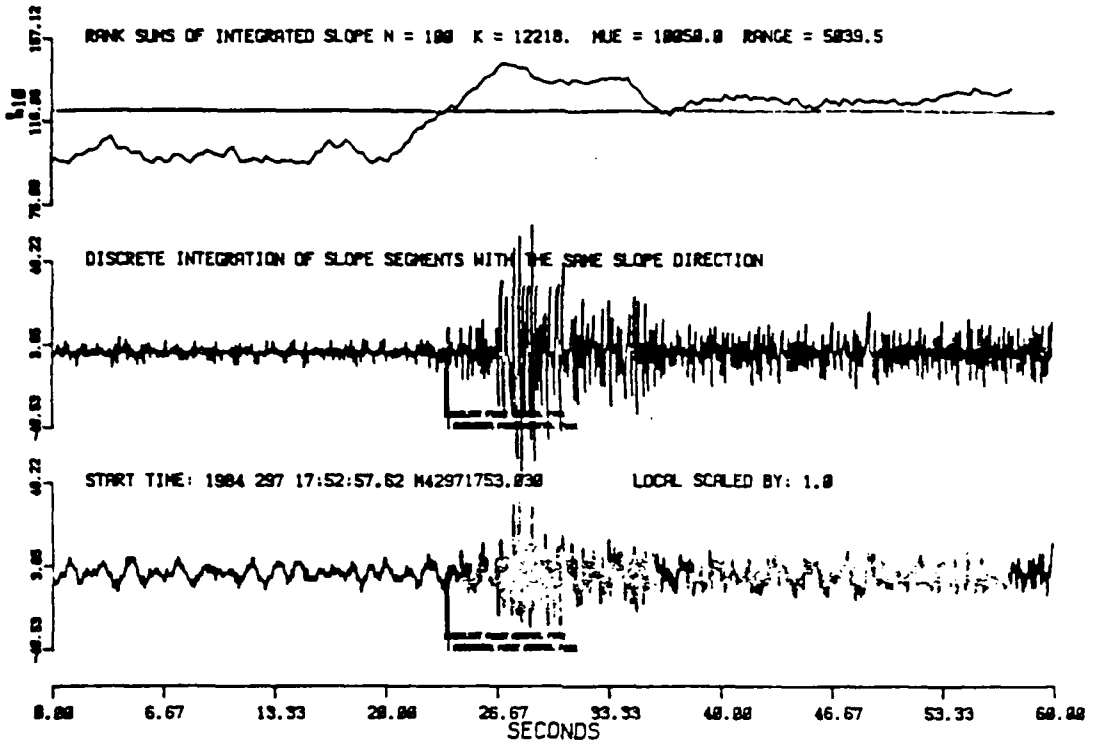

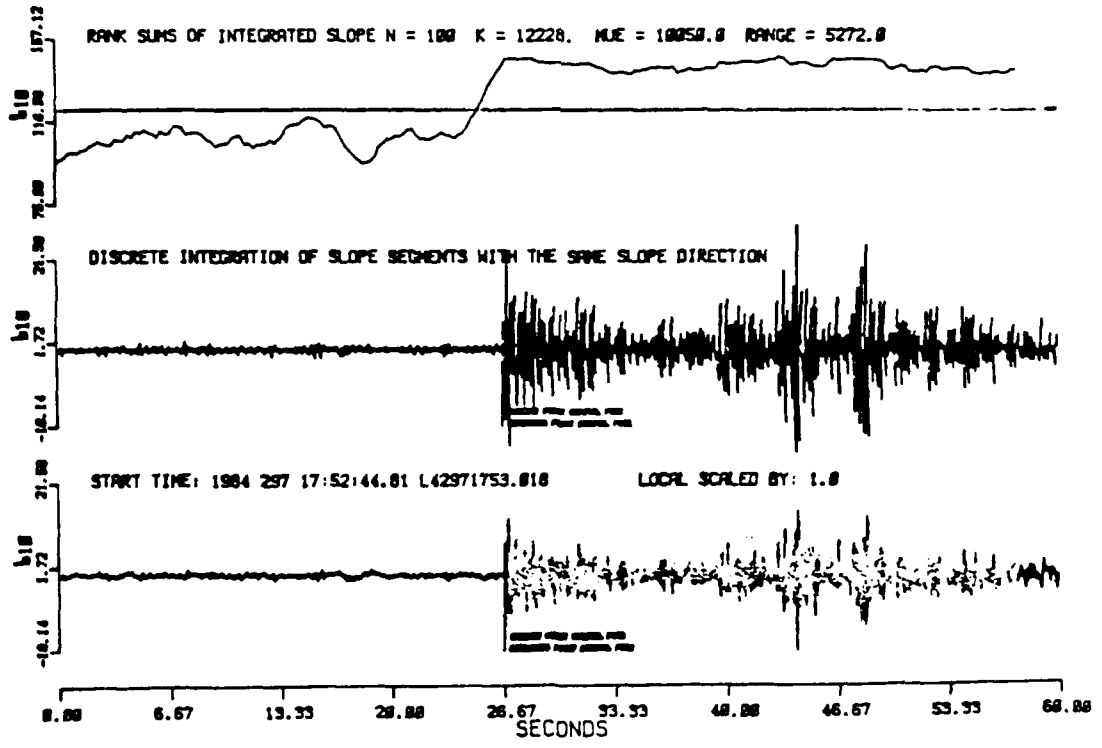

Event 37 Local P Arrival

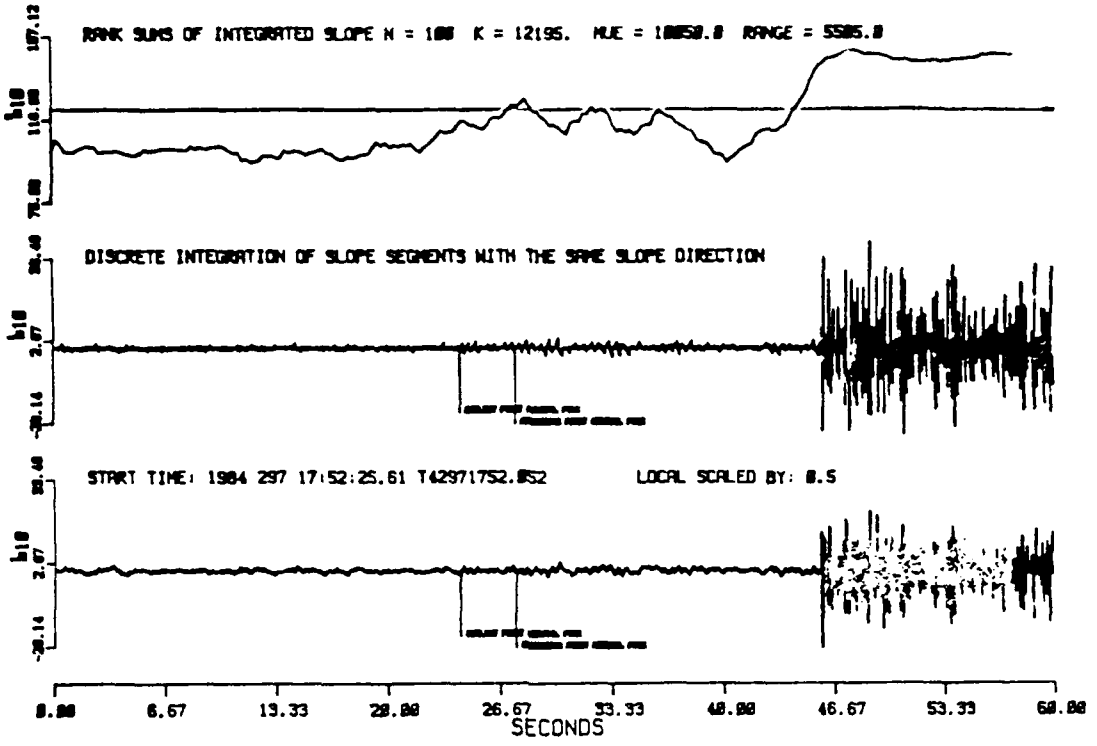
RANK SUMS OF INTEGRATED SLOPE N = 100 K = 12195. MUE = 10050.0 RANGE = 5585.0
DISCRETE INTEGRATION OF SLOPE SEGMENTS WITH THE SAME SLOPE DIRECTION
START TIME: 1984 297 17:52:25.61 T429717S2.852 LOCAL SCALED BY: 0.5
0.00
6.67
13.33
20.00
26.67
33.33
40.00
46.67
53.33
60.00
SECONDS

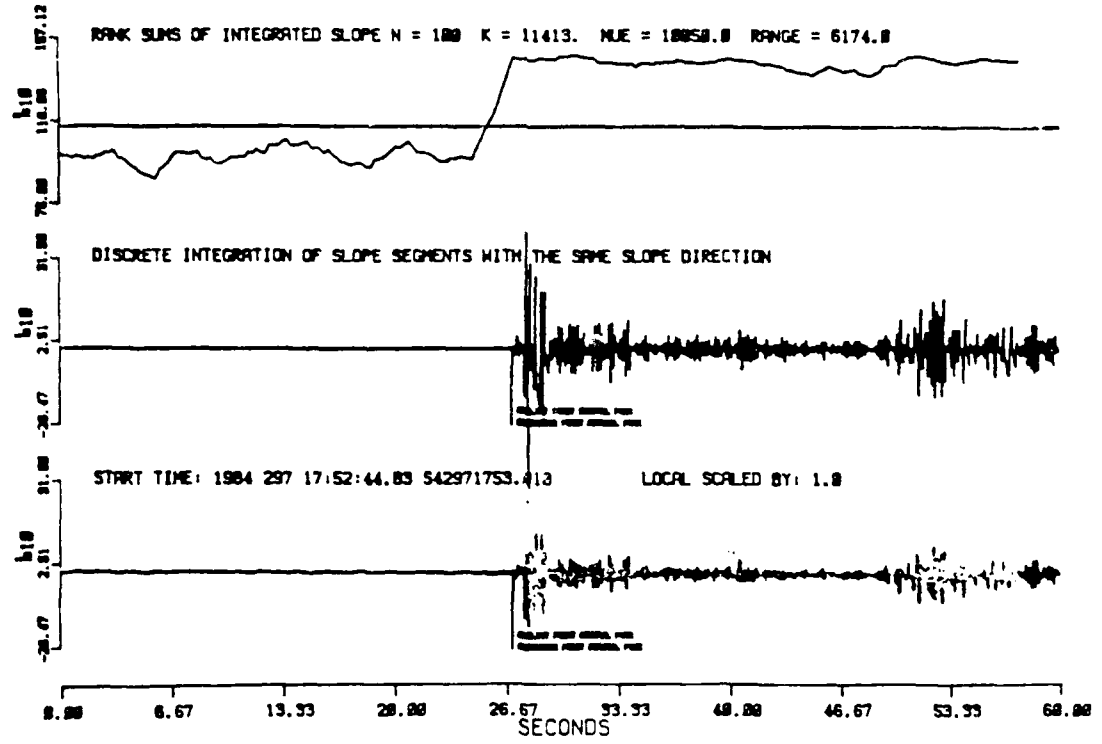
RANK SUMS OF INTEGRATED SLOPE N = 100 K = 11413. MUE = 10050.0 RANGE = 6174.0
DISCRETE INTEGRATION OF SLOPE SEGMENTS WITH THE SAME SLOPE DIRECTION
START TIME: 1984 297 17:52:44.83 S429717S3.413 LOCAL SCALED BY: 1.0
0.00
6.67
13.33
20.00
26.67
33.33
40.00
46.67
53.33
60.00
SECONDS

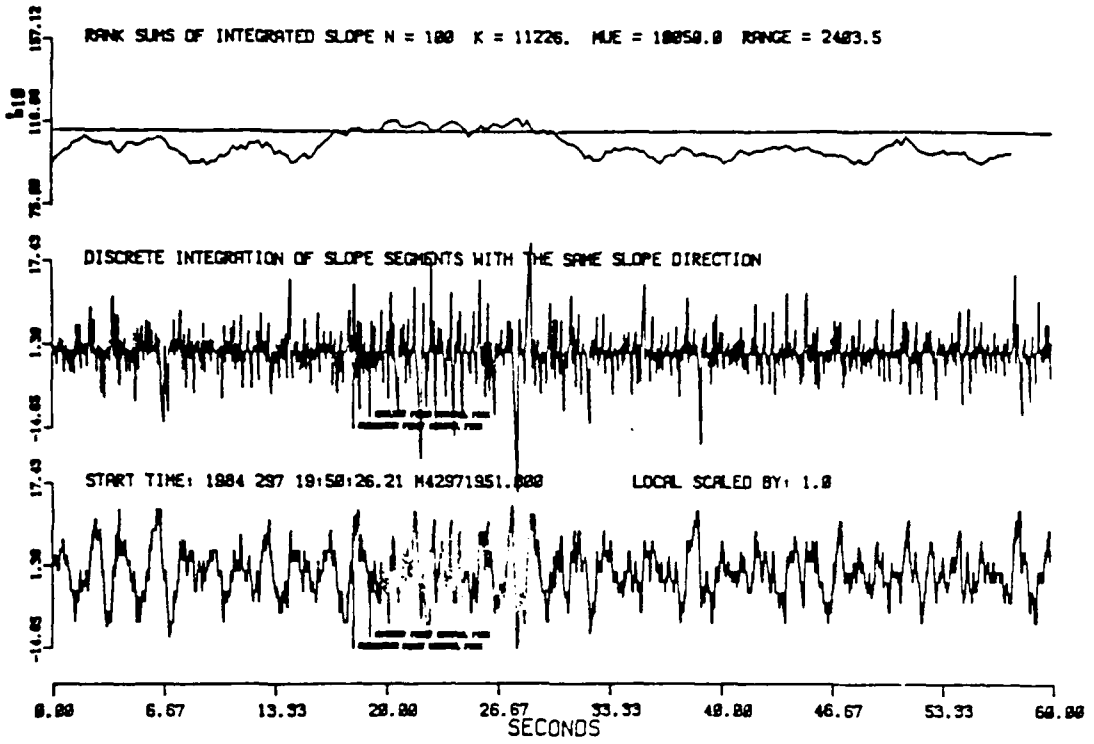

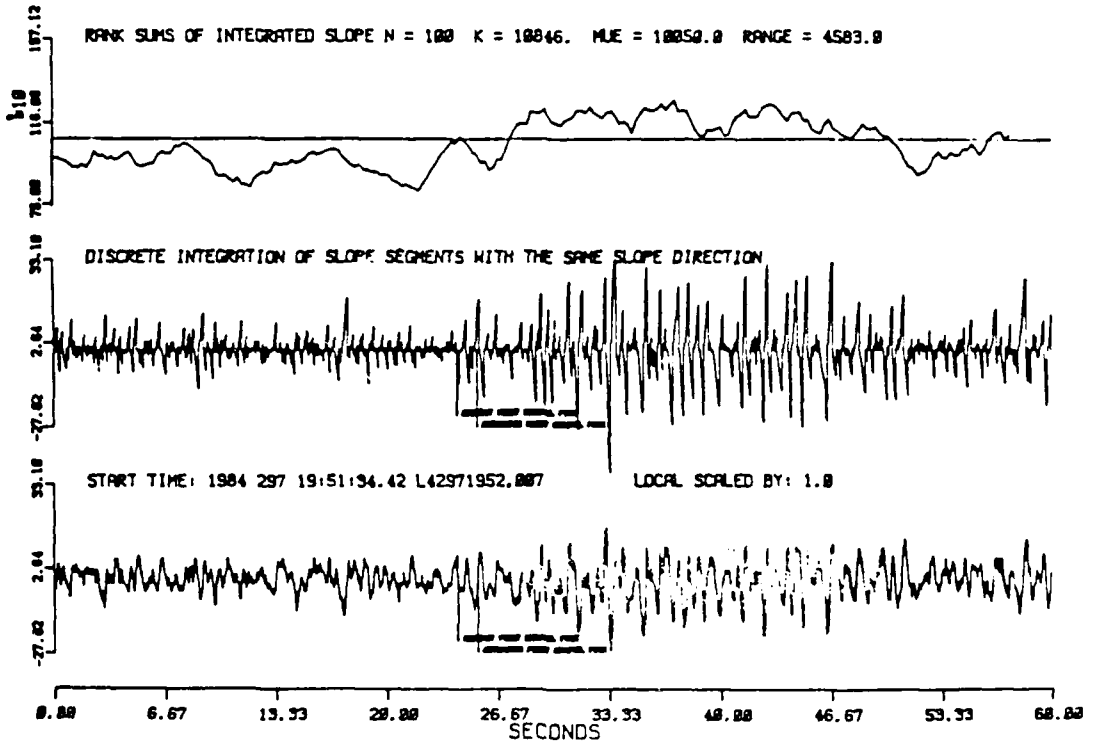

Event 38 Local P Arrival

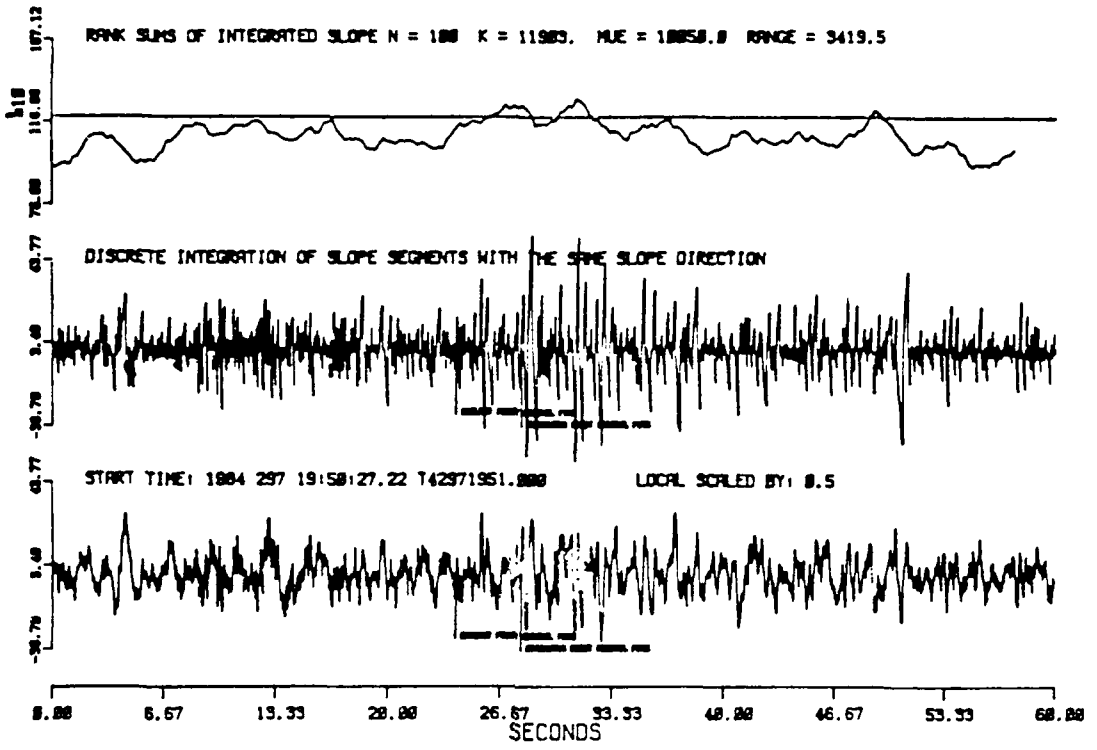
RANK SUMS OF INTEGRATED SLOPE N = 100 K = 11903. MUE = 10050.0 RANGE = 3419.5
DISCRETE INTEGRATION OF SLOPE SEGMENTS WITH THE SAME SLOPE DIRECTION
START TIME: 1984 297 19:50:27.22 T42971951.000 LOCAL SCALED BY: 0.5
0.00
6.67
13.33
20.00
26.67
33.33
40.00
46.67
53.33
60.00
SECONDS

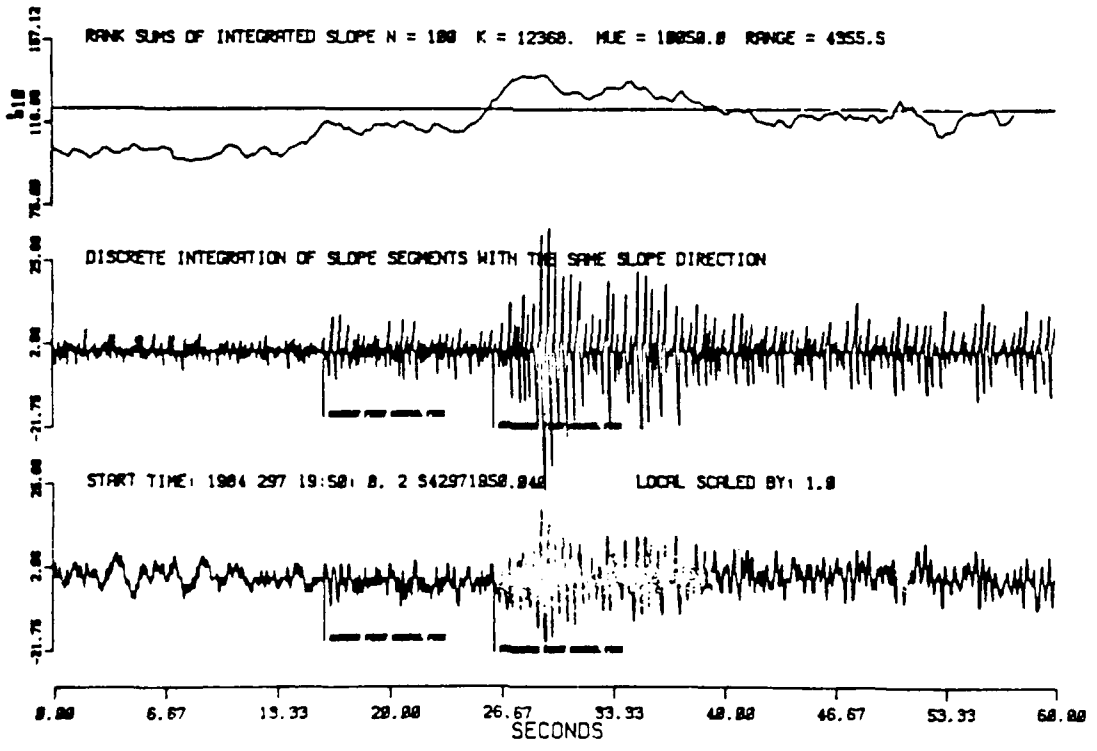
RANK SUMS OF INTEGRATED SLOPE N = 100 K = 12360. MUE = 10050.0 RANGE = 4355.5
DISCRETE INTEGRATION OF SLOPE SEGMENTS WITH THE SAME SLOPE DIRECTION
START TIME: 1984 297 19:50: 0. 2 S42971850.040 LOCAL SCALED BY: 1.0
0.00
6.67
13.33
20.00
26.67
33.33
40.00
46.67
53.33
60.00
SECONDS

BIBLIOGRAPHY

-----.Digital Waveform Processing and Recognition.

Abdrabbo, N.A. and M.B. Priestley, On the prediction of non-stationary processes, J. Roy. Statist. Soc. B, Vol. 29, 570-585, 1967.

Agrawala, A., Ed., Machine recognition of patterns, IEEE Press, (reprints) 1977.

Allen, R.V., Automatic earthquake recognition ..., BSSA, Vol. 68, 1521-1532, 1978.

Allen, R., Automatic phase pickers: their present use and future prospects, BSSA, Vol. 72, no. 6B, S225-S242, 1983.

Anderson, K.R., Automatic analysis of micro-earthquake network data, Geoexploration, Vol. 16, 159-175, 1978.

Anderson, K.R., Automatic processing of local earthquake data, Ph.D. Thesis, MIT, Cambridge, 1978.

Anderson, K.R. and J.E. Gaby, Dynamic waveform matching, 3rd Int'l. Symp. Comput. Aided Seismic Analysis and Discrimination, 98-108, 1983.

Anderson, K.R., Epicentral location using arrival time order, BSSA, Vol. 71, no. 2, 541-545, 1981.

Anderson, K.R., Syntactic Analysis of Seismic Waveforms Using Augmented Transition Network Grammers, IEEE, 54-65, 1981.

Bevington, P.R., Data reduction and error analysis for the physical sciences, McGraw-Hill, Inc., 1969.

Blandford, R.R., Seismic event discrimination, BSSA, Vol. 72, no. 6B, S69-S88, 1983.

Box and Jenkins, Some Recent Advances in Forecasting and Control, Applied Statistics, 91-109, 1970?

Box and Jenkins, Time Series Analysis: forecasting and control, Holden Day 1976.

Chen, C.H., Application of pattern recognition to seismic wave interpretation, in applications of pattern recognition, K.S. Fu, Ed., CRC Press, Boca Raton, FL

Chen, C.H., Ed., Computer-aided seismic analysis and discrimination, Elsevier, Amsterdam, 1978.

Chen, C.H., Ed., Digital waveform processing and recognition, CRC Press, Inc., 104-123, 1982.

Chen, C.H., Feature extraction and computational complexity in seismological pattern recognition, Proc. 2nd Int'l. Jt. Conf. on Pattern Recognition, IEEE, Piscataway, NJ, 1974.

Chen, C.H., Pattern Analysis of acoustical and seismic events, 3rd Int'l. Symp. Comput. Aided Seismic Analysis and Discrimination, 1983.

Chen,C.H., A Review of Geophysical Signal Analysis and Recognition, IEEE, 144-147, 1981.

Chen, C.H., Seismic pattern recognition, Geoexploration, Vol. 16, 133-146, 1978.

Cobben,W., A Nonparametric Signal Detector for Trend with Dependent Input Data, Signal Processing, Vol.4, 125-137, 1982.

Cox,D.R.and A.Stuart, Some quick sign tests for trend in location and dispersion, Biometrika, Vol.42, 80-95, 1955.

Davis, L.S., A survey of edge detection techniques, Computer Graphics and Image Processing, Vol. 4, 248-270, 1975.

Documentation of earthquake algorithms, report SE-35, World Data Center A for Solid Earth Geophysics, National Geophysical Data Center, July, 1984.

Faure, C., H. Soldano, Th. VanDerPyl, Descriptive methods and processing of seismic signals, 3rd Int'l. Symp. Comput. Aided Seismic Analysis and Discrimination, 1983.

Fu, K.S., Ed., Applications of pattern recognition, CRC Press, 1982.

Fu, K.S., Error-correcting for syntactic pattern recognition, Data Structure, Computer Graphics and Pattern Recognition, Klinger et. al. Eds., Academic Press, NY, 1976.

Fu, K.S., Syntactic pattern recognition and applications, Prentice-Hall, Englewood Cliffs, NJ, 1982.

Fukunaga, K., Introduction to statistical pattern recognition, Academic Press, New York, 1972.

Fuller, W.A., Introduction to statistical time series, Wiley, 1976.

Gaby, J.E. and K.R. Anderson, Using affinity to derive the morphological structure of seismic signals, 3rd Int'l. Symp. Comput. Aided Seismic Analysis and Discrimination, 1983.

Gaby,J.E.,K.R.Anderson, Primitive Extraction for a Syntactic Pattern Recognizer of Features in Seismic Signals, ICASSP 83, Boston, IEEE, 993-996, 1983.

Gaby,J.E.,K.R.Anderson, Using Affinity to Derive the Morphological Structure of Seismic Signals, IEEE, 20-28, 1983.

Goforth, T. and E. Herrin, An automatic seismic signal detection algorithm based on the Walsh transform, BSSA, Vol. 71, 1351-1360, 1981.

Golden, P., Draft summary report GSETT experiment, 15 Oct 1984 - 14 Dec 1984, station LTX, Southern Methodist University, February 11, 1985.

Goncz, J.H., Present status and dynamic planning for automatic association programs, Seismic Data Analysis Center, SDAC-TR-80-2, Teledyne Geotech, Alexandria, VA, 1980.

Harrison,J.P., Short term sales forecasting development and methods for seasonal estimation, Applied Statistics, 1964.

Hatherly,P.J., A computer method for determining seismic first arrival times, Geophysics, 1431-1436, 1982.

Heuts,P.M.J., Asymptotic Robustness of Prediction Intervals of ARIMA Models to Deviations from Normality, Australian J. Statistics, Vol.23, No.3, 300-308, 1981.

Hollander, M. and D.A. Wolfe, Nonparametric statistical methods, John Wiley & Sons, 1973.

Ives, R.B., Dynamic spectral ratios as features in seismological pattern recognition, Conf. on Computer Graphics, Pattern Recognition and Data Structures, May 1975, IEEE, Piscataway, NJ, Vol. 10, 64, 1975.

Kanal, L., Patterns in pattern recognition: 1968-1974, IEEE Trans. Inform. Theory, Vol. IT-20, 697-722, Nov. 1974.

Kay, S.M. and S.L. Marple, Spectrum analysis - A modern perspective, Proc. IEEE 69, 1380-1419, 1981.

Kassam,S.A.and J.B.Thomas, A class of nonparametric detectors for dependent input data, IEEE Transactions Information Theory, Vol.IT-21, July 1975.

Liu,H.H.and K.S.Fu, An Application of syntactic Pattern Recognition to Seismic Discrimination, IEEE, 49-53, 1981.

Lu, N.H. and B.A. Eisenstein, Suboptimum detection of weak signals in non-gaussian noise, IEEE Transactions on Information Theory, Vol. IT-29, no. 3, 462-466, 1983.

Martin, W., Line tracking in non-stationary processes, Signal Processing, no. 3, 147-155, 1981.

Monmonier, M.S., Computer-assisted cartography principles and prospects, Prentice-Hall, Englewood Cliffs, New Jersey, 1982.

Mood, A.M., F.A. Graybill and D.C. Boes, Introduction to the Theory of Statistics, 3rd Ed., McGraw-Hill, New York, 1974.

Myers, C.S., A comparative study of several dynamic time-warping algorithms for speech recognition, Master's Thesis, MIT, Cambridge, MA, 1980.

Myers, C.S. and L.R. Rabiner, A comparative study of several time-warping algorithms for connected-word recognition, Bell Systems Tech. J., Vol. 60, no. 7, 1389-1409, 1981.

Naimark, B.M., Algorithm for automatic recognition of a seismic signal by a computer, Reviews of Geophysics, Vol. 3, no. 1, 187-191, 1965.

Niemi, On the Effects of a Nonstationary Noise on ARMA Models, Scandanavian J. Statistics, Vol.10, 11-17, 1983.

Odeh, R.E., Owen, Birnbaum, Fisher, Pocket book of statistical tables, Marcel Dekker, Inc., NY, 1977.

Owen, Handbook of statistical tables, Addison-Wesley Publishing Co., Inc., Reading, MA, 1962.

Philippe and Dennery, An introduction to statistical mechanics, John Wiley & Sons, NY, 1972.

Priestley, M.B., Spectral analysis and time series, Academic Press (paperback), Vol. 1-2, 1981.

Robinson, E.A., Multichannel time series analysis with digital computer programs, Holden-Day, San Francisco, CA, 1967.

Schowengerdt, R.A., Techniques for image processing and classification in remote sensing, Academic Press, 1983.

Schumway, R.H. and A.N. Unger, Linear discriminant functions for stationary time series, J. Amer. Stat. Assoc., Vol. 67, 948-, 1974.

Serfling, R.J., The Wilcoxon two-sample statistic on strongly mixing prodesses, Ann. of Mathe. Statistics, Vol. 39, no. 4, 1202-1209, 1968.

Shin, J.G. and S.A. Kassam, Robust detector for narrow-band signals in non-Gaussian noise, J. Acoust. Soc. Am., Vol. 75, no. 2, 527-533, 1983.

Shtemenko, Y.N., Reconstruction of seismic signals, distorted by correlated noise in multi-channel systems, Izvestiya, Earth Physics, Vol. 16,no. 4, 289-295, 1980.

Simon, R.B., Earthquake interpretations a manual for reading seismograms, William Kaufmann, Inc., Los Altos, CA, 1981.

Swain, P.H. and H. Hauska, The decision tree classifier: Design and potential, IEEE Trans. on Geoscience Electronics, Vol. GE-15, no. 3, 142-147, July 1977.

Tables of normal probability functions, National Bureau of Standards, Applied Mathematics Series no. 23, U.S. Government Printing Office, Washington, D.C., 1953.

Taner, M.T., F. Koehler and R.E. Sheriff, Complex seismic trace analysis, Geophysics, Vol. 44, 1041-1063, 1979.

Tiberio, M.A., Detection algorithm, Seismic Discrimination Semiannual Technical Summary, Lincoln Lab., MIT, Cambridge, MA, 15-17, Sept. 1981.

Tjostheim, D., Recognition of waveforms using autoregressive feature extraction, IEEE Trans. Comput., Vol. C-26, 268, 1977.

Walsh, J.E., Some significance tests for the median which are valid under very general conditions, Ann. of Mathe. Statistics, Vol. 20, 64-81, 1949.

Walsh, J.E., Some bounded significance level properties of the equal-tail sign test, Ann. of Mathe. Statistics, Vol. 22, 408-417, 1951.

Whittle,P., Recursive Relations for Predictors of Non-stationary Processes, J. Royal Statistic. Society B., Vol.27, 523-532, 1965.

Willis, M.E. and M.N. Toksoz, Automatic P and S wave velocity determination from full waveform digital acoustic logs, Geophysics (submitted 1981).

THE CURIOUS CASE OF THE MISSING EXPLOSION

Eugene Herrin
Geophysical Laboratory
Southern Methodist University

"Is there any point to which you would wish to draw my attention?"
"To the curious incident of the dog in the night-time."
"The dog did nothing in the night-time."
"That was the curious incident," remarked Sherlock Holmes.
("Silver Blaze", A. Conan Doyle)

This narrative could properly be classified as historical fiction. Most of what is reported here actually happened, but some of the events occurred only in the imagination of the writer. We begin by considering the capabilities of a regional network designed to monitor an area of thick salt deposits in the western portion of the Permian Basin of Texas and New Mexico. The stations in the network are at Lajitas, Texas; Hobart, Oklahoma; and Winnemucca, Nevada (see Figure 3). Noise levels at the three stations are based upon actual noise observed at these sites and at similar sites. The minimum background noise at Lajitas is the lowest ever observed in the frequency band of 5 to 40 Hz. This minimum noise level is shown in Figure 1. The minimum levels reported for NORSAR (NORESS site) are somewhat higher, by about 10 dB or more. Measurements at Hobart in the frequency band 1 to 4 Hz show noise levels similar to NORSAR. The background level at Winnemucca based on early measurements is between the Lajitas and the Hobart values. The Lajitas and Winnemucca stations have state-of-the-art, three-component, short

period instruments in 50 ft. boreholes. At Hobart, a 15 element, short period array of surface instruments is located on basement rock. This array is identical to the NORESS array without the outer ring.

Background levels shown in Figure 1 are the minimum noise levels under ideal conditions which exist only a small fraction of the time. The major source of background noise is the effect of wind at the site as is shown in Figure 2. NORSAR has noise levels similar to those at Lajitas under high-wind conditions. We expect to observe the same effect at the Hobart array.

Figure 3 shows the location of a number of events as well as the locations of the stations. GNOME was a 3 kt explosion tamped in salt which was actually observed at Lajitas, Hobart and Winnemucca. SLEUTH is a planned 3 kt decoupled shot in the Salado formation in the same general area as the GNOME event. Figure 4 shows the stratigraphic units in the area. The Salado salt provides the depth and thickness needed to decouple a 3 kt nuclear explosion.

The southeastern corner of New Mexico is an area dotted with potash mines as shown in Figure 5. Mining potassium bearing minerals from the salt and anhydrite units is accomplished using the room-and-pillar method with the separation of the ore being done on the surface near the working shafts. The area is almost a wasteland covered with mounds of discarded evaporites and dessication ponds. Once the mining has proceeded as far away from the working shaft as is practical, the pillars are systematically removed allowing the mine to subside. This

collapse leads to obvious surface effects over the area which has been mined. After this procedure is completed, a new shaft is dug and the operation is repeated. Travellers crossing this region must beware of dangerous scarps which develop in the highways above collapsing mines.

In the midst of this region under one of the mined areas a cavity with a 40 meter radius has been constructed at a depth of 1000 meters in the Salado salt. The salt removed in this process represents only a small addition to the wastes already present on the surface. A 3 kt nuclear device is placed in the cavity ready for the decoupled test which has been code-named SLEUTH.

The Pn signal levels from a 3 kt shot fully tamped in salt (GNOME) observed at the three stations in the monitoring network are given in Table 1, along with the distances to the stations. The very low signal level at Winnemucca resulted from the high attenuation of Pn across the Basin and Range province. Propagation to Lajitas and Hobart, however, is as expected in the mid-continent. We assume a decoupling ratio of 100 at 1 to 2 Hz for SLEUTH compared to GNOME, thus we can accurately predict the Pn amplitude levels (1-2 Hz) at the three stations for the decoupled shot.

On Tuesday, 25 June 1985, preparations were being made for a 4 kt HE shot (MINOR SCALE) at the White Sands test site (see Figure 3). A cold front was crossing Colorado and Utah at that time as shown in Figure 6. The pattern of fronts moving west to east shown in this map is typical of the weather pattern in this region in the spring and early summer and again in the fall. The frontal movements and wind patterns are highly predictable. On

Wednesday, 26 June (Julian day 177), the cold front had passed into New Mexico, but had not yet begun to affect the wind patterns at Lajitas. That afternoon an earthquake of about magnitude 3 occurred west of Amarillo, Texas, and was recorded on the high-frequency (sample rate 250 per sec) system operating at the Lajitas station. The distance to Lajitas from the epicenter is 670 km. Figure 8 shows the signal and the signal-to-noise spectrum for this event. There is good signal-to-noise-ratio to frequencies greater than 15 Hz. This event was located within the 16-element seismic network operated by Stone and Webster Engineering as part of the nuclear waste disposal survey in the Texas Panhandle; therefore, we were able to compute an accurate epicenter for the event using the network records. Digital data were available for a station 48 km from the epicenter so that a good displacement spectrum could be computed. This spectrum showed a clear corner at 6 Hz, a constant level at lower frequencies and a roll-off above the corner frequency of 60 dB/decade (f^{-3}). Using this spectrum and the digital record at Lajitas, we were able to produce a good estimate of the apparent Q for Pn along this path. The value of Q was 246 which is consistent with Q(Pn) reported from northeast of Moscow along a line from the Volga River to Vorkuta (Yegorkin and Kun, Izvestiya, 1978, Vol. 14, No. 4, 262-269).

On Thursday, 27 June (Day 178) 1985, the cold front had moved through Oklahoma and much of Texas (Figure 9). Winds at Hobart and Lajitas were 20 to 30 mph from the north. That morning MINOR SCALE was fired at White Sands, and thirty seconds

later the decoupled nuclear shot, SLEUTH, was fired. Figure 10 shows the signal from MINOR SCALE. The amplitude of Pn from this event was about 4 times as large as from the Amarillo earthquake the previous day, as would be expected based on the yield of MINOR SCALE. The wind at Lajitas was 20-30 mph at the time of the event (Figure 10), whereas conditions had been nearly calm during the recording of the Amarillo earthquake on the previous day. Even though the vertical instrument was located at a depth of 100 meters, wind-noise was a major problem on day 178. This effect is clearly seen in Figure 11, where the signal-to-noise spectrum falls to zero dB at 6 Hz for MINOR SCALE. This result can be contrasted with the effective bandwidth of 16 Hz seen for the more distant, significantly smaller event recorded on the previous day when the wind was nearly calm.

SLEUTH was not detected at Lajitas. Pn was below the noise level and the Lg wave train was swamped by the Lg signal from MINOR SCALE. Figure 12 shows the predicted displacement spectra for GNOME and SLEUTH based on the corner frequencies for 3 kt tamped and decoupled events given by Archambeau and the Q-value obtained from the Amarillo earthquake. The displacement spectra of the background noise on days 177 and 178 are also shown. From this figure we see that if SLEUTH had been fired on day 177, Pn would have been detected at Lajitas, in agreement with Archambeau's predictions. By picking the right time to fire SLEUTH, based on the weather patterns and the known time of MINOR SCALE, the most sensitive high-frequency station in the network was made incapable of detecting the event. At Hobart, Oklahoma, the wind was 15 to 20 knots (around 25 mph) from the north

(Figure 9). The surface array there could be expected to produce signal-to-noise improvement over a single surface instrument of about 3.5 at 1 to 2 Hz and about 2 at 10 Hz. The background noise; however, could be expected to be higher by at least a factor of 5 because of the high winds. Thus the Hobart array would fail to detect Pn from SLEUTH. Again, Lg would be lost in the coda of MINOR SCALE, and could not be pulled out by array processing because of the similarity of azimuths for the two events relative to the array. Because of poor propagation across the Basin and Range Province, Pn from SLEUTH could not be detected at Winnemucca no matter what the noise conditions were at that station. Thus we see that an excellent reginal network designed to monitor an area with salt deposits failed to detect a 3 kt decoupled shot.

"The dog did nothing in the night-time."

The failure of the network occurred because the evader could pick the most advantageous time to fire the clandestine test. SLEUTH is not one-of-a-kind. Predictable weather conditions similar to those on 27 June 1985, occur in West Texas and Oklahoma several times each year. Shots of 1/2 kt of HE or larger are not uncommon at White Sands Test Site. Cavity mining could go on year after year in southeastern New Mexico completely masked by the potash mining in the area. By waiting for the

same sequence of events that occurred on 27 June, several decoupled nuclear tests a year could be carried out with virtually no chance of detection.

Two factors are required for a successful clandestine test of the kind described in this paper. The first is a degradation of detection capability at the critical stations because of high wind. The second is a legitimate HE test under the control of the evader which can be used to mask the decoupled shot. The second factor must be regulated by legal means. Control of the first factor depends upon our ability to protect instruments from the effect of wind-induced seismic noise. Until these problems are solved, a clever evader can pick the right time to fire a decoupled shot with little risk of detection.

Acknowledgements. Dick Cromer (Sandia) and Paul Golden (SMU) computed the spectra used in this paper. Stone and Webster Engineering provided digital data from their network in the Texas Panhandle. This work was supported by DARPA/AFGL under contract No. F19628-85-K-0032 and by Sandia National Laboratories. John W. Harrington suggested the use of the quotation from A. Conan Doyle.

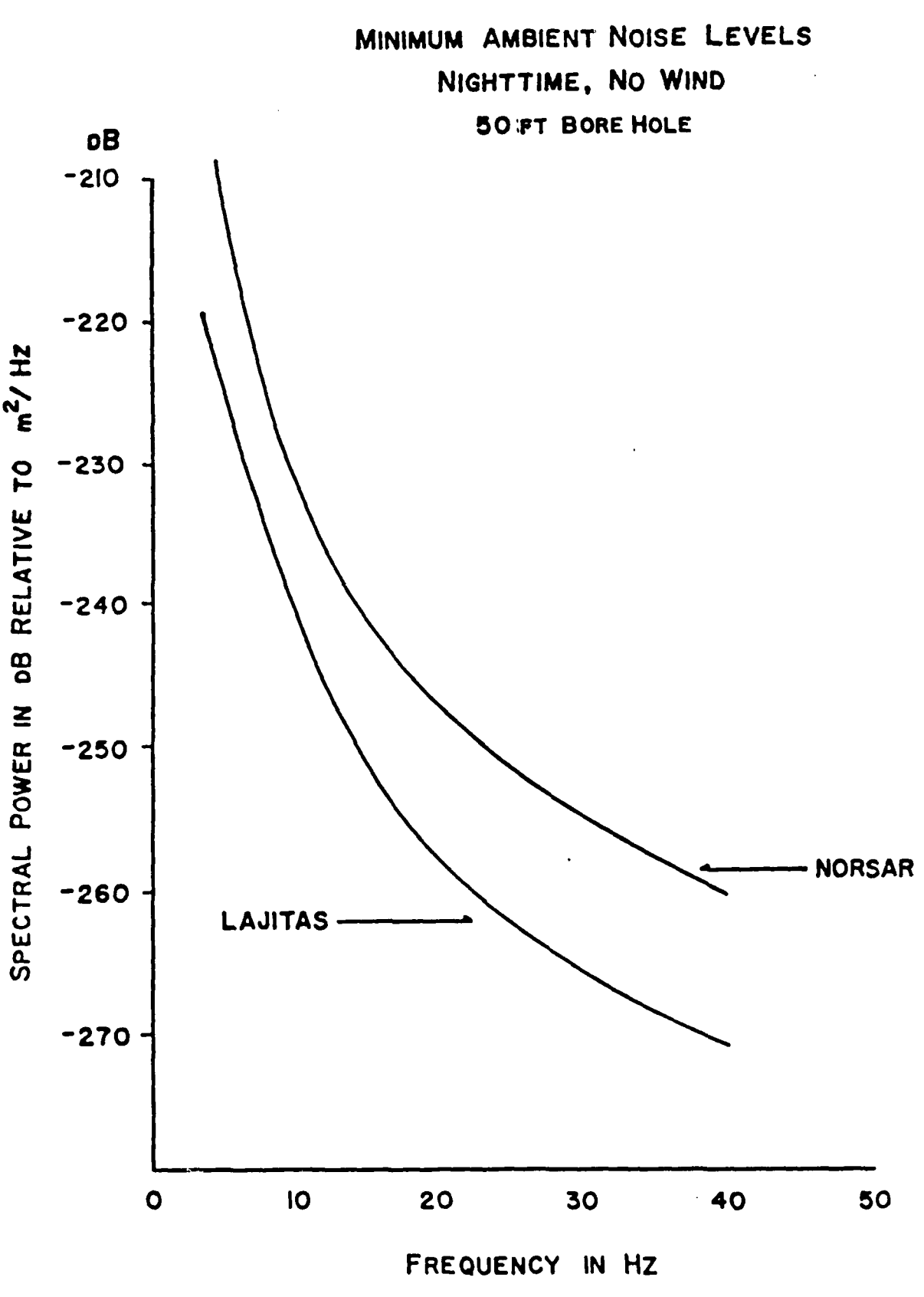

Figure 1. Minimum Seismic Noise Levels at Lajitas and Norsar.

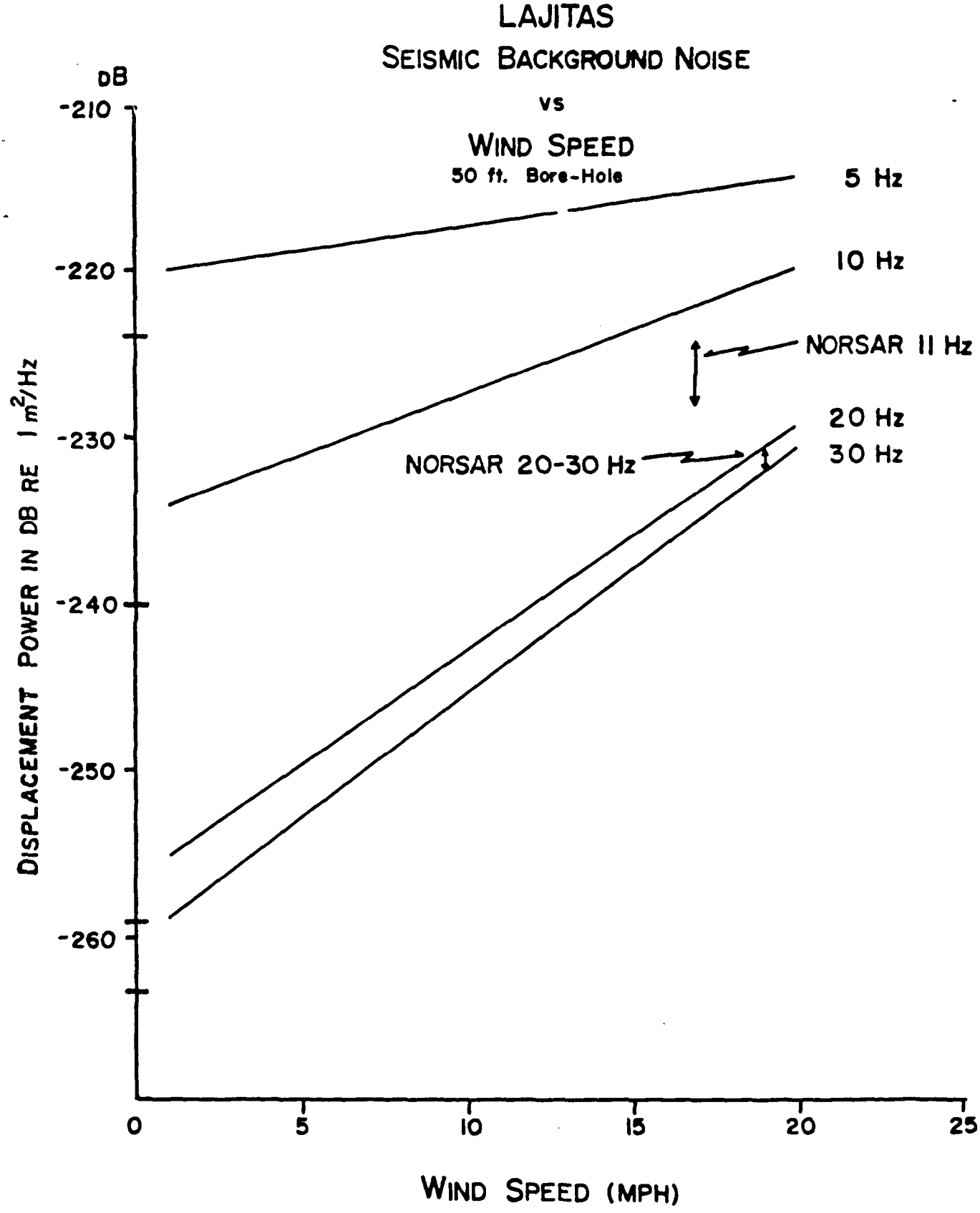

Figure 2. Seismic background versus wind speed at Lajitas.

Figure 3. Map showing locations of seismic stations and events.

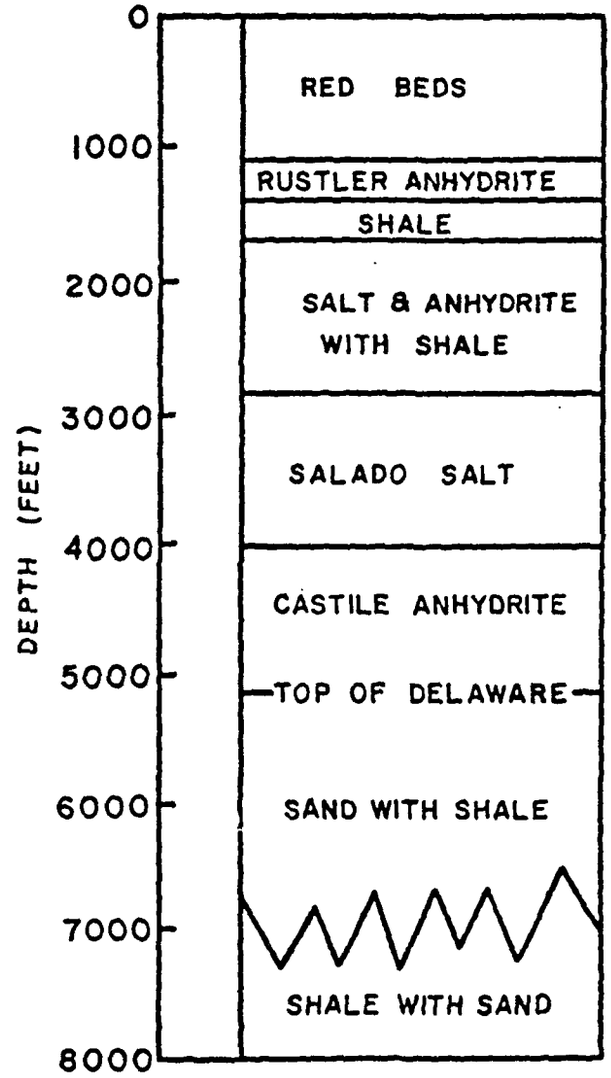

Figure 4. Stratigraphic section of GNOME/SLEUTH site.

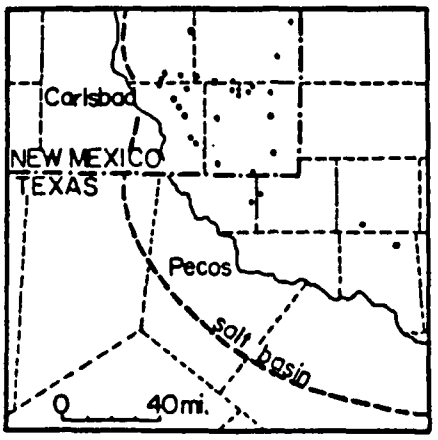

Figure 5. Map showing potash mining activity in the GNOME/SLEUTH vicinity. Dots indicate location of potash mines.

Table 1.

SIGNAL LEVELS

Station	(km) Distance	Pn Amplitudes (millimcrons) GNOME	SLEUTH
Lajitas	378	42	0.4
Hobart	561	35	0.3
Winnemucca	1574	1	0.01

GNOME	3 kt	tamped in salt
SLEUTH	3 kt	in salt cavity, radius 40 meters depth 1000 meters in Salado formation.

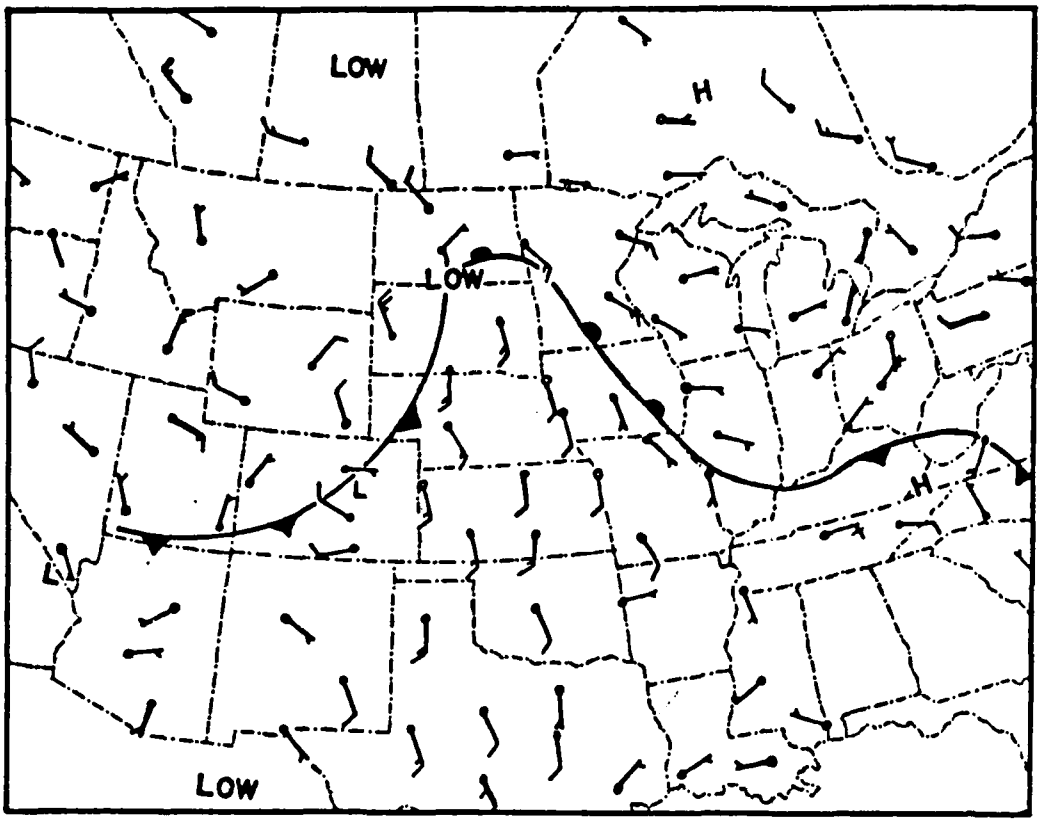

Figure 6. Weather map for Tuesday, 25 June 1985.

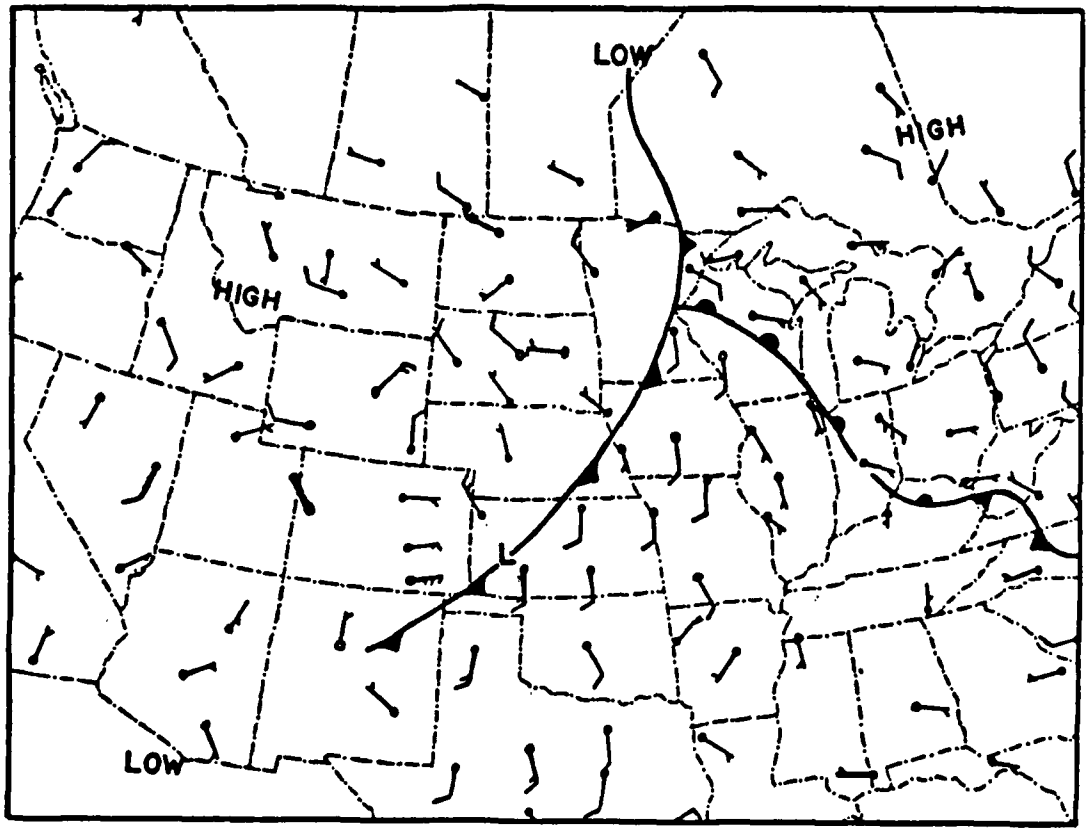

Figure 7. Weather map for Wednesday, 26 June 1985.

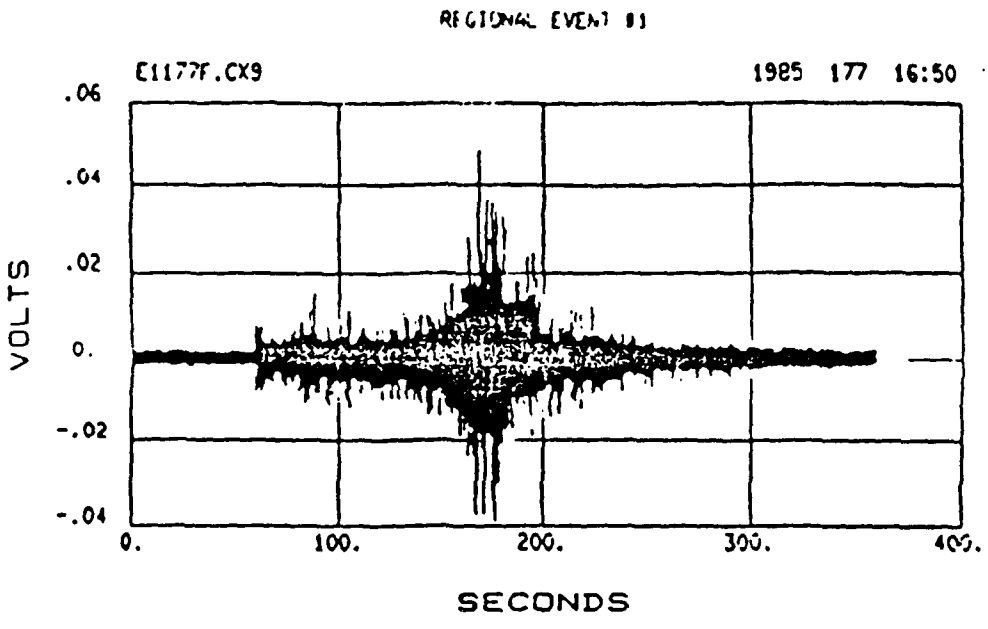

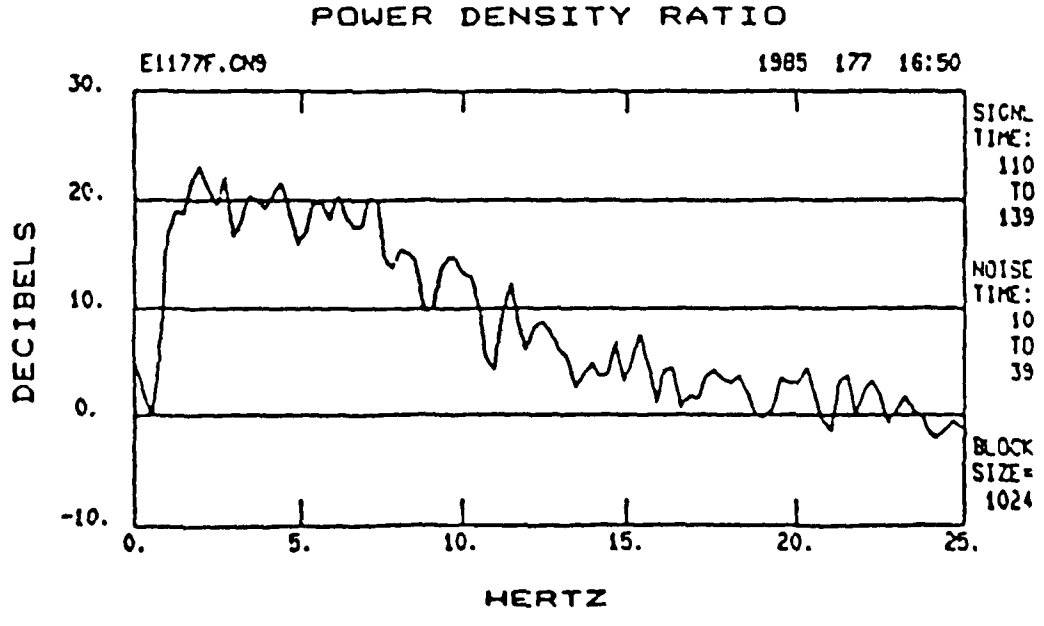

Figure 8. Amarillo earthquake, High-frequency recording (250 samples per second) from 330 ft. Z component at Lajitas and signal-to-noise spectrum for this record.

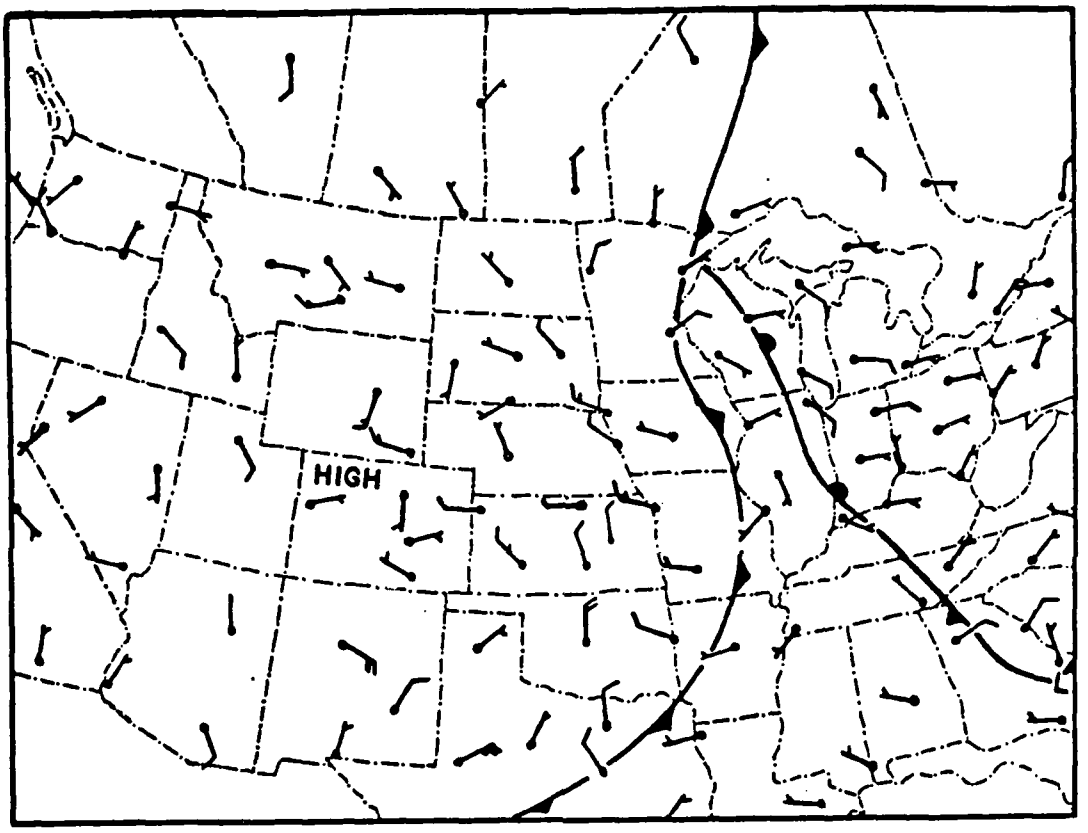

Figure 9. Weather map for Thursday, 27 June 1985.

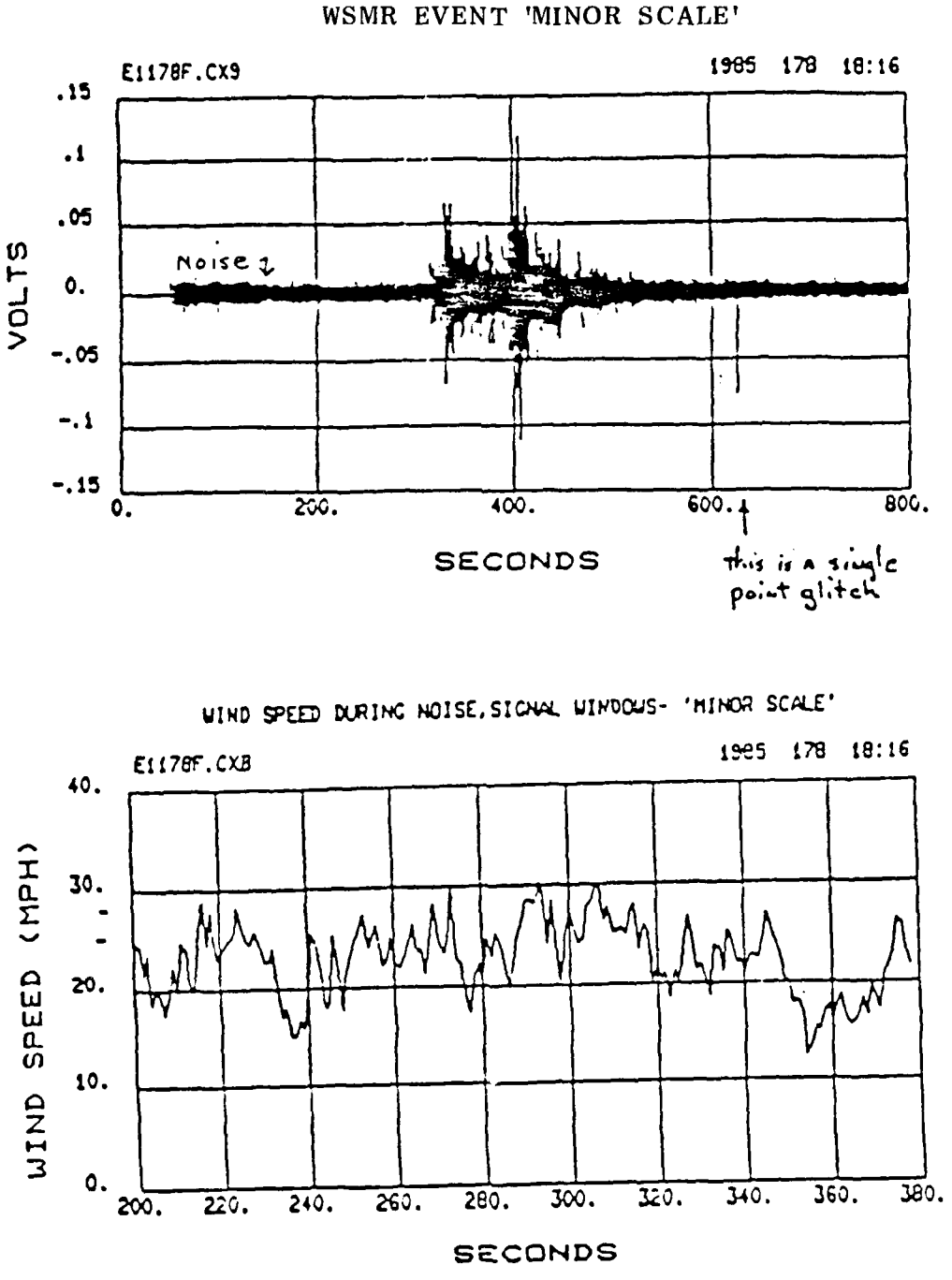

Figure 10. Minor Scale: Record from 330 ft. borehole instrument and plot of wind speed during P-wave arrival time.

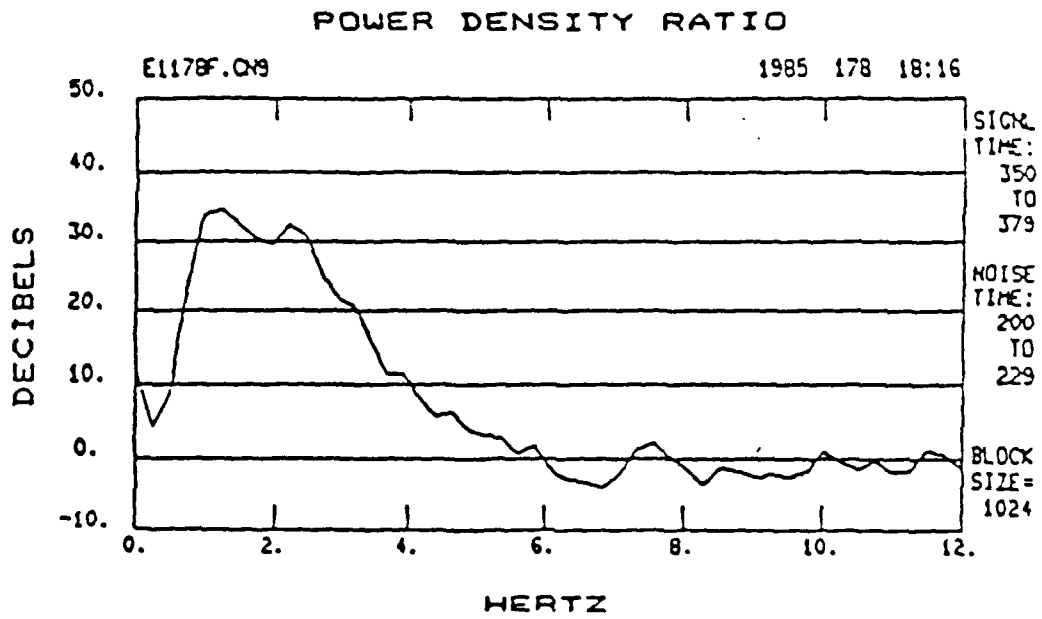

Figure 11. Minor Scale: Signal-to-noise spectrum from P-wave, 330 ft. borehole instrument.

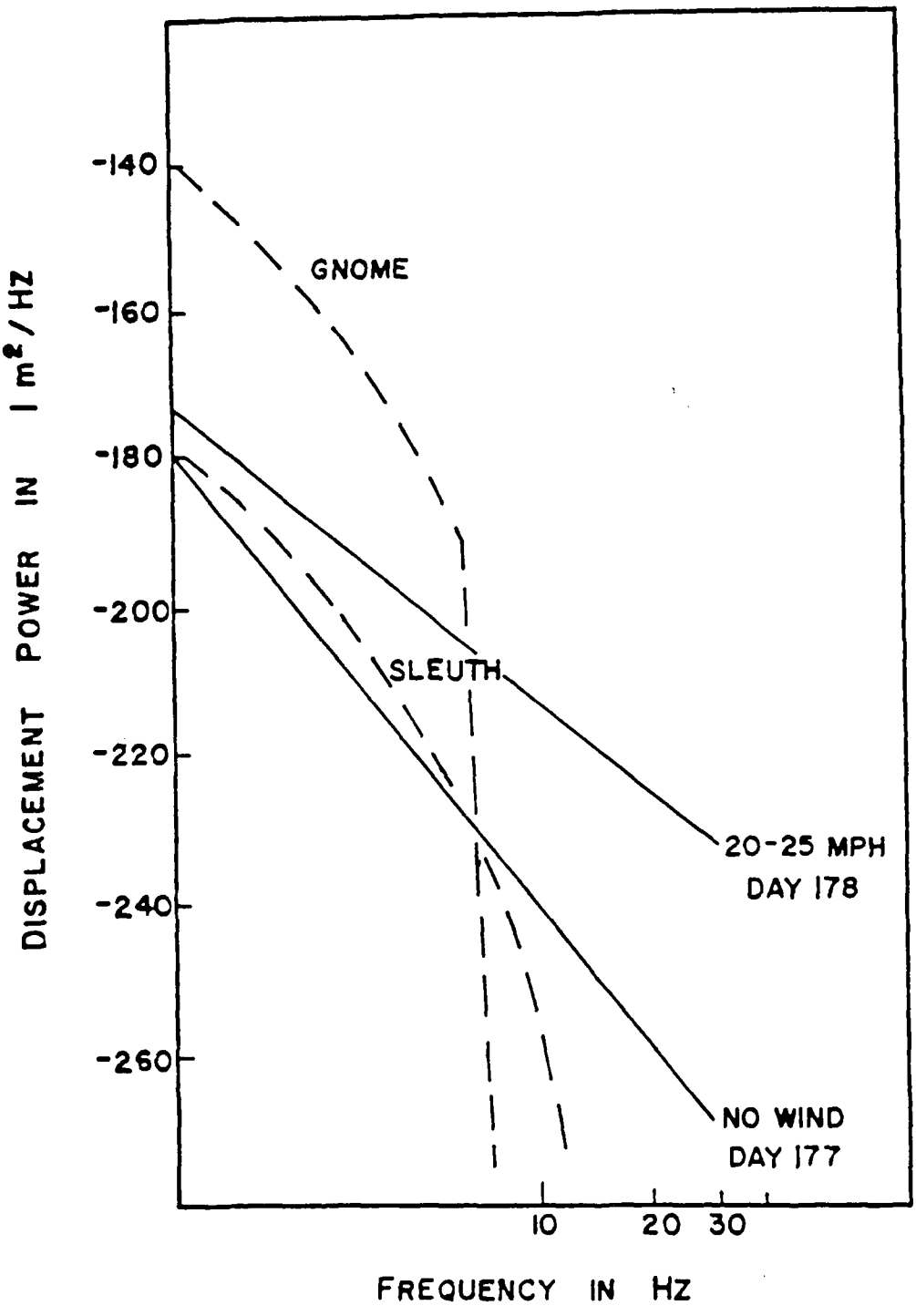

Figure 12. Displacement spectra for GNOME and SLEUTH at Lajitas and the background noise at Lajitas.

DISTRIBUTION LIST

Dr. Monem Abdel-Gawad
Rockwell Internat'l Science Center
1049 Camino Dos Rios
Thousand Oaks, CA 91360

Professor Keiiti Aki
Center for Earth Sciences
University of Southern California
University Park
Los Angeles, CA 90089-0741

Dr. Raplh Alewine III
DARPA/STO/GSD
1400 Wilson Boulevard
Arlington, CA 22209-2308

Professor Shelton S. Alexander
Geosciences Department
403 Deike Building
The Pennsylvania State University
University Park, PA 16802

Professor Charles B. Archambeau
Cooperative Institute for Resch
in Environmental Sciences
University of Colorado
Boulder, CO 80309

Dr. Thomas C. Bache Jr.
Science Applications Int'l Corp.
10210 Campus Point Drive
San Diego, CA 92121

Dr. Robert Blandford
DARPA/STO/GSD
1400 Wilson Boulevard
Arlington, CA 22209-2308

Dr. Lawrence Braile
Department of Geosciences
Purdue University
West Lafayette, IN 47907

Dr. James Bulau
Rockwell Int'l Science Center
1049 Camino Dos Rios
P.O. Box 1085
Thousand Oaks, CA 91360

Dr. Douglas R. Baumgardt
Signal Analysis & Systems Div.
ENSCO, Inc.
5400 Port Royal Road
Springfield, VA 22151-2388

Dr. G. Blake
US Dept of Energy/DP 331
Forrestal Building
1000 Independence Ave.
Washington, D.C. 20585

Dr. S. Bratt
Science Applications Int'l Corp.
10210 Campus Point Drive
San Diego, CA 92121

Woodward-Clyde Consultants
ATTN: Dr. Lawrence J. Burdick
Dr. Jeff Barker
P.O. Box 93245
Pasadena, CA 91109-3245 (2 copies)

Dr. Roy Burger
1221 Serry Rd.
Schenectady, NY 12309

Professor Robert W. Clayton
Seismological Laboratory/Div. of
Geological & Planetary Sciences
California Institute of Technology
Pasadena, CA 91125

Dr. Vernon F. Cormier/Earth Resources
Lab, Dept of Earth, Atmospheric and
Planetary Sciences
MIT - 42 Carleton Street
Cambridge, MA 02142

Professor Anton W. Dainty
AFGL/LWH
Hanscom AFB, MA 01731

Dr. Zoltan A. Der
ENSCO, Inc.
5400 Port Royal Road
Springfield, VA 22151-2388

Professor Adam Dziewonski
Hoffman Laboratory
Harvard University
20 Oxford St.
Cambridge, MA 02138

Professor John Ebel
Dept of Geology & Geophysics
Boston College
Chestnut Hill, MA 02167

Dr. Jack Evernden
USGS-Earthquake Studies
345 Middlefield Road
Menlo Park, CA 94025

Professor John Ferguson
Center for Lithospheric Studies
The University of Texas at Dallas
P.O. Box 830688
Richardson, TX 75083-0688

Mr. Edward Giller
Pacific Seirra Research Corp.
1401 Wilson Boulevard
Arlington, VA 22209

Dr. Jeffrey W. Given
Sierra Geophysics
11255 Kirkland Way
Kirkland, WA 98033

Professor Steven Grand
Department of Geology
245 Natural History Building
1301 West Green Street
Urbana, IL 61801

Professor Roy Greenfield
Geosciences Department
403 Deike Building
The Pennsylvania State University
University Park, PA 16802

Dr. James Hannon
Lawrence Livermore Nat'l Lab.
P.O. Box 808
Livermore, CA 94550

Professor David G. Harkrider
Seismological Laboratory
Div of Geological & Planetary Sciences
California Institute of Technology
Pasadena, CA 91125

Professor Donald V. Helmberger
Seismological Laboratory
Div of Geological & Planetary Sciences
California Institute of Technology
Pasadena, CA 91125

Professor Eugene Herrin
Institute for the Study of Earth
& Man/Geophysical Laboratory
Southern Methodist University
Dallas, TX 75275

Professor Robert B. Herrmann
Department of Earth & Atmospheric
Sciences
Saint Louis University
Saint Louis, MO 63156

U.S. Arms Control & Disarm. Agency
ATTN: Mrs. M. Hoinkes
Div. of Multilateral Affairs
Room 5499
Washington, D.C. 20451

Professor Lane R. Johnson
Seismographic Station
University of California
Berkeley, CA 94720

Professor Thomas H. Jordan
Department of Earth, Atmospheric
and Planetary Sciences
Mass Institute of Technology
Cambridge, MA 02139

Dr. Alan Kafka
Department of Geology &
Geophysics
Boston College
Chestnut Hill, MA 02167

Ms. Ann Kerr
DARPA/STO/GSD
1400 Wilson Boulevard
Arlington, VA 22209-2308

Professor Charles A. Langston
Geosciences Department
403 Deike Building
The Pennsylvania State University
University Park, PA 16802

Professor Thorne Lay
Department of Geological Sciences
1006 C.C. Little Building
University of Michigan
Ann Harbor, MI 48109-1063

Dr. Arthur Lerner-Lam
Lamont-Doherty Geological Observatory
of Columbia University
Palisades, NY 10964

Dr. George R. Mellman
Sierra Geophysics
11255 Kirkland Way
Kirkland, WA 98033

Professor Brian J. Mitchell
Department of Earth & Atmospheric
Sciences
Saint Louis University
Saint Louis, MO 63156

Professor Thomas V. McEvilly
Seismographic Station
University of California
Berkeley, CA 94720

Dr. Keith L. McLaughlin
Teledyne Geotech
314 Montgomery Street
Alexandria, VA 22314

Mr. Jack Murphy - S-CUBED
Reston Geophysics Office
11800 Sunrise Valley Drive
Suite 1212
Reston, VA 22091

Dr. Carl Newton
Los Alamos National Lab.
P.O. Box 1663
Mail Stop C335, Group E553
Los Alamos, NM 87545

Professor Otto W. Nuttli
Department of Earth &
Atmospheric Sciences
Saint Louis University
Saint Louis, MO 63156

Professor J. A. Orcutt
Geological Sciences Div.
Univ. of California at
San Diego
La Jolla, CA 92093

Dr. Frank F. Pilotte
Director of Geophysics
Headquarters Air Force Technical
Applications Center
Patrick AFB, Florida 32925-6001

Professor Keith Priestley
University of Nevada
Mackay School of Mines
Reno, Nevada 89557

Mr. Jack Raclin
USGS - Geology, Rm 3 C136
Mail Stop 928 National Center
Reston, VA 22092

Professor Paul G. Richards
Lamont-Doherty Geological
Observatory of Columbia Univ.
Palisades, NY 10964

Dr. Norton Rimer
S-CUBED
A Division of Maxwell Lab
P.O. 1620
La Jolla, CA 92038-1620

Dr. George H. Rothe
Chief, Research Division
Geophysics Directorate
HQ Air Force Technical
Applications Center
Patrick AFB, Florida 32925-6001

Professor Larry J. Ruff
Department of Geological Sciences
1006 C.C. Little Building
University of Michigan
Ann Arbor, MI 48109-1063

Dr. Alan S. Ryall, Jr.
Center of Seismic Studies
1300 North 17th Street
Suite 1450
Arlington, VA 22209-2308

Professor Charles G. Sammis
Center for Earth Sciences
University of Southern California
University Park
Los Angeles, CA 90089-0741

Dr. David G. Simpson
Lamont-Doherty Geological Observ.
of Columbia University
Palisades, NY 10964

Dr. Jeffrey L. Stevens
S-CUBED,
A Division of Maxwell Laboratory
P.O. Box 1620
La Jolla, CA 92038-1620

Professor Brian Stump
Institute for the Study of Earth & Man
Geophysical Laboratory
Southern Methodist University
Dallas, TX 75275

Professor Ta-liang Teng
Center for Earth Sciences
University of Southern California
University Park
Los Angeles, CA 90089-0741

Dr. R. B. Tittmann
Rockwell International Science Ctr
1049 Camino Dos Rios
P.O. Box 1085
Thousand Oaks, CA 91360

Professor M. Nafi Toksoz/Earth Resources
Lab - Dept of Earth, Atmospheric and
Planetary Sciences
MIT - 42 Carleton Street
Cambridge, MA 02142

Dr. Lawrence Turnbull
OSWR/NED
Central Intelligence Agency
CIA, Room 5G48
Washington, D.C. 20505

Professor Terry C. Wallace
Department of Geosciences
Building #11
University of Arizona
Tucson, AZ 85721

Professor John H. Woodhouse
Hoffman Laboratory
Harvard University
20 Oxford St.
Cambridge, MA 02138

***

DARPA/PM
1400 Wilson Boulevard
Arlington, VA 22209

Defense Technical
Information Center
Cameron Station
Alexandria, VA 22314
(12 copies)

Defense Intelligence Agency
Directorate for Scientific &
Technical Intelligence
Washington, D.C. 20301

Defense Nuclear Agency/SPSS
ATTN: Dr. Michael Shore
6801 Telegraph Road
Alexandria, VA 22310

AFOSR/NPG
ATTN: Director
Bldg 410, Room C222
Bolling AFB, Wash D.C. 20332

AFTAC/CA (STINFO)
Patrick AFB, FL 32925-6001

U.S. Geological Survey
ATTN: Dr. T. Hanks
Nat'l Earthquake Resch Center
345 Middlefield Road
Menlo Park, CA 94025

SRI International
333 Ravensworth Avenue
Menlo Park, CA 94025

Center for Seismic Studies
ATTN: Dr. C. Romney
1300 North 17th St., Suite 1450
Arlington, VA 22209 (3 copies)

Science Horizons, Inc.
ATTN: Dr. Bernard Minster
Dr. Theodore Cherry
710 Encinitas Blvd., Suite 101
Encinitas, CA 92024 (2 copies)

Dr. G. A. Bollinger
Department of Geological Sciences
Virginia Polytechnical Institute
21044 Derring Hall
Blacksburg, VA 24061

Dr. L. Sykes
Lamont Doherty Geological Observ.
Columbia University
Palisades, NY 10964

Dr. S. W. Smith
Geophysics Program
University of Washington
Seattle, WA 98195

Dr. L. Timothy Long
School of Geophysical Sciences
Georgia Institute of Technology
Atlanta, GA 30332

Dr. N. Biswas
Geophysical Institute
University of Alaska
Fairbanks, AK 99701

Dr. Freeman Gilbert - Institute of
Geophysics & Planetary Physics
Univ. of California at San Diego
P.O. Box 109
La Jolla, CA 92037

Dr. Pradeep Talwani
Department of Geological Sciences
University of South Carolina
Columbia, SC 29208

Dr. Donald Forsyth
Dept. of Geological Sciences
Brown University
Providence, RI 02912

Dr. Jack Oliver
Department of Geology
Cornell University
Ithaca, NY 14850

Dr. Muawia Barazangi
Geological Sciences
Cornell University
Ithaca, NY 14853

Rondout Associates
ATTN: Dr. George Sutton,
Dr. Jerry Carter, Dr. Paul Pomeroy
P.O. Box 224
Stone Ridge, NY 12484 (3 copies)

Dr. Bob Smith
Department of Geophysics
University of Utah
1400 East 2nd South
Salt Lake City, UT 84112

Dr. Anthony Gangi
Texas A&M University
Department of Geophysics
College Station, TX 77843

Dr. Gregory B. Young
ENSCO, Inc.
5400 Port Royal Road
Springfield, CA 22151

Weidlinger Associates
ATTN: Dr. Gregory Wojcik
620 Hansen Way, Suite 100
Palo Alto, CA 94304

Dr. Leon Knopoff
University of California
Institute of Geophysics
& Planetary Physics
Los Angeles, CA 90024

Dr. Kenneth H. Olsen
Los Alamos Scientific Lab.
Post Office Box 1663
Los Alamos, NM 87545

Professor Jon F. Claerbout
Professor Amos Nur
Dept. of Geophysics
Stanford University
Stanford, CA 94305 (2 copies)

Dr. Robert Burridge
Schlumberger-Doll Resch Ctr.
Old Quarry Road
Ridgefield, CT 06877

Dr. Robert Phinney/Dr. F.A. Dahlen
Dept of Geological
Geophysical Sci. University
Princeton University
Princeton, NJ 08540 (2 copies)

New England Research, Inc.
ATTN: Dr. Randolph Martin III
P.O. Box 857
Norwich, VT 05055

Sandia National Laboratory
ATTN: Dr. H. B. Durham
Albuquerque, NM 87185

AFGL/XO
Hanscom AFB, MA 01731-5000

AFGL/LW
Hanscom AFB, MA 01731-5000

AFGL/SULL
Research Library
Hanscom AFB, MA 01731-5000 (2 copies)

Secretary of the Air Force (SAFRD)
Washington, DC 20330

Office of the Secretary Defense
DDR & E
Washington, DC 20330

HQ DNA
ATTN: Technical Library
Washington, DC 20305

Director, Technical Information
DARPA
1400 Wilson Blvd.
Arlington, VA 22209

Los Alamos Scientific Laboratory
ATTN: Report Library
Post Office Box 1663
Los Alamos, NM 87544

Dr. Thomas Weaver
Los Alamos Scientific Laboratory
Los Almos, NM 97544

Dr. Gary McCartor
Mission Research Corp.
735 State Street
P.O. Drawer 719
Santa Barbara, CA 93102

Dr. Al Florence
SRI International
333 Ravenwood Avenue
Menlo Park, CA 94025-3493

Dr. W. H. K. Lee
USGS
Office of Earthquakes, Volcanoes,
& Engineering
Branch of Seismology
345 Middlefield Rd
Menlo Park, CA 94025

***

Dr. Peter Basham/Earth Physics Branch
Department of Energy and Mines
1 Observatory Crescent
Ottawa, Ontario
CANADA K1A 0Y3

Dr. Eduard Berg
Institute of Geophysics
University of Hawaii
Honolulu, HI 96822

Dr. Michel Bouchon - Universite
Scientifique et Medicale de Grenob
Lab de Geophysique - Interne et
Tectonophysique - I.R.I.G.M-B.P.
38402 St. Martin D'Heres
Cedex FRANCE

Dr. Hilmar Bungum/NTNF/NORSAR
P.O. Box 51
Norwegian Council of Science,
Industry and Research, NORSAR
N-2007 Kjeller, NORWAY

Dr. Kin-Yip Chun
Geophysics Division
Physics Department
University of Toronto
Ontario, CANADA M5S 1A7

Dr. Alan Douglas
Ministry of Defense
Blacknest, Brimpton,
Reading RG7-4RS
UNITED KINGDOM

Professor Peter Harjes
Institute for Geophysik
Rhur University/Bochum
P.O. Box 102148, 4630 Bochum 1
FEDERAL REPUBLIC OF GERMANY

Dr. E. Husebye
NTNF/NORSAR
P.O. Box 51
N-2007 Kjeller, NORWAY

Mr. Peter Marshall, Procurement
Executive, Ministry of Defense
Blacknest, Brimpton,
Reading FG7-4RS
UNITED KINGDOM

Dr. B. Massinon
Societe Radiomana
27, Rue Claude Bernard
75005, Paris, FRANCE

Dr. Pierre Mechler
Societe Radiomana
27, Rue Claude Bernard
75005, Paris, FRANCE

Dr. Ben Menaheim
Weizman Institute of Science
Rehovot, ISRAEL 951729

Dr. Svein Mykkeltveit
NTNF/NORSAR
P.O. Box 51
N-2007 Kjeller, NORWAY

Dr. Frode Ringdal
NTNF/NORSAR
P.O. Box 51
N-2007 Kjeller, NORWAY

University of Hawaii
Institute of Geophysics
ATTN: Dr. Daniel Walker
Honolulu, HI 96822

***